CHARLES UNIVERSITY
Faculty of Science
Developmental and Cell Biology

The role of Kit ligands in hematopoiesis of *Danio rerio*

Dissertation

Jana Oltová

Supervisor: Petr Bartůněk, Ph.D.

Department of Cell Differentiation

Institute of Molecular Genetics of the Czech Academy of Sciences

Prague, 2020

DECLARATION

I declare that I wrote this dissertation independently and that I cited all the information sources and literature. This work or a substantial part of it was not presented to obtain another academic degree or equivalent.

Prague, 1.3.2020

Jana Oltová

PROHLÁŠENÍ

Prohlašuji, že jsem závěrečnou práci zpracovala samostatně a že jsem uvedla všechny použité informační zdroje a literaturu. Tato práce ani její podstatná část nebyla předložena k získání jiného nebo stejného akademického titulu.

V Praze, dne 1.3.2020

Jana Oltová

ACKNOWLEDGEMENT

I am happy to take this opportunity to thank everyone who supported me on the journey towards completing this project. I have been really lucky to work in a great team of the Laboratory of Cell Differentiation and CZ-OPENSCREEN and I would like to thank all present and past members of these laboratories for helping me and for creating such a friendly and productive atmosphere.

First and foremost, my very special thanks goes to Petr Bartůněk, my visionary supervisor, for supporting me in hard times and for giving me the opportunity to be a part of all this. I am also extremely thankful to Olga Machoňová and Ondřej Svoboda, two of my colleagues who became my closest friends, for everything they have done for me. Without them, many of the experiments would not have been possible. Furthermore, I would like to thank Trevor Epp and Bjoern Schuster for critically reading the manuscripts. My thanks also goes to all the members of our fish facility for taking care of the animals and also I would like to acknowledge Tereza Mikulášová for providing some of the graphical schemes.

Moreover, I also want take the opportunity to acknowledge the whole Zebrabase team for their dedication to the project - especially Jindřich Jindřich for bringing Zebrabase to life in 2014 and developing it with me ever since, and Ctibor Škuta for creating the best user interface we could have wished for. Personally, I feel honored for being given the opportunity to work in such a great team on a dynamically growing project whose outcomes are helping scientist from all around the work. Furthermore, I want to thank to Petr Divina and the IT department at the Institute of Molecular Genetics for providing the technical support and resources necessary for the development of Zebrabase.

Finally, I want to express my deep gratitude to my parents for their never-ending support.

Thank you all. Without you, none of this would have been possible.

FINANCIAL SUPPORT

This work was supported by the Czech Science Foundation (16-21024S), Ministry of Health (NV19-07-00412), Ministry of Education, Youth and Sports - Program NPU I (LO1419) to Petr Bartůněk, and Grant Agency of the Charles University (1272214) to me.

TABLE OF CONTENTS

ABSTRACT (ENGLISH)

Hematopoiesis is a precisely regulated process, dependent on the activity of hematopoietic cytokines and their receptors. Due to an extra round of whole genome duplication in teleost fish, two paralogs of many important genes, including some hematopoietic cytokines and their receptors, are present in the zebrafish (*Danio rerio*) genome. In this project, we have been investigating the role of zebrafish Kit ligands in hematopoiesis. Kit ligand is a pleiotropic cytokine, which is essential for vertebrate erythropoiesis; however, in zebrafish, no such role has been reported so far. To determine the function of zebrafish paralogs of Kit ligand (Kitlga and Kitlgb) in hematopoiesis, we performed *in vivo* and *ex vivo* gain- and loss-of-function experiments. Strikingly, we were the first to report the synergistic cooperation of zebrafish Kitlga with erythropoietin and dexamethasone, enabling the growth of kidney marrow-derived suspension cells and providing optimal conditions for the expansion of adult erythroid progenitors. We assume that by using different cytokine combinations, optimal conditions for the growth of other hematopoietic cell types can be established, and therefore, this new approach now available for the zebrafish model will be particularly useful for studies of normal and aberrant hematopoiesis (e.g. using hematopoietic mutant lines and disease models). Finally, we developed an intuitive fish tracking database system, Zebrabase, and we are providing it as a hosted service to the zebrafish community. Zebrabase is currently used in more than 40 zebrafish facilities worldwide and is continuously gaining popularity as a tracking solution of choice for both small and large facilities. Taken together, the results of this project reinforce the role of zebrafish as a relevant model for human hematopoiesis.

Keywords

Danio rerio, hematopoiesis, cytokine, Kit ligand, whole-genome duplication, erythropoiesis, database

ABSTRAKT (CZECH)

Hematopoetická regulace závisí z velké části na aktivitě hematopoetických cytokinů a jejich receptorů. Díky celogenomové duplikaci je u kostnatých ryb včetně Dánia pruhovaného (*Danio rerio*) mnoho duplikovaných paralogů, mimo jiné i pro některé hematopoetické cytokinové geny. V tomto projektu jsme se zabývali rolí duplikovaného Kit ligandu v hematopoeze *D. rerio*. Kit ligand (Kitlg) je cytokin s pleiotropním efektem, který je zcela zásadní pro erytropoezu u obratlovců, ale u *D. rerio* tato role zatím nebyla prokázána. Za účelem ověření této funkce jsme použili *in vivo* a *ex vivo* nástroje a gain-of-function i loss-of-function přístupy. Jako první jsme prokázali synergistickou kooperaci rybího Kitlga s erythropoetinem (Epo) a dexamethasonem (Dex), která umožňuje kultivovat buňky ledvinné dřeně v suspenzi a vytváří optimální podmínky pro expanzi dospělých erytroidních progenitorů. Předpokládáme, že námi navržené podmínky bude dále možné optimalizovat za pomocí dalších cytokinových kombinací tak, aby umožňovaly růst a expanzi jiných typů hematopoetických buněk. Proto bude tento přístup velmi užitečný pro studium normální a aberantní hematopoezy, například za využití rybích hematopoeitckých mutantních linií a modelů onemocnění. Dále jsme vyvinuli intuitivní rybí databázi pro rybí chovy, Zebrabase, a poskytujeme ji vědecké komunitě jako hostovanou službu. Zebrabase je momentálně používána ve více než čtyřiceti laboratořích po celém světě a stává se stále více populární jako databázové řešení pro sledování zvířat v malých i velkých chovech. Závěrem, výsledky tohoto projektu upevňují roli *D. rerio* jako relevantního modelu pro studium lidské hematopoezy.

Klíčová slova

Danio rerio, hematopoeza, cytokin, Kit ligand, celogenomová duplikace, erythropoeza, databáze

LIST OF ABBREVIATIONS

BFU-E	burst forming units-erythroid
CFU-E	colony forming unit erythroid
CFU-T	colony forming unit thrombocyte
CHT	caudal hematopoietic tissue
CLP	common lymphoid progenitor
CMP	common myeloid progenitors
CSF1	colony stimulating factor 1
CSF3	colony stimulating factor 3
Dex	dexamethasone
DOB	date of birth
dpf	days post-fertilization
EMP	erythro-myeloid progenitors
EPO	erythropoietin
FACS	flow cytometry and fluorescence-activated cell sorting
FELASA	Federation of European Laboratory Animal Science Associations
FGF2	fibroblast growth factor 2
FLT3L	FMS-like tyrosine kinase 3 ligand
GR	glucocorticoid receptor
G-CSF	granulocyte colony-stimulating factor
GM-CSF	granulocyte-macrophage colony-stimulating factor
GMP	granulocyte-monocyte progenitor
hbb	b-globin
hpf	hours post-fertilization
HSC	hematopoietic stem cell
ICM	intermediate cell mass
IGF1	insulin-like growth factor 1
IL3	interleukin 3
INS	insulin

JAK2	Janus kinase 2
kDa	kilodalton
LT-HSC	long-term hematopoietic stem cell
MAPK	mitogen-activated protein kinase
M-CSF	macrophage colony-stimulating factor
MEP	megakaryocyte-erythrocyte progenitor
MPP	multipotent progenitor cell
PI-3K	phosphatidylinositol 3-kinase
qPCR	quantitative reverse transcriptase-polymerase chain reaction
RBC	red blood cell
STAT5	signal transducer and activator of transcription 5
ST-HSC	short-term hematopoietic stem cell
TEP	thrombocyte-erythrocyte progenitors
TGFα/β	transforming growth factor α/β
TPO	thrombopoietin

INTRODUCTION

1. Vertebrate hematopoiesis

In vertebrates, the multistep process of formation and turnover of all blood is tightly regulated by a complex network of intrinsic and extrinsic factors **(Kaushansky 2006, Orkin and Hochedlinger 2011)**. The core elements of the hematopoietic regulation are cytokines and growth factors that bind to their cognate receptors, triggering downstream signaling events. Consequently, by controlling the activity of transcriptional repressors and activators, cellular responses like proliferation, self-renewal or differentiation are modulated. Typically, cytokines are functionally pleiotropic, affecting a wide range of cell types **(Nicola 1994)**.

The process of hematopoiesis first occurs already early in the development, in the primitive wave of the production of red blood cells and macrophages that provide the crucial support to the developing embryo. The primitive wave of hematopoiesis is independent of hematopoietic stem cells **(**reviewed in **Galloway and Zon 2003)**. On the other hand, during definitive hematopoiesis, the whole network is secured by proliferation, self-renewal and differentiation of hematopoietic stem cells (HSCs), as well as cells with reduced self-renewal capabilities - hematopoietic multipotent progenitor cells (MPPs) and lineage restricted progenitors. With the exception of a subset of tissue resident macrophages, all erythroid and myeloid cells are derived from HSCs **(Ginhoux et al. 2010)**. The classical hierarchical model of definitive hematopoiesis **(Akashi et al. 2000, Reya et al. 2001)** claims that HSCs lose their long-term self-renewing capabilities in an asymmetrical manner, which results in the formation of MPPs that further give rise to the common myeloid progenitor (CMP) and common lymphoid progenitor (CLP). CMPs differentiate into bipotent megakaryocyte-erythrocyte progenitors (MEPs) and restricted common granulocyte-monocyte progenitors (GMPs) **(Figure 1)**.

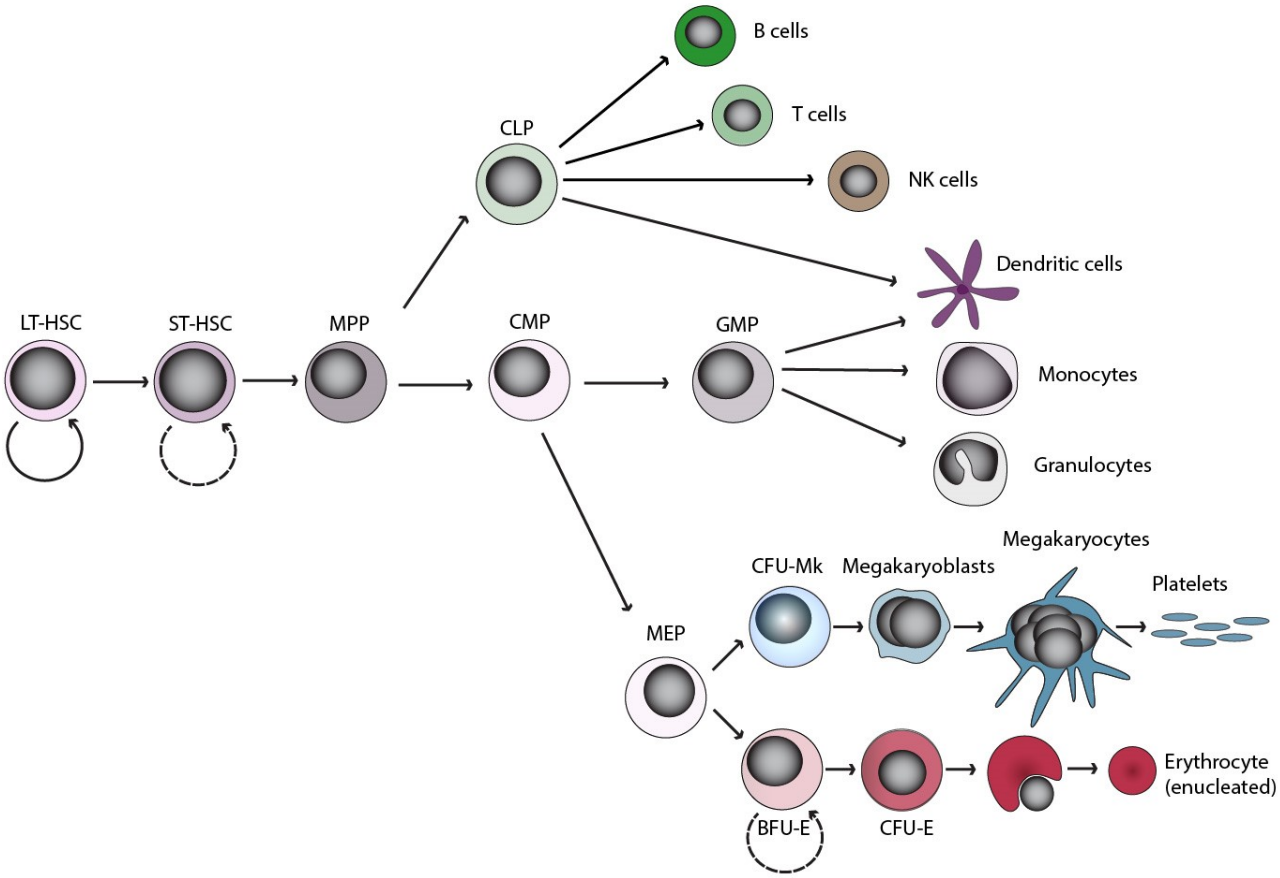

Figure 1 | Classical hierarchical model of mammalian definitive hematopoiesis. LT-HSCs give rise to ST-HSCs and MPPs. MPPs differentiate into CLPs crucial for lymphoid production and CMPs that give rise to GMPs and bi-potent MEPs. MEPs can further differentiate through several subsequent steps into megakaryocytes and erythrocytes. LT-HSC – long term hematopoietic stem cell, ST-HSC – short term hematopoietic stem cell, MPP – multipotent progenitor cell, CLP – common lymphoid progenitor, CMP - common myeloid progenitor, BFU-E – burst forming unit-erythroid, CFU-E - colony forming unit-erythroid, GMP – granulocyte-monocyte progenitor **(**figure adapted from **Akashi et al. 2000)**

2. Hematopoietic regulation of the erythro-myeloid lineage

The precise spatiotemporal orchestration of the entire hematopoietic network is essential both in the course of development and in adult organisms. When disrupted, severe hematopoietic disorders may occur, such as myeloid leukemia, anemia, thrombocytopenia, or neutropenia, often linked to defects in the erythro-myeloid compartment **(Wickrema and Crispino 2007, Crispino and Weiss 2014)**.

In vertebrates, Kit ligand (KITLG, or Stem Cell Factor, SCF) and erythropoietin (EPO), are the major regulators of the process of red blood cell (RBC) development from bipotent mammalian MEPs or non-mammalian TEPs through committed burst and colony forming units – erythroid (BFU-E, CFU-E). Moreover, erythroid development is further supported by insulin (INS) and insulin-like growth factor (IGF1) that promote self-renewal of erythroid progenitors **(Miyagawa et al. 2000)**, transforming growth factor a (TGFa) and TGFb family members **(Krystal 1994, Huber et al. 1998, Gandrillon et al. 1999, Fuchs et al. 2002, Harandi et al. 2010)**, interleukin 3 (IL3), and fibroblast growth factor 2 (FGF2) **(Bartunek et al. 2002)**.

On the other hand, the cytokine critical for the development of thrombocytes from TEPs and the formation of platelets from polyploid megakaryocytes is thrombopoietin (TPO) **(Kaushansky et al. 1995, Kato et al. 1998)**. TPO binds to TPOR (c-MPL), its cognate receptor, to trigger downstream signaling essential for proper thrombopoiesis **(de Sauvage et al. 1994, Alexander 1999a, Alexander 1999b)**. Other factors involved in megakaryocytic maturation and platelet formation are IL12 and SDF1 **(Gordon and Hoffman 1992)**. In the thrombo-erythroid development, lineage restricted cytokines are complemented by those with a broader effect, especially interleukins (IL3, IL6, IL11), G-CSF and GM-CSF **(McNiece et al. 1991, Gordon and Hoffman 1992)** and KITLG **(Steinlein et al. 1995, Broudy 1997)**, which are able to promote both erythroid and thrombocytic differentiation.

Other myelo-monocytic cell types originate from CMPs – granulocytes, monocytes/macrophages and dendritic cells **(Akashi et al. 2000)**, whose differentiation and proliferation from hematopoietic stem and progenitor cells (HSPCs) is controlled by granulocyte colony-stimulating factor (G-CSF or CSF3), macrophage colony-stimulating factor (M-CSF or CSF1), granulocyte-macrophage CSF (GM-CSF or CSF2), and interleukin 3 (IL3) **(Metcalf and Nicola 1983, Metcalf 1985, Migliaccio et al. 1991, Lieschke et al. 1994, Lieschke et al. 1994, Liu et al. 1996)**. These cytokines bind to their corresponding receptors - CSF receptor (M-CSFR, or CSF1R), G-CSF receptor (G-CSFR, or CSF3R), GM-CSF receptor (GM-CSFR, or CSF2RA) and interleukin 3 receptor (IL3RA), respectively.

3. Mammalian versus non-mammalian hematopoiesis

The process of hematopoiesis is well conserved in vertebrates and all three major lineages – myeloid, erythroid and lymphoid – are present from fish to men. Similarly, also the sequential waves of the hematopoietic development, finally leading to a fully functional adult hematopoietic system, have been described in all vertebrate models, including the zebrafish **(reviewed in Davidson and Zon 2004, de Jong and Zon 2005)**. However, especially in the erythro-megakaryocytic lineages, there are subtle differences between mammalian and non-mammalian hematopoiesis that have to be taken into account when using non-mammalian models **(Svoboda and Bartunek 2015)**. In mammals, bi-potent MEPs give rise either to enucleated erythrocytes **(Muir and Kerr 1958, Simpson 1967)** or to endoreduplicated megakaryocytes **(Svoboda et al. 2014)** that serve as precursors for platelet biogenesis. On the contrary, non-mammalian vertebrates possess the bi-potent thrombocyte-erythrocyte progenitors (TEPs) instead, capable of differentiation into functional platelet homologs, termed thrombocytes, or to nucleated erythrocytes **(Ratnoff 1987, Schneider and Gattermann 1994, Svoboda et al. 2014)**. However, besides these differences, the rest of the hematopoietic hierarchy is well conserved between mammalian and non-mammalian organisms **(**reviewed in **Svoboda and Bartunek 2015)**.

As suggested earlier by my colleagues **(Svoboda and Bartunek 2015)**, the investigation of precise relationship between mammalian and non-mammalian hematopoiesis is essential for future hematopoietic research. The use of non-mammalian models can help overcome the obstacles posed by the erythroid and megakaryocytic enhancements in mammals (e.g. megakaryocyte endoreduplication, platelet formation and erythroid enucleation), which are complicating the task of identifying novel key regulators of cell fate determination.

Due to substantial sequence divergence between teleost and mammalian cytokines, most of the mammalian cytokines are generally not effective in zebrafish cultures **(Stachura et al. 2009, Stachura et al. 2011, Stachura et al. 2013, Svoboda et al. 2014)**. The same fact also makes the identification of zebrafish orthologs challenging but in spite of it, many successful attempts to identify and use recombinant zebrafish cytokines have been reported in the recent years **(**reviewed in **Svoboda et al. 2016)**.

4. *D. rerio* as a model of hematopoiesis

Small fish species are gradually gaining popularity in research as a useful alternative to rodent model organisms. Zebrafish (*D. rerio*) is a freshwater cyprinid fish originating from eastern Asia. There are multiple advantages that make it a powerful vertebrate model organism – especially optical transparency of the embryos, high fecundity and external fertilization. Moreover, zebrafish are genetically amenable and combined with the extensive toolbox for genetic manipulation, this fact provides a great basis for the establishment of transgenic and mutant strains. Finally, due to rapid early development and small size of the embryos, zebrafish are suitable for developmental imaging and screening *in vivo*. In the past, zebrafish have been used to answer number of questions related to hematopoiesis **(reviewed in de Jong and Zon 2005, Boatman et al. 2013, Carroll and North 2014)**.

The zebrafish hematopoietic development initiates with the generation of primitive macrophages and granulocytes before 24 hours post fertilization (hpf) **(Herbomel et al. 1999, Le Guyader et al. 2008)**, followed by the development of primitive erythroid cells from intermediate cell mass (ICM) and their entering of circulation at about 26 hpf **(Long et al. 1997)**. These primitive blood cells arise only transiently in the development and are independent of HSCs or MPPs. In the following temporary phase, multipotent erythro-myeloid progenitors (EMPs) presumably arise from the posterior blood island (PBI) at around 28 hpf, giving rise to adult-type of erythroid and myeloid cells in the zebrafish embryo **(Bertrand et al. 2007, Bertrand et al. 2010)**. The final stage begins with transdifferentiation of the endothelium of ventral aorta into HSCs, which migrate into caudal hematopoietic tissue (CHT). Finally between 36 – 72 hpf, HSCs colonize the definitive sites of adult hematopoiesis in zebrafish – kidney and thymus **(North et al. 2007, Bertrand et al. 2008, Kissa et al. 2008, Bertrand et al. 2010)** - to further generate erythroid, myeloid, and lymphoid cells for the rest of the life of the animal.

5. Genome evolution in teleost

In teleost, the extra round of whole genome duplication (WGD) occurred approximately 320-350 million years ago **(Hoegg et al. 2004, Amores et al. 2011)**, resulting in two paralogs of many important genes in zebrafish, including some of the hematopoietic cytokine genes. After such an event, very often, one of the duplicated paralogs is lost after detrimental mutations

accumulate in its genomic sequence in a process called pseudogenization **(Nei and Roychoudhury 1973, Takahata and Maruyama 1979, Watterson 1983)**. Alternatively, the two paralogs of the ancestral gene can be retained and either split the original function (subfunctionalization) or acquire new functions (neofunctionalization) **(Force et al. 1999)**.

Naturally, the event of duplication leads to an increased complexity of the signaling network, especially in cases, when both the duplicated receptors and ligands are retained. The understanding of potential functional differences, binding specificities, and differences in spatiotemporal expression are crucial for the utilization of zebrafish as a model organism for further studies. Although some functions of the duplicated erythro-myeloid cytokines have been already reported **(Hultman et al. 2007, Wang et al. 2008, Stachura et al. 2013, Butko et al. 2015)**, as described in the next section, there are still many unknowns.

Nevertheless, in addition to duplication, genome evolution in teleost also brought some losses of individual hematopoietic cytokine genes or whole gene clusters, including some of the class I cytokine family members **(Liongue and Ward 2007)**. One example is a missing cluster of genes belonging to the *il3* family, including ligands and receptors for *il3*, *il5* and *gmcsf*. These factors are the regulators of the myelo-monocytic lineage, but it has been suggested that they might be functionally substituted by different cytokines in zebrafish **(Stachura et al. 2013)**. Another example of a potentially missing cytokine is *flt3l,* a crucial regulator of myeloid cells and HSCs **(Guermonprez et al. 2013, Jacobsen et al. 2016, Tornack et al. 2017)**, which has so far not been identified in the zebrafish genome, although its receptor is present and expressed **(He et al. 2014, Macaulay et al. 2016, Tang et al. 2017)**.

6. Duplicated erythro-myeloid cytokines in *D. rerio*

This section gives a brief overview of the current knowledge regarding the functional diversification or redundancy of duplicated zebrafish cytokines and their receptors with respect to the erythro-myeloid lineage. Part of this chapter has been included in the review article: **Oltova, J, Svoboda, O & Bartunek, P. Hematopoietic Cytokine Gene Duplication in Zebrafish Erythroid and Myeloid Lineages. Frontiers in Cell and Developmental Biology, 2018.** (10.3389/fcell.2018.00174)

6.1. Kitlga/b

In vertebrates, proliferation and differentiation of erythroid cells is regulated most prominently by two cytokines, erythropoietin (EPO) and Kit ligand (KITLG or stem cell factor, SCF), which ensure erythroid lineage commitment by binding to their cognate receptors, which in turn triggers specific signaling events **(Krantz 1991, Broudy 1997, Panzenbock et al. 1998)**. The proper balance between Epo and Kit signaling is essential to control erythroid progenitor self-renewal and proliferation versus terminal differentiation of erythrocytes **(Wessely et al. 1999, Munugalavadla and Kapur 2005, Dzierzak and Philipsen 2013)**.

KITLG is a pleiotropic cytokine that, besides its role in erythropoiesis, affects a wide range of tissues and cells and it is an important regulator of many processes, both in the adult organism and during the development **(Ding et al. 2012, Lennartsson and Ronnstrand 2012)**. In mammals, KIT signaling has been reported in neurogenesis, pigmentation **(Grabbe et al. 1994, Alexeev and Yoon 2006, Lennartsson and Ronnstrand 2012, Gong et al. 2019)**, as well as erythro-myelopoiesis **(Hayman et al. 1993)** and primordial germ cell development **(De Miguel et al. 2002)**. Two distinct forms naturally occurring *in vivo*, transmembrane and soluble, are associated with different processes. Transmembrane form has been reported in regulation of stem cells in their niches, whereas the soluble form is transported in circulation, and can affect distant tissues **(Ashman 1999, Lennartsson and Ronnstrand 2012)**. Upon binding of the Kit ligand to its cognate receptor, KIT, a receptor tyrosine kinase type-III family member, dimerization and autophosphorylation of the receptor leads to triggering of various signaling cascades, e.g. PI-3K, MAPK, SRC and JAK kinase pathways **(Ashman 1999, Abbaspour Babaei et al. 2016)**.

In teleost, the whole Kit ligand-receptor signalosome has been duplicated, which makes the scenario more complex. The understanding of diversification of the functions of both ligands (Kitlga, Kitlgb) and receptors (Kita, Kitb), including their binding specificities, is essential for future studies. Current available data indicate that both Kit receptor and ligand paralogs have subspecialized during evolution. This is demonstrated by their different tissue specific expression in the development: Kita is expressed in melanocytes and melanoblasts, lateral mesoderm (the location of hematopoietic precursors), and notochord **(Parichy et al. 1999)**. On the other hand, Kitb was detected in neural tube and otic vesicles **(Mellgren and Johnson 2005)**. Moreover, there are also functional differences between the two receptors: *kita* receptor mutants (*kita*$^{b5/b5}$ or *sparse*) exhibit defects in pigmentation **(Parichy et al. 1999)**, whereas *kitb*

has not been associated with melanogenesis so far **(Mellgren and Johnson 2005, Mahony et al. 2018)**. Regarding the ligands, a similar diversification has been observed in gain-of-function studies. Hyperpigmentation phenotype was reported after overexpression of Kitlga **(Hultman et al. 2007)** but so far, no role in pigmentation has been observed for Kitlgb **(Mahony et al. 2018)**. These findings suggest that pigmentation might be controlled specifically by the Kitlga – Kita pair. Interestingly, although the homology of the genomic sequence of zebrafish Kit ligands with their murine counterpart is relatively low, the exon intron structure is remained conserved as showed in **Figure 2** **(Hultman et al. 2007)**

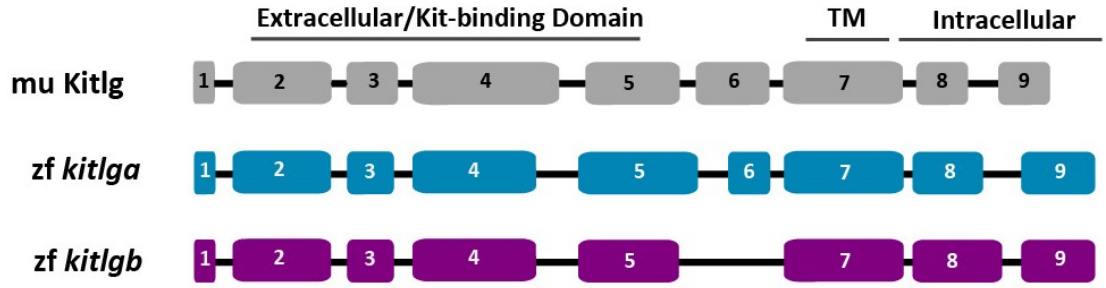

Figure 2 | Genomic structure of duplicated zebrafish *kit* ligands aligned with murine Kitlg. Exons are numbered according to their homology with murine sequence. Although the sequence is quite diverged - zfKitlga 29% identity, 43% similarity and zfKitlgb 20% identity and 50% similarity with the murine coding sequence, the intron-exon locations are conserved. TM – transmembrane domain. **(figure reproduced from Hultman et al. 2007)**

Despite extensive studies, the role of Kit signaling in hematopoiesis of zebrafish has remained unnoticed for a long time. Even though Kit receptors are expressed in hematopoietic tissues **(Parichy et al. 1999, Mahony et al. 2018)**, under steady state conditions hematopoiesis is not affected in the adult *kita*$^{b5/b5}$ (*sparse*) mutants lacking the functional Kita receptor **(Parichy et al. 1999)**. This is in contradiction to the findings in other vertebrate models, where the absence of c-kit leads to severe anemia and is embryonically lethal **(Geissler et al. 1988)**. So far, there are only two reports indicating potential roles of zebrafish Kit signaling in zebrafish hematopoiesis. Mahony et al. observed a mild increase in the number of HSCs after overexpression of Kitlgb **(Mahony et al. 2016)**, and also a decrease in the number of HSCs after downregulation of Kitb **(Mahony et al. 2018)**. The authors concluded that in agreement with previous studies, the role of Kita and Kitlga is likely restricted to melanocyte formation, with no involvement in the process of hematopoiesis.

6.2. Epoa/b

In vertebrates, the major regulator of the development of red blood cells is erythropoietin (EPO), which mediates self-renewal, survival and differentiation of erythroid cells by binding to its cognate receptor, EPOR **(Krantz 1991)**. EPO binding leads to homodimerization of EPOR, which results in autophosphorylation of JAK2 bound to Box1/2, which then phosphorylates other signaling molecules, like STAT5 (signal transducers and activators of transcription), PI-3K (phosphatidylinositol 3-kinase) or MAPK (mitogen-activated protein kinase), as well as the EPO receptor itself **(Drachman and Kaushansky 1997, Constantinescu et al. 1999)**. Two copies of the zebrafish *epo* gene have been previously identified in our laboratory, *epoa* and *epob*. The role of *epoa* seems to be similar to its mammalian orthologue - stimulation of proliferation and differentiation of erythroid cells **(Paffett-Lugassy et al. 2007, Stachura et al. 2011)** but *epob* has not been associated with any hematopoietic process so far (Svoboda O., Bartunek P., *unpublished)* and it is possible that it even formed a pseudogene without any biological function. It was shown that recombinant zebrafish Epoa is able to promote the expansion and differentiation erythroid cells *ex vivo* **(Stachura et al. 2009)** and when combined with other factors (Gcsfa, Tpo), it promotes multilineage erythro-myeloid cell fates in semisolid media **(Stachura et al. 2011, Svoboda et al. 2014)**. For simplicity, I will use the designation Epo/*epo* for Epoa/*epoa* in the whole dissertation. So far, only a single erythropoietin receptor has been identified in zebrafish **(Paffett-Lugassy et al. 2007)**.

6.3. Csf1a/b and IL34

The main regulator of a majority of myeloid cells, such as monocytes, macrophages, dendritic cells, microglia, osteoclast and also Langerhans and Kupffer cells in mammals is the Colony stimulating factor 1 (CSF1, or Macrophage colony-stimulating factor – M-CSF), playing also an important role in disease development **(Hamilton 2008, Hamilton and Achuthan 2013)**. The ligand binds to the CSF1 receptor (CSF1R), a RTKIII family member, which leads to activation of JAK2/STAT5, PI3K and MEK signaling **(Pixley and Stanley 2004, Martinez and Gordon 2014)**. In addition to CSF1, in certain tissues (Langerhans cells and microglia), the receptor can be also activated by IL34 **(Greter et al. 2012, Wang et al. 2012)**.

In zebrafish, also *csf1* have been identified in the form of two paralogs (*csf1a/b*) **(Wang et al. 2008)**. Along with two *csf1* receptors (*csf1ra/b*), this in another relatively unique example of duplication of the whole ligand-receptor signalosome **(Braasch et al. 2006)**. Even though two copies of IL34 have been reported in salmon **(Pagan et al. 2015)**, in zebrafish, only a single copy has been identified so far. Csf1a and Il34 signaling has been associated with microglia development in the retina **(Huang et al. 2012)** as well as pigment pattern formation during development **(Patterson et al. 2014)** (Csf1a only). IL34 has been show to regulate macrophages and microglial precursors **(Kuil et al. 2018, Wu et al. 2018)**. Moreover, *csf1ra* mutant fish (*panther*) display decreased numbers of microglia and macrophages **(Herbomel et al. 1999, Pagan et al. 2015)** but any information about the role of *csf1rb* are missing so far.

6.4. Csf3a/b

Colony stimulating factor 3 (CSF3), also known as Granulocyte colony stimulating factor (G-CSF), is a cytokine essential for survival, proliferation and differentiation of macrophages, monocytes and neutrophils **(Metcalf and Nicola 1983, Nicola et al. 1983, Nicola et al. 1985, Lieschke et al. 1994, Liu et al. 1996)**. Its action is mediated by its receptor, CSF3R. Ligand binding triggers signaling cascades including JAK2/STAT5 and MAPK pathway, crucial for the production of neutrophils both in steady state and under stress conditions **(Touw and van de Geijn 2007)**.

In zebrafish, two paralogs of Csf3 have been reported, whose function are slightly diversified **(Stachura et al. 2013)**, although both paralogs stimulate granulocytic and monocytic/macrophage differentiation, as reported in mammals **(Nicola et al. 1983, Nicola et al. 1985, Migliaccio and Migliaccio 1988)**. However, in zebrafish hematopoiesis, they appear to play a broader role, including the specification and expansion of HSCs. Both paralogs are expressed differentially in the course of development, with *csf3a* expression being low in the early development and rising gradually over time, whereas *csf3b* expression being high from 6 hpf, but decreasing over time. Gain-of-function studies indicate functional redundancy, although changes in binding kinetics to Csf3r receptor have been reported, potentially serving as another mechanism of spatiotemporal control of Csf3a/b activity **(Stachura et al. 2013)**. Although in adult kidney marrow, the main site of hematopoiesis in zebrafish, Csf3b expression was predominant, both ligands retain their ability to trigger differentiation of myeloid progenitors *ex vivo.* It was shown that as in mammals, Csf3 is important for both primitive and definitive waves of

generation of myelo-monocytic cells also in zebrafish **(Stachura et al. 2013)**. Altogether, the results indicate that Csf3 was involved in many different levels of hematopoiesis, but after the diversification of mammals, other specialized cytokines have likely taken over some parts of the original Csf3 function **(Avery et al. 2004, Huising et al. 2006, Stachura et al. 2013)**

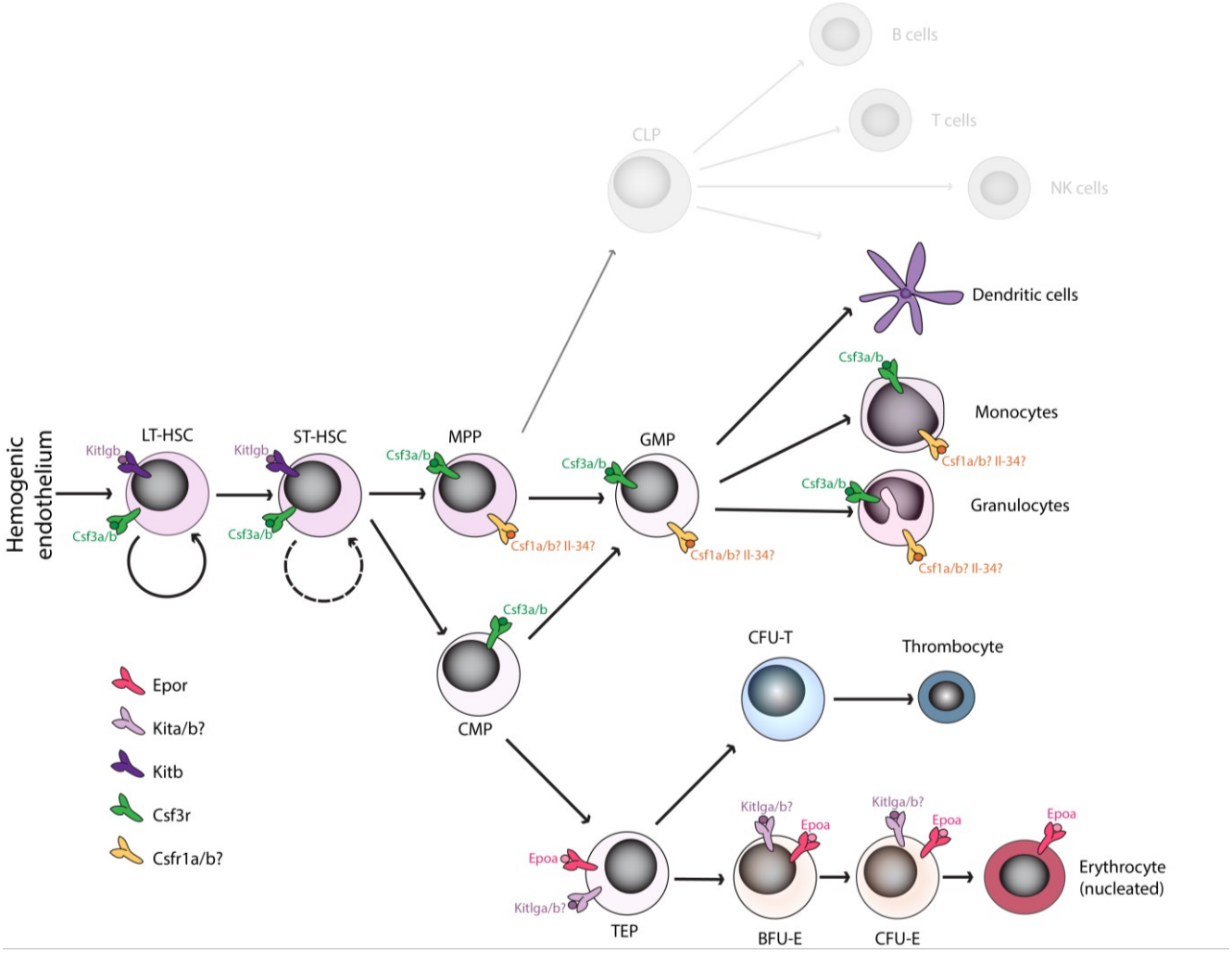

Figure 3 | Overview of duplicated hematopoietic cytokines and receptors regulating the erythro-myeloid lineage in *Danio rerio*. Various cytokine receptors have been proposed to act at the level of hematopoietic stem cells (Kitb, Csf3r), the myeloid lineage (Csf1ra/b, Csf3r), or the erythroid lineage (Epor, Kita/b) in *D. rerio* binding the corresponding ligands. Some duplicated paralogs seem to have lost their function in hematopoiesis (e.g., Epob), whereas other have undergone sub-specialization (e.g. Kitlga/b). The function of missing cytokines (Il-3, Il-5, GM-CSF, Flt3l) is most likely compensated by other factors. LT-HSC, long-term hematopoietic stem cells; ST-HSC, short-term hematopoietic stem cells; MPP, multipotent progenitor cells; GMP, granulocyte-macrophage progenitors; CMP, common myeloid progenitors; TEP, thrombo-erythroid progenitors; BFU-E, burst forming unit-erythroid, CFU-E, colony forming unit-erythroid; CFU-T, colony forming unit-thrombocytic.

7. Zebrafish tracking and reporting

As mentioned earlier, zebrafish is a powerful and popular model organism. The zebrafish community has been growing rapidly and so is the amount of resources in the form of genetically modified fishlines, further accelerated by the rapid development in the field of zebrafish genome editing – especially CRISPR technology **(Ablain et al. 2015, Burger et al. 2015)** and site specific transgenesis **(Mosimann and Zon 2011, Mosimann et al. 2013, Felker and Mosimann 2016)**. Therefore, the proper animal tracking system and organization of animal-related records is more important than ever. A database system that would facilitate tracking of the fish of the F0 and F1 generations of newly created genetically modified lines, as well as the fish stocks of already established lines, would be of great benefit. Without a well-designed tool, this task is both highly laborious and space demanding and requires a high level of organization in the facility.

Notably, in zebrafish inbred lines are not established, as is common in the mouse model. Rather, the animals defined by their backgrounds based on the origin of the founder population and its characteristics (for a list of wild-type backgrounds, see https://zfin.org/action/feature/wildtype-list). The reason is that zebrafish are sensitive to inbreeding depression and therefore require outcrossing preferably every second or third generation **(Monson and Sadler 2010)**, otherwise, substantial issues can arise, including detrimental developmental defects, low productivity and poor survival of the embryos.

Moreover, there is basically no simple way to distinguish fish individuals, unless they possess a distinguishable phenotypic feature caused by their genotype or background. Up to day, there is no cost-effective system designed to distinguish single fish individuals in a tank, and although emerging technologies such as subdermal chipping are developing fast, the technology is not yet sufficiently miniaturized to enable its routine use in tracking small fish species, although some significant advances have been reported using the radio frequency identification microtags **(Cousin et al. 2012)**. The workaround of keeping the fish in solitude or in sexually dimorphic pairs is suboptimal due to social requirements of *D. rerio*, and should be avoided when possible as it is detrimental to the development and health of the animals **(Spence et al. 2008, Alestrom et al. 2019)**, and moreover, it is also very space inefficient. Rather,

zebrafish should be kept within a specified density range, preferably with both males and females present in a single tank **(Castranova et al. 2011, Ribas et al. 2017)**.

According to the 3R's replacement principle **(Russell and Burch 1959, Kirk 2018)** and EU Directive on protection of laboratory animals **(Alestrom et al. 2019)** researches should always prefer the evolutionary lowest animal model relevant for the specific study. Therefore, promoting non-mammalian models and establishing proper conditions for their utilization, tracking and reporting should be of broad interest of the scientific community. Nevertheless, the options available for tracking of zebrafish were rather limited at the time when we started our own facility in 2014. Scientist were using outdated software solutions or simple spreadsheets. One element contributing to the fact was that the requirements for aquatic organism tracking significantly differ from the rodent tracking, wherein systems such as PyRat (https://www.scionics.com/pyrat.html) or open-source JAX Colony Management System **(Donnelly et al. 2010)** have long been established as a standard. In contrast to the individually identifiable rodents, the aquatic animal tracking requires following groups of animals and their rearrangement, as explained earlier, and therefore also a completely different database design.

A handful of solutions designed for fish tracking was available in 2014, either commercial (e.g., www.daniodata.com, www.scionics.com/pyrat_aquatic.html) or open-source **(Anderson et al. 2010, Hensley et al. 2012, Yakulov and Walz 2015)** (http://zebase.bio.purdue.edu, http://aqacs.uoregon.edu/zf/files, https://zebrafish.jimdo.com); however, none of them was predominant in the zebrafish community. This was possibly due to the fact that each of them was tailored to a specific set of requirements but none presented a universal solution that would work well for both small and large zebrafish facilities. The main drawbacks we could identify was the price, which made the commercial databases unsuitable for small or starting facilities on a budget, and dedication to a single platform (e.g. iPad in the case of Danio Data). Even more importantly, the sustainability of both open-source and commercial solutions proved to be limited in long term. This aspect should not be underestimated because switching from one system to another can be very tedious and recovering the whole tracking history can be in some cases even impossible. Finally, a feature which was missing in most of the existing database systems was a simple way to view detailed fish usage statistics that would enable the export of animal reports, which are required by legal authorities.

AIMS OF THE PROJECT

The objective of this project is to reinforce the role of zebrafish as a model for human hematopoiesis using *in vivo* and *ex vivo* approaches. Zebrafish is continuously gaining popularity in the field of blood development, due to the numerous practical advantages it has to offer. Therefore, we believe that by elucidating specific questions about evolutionary conservation of hematopoietic system and providing novel experimental tools and approaches to study it, we can significantly contribute to the field and help to establish the zebrafish as model organism of choice for studying normal and aberrant hematopoiesis.

Specifically, we will focus on these aims:

1. **Investigate the role of zebrafish Kit ligands in hematopoiesis.**
   Kit signaling is crucial for mammalian hematopoiesis but strikingly, no such role has been reported in zebrafish. Using *in vivo* and *ex vivo* approaches, we will investigate the role of the two zebrafish Kit ligand paralogs, especially with respect to erythropoiesis.

2. **Develop new approaches to study hematopoiesis that were previously missing.**
   Although the expansion of erythroid progenitors *ex vivo* has been described in different vertebrates, a similar approach in zebrafish is missing. We believe that establishing proper condition for *ex vivo* suspension culture of kidney marrow cells, together with already available protocols for clonal assay, will provide a set of indispensable tools to study normal and aberrant hematopoiesis.

3. **Provide a novel tool for systematic tracking of the animals.**
   We aim to establish an animal tracking system tailored specifically to small fish species that will enable advanced fish tracking, data visualization and reporting, experiment planning and facility management. We aim to optimize the user interface to be intuitive and providing excellent user experience. Moreover, the system must be compliant with the national legislation and EU directives for the use of vertebrate animals for scientific purposes.

MATERIALS AND METHODS

Animal stocks and embryos

Fish were raised, housed and staged according to zebrafish husbandry recommendations **(Westerfield 2000, Alestrom et al. 2019)**. For animal housing, ZebTEC aquatic system with recirculation (Tecniplast) was used and animals were tracked using our dedicated database solution, Zebrabase **(Oltova et al. 2018)**. For visualization of specific cells types, we used *gata1*:*DsRed* transgenic animals for visualization of erythroid progenitors **(Traver et al. 2003)** and *LCR*:*EGFP* animals, with locus control region upstream of b-globin promoter, for strong and specific erythrocyte visualization **(Ganis et al. 2012)**. Moreover, we used the kita mutant line (*kita*$^{b5/b5}$ or *sparse*), with a 1 nucleotide deletion resulting in a premature stop codon and the absence of the tyrosine kinase domain of the receptor **(Parichy et al. 1999)**, as well as and wild-type animals of the AB background. Here I would like to thank Leonard Zon and David Traver for providing the genetically modified animals.

The experimental and animal care procedures were approved by the Animal Care Committee of the Institute of Molecular Genetics of the Czech Academy of Sciences (13/2016 and 96/2018), in compliance with national and institutional guidelines.

Ex vivo cultures

For isolation of kidney marrow cells, we used 6-month old adult zebrafish animals. We performed the procedure as previously described **(Svoboda et al. 2016)** and plated and cultivated the cells in zfS13 medium (see **Table 1** for composition). The crucial component of the medium is carp serum, which was obtained as described previously **(Svoboda et al. 2016)**. Specific cytokines were added at 100 ng/ml and dexamethasone was added at 1uM final concentration. To ensure optimal growth in suspension, 30% of the medium was exchanged every other day. Cells were counted using a CASY Cell Counter. To study the colony forming capabilities, we also performed assays in semi-solid media, which prevents the movement of single cells and enables colony growth. A detailed protocol was published previously **(Svoboda et al. 2016)**.

Table 1 | Composition of zebrafish S13 medium.

zf S13 medium	**final concentration**
DMEM (Gibco, cat. no. 41966-029)	
Distilled Water (Gibco, cat. no. 15230-089)	
FBS, embryonic-stem-cell qualified (Biosera, cat. no. FB-1001S/500)	10%
Carp Serum	2%
BSA 10% (StemCell Technologies, cat. no. 09300)	0.5%
NaHCO3, 7.5%	0.2%
beta-Mercaptoethanol (Sigma-Aldrich, cat. no. M6250)	0.1 mM
L-Glutamine, 0.2 M (Gibco, cat. no. 25030-081)	4 mM
Hypoxanthine (Sigma-Aldrich, cat. no. H9636)	200mg/100ml
FE-SIH iron supplement, 1000x (Sigma-Aldrich, cat. no. I3153)	
Penicillin-streptomycin, 100× (Gibco, cat. no. 15140122)	
solution A (1000x)	
solution B (50x)	

solution B in water	**final concentration**
L-Methionine	10 mM
L-Phenylalanine	20 mM
L-Alanine	10 mM
Glycine	50 mM
L-Threonine	40 mM
L-Isoleucine	40 mM
L-Proline	10 mM
L-Valine	40 mM
L-Aspartic Acid	10 mM
L-Glutamic Acid	25 mM

solution A in water	**final concentration**
Biotin (Sigma B4639)	0.1%

Generation of recombinant cytokines and cytokine mRNA

The zebrafish Kitlga/b amino acid sequence was first inspected by Phobius tool (http://phobius.sbc.su.se/) to predict protein structure and hydrophobicity. Putative signal peptide (SP) and transmembrane (TM) domains were identified in amino acid positions 1 to 24 and 206 to 224 of Kitlga, and amino acid positions 1 to 31 and 185 to 209 of Kitlgb (see **Figure 4A**).

To produce the soluble form of both Kitlga and Kitlgb, we used sequence specific primers (**Table 2**) for the amplification of cDNA fragments corresponding to amino acid 25 to 182 (Kitlga) and 31 to 187 (Kitlgb) from adult zebrafish retina. To produce recombinant cytokines in sufficient quantities, we used the baculoviral expression system. The amplified fragment was cloned into pAc-GP67-B vector supplemented with 6xHis tag sequence. By cotransfection of pAc-His-Kitlga/b and BaculoGold Bright Baculovirus DNA into sf21 insect cells, we generated the recombinant baculovirus. Infected GFP-positive cells secreted recombinant cytokines into the medium, which were then purified on a Ni2+-NTA agarose column (**Figure 4B**). Plasmids for cytokine expression are available from Addgene with the accession numbers 140292 (pAc-His-zfKitlga), and 140293 (pAc-His-zfKitlgb).

To generate constructs for *in vitro* transcription of *kitlga/b* mRNA for microinjection, we amplified the full length cDNA fragment using sequence specific primers (**Table 2**) and the fragment was cloned into pCS2+ vector. We transcribed mRNAs from the linearized plasmid using the mMessage mMachine SP6 kit (Roche) and purified the transcript by lithium chloride extraction.

Recombinant Epo protein and *epo* mRNA were prepared as described previously **(Paffett-Lugassy et al. 2007, Stachura et al. 2009, Svoboda et al. 2016)**.

Table 2 | Primers for cloning of kit ligands.

	Forward primer	**Reverse primer**
Protein expression		
Kitlga	CGGGATCCATTGAAATAGGAAATCCCAT	GCGGATCCTTACTCATTTGTACTATGTTGCGC
Kitlgb	GCGGATCCGGGAGCCCTTTAACAGATGA	GCGGATCCTTAATGAACCGCAGAGTTCATGCC
mRNA microinjection		
kitlga	GCGGATCCGGTTTCGCTGACATTGGAGT	GCGGATCCTTTGTTCCTGTAGGTTGGGC
kitlgb	GCGGATCCGGAGACACGGCTGATTTGTT	GCGGATCCATCCCGTTCTGGATATTCCC

mRNA microinjections and dexamethasone treatment

Embryos were injected immediately after fertilization, at the 1-cell stage, using 600 pg of each mRNA per embryo. Zebrafish embryos have been kept according to the approved animal care

procedures until reaching 24 hpf. Then, they have been dechorionated using pronase and optionally, treated with 50µM dexamethasone diluted in E3 medium. Treatment has been exchanged every day until 72 hpf.

Benzidine staining and image analysis

72 hpf zebrafish larvae were anesthetized by Tricane (MS-222), while incubated on ice for 5 minutes. The purpose of this procedure is to stop the blood flow gradually before staining to prevent artifacts. Anesthetized larvae were washed with cold PBS and fresh benzidine solution was added immediately (composition: o-dianisidine (Sigma-Aldrich, D9143) (0.6 mg/ml), sodium acetate pH 4.5 (0.01 M), hydrogen peroxide (0.65%) and ethanol (40%)) and incubated for 10 mins in the dark. Staining solution was washed away and larvae were imaged in glycerol.

Imaging and image analysis

For Imaging of benzidine stained larvae, we used Zeiss Axio Zoom.V16 with Plan Neofluar Z 1.0x objective equipped with Zeiss Axiocam 105 mono camera. Z-stacks were processed using the Extended Depth of Focus module in ZEN blue 2.3 software and images were quantified using a custom developed FiJi script (see **Script 1** in the supplement). Images of *gata1:DsRed* larvae were acquired on Zeiss Axio Zoom.V16 with Zeiss Axiocam 506 mono camera and ZEN Blue software.

Images of cells cultured *ex vivo* were acquired on Olympus IX70 inverted microscope equipped with the Olympus DP72 camera using a 20x objective (suspension cultures) and 10x objective (colony assays). Moreover, colony assays were also imaged using Zeiss Axio Zoom.V16 with Plan Neofluar Z 1.0x objective and Zeiss Axiocam 506 mono camera and analyzed automatically using custom developed FiJi script (see **Script 2** in the supplement).

FACS Sorting of embryos and RNA isolation

We treated the embryos at 24 hpf, 48 hpf and 72 hpf with 100x diluted Liberase TM (Roche, 05401119001) in PBS. Samples were incubated at 37°C for 1, 1.5 or 2.5 hours, respectively for each stage. We filtered cell suspension using a 30um filter, centrifuged and resuspended in

PBS. We collected sorted cells into TRI Reagent (Sigma, T3934). RNA was isolated with RNeasy Plus Mini Kit (Qiagen, 74136).

Isolation of RNA from whole embryos and tissues and qPCR

We isolated RNA from whole injected or uninjected embryos or tissues using PureLink Micro Kit (Invitrogen, 12183-016), following the manufacturer's instruction, including DNase I treatment. cDNA was synthesized using iScript™ cDNA Synthesis Kit (Bio-Rad). We run qPCR in triplicates on a LightCycler 480 machine using SYBR Green I (Roche). For normalization of the RNA content we used *ef1a* and *mob4* housekeeping genes and we calculated the relative expression levels using the ΔΔCt method. The list of qPCR primers is in **Table 3.**

Table 3 | Primers of qPCR analysis.

	Forward primer	**Reverse primer**
gata1a	GTTTACGGCCCTTCTCCACA	CACATTCACGAGCCTCAGGT
hbbe1	CTTGACCATCGTTGTTG	GATGAATTTCTGGAAAGC
kita	CTATGTTGTCAAAGGCAATGCT	CCAGACGTCACTCTCAAAGGT
kitb	GGATACAGAATGAGTGAGCCTGA	CTCCAGCACCATCTCATCAC
efa1	GAGAAGTTCGAGAAGGAAGC	CGTAGTATTTGCTGGTCTCG
mob4	CACCCGTTTCGTGATGAAGTACAA	GTTAAGCAGGATTTACAATGGAG

RNAseq and transcriptomics

We isolated total RNA from 6-7×10^6 kidney marrow cells cultivated either in the presence of **Epo, Dex** or **Epo, Dex, Kitlga** in biological duplicates using Purelink Micro kit (Invitrogen). We assessed the quantity of isolated RNA on NanoDrop ND 1000 (Thermo Fisher Scientific) and analyzed its integrity on Agilent 2100 Bioanalyser (Agilent Technologies). The RNA integrity number ranged between 9.5 and 10. Samples were sequence on Illumina NextSeq® 500 instrument using 75bp single-end configuration yielding on average 47 million reads per sample.

The criterion for differentially expressed genes was statistical significance (adjusted p-value) of <0.1 and minimal absolute log2-fold change value of -2.32 (for the genes that were downregulated in Epo, Dex, Kitla treatment) or 1 (for the genes that were upregulated in Epo, Dex, Kitla treatment). These candidates were further analyzed and visualized. Next, gene

ontology (GO) enrichment was analyzed for the up and down regulated genes fulfilling the criteria of log2-fold change > 0.415 and adjusted p-value < 0.1. GO terms with the cutoff of log2-fold change > 0.3 and p<0.0001 sorted by Odds ratio are shown in the **Supplementary Table 3**. For more details on the library preparation, library size distribution, and bioinformatical pipeline used for data processing, please, refer to the supplemental information of the submitted manuscript: **Oltova, J, Svoboda, O, Machonova, O, Svatonova, P, Traver, D, Kolar, M, Bartunek, P. Zebrafish Kit ligands cooperate with erythropoietin to promote erythroid cell expansion, Blood Advances, 2020** (preprint version available online: 10.1101/2020.02.03.931634)

RNAseq data were uploaded to ArrayExpress under accession number E-MTAB-8800.

Database development and architecture

Zebrabase is a cross-platform web application (Windows, Mac OS, Android, iOS, Linux-based systems) that works in all modern internet browser. We create a dedicated PostgreSQL database (https://www.postgresql.org/) for every Zebrabase customer (e.g. facility or laboratory) to ensure high data separation, security and consistency. The application back-end is using Python programming language (https://www.python.org/) with the Django web framework (https://www.djangoproject.com/) that ensures data exchange between the database and web browser. On the other hand, front-end part of the application is utilizing the latest HTML5/CSS3 and Bootstrap framework for high responsibility, interactivity and data visualization.

Communication of the users with the Zebrabase system is secured by SSL connection. Database dumps are created every day and stored for 6 months. The system is operated with utmost effort to ensure service availability – virtual server environment used to run the system consists of two clusters of hardware servers in different data centers of the Institute of Molecular Genetics and the system is replicated from the primary to secondary cluster twice per hour, so that the service can be restored in case the primary cluster becomes unavailable.

For more details on database development and system architecture, please, refer to the publication: **Oltova, J*, Jindrich, J*, Skuta, C, Svoboda, O, Machonova, O & Bartunek, P. Zebrabase: An Intuitive Tracking Solution for Aquatic Model Organisms. Zebrafish, 2018, 15: 642-647** (10.1089/zeb.2018.1609)

RESULTS

1. The role of Zebrafish Kit ligands in hematopoiesis in D. rerio

Results presented in this chapter have been included in the submitted manuscript : **Oltova, J, Svoboda, O, Machonova, O, Svatonova, P, Traver, D, Kolar, M, Bartunek, P. Zebrafish Kit ligands cooperate with erythropoietin to promote erythroid cell expansion, Blood Advances, 2020** (preprint version is available on bioRxiv: 10.1101/2020.02.03.931634)

1.1. Cytokine expression

First, we cloned and expressed zebrafish Kit ligands, to obtain the recombinant proteins to use in *ex vivo* assays. Using sequence specific primers, we amplified the mature form of zebrafish *kitlga* and *kitlgb* from adult retina. As shown in **(Figure 4A)**, the amplified region was devoid of signal-peptide, intracellular and transmembrane region. The amplified fragment was cloned into baculoviral expression vector to produce the soluble form of recombinant Kitlga and Kitlgb using the sf21 insect cells **(Figure 4B)**.

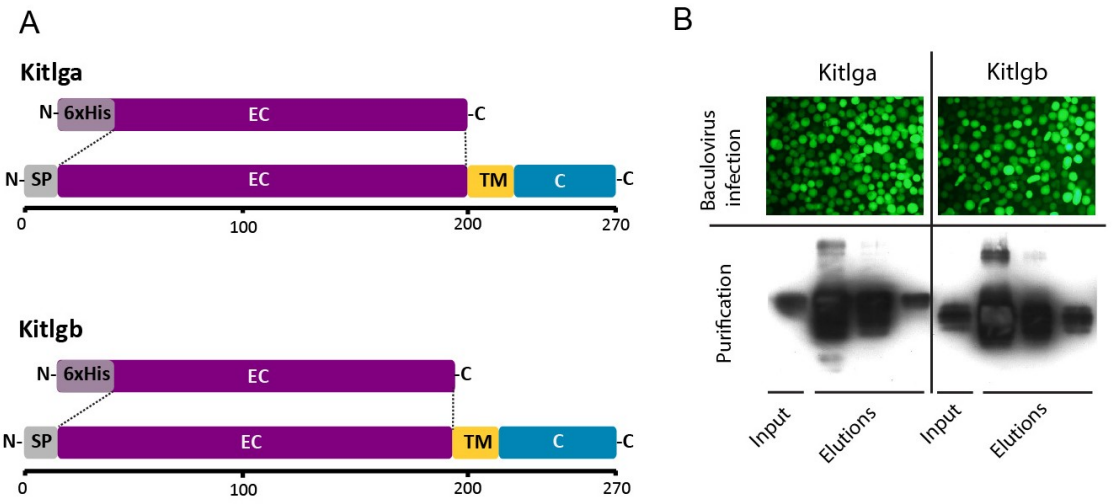

Figure 4 | Cloning and expression of zebrafish Kitlga and Kitlgb. (A) Sequence encoding the mature extracellular form of each of the Kit ligands was amplified using RT-PCR from adult zebrafish retina and cloned into pAc-GP67-B vector to generate recombinant His-tagged Kitlga and Kitlgb proteins. SP - signaling peptide, EC – extracellular part, TM – transmembrane domain, C – cytosolic part, 6xHis - 6x histidine tag. (B) sf21 insect cells were co-transfected with BaculoGold Bright DNA (BD Biosciences) and Kitlga/b transfer vector. Virus-infected cells were GFP-positive (top). Recombinant proteins were secreted from infected cells, purified using affinity chromatography and detected using anti-His antibody (bottom). This figure has been reproduced from the submitted manuscript **(Oltova et al., 2020)**.

In the following *ex vivo* experiments, we used these His-tagged purified proteins. For mRNA injections, we amplified the full-length cDNA fragment using sequence specific primers **(Table 2)** and cloned it into pCS2+ vector. Epo protein and mRNA have been prepared according to previously published studies **(Paffett-Lugassy et al. 2007, Stachura et al. 2009, Svoboda et al. 2016)**.

1.2. The effect of Kit ligands on zebrafish kidney marrow cells

With the purpose of testing the biological activity of recombinant Kit ligands, we isolated kidney marrow cells from adult zebrafish as described previously **(Svoboda et al. 2016)** and treated the cells with various cytokines, or their combination, and subsequently counted them at specific time points. The potential enhancement in the myeloid lineage was assessed after 3 days in culture. We added both Kit ligands, either separately or combined with Gcsfa, which has been previously shown to support myeloid cell fate **(Stachura et al. 2013)**, and we also tested Gcsfa alone. In all conditions, we observed an increase in cell number compared to untreated control, however, only Gcsfa boosted the growth of kidney marrow cells significantly and the effect was further potentiated by the addition of either of the Kit ligands. The Kit ligands alone exhibited mild activity, which was reproducible but statistically not significant (**Figure 5A**).

Furthermore, Kit ligands were tested for their role in erythroid cell expansion. Cells were treated with each of the two Kit ligands, either separately or combined with Epo. The number of cells was quantified after 7 days in culture. In agreement with previous studies, Epo alone was able to boost the growth significantly **(Paffett-Lugassy et al. 2007, Stachura et al. 2009)**, and again, we noticed a mild increase in the number of cells when treated with any of the Kit ligands alone. Interestingly, when we combined Epo with Kitlga, the number of cells was significantly higher than in Epo alone, implying cooperation of the two factors exceeding the level of a simple additive effect (**Figure 5B**). Taken together, our results showed that zebrafish Kit ligands are able to promote the growth of erythroid and myeloid cells *ex vivo*.

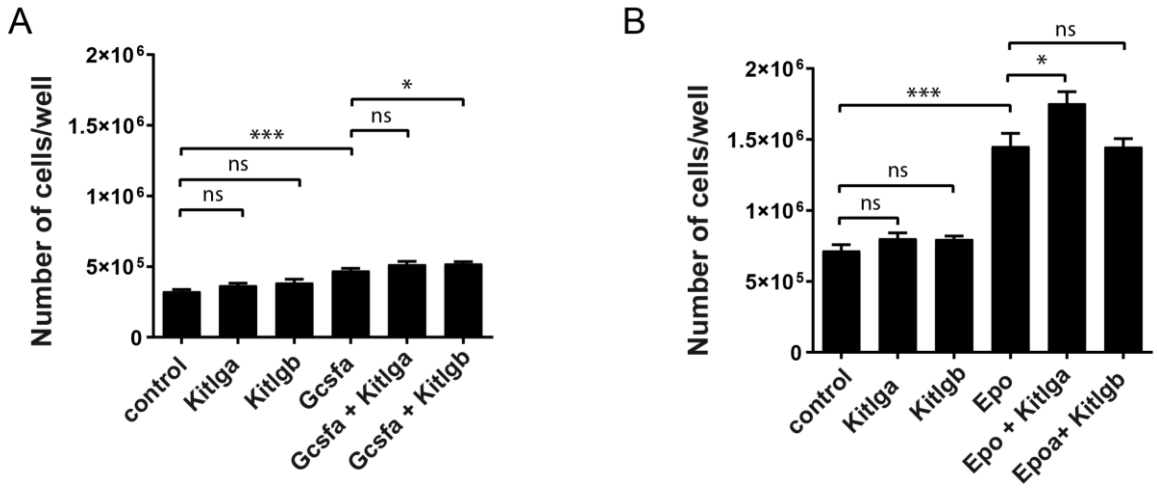

Figure 5 | The effect of Kitlga and Kitlgb on erythroid and myeloid expansion of zebrafish kidney marrow cells. Quantification of the number of kidney marrow cells after treatment with PBS (control) or specific cytokines for 3 days (A) and 7 days (B). Statistical significance was determined using standard one-way ANOVA. This figure has been reproduced from the submitted manuscript **(Oltova et al., 2020)**.

Our next aim was to maximize the expansion of erythroid progenitors from kidney marrow cells. As a starting point, we took the Epo + Kitlga combination that was the most potent in the previous experiments and tested the addition of other factors in the culture of kidney marrow cells isolated from *gata1:DsRed* transgenic animals. Although no reports of the suspension culture of kidney marrow cells in zebrafish was reported previously, we hypothesized that conditions functional in other vertebrates could be effective in zebrafish as well **(Panzenbock et al. 1998, Kolbus et al. 2003)**. As the addition of particular steroids was associated with self-renewal and proliferation of erythroid progenitors in other vertebrates **(Schroeder et al. 1993, Kolbus et al. 2003, Leberbauer et al. 2005, England et al. 2011)**, we included dexamethasone as one of the factors. In agreement with previous findings in vertebrates, Kitlga, Epo and Dex acted synergistically in *ex vivo* cultures, promoting erythroid expansion of kidney marrow cells (**Figure 6A**). Moreover, cells treated with Epo, Dex and Kitlga formed islets of round, highly *gata1:DsRed*-positive cells, corresponding to erythroid progenitors (**Figure 6B**).

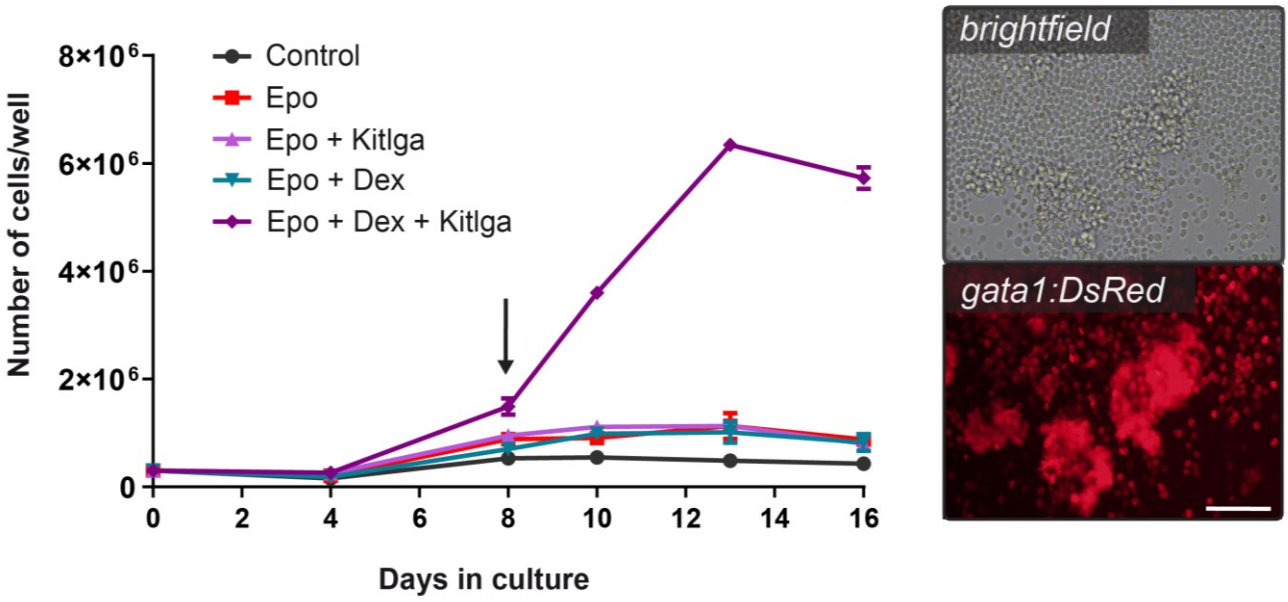

Figure 6 | Optimizing culture conditions for erythroid cell expansion of zebrafish kidney marrow cells. Left - Growth curve for *ex vivo* culture of whole kidney marrow cells with different cytokine combinations. Each point represents a mean of a biological duplicate with SD. Right - Representative images of whole kidney marrow cells isolated from transgenic *gata1:DsRed* fish treated with PBS (control) or a specific cytokines and cultivated for 8 days. Scale bar represents 100 um. This figure has been reproduced from the submitted manuscript **(Oltova et al., 2020)**.

Also in colony forming assays, we observed that Epo can cooperate with Kitlga to promote the growth of large erythroid colonies (**Figure 7A**). When Kitlga was combined with Epo, we observed significantly more, highly *gata1*:*DsRed*-positive colonies that were also noticeably larger, compared to those growing in Epo alone (**Figure 7B**, **C**). However, neither in liquid cultures nor semisolid media, we observed a similar cooperation of Epo with Kitlgb (data not shown).

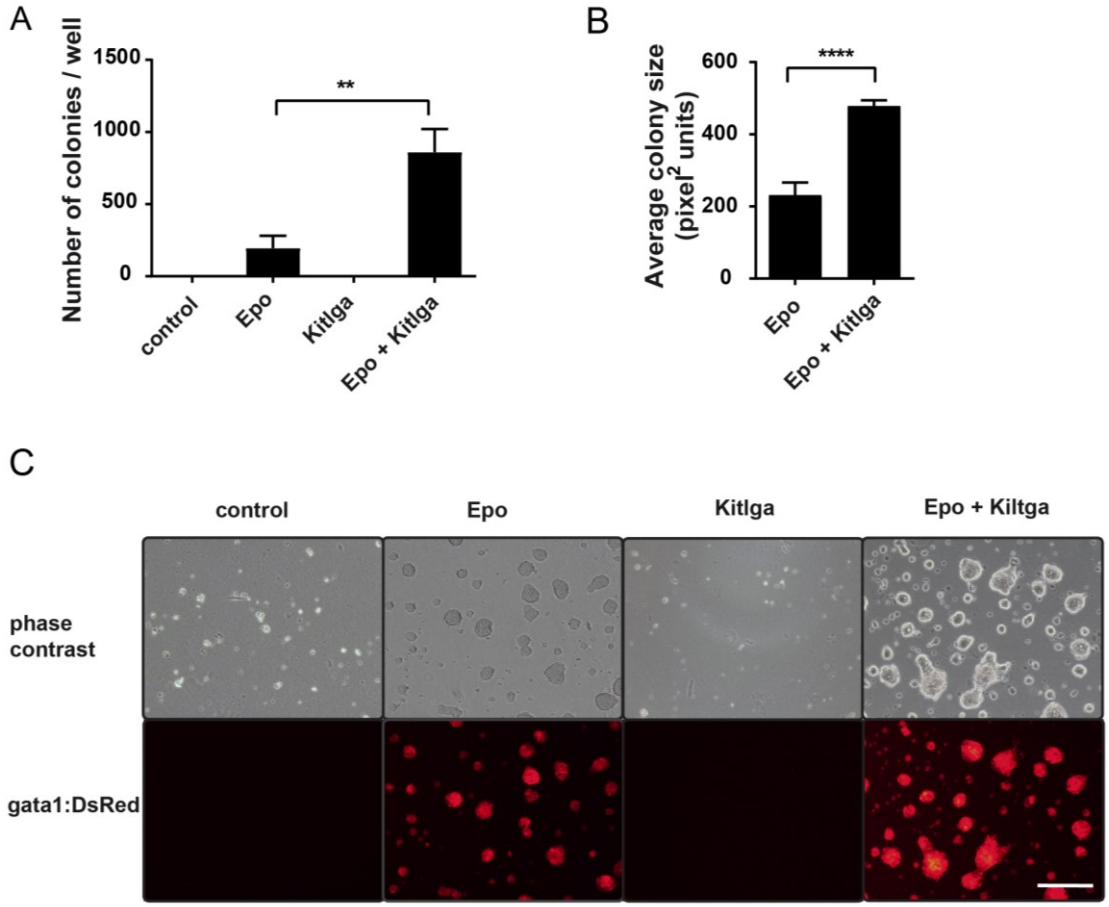

Figure 7 | Cooperation of Kiltga with Epo in colony forming assays. (A) Quantification of the number of colonies formed from kidney marrow cells plated in semisolid media after the treatment with PBS (control) or specific cytokines for 7 days. Each condition was counted in three separate wells from images acquired on Zeiss Axio Zoom.V16. Each bar represents mean with SD. Statistical significance was determined by one-way ANOVA. (B) Quantification of the size of the colonies in (A). Each bar represents a triplicate mean with SD. Statistical significance has been determined by t-test.(C) Representative brightfield (top) and *gata1:DsRed* fluorescence (bottom) images of gata1:DsRed positive colonies for each cytokine and their combination. Images were acquired on Olympus IX70 inverted microscope. Scale bar represents 200 um. This figure has been reproduced from the submitted manuscript **(Oltova et al., 2020)**.

1.3. The mechanism of erythroid expansion *ex vivo*

With the aim to gain better understanding of the mechanism of Kitlga cooperation with the other factors, we performed an RNAseq experiment, comparing **Epo, Dex, Kitlga**-treated cells that were reaching the first point of substantial expansion after 8 days in culture, to **Epo, Dex**-treated cells. Our goal was to see what are the early changes in response to Kitlga, that could help us clarify the erythroid expansion later (see the arrow in **Figure 6A**, **left**). The analysis

revealed that in both culture conditions, erythroid hallmarks are prominent (data not shown) but the addition of Kitlga to Epo and Dex caused an additional increase in the erythroid gene expression. We identified several erythroid (*g6fl*, *lias*) and cell cycle (*cdc27*) specific genes among the upregulated differentially expressed genes (**Figure 8D** and **Supplementary Table 1**), confirming additional erythroid cell expansion when Epo and Dex were combined with Kitlga. Downregulated genes, on the other hand, were mostly associated with myeloid cell fate (e.g. *pigrl2*.3, *blnk*, *nfkbiz*, *alox5a*, *inpp5d*). These data indicate that the expansion induced by **Epo, Dex, Kitlga** led to an erythroid-enriched cell population compared to **Epo, Dex** culture alone, which exhibited slightly more myeloid character.

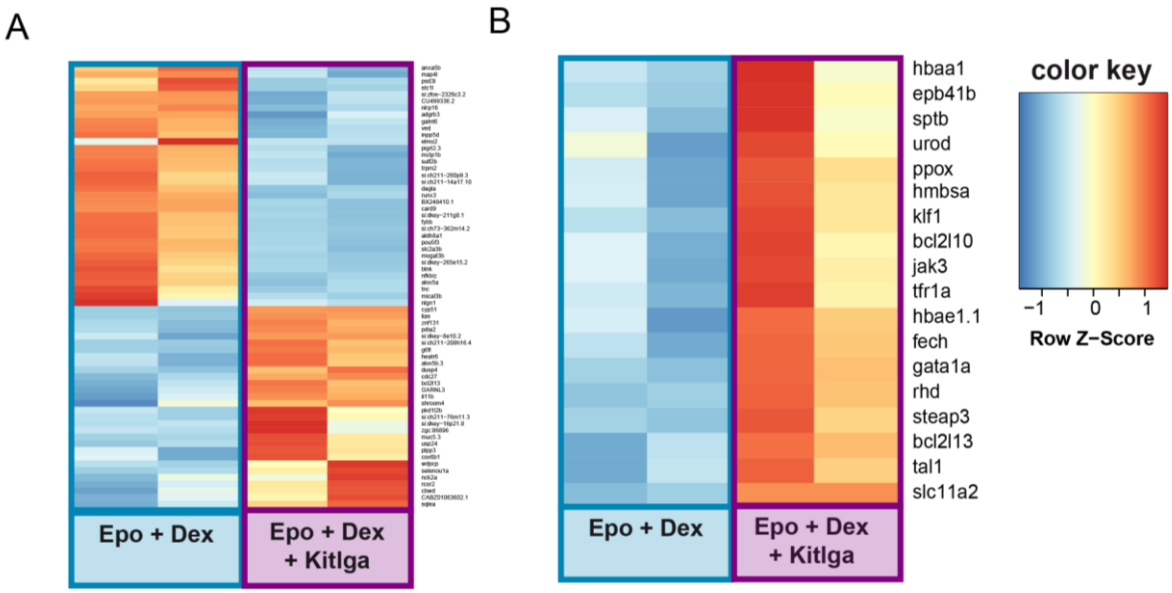

Figure 8 | RNA sequencing data showing differences between Epo, Dex, Kitlga- and Epo, Dex-treated cells after 8 days in liquid culture. An expression heatmap of Epo, Dex- and Epo, Dex, Kitlga-treated cells showing the top predicted differentially expressed genes (A) and representative markers of erythroid differentiation (B). Color coding by z-score for heatmaps in A and B. This figure has been reproduced from the submitted manuscript **(Oltova et al., 2020)**.

Finally, we analyzed separately changes in expression of erythroid genes and revealed that, compared to cells treated with **Epo, Dex**, cells treated with all three factors exhibited an increase in expression of many of the erythroid genes, namely globin genes (*hbae1.1*, *hbaa1*), genes involved in heme and iron metabolism (e.g. *urod*, *slc11a2*, *steap3*), erythroid cytoskeleton (e.g. *rhd*, *sptb*, *eph41b*) and signaling (*gata1a*, *jak3*) (**Figure 8B, Supplementary Table 2)**. Based on Gene Ontology terms prediction, we revealed categories enriched in

upregulated genes, that were associated with translation (GO:0006412, GO:0002181, GO:0000028, GO:0000027), erythropoiesis (GO:0042541, GO:0030218, GO:0048821) and cell cycle regulation (GO:0051726). For a full list of enriched GO terms in all three standard GO term categories, please, refer to **Supplementary Table 3**. Interestingly, when we examined the expression of both *kit* receptors, the expression of *kita* was predominant both in the **Epo, Dex** and **Epo, Dex, Kitlga** samples, whereas *kitb* expression was almost negligible.

1.4. The role of Kit ligands in vivo

Next, we microinjected cytokine mRNA(s) into 1-cell stage embryos, to test the function of both Kit ligands *in vivo*. When combined with *epo*, both *kitlga* and *kitlgb* lead to an increase in number of *gata1*:*DsRed*-positive cells (**Figure 9A**) and enhanced hemoglobinization at 72 hpf, visualized by the whole mount benzidine staining. Also, in agreement with previous studies, we noticed an increase in pigmentation in embryos injected with *kitlga* mRNA (**Figure 9B**).

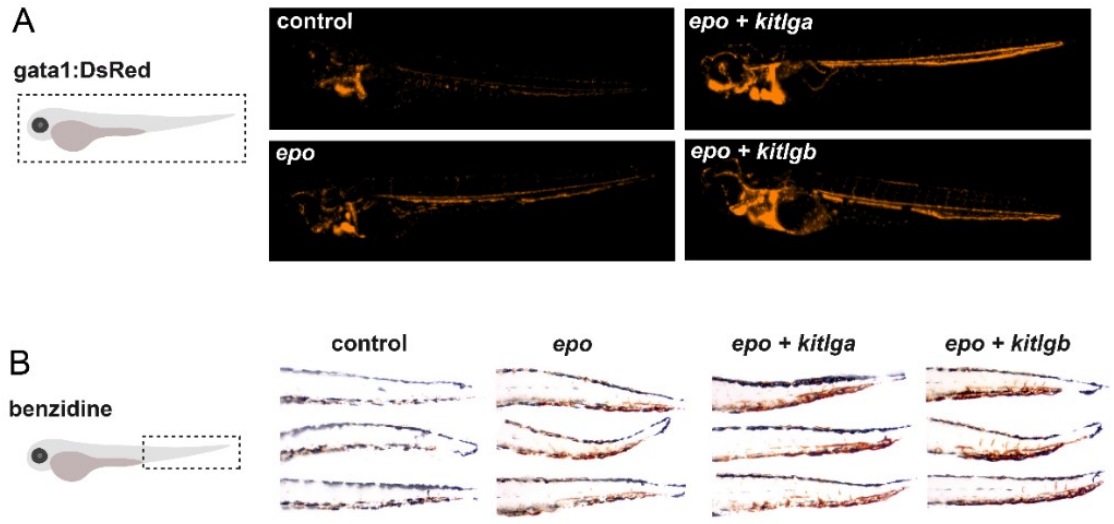

Figure 9 | In vivo effects of *kitlga* and *kitlgb* at 72 hpf. (A) Representative images of 72 hpf *gata1:DsRed*+ transgenic reporter larvae after injection of corresponding mRNAs. Control represents uninjected larvae. Images were acquired on Zeiss Axio Zoom.V16. (B) Representative images of benzidine stained tails of larvae at 72 hpf after the injection of corresponding mRNAs. Control represents uninjected embryos. Note the increase in pigmentation in *epo*, *kitlga*-injected embryos. Z-stacks were acquired on Zeiss Axio Zoom.V16 and processed using Extended Depth of Focus module (ZEN blue software). This figure has been reproduced from the submitted manuscript **(Oltova et al., 2020)**.

Furthermore, we performed an automated image analysis using a custom developed script for Fiji and quantified the differences in benzidine staining, which confirmed the observed trend. Moreover, also in quantitative PCR (qPCR) analysis from whole injected embryos there was a subtle increase in the expression of erythroid markers at 72 hpf (**Figure 9D**) when *epo* was combined with either of the ligands. In a following experiment, we combined mRNA microinjection with *in vivo* dexamethasone (Dex) treatment and we could observe that Dex could further enhance hemoglobinization, although the effect was rather subtle.

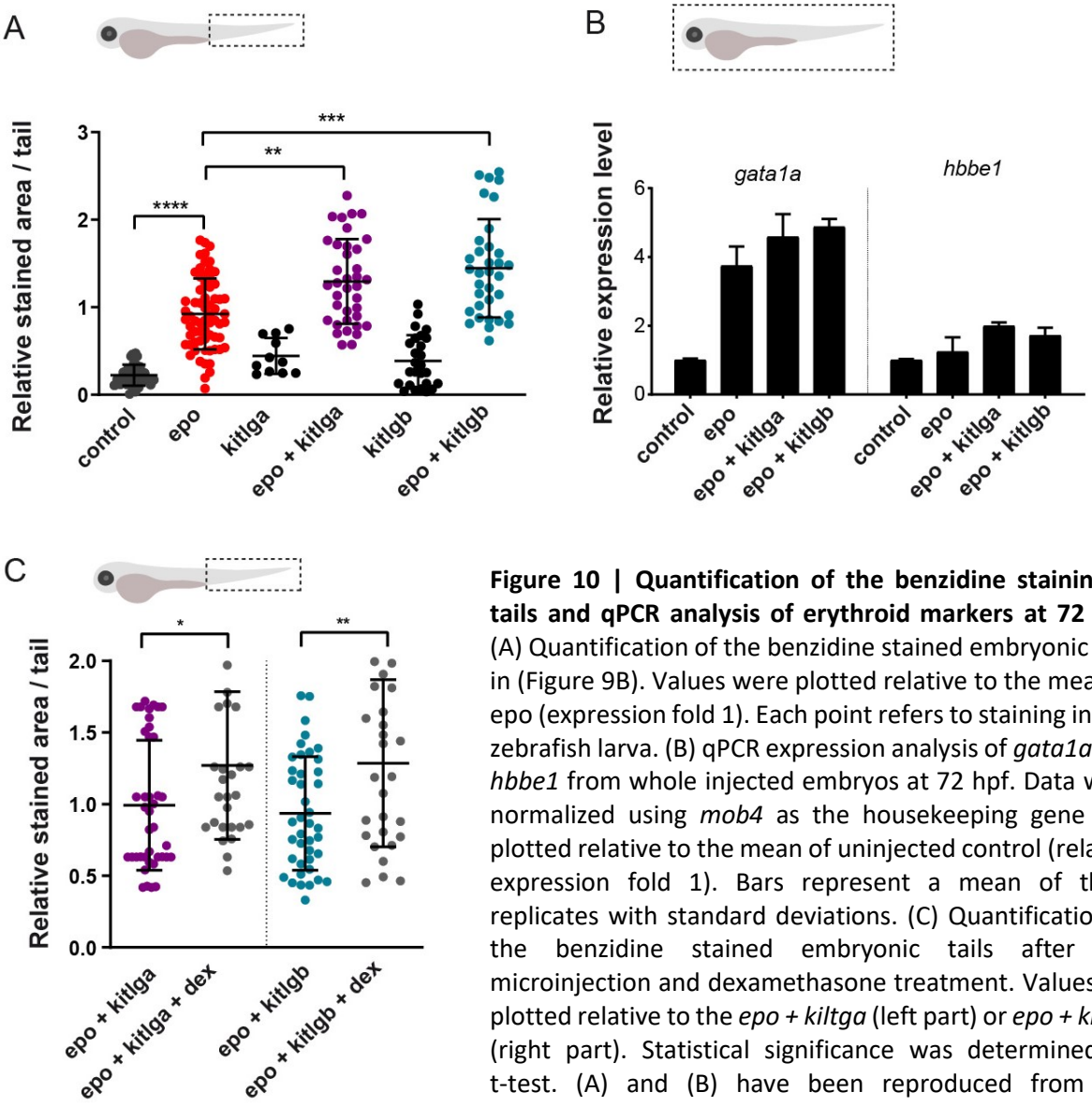

Figure 10 | Quantification of the benzidine staining in tails and qPCR analysis of erythroid markers at 72 hpf. (A) Quantification of the benzidine stained embryonic tails in (Figure 9B). Values were plotted relative to the mean of epo (expression fold 1). Each point refers to staining in one zebrafish larva. (B) qPCR expression analysis of *gata1a* and *hbbe1* from whole injected embryos at 72 hpf. Data were normalized using *mob4* as the housekeeping gene and plotted relative to the mean of uninjected control (relative expression fold 1). Bars represent a mean of three replicates with standard deviations. (C) Quantification of the benzidine stained embryonic tails after the microinjection and dexamethasone treatment. Values are plotted relative to the *epo + kiltga* (left part) or *epo + kitlgb* (right part). Statistical significance was determined by t-test. (A) and (B) have been reproduced from the submitted manuscript **(Oltova et al., 2020)**.

1.5. Spatiotemporal expression of kita and kitb

With the aim to investigate the mechanism of cooperation of *epo* with *kit* ligands, we used qPCR to analyze the expression of both kit receptors in tissues and during the development. In tissues, we could observe the highest *kita* expression in kidney, the major site of definitive hematopoiesis, (**Figure 11A**) and the highest *kitb* expression in retina (**Figure 11B**). In the course of embryonic development, the expression of both kit receptors was gradually increasing with the highest level at 7 dpf (*kita*) and 72 hpf (*kitb*), respectively.

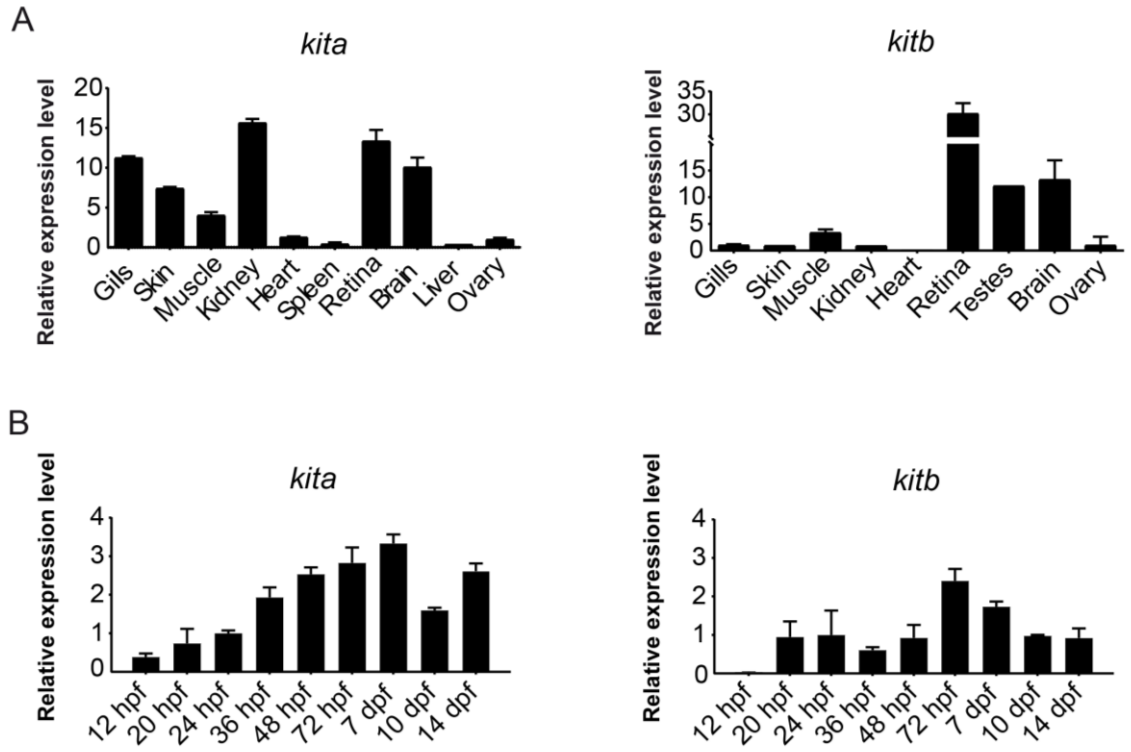

Figure 11 | Expression of zebrafish kit receptors. (A) qPCR expression analysis of *kita* (left) and *kitb* (right) in various adult tissues. Data was normalized using *ef1a* as the housekeeping gene and using the ovary sample as relative expression fold 1. (B) qPCR expression analysis of *kita* (left) and *kitb* (right) during development. Data was normalized using *ef1a* as the housekeeping gene and using the ovary sample as relative expression fold 1. This figure has been reproduced from the submitted manuscript **(Oltova et al., 2020)**.

Based on the *ex vivo* erythroid expansion of *gata1:DsRed*+ cells from adult animals, we next analyzed the receptor expression in erythroid cells in the development. We FACS-sorted *gata1:DsRed*+ cells corresponding mostly to erythroid progenitors and erythrocytes (**Figure 12A**) and *LCR:EGFP*+ (b-globin reporter) corresponding mostly to erythrocytes (**Figure 12B**) from transgenic embryos at three developmental stages. Interestingly, we could observe a gradual increase in the expression of both receptors in the course of development (**Figure 12**).

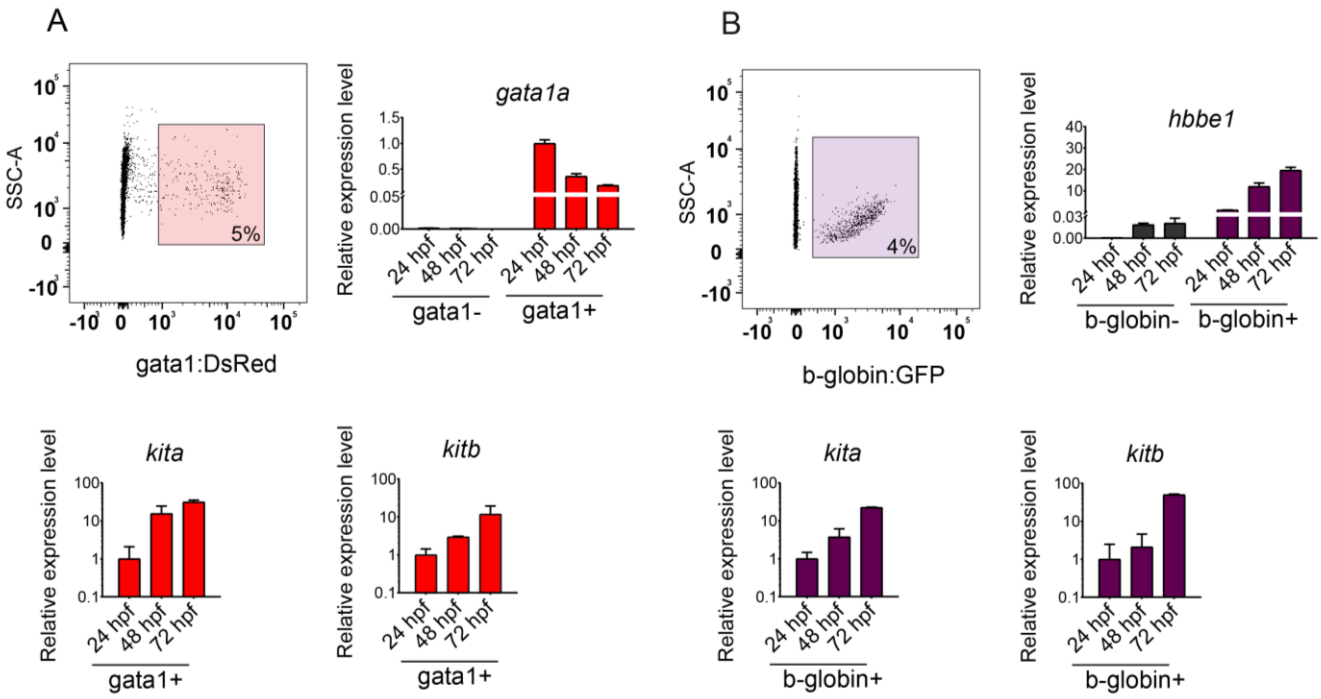

Figure 12 | Expression of *kita* and *kitb* in erythroid development. (A) FACS-sorting of *gata1:DsRed*-positive cells from transgenic embryos at 24 hpf (to left). qPCR analysis of *gata1a* (top right], kita (bottom left) and kitb (bottom right) expression. (B) FACS-sorting of *LCR:EGFP*-positive cells (expressing b-globin) from transgenic embryos at 24 hpf (to left). qPCR analysis of *gata1a* (top right), kita (bottom left) and kitb (bottom right) expression. (A, B) Data was normalized using *ef1a* as a housekeeping gene and 24hpf DsRed+ or EGFP+ positive sample as the relative expression fold 1. This figure has been reproduced from the submitted manuscript **(Oltova et al., 2020)**.

1.6. The role of Kita receptor in erythroid expansion

Finally, we wanted to investigate the mechanism of the erythroid expansion effect we observed when *epo* was combined with *kit* ligands. For that purpose, we used *sparse* mutant fish (*kita*$^{b5/b5}$) lacking the functional Kita receptor. When we injected *epo* together with either of the kit ligands, we failed to observe the cooperation like we have seen previously in wild-type animals, suggesting that Kita is required for Kitlg-dependent erythroid expansion *in vivo*. Moreover, also qPCR from whole embryos using erythroid marker genes *gata1a* and

hbbe1 did not reveal any cooperation of *epo* and any of the kit ligands in *sparse* mutants (**Figure 13B**). Interestingly, we noticed a slight decrease in the number of erythrocytes in mutant uninjected control compared to wild-type uninjected control (data not shown). However, the effect of *epo* mRNA alone remained on a similar relative level as in wild-type embryos (**Figure 13A**).

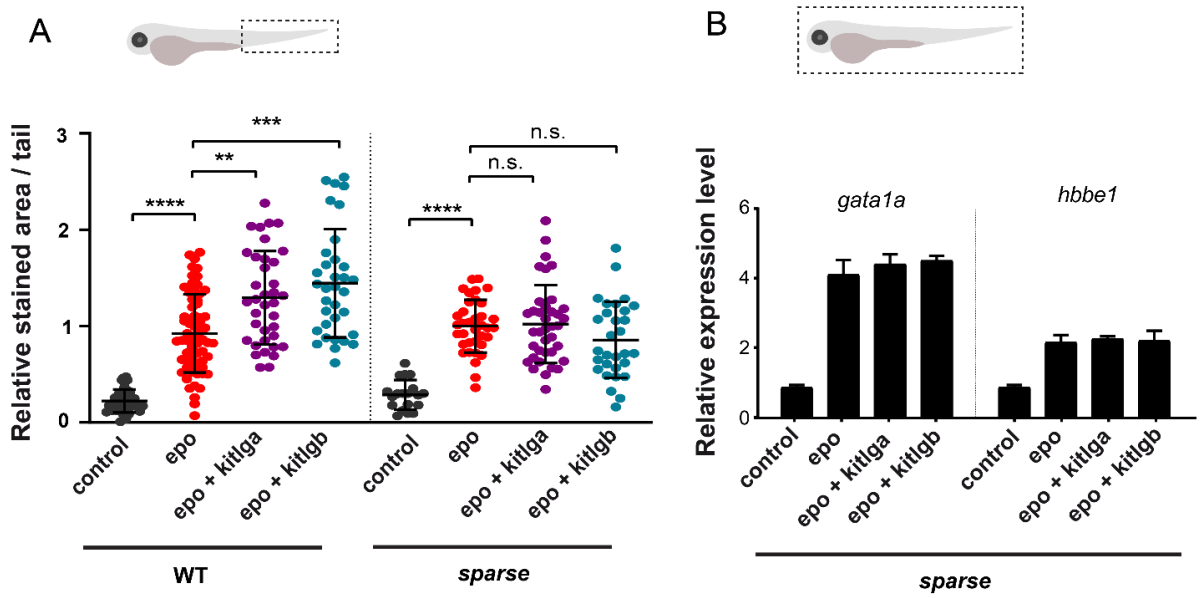

Figure 13 | The effect of kit ligands in *sparse* mutants. (A) Benzidine staining quantified in uninjected control or injected wild-type or sparse embryos. Values are plotted relatively to the mean of epo samples, which corresponds to 1. Note that for demonstrative purposes, part A, left is reused from **Figure 10**. (B) The expression of *gata1a* and *hbbe1* in whole injected embryos analyzed by qPCR using mob4 as a housekeeping gene and the mean of uninjected control as the relative expression fold 1. Bars represent mean of three replicates with SD. This figure has been reproduced from the submitted manuscript **(Oltova et al., 2020)**.

Summary

We cloned and expressed both paralogs of the zebrafish Kit ligand, either in the soluble form for *ex vivo* assays or in full-length form for *in vivo* mRNA microinjection. We tested various cytokines in the culture of kidney marrow cells using the purified recombinant cytokines and established an optimal factor combination consisting of Epo, Kitlga and dexamethasone. Moreover, in gain-of-function experiments we revealed that both *kitlga* and *kitlgb* cooperate with *epo* to increase the number of erythroid cells in zebrafish larvae. Finally, using the *kita*$^{b5/b5}$ (*sparse*) mutants, we showed that Kitlg-dependent erythroid expansion *in vivo* is mediated by the Kita receptor.

2. A novel tracking solution for aquatic model organisms

Part of the results presented in this chapter were included in the manuscript: **Oltova, J, Jindrich, J, Skuta, C, Svoboda, O, Machonova, O & Bartunek, P. Zebrabase: An Intuitive Tracking Solution for Aquatic Model Organisms. Zebrafish, 2018, 15: 642-647** (10.1089/zeb.2018.1609). Zebrabase is continuously developed and new features are added with every release. For more information about the current version, please visit zebrabase.org. For testing of the database demo, please visit public.zebrabase.org.

2.1. Origins of the project (preface)

Shortly after I started my Ph.D. studies, our animal facility significantly expanded, and also the number of genetically modified animals we had to track was gradually increasing. Therefore, it became obvious that a proper tracking system that would allow browsing the animals stocks, filtering, and searching was essential to manage our facility data. Due to lack of any other solution that would fulfill our requirements, we decided to design one on our own, with the help of the skilled database developers at CZ-OPENSCREEN. Although we originally had no intention to develop Zebrabase as a community tool, soon we were asked by a number of our collaborators and colleagues to provide the service to their facilities. Being convinced by their interest that a tool like Zebrabase is really needed in the community, we built an interdisciplinary team of zebrafish researchers, programmers, database developers and web designers, which is able to react to the dynamically evolving needs of the zebrafish community and the legal requirements associated with the use of this model (EU directives, FELASA guidelines and recommendations). From version 2.0, Zebrabase is available for any external scientific institution or non-profit organization via our website (https://zebrabase.org/contact). As our initial idea was to help promote and establish zebrafish as a model organism, small and starting facilities can use Zebrabase completely free of charge.

The following chapters will relate to the current version of the software at the time when I was writing this dissertation (Zebrabase 2.7.5).

2.2. General concept and basic operation principles

Zebrabase is a web-based solution developed specifically for tracking of aquatic animals. It is cross-platform (accessed via web browser), supporting both desktop and mobile use on Windows, Mac, Linux, Android and iOS. The access to the database is ensured via an optimized interface that enables browsing, creating and editing fish stock records. One of the features of Zebrabase is a built-in QR code generator and reader functionality that can help to streamline the workflow significantly, especially in larger facilities. Zebrabase provides a tracking platform to follow the animals from birth to death, and to store detailed records about all fish stocks. Every action performed in the software creates a record in the database that can be later used for reporting purposes. Optimization for touch devices has been included to all main parts of the database including the homepage (**Figure 14**).

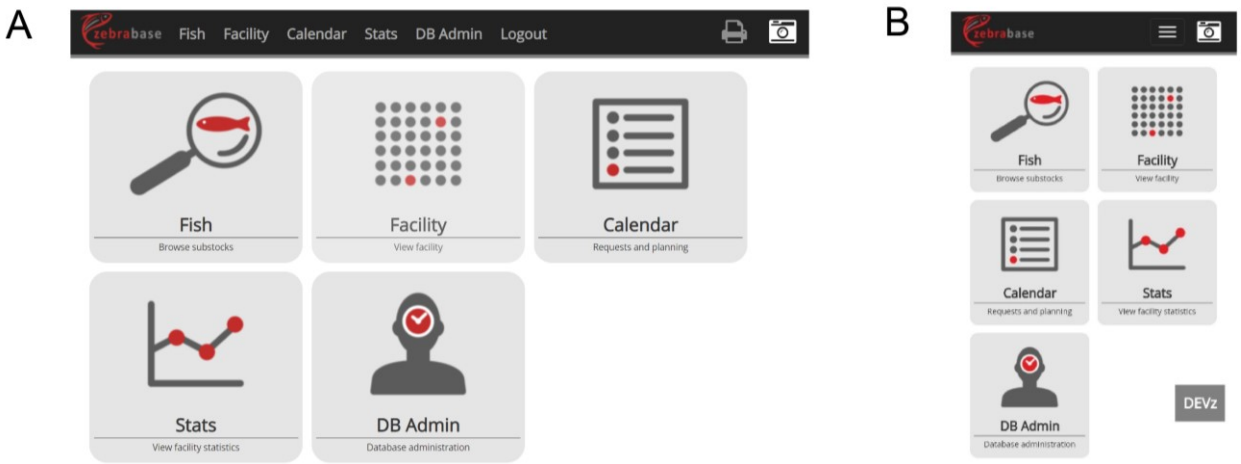

Figure 14 | Zebrabase Home Page. Desktop (A) and mobile optimized (B) version of the homepage. The page serves as a hub to get quickly to all the important functions of the database – fish stocks, facility overview, calendar, statistics and administrator interface.

The cornerstone of Zebrabase is comprehensive tracking of the animals, which is based on systematic fish characterization and grouping. All facility animals are divided into fishlines defined by the database administrator by their genomic features (genotypes, for short), the date of their establishment or import and other auxiliary information. Fishlines are further separated into stocks – groups of fish sharing the same genotype and background (defined by the fishline), as well as parents and date of birth (DOB). Because in reality, the number of fish

in a stock can often exceed the capacity of a single tank, we introduced another level of animal grouping – so-called substocks, which refer to a defined stock subset sharing a single container (e.g. a tank or Petri dish) and represent the basic trackable unit in the database (**Figure 15**). In the user interface, animals are identified by an internal stock and substock ID. In line with the grouping logic, stock ID is a common identifier for a group of siblings originating from a single crossing event, whereas substock ID is a unique identifier for each of the fish group sharing a single container.

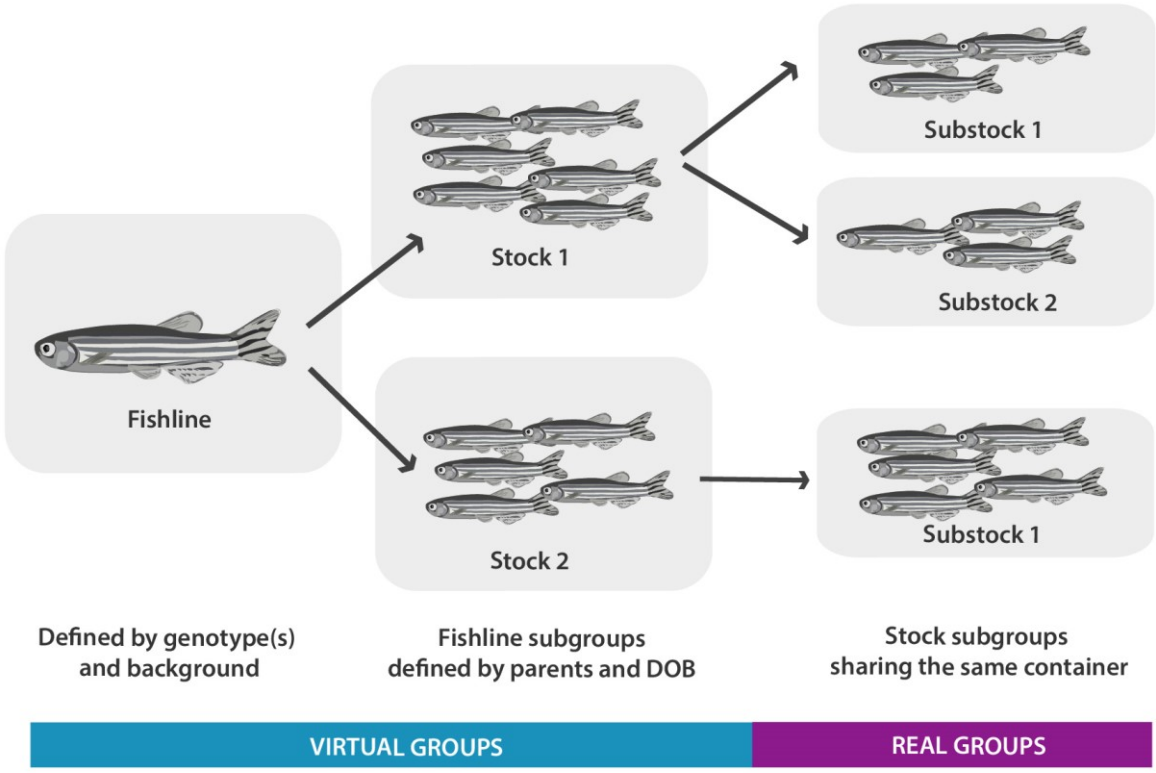

Figure 15 | Schematic representation of fish grouping logic in Zebrabase. Fishlines are defined by their genotypes and background. Stocks are groups of fish within a single fishline originating from a single crossing event and are defined by date of birth (DOB) and parents. Substocks reflect the physical group of fish in the facility and correspond to stock subgroups sharing the same container (e.g. tank or a dish)

In Zebrabase, generation of the fishline names are based on the ZFIN nomenclature (https://wiki.zfin.org/display/general/ZFIN+Zebrafish+Nomenclature+Guidelines). The names are generated automatically from the information about genotypes of the specific fishline (type of modification, driver, triggered gene, affected gene, allele etc.). Alternatively, for specific fishlines the administrator can opt for the use an alias instead of the generated names. This is

particularly useful for lines that have a well-known trivial name (for examples see **Table** 4) or those a very long generated name, e.g. in the case of multiple complex genomic features. Moreover, background can be specified in a dedicated field and also a suffix can be appended to the generated name with additional information about the fishline.

Table 4 | Examples of commonly used trivial names for zebrafish mutant lines

Trivial name	Affected gene	Phenotypic defect
casper	*mitfa, mpv17*	pigmentation
panther	*csf1ra*	pigmentation
sparse	*kita*	pigmentation
moonshine	*trim33*	erythroid development
cloche	*npas4l*	hematopoietic and endothelial development
vlad tepes	*gata1*	erythroid development
spadetail	*tbx16*	mesodermal and hematopoietic development

Zebrabase also enables users to store attachments and effectively organize publications or genotyping protocols associated with a particular fishline. Same is true for visual content – for instance, observed phenotypes of mutant lines, or transgenic reporter expression patterns can be stored as .jpg files associated with a particular fishline.

2.3. Animal tracking

For efficient spatial tracking of the substocks, we developed an intuitive positional widget called **Facility** (**Figure 16**), which serves as a visual interface for user-defined rooms, racks and tanks. The status of each substock is consistently color-coded (more on that topic later), which provides a useful reference for the users. Clicking on a position opens the action menu for quick actions, whereas when clicked twice, the substock record (**Figure 17A)** pops up. Alternatively, the QR code printed on tank labels also serves as a direct link to the substock record (**Figure 17C**). From the substock record page, various actions associated with the animals can be performed. Moreover, an interactive pedigree is visualized at the bottom of the page, which provides links to all the substock in the whole hierarchy, as well as the corresponding action records (**Figure 17B)**. Also, action history for the particular substock and

links to all the living siblings and offspring in the database are also provided at the substock record page. Finally, under the Fish tab there is a complete list view of all the substocks, including the dead ones (**Figure 18**). The list view also includes an extensive filtering section and quick search function, which enables to search efficiently by genomic features, IDs, owners or project licenses.

2.4. Animal age and productivity

The visualization of animal age and productivity is an essential feature of an animal tracking database. Therefore, we implemented color-coded statuses that are determined by productivity (the ability to spawn), age and auxiliary information entered by the database users. Each status type is consistently visualized by using a specific color throughout the database:

- **grey** - juvenile and unproductive fish
- **green** – productive adult fish
- **yellow** – adult fish with a temporary alert status entered by a database user (default options: progeny survival low, temporary unproductive)
- **red** – retired fish (default threshold: 18 month of age)

Based on the standard operating procedures (SOP), each facility manager can decide independently, what are the specific reason to assign a temporary status - e.g. embryonic survival rate below 30% (“progeny survival low”), or three consecutive unsuccessful crossing attempts (“temporary uproductive”). Productivity changes are reported by a dedicated action **Productivity** in Zebrabase.

Figure 16 | Zebrabase Facility View. Facility view is a visual facility interface that enables users to browse the racks within the facility and to perform the actions. Combined with the room and rack name, each position is uniquely defined within the whole facility using rows (letters) and column (numbers) identifiers. On mouse over, additional information appear in the tooltip. When clicked, the action menu appears and enables users to perform all actions available for a particular substock. When double clicked, the substock records pops up.

2.1. Actions

In Zebrabase, a number of actions can be performed virtually with the fish tank. We tried to reflect most accurately the real situations in a fish facility. The currently implemented actions include basic record update, count, crossing, split, transfer, productivity, genotyping, termination, adding request for a specific substock and printing a QR code. All of these can be fully tracked and browsed in the action history accessible to the administrators. The action history is also a part of the substock record, to provide an indication of the actions associated with a particular tank of fish. Examples of the functionalities provided by specific actions are provided later in this chapter. Recently, we implemented the batch support for actions, which enables to select multiple substocks and apply the action at once (currently available for record update, count, productivity and termination). Also, batch QR code print option is available in the Facility view.

A

Substock

gata1:DsRed $^{+/+}$ 2020-01-14 F01_A09 (6/9)

Delete | Update | Count | Terminate tank | Crossing | Split | Genotyping | Productivity | Transfer | Print QR Code ... | View position | Add request | Update stock

Stock	gata1:DsRed 2020-01-14
Fishline	gata1:DsRed
Suffix	
Position	F01_A09
Tank type	1x1
Substock use	
Substock number	6/9
Substock siblings	gata1:DsRed $^{+/+}$ 2020-01-14 F01_B10 (5/9) gata1:DsRed $^{+/+}$ 2020-01-14 F14_B09 (1/9) gata1:DsRed $^{+/+}$ 2020-01-14 F14_B08 (2/9) gata1:DsRed $^{+/+}$ 2020-01-14 F14_B07 (3/9) gata1:DsRed $^{+/+}$ 2020-01-14 F14_B06 (4/9) gata1:DsRed $^{+/+}$ 2020-01-14 F01_A01 (9/9) gata1:DsRed $^{+/+}$ 2020-01-14 F01_A02 (8/9) gata1:DsRed $^{+/+}$ 2020-01-14 F01_A08 (7/9)
Substock offspring	
Count	30
Substock status	unproductive
Description	
Date of birth	2020-01-14
Date of death	
Substock inputs	transfer 2020-02-17 transfer 2020-01-20 count 2020-01-20
Owners	
Substock projects	
Loc.stock ID	04181
Substock ID	9085
Genotypes with zygosities	gata1:DsRed $^{+/+}$

B

Parent tree

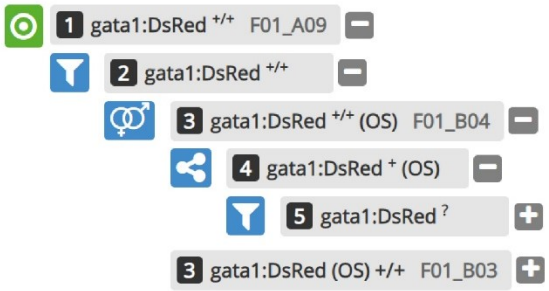

C

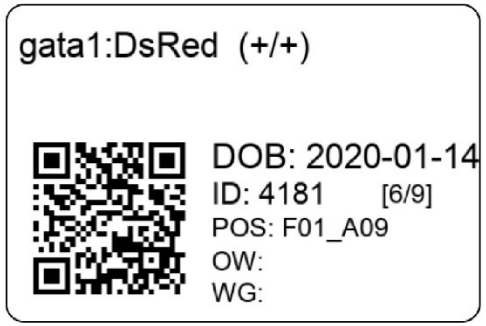

Figure 17 | Substock record page. (A) The substock record provides an overview of the essential information about a particular substock. It can be accessed either via the database itself from the Fish list or Facility view, or alternatively, by scanning the QR code on a tank. (B) Parent tree shows past generations and actions that lead to the creation of the current substock. All parts of the pedigree are interactive, providing links to the respective parts of the database. (C) QR code tank label that serves as a direct link to the substock record in the database when scanned.

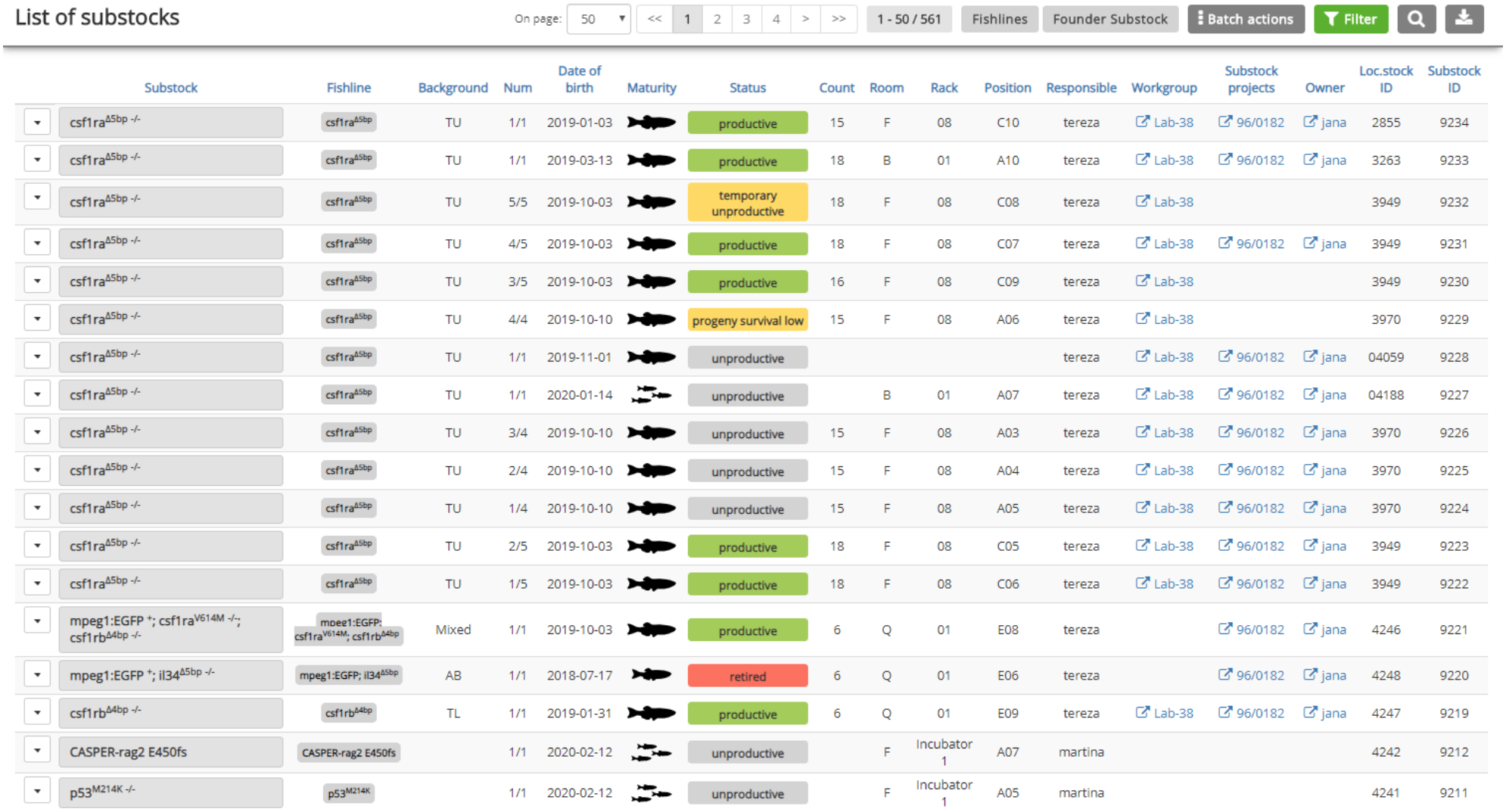

List of substocks

On page: 50 | << 1 2 3 4 > >> | 1 - 50 / 561 | Fishlines | Founder Substock | Batch actions | Filter

Substock	Fishline	Background	Num	Date of birth	Maturity	Status	Count	Room	Rack	Position	Responsible	Workgroup	Substock projects	Owner	Loc.stock ID	Substock ID
csf1ra$^{\Delta 5bp\ -/-}$	csf1ra$^{\Delta 5bp}$	TU	1/1	2019-01-03		productive	15	F	08	C10	tereza	Lab-38	96/0182	jana	2855	9234
csf1ra$^{\Delta 5bp\ -/-}$	csf1ra$^{\Delta 5bp}$	TU	1/1	2019-03-13		productive	18	B	01	A10	tereza	Lab-38	96/0182	jana	3263	9233
csf1ra$^{\Delta 5bp\ -/-}$	csf1ra$^{\Delta 5bp}$	TU	5/5	2019-10-03		temporary unproductive	18	F	08	C08	tereza	Lab-38			3949	9232
csf1ra$^{\Delta 5bp\ -/-}$	csf1ra$^{\Delta 5bp}$	TU	4/5	2019-10-03		productive	18	F	08	C07	tereza	Lab-38	96/0182	jana	3949	9231
csf1ra$^{\Delta 5bp\ -/-}$	csf1ra$^{\Delta 5bp}$	TU	3/5	2019-10-03		productive	16	F	08	C09	tereza	Lab-38			3949	9230
csf1ra$^{\Delta 5bp\ -/-}$	csf1ra$^{\Delta 5bp}$	TU	4/4	2019-10-10		progeny survival low	15	F	08	A06	tereza	Lab-38			3970	9229
csf1ra$^{\Delta 5bp\ -/-}$	csf1ra$^{\Delta 5bp}$	TU	1/1	2019-11-01		unproductive					tereza	Lab-38	96/0182	jana	04059	9228
csf1ra$^{\Delta 5bp\ -/-}$	csf1ra$^{\Delta 5bp}$	TU	1/1	2020-01-14		unproductive		B	01	A07	tereza	Lab-38	96/0182	jana	04188	9227
csf1ra$^{\Delta 5bp\ -/-}$	csf1ra$^{\Delta 5bp}$	TU	3/4	2019-10-10		unproductive	15	F	08	A03	tereza	Lab-38	96/0182	jana	3970	9226
csf1ra$^{\Delta 5bp\ -/-}$	csf1ra$^{\Delta 5bp}$	TU	2/4	2019-10-10		unproductive	15	F	08	A04	tereza	Lab-38	96/0182	jana	3970	9225
csf1ra$^{\Delta 5bp\ -/-}$	csf1ra$^{\Delta 5bp}$	TU	1/4	2019-10-10		unproductive	15	F	08	A05	tereza	Lab-38	96/0182	jana	3970	9224
csf1ra$^{\Delta 5bp\ -/-}$	csf1ra$^{\Delta 5bp}$	TU	2/5	2019-10-03		productive	18	F	08	C05	tereza	Lab-38	96/0182	jana	3949	9223
csf1ra$^{\Delta 5bp\ -/-}$	csf1ra$^{\Delta 5bp}$	TU	1/5	2019-10-03		productive	18	F	08	C06	tereza	Lab-38	96/0182	jana	3949	9222
mpeg1:EGFP $^{+}$; csf1ra$^{V614M\ -/-}$; csf1rb$^{\Delta 4bp\ -/-}$	mpeg1:EGFP; csf1ra^{V614M}; csf1rb$^{\Delta 4bp}$	Mixed	1/1	2019-10-03		productive	6	Q	01	E08	tereza		96/0182	jana	4246	9221
mpeg1:EGFP $^{+}$; il34$^{\Delta 5bp\ -/-}$	mpeg1:EGFP; il34$^{\Delta 5bp}$	AB	1/1	2018-07-17		retired	6	Q	01	E06	tereza		96/0182	jana	4248	9220
csf1rb$^{\Delta 4bp\ -/-}$	csf1rb$^{\Delta 4bp}$	TL	1/1	2019-01-31		productive	6	Q	01	E09	tereza	Lab-38	96/0182	jana	4247	9219
CASPER-rag2 E450fs	CASPER-rag2 E450fs		1/1	2020-02-12		unproductive		F	Incubator 1	A07	martina				4242	9212
p53$^{M214K\ -/-}$	p53^{M214K}		1/1	2020-02-12		unproductive		F	Incubator 1	A05	martina				4241	9211

Figure 18 | Zebrabase List View. Accessible from the Fish tab, list view is an interface designed for browsing, filtering and searching for specific substock records. It shows all the relevant information like fishline, background, date of birth, status, number, position and owner, as well as the corresponding fishline responsible user. Moreover, project ID/ IACUC codes can be specified in the Project field and also Workgroup information is displayed if available. This interface allows to perform quick actions via the action menu button on left hand side of each row.

2.2. Breeding management

A dedicated **Crossing** action serves for incrossing and outcrossing of substocks. Thanks to the internal database structure, when outcrossing substocks with different genotypes, new fishline with the corresponding genotype combination is created automatically, in case the combination is unique. The action can, consistently with the other actions, be initialized from the Facility view or the Fish list. Moreover, zygosity is determined automatically for the progeny substock from the information available for the parents – for example incrossing homozygotes for a certain genomic feature will yield homozygous progeny. In case where the parental information is not sufficient to determine the zygosity, "?" sign is shown for the particular genotype in the substock name.

2.3. Calendar

To streamline the communication between researchers and the facility staff, users can submit requests via a dedicated interface in the **Calendar** or they can choose the **Add request** option from the Action menu or from the substock record page. A handful of request types are available from the dropdown menu, like genotyping or terminating substocks, setting up fish for crossing, and importing and exporting the animals. The number of request types is still growing based on the feedback we get from Zebrabase users. Every new entry is visualized in the **Calendar** (**Figure 19**) and email notification is sent to facility staff users. Members of the facility staff are then able to accept the requests, mark them as performed, or decline them, optionally attaching an explanatory note to the researcher. Using the same interface, researchers can plan their experiments by checking the "self-request" box when creating the request record. Such an entry is then only visible to the user who entered it.

2.4. Data management

Automated data import from previous database or spreadsheet is possible with the use of the import template we provide. Complete dataset, including the breeding history, can be imported to a new Zebrabase database. On the other hand, data can be exported to .csv or .xls including a current substock data, action history and statistics. Moreover, we are also able to provide complete database dumps from the daily backups, if required by the customer.

For the not uncommon situation where multiple research groups are sharing the zebrafish facility and wish to have their data separated, we have designed an option to compartmentalize the data in the user interface. This not only means that a portion of the data can stay undisclosed, but it also prevents users from other workgroups to mistakenly edit or delete records that do not belong to them, and therefore the use of **Workgroups** is always recommended for large facilities. This data separation takes place at the level of fishlines and can be adjusted by the database administrator. Typically, fish facility staff and animal caretakers still retain the right to see and use the full dataset. Within each workgroup, the permission groups can further refine the user rights in more detail ranging from the view-only guest access to the most advanced administrator rights.

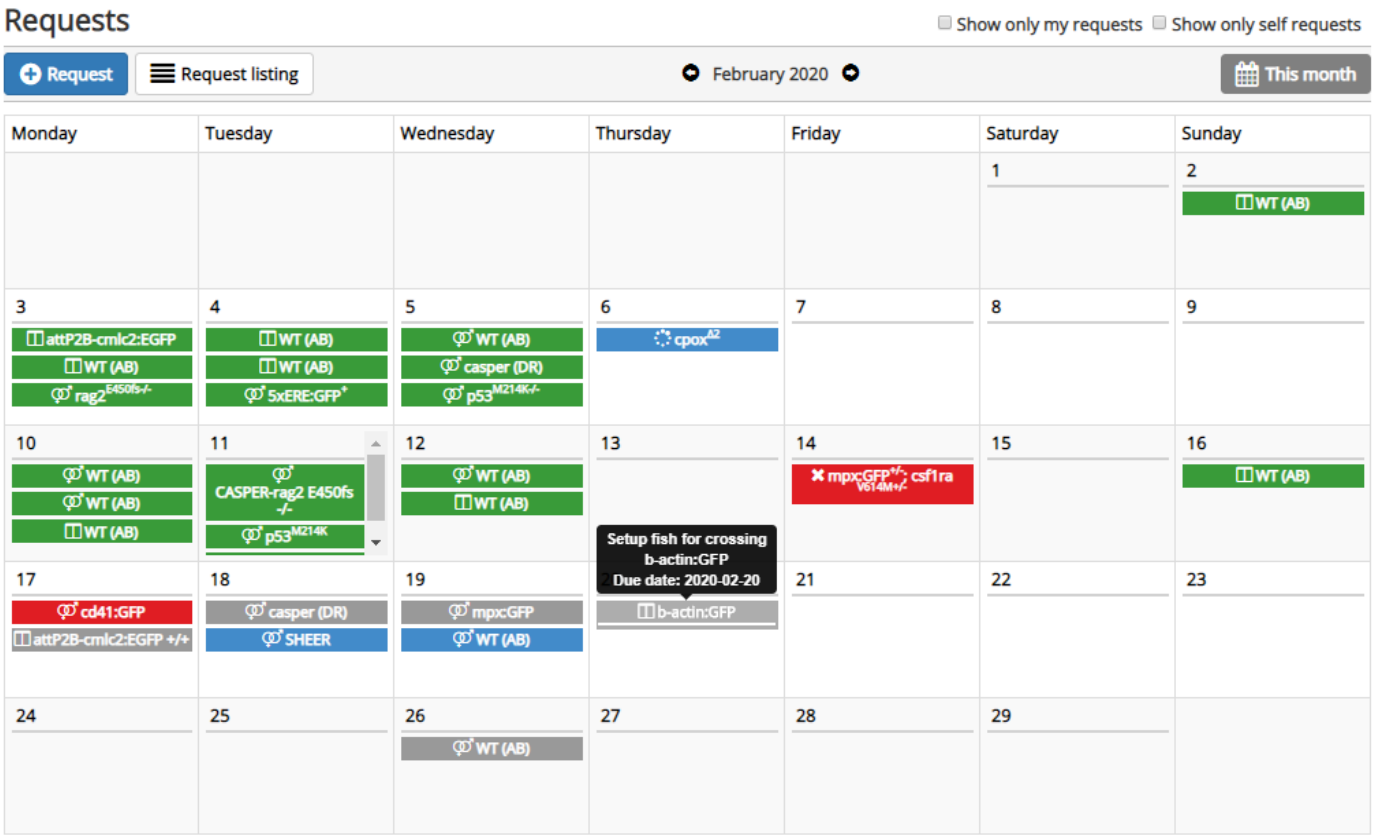

Figure 19 | Calendar interface. The calendar serves for entering requests for the animal facility staff or research plans for researchers themselves (designated by a horizontal line). These can be typically requests or plans for crossing, genotyping or termination of a tank. The number of request types is continuously growing based on the user feedback. Color coding: grey – new requests, blue – accepted request, green – performed requests, red – declined request.

2.5. Statistics and reporting

We implemented an in-built comprehensive reporting system of animal usage or death mediated by the action **Count**. First, a so-called "Start count" must be specified for a fish substock, which is typically performed when the juvenile fish are introduced into the facility system. Once this number is available for a particular substock, all subtractive count types (Died, Euthanized, Used for experiment) are used to create animal reports in the Statistics. For the count type "Used for experiment", it is also possible to specify the experiment type, which can be also linked to specific Project ID. All the records are then visualized in the **Statistics** (**Figure 20**), which include a detailed filtering section and can be used for creating custom animal reports.

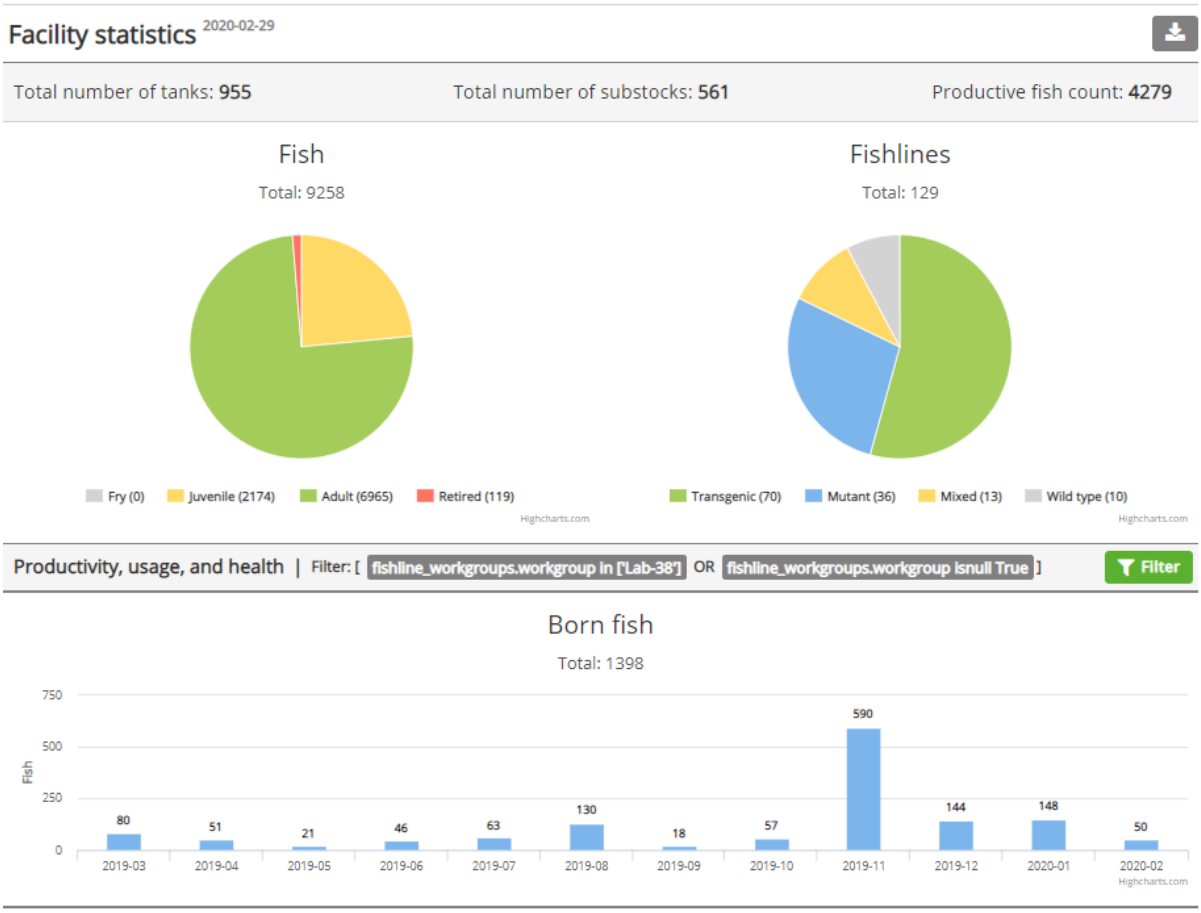

Figure 20 | Facility statistics. (A) Pie chart overview of the current number of fish and fishlines in the facility. (B) Bar chart section with detailed statistics per month (default, can be changed to daily or weekly statistics), which can be filtered by various characteristics and displayed for a defined date range.

2.6. Zebrabase 3.0

After five years of development, complete update of the code to the new programming languages and frameworks was inevitable, because the older version were either no longer supported or they were restricting the development of new features. The redesigned version 3.0 will include significant functional improvements, like drag and drop support, position sharing and merging, improved configuration for administrators or enhanced communication functionalities, to name a few.

Summary

We developed a scalable, cross-platform tracking database designed specifically for small fish species, which is suitable for zebrafish facilities of any size. Zebrabase is optimized for mobile devices as well as the use on desktop computers and it provides also the QR code functionality for efficient record browsing and editing. We implemented a smart user interface, interactive view of the data and facility, comprehensive animal tracking features and detailed statistics and reporting functionalities. New features are continuously added based on the user feedback and a completely redesigned version 3.0 is planned to be released in the summer 2020.

DISCUSSION

Duplicated erythro-myeloid cytokines in zebrafish

In teleost including zebrafish, an extra round of whole genome duplication 250-350 million years ago resulted in formation of multiple paralogs of many important genes **(Hoegg et al. 2004, Amores et al. 2011)**, including hematopoietic cytokines. After such an event, multiple scenarios can occur - pseudogenization often leading to a loss of function of one of the paralogs **(Nei and Roychoudhury 1973, Takahata and Maruyama 1979, Watterson 1983)**, subfunctionalization, neofunctionalization or functional redundancy of the duplicated counterparts **(Force et al. 1999)**. In the introductory part of this dissertation, particular examples of all of these outcomes are discussed including examples of cytokines regulating the development of zebrafish erythro-myeloid lineage - e.g. *epob* loss of function, potential sub-specialization of *kitlga*/*b*, or the partial redundancy between *csf3a*/*b*. In addition, we hypothesize that some specific gene duplications might even have enabled or compensated for the loss of particular genes or clusters in the zebrafish genome (GM-CSF/IL3 cluster).

Despite the fact, that zebrafish is gaining popularity in the hematopoietic field, zebrafish genome duplication brought an increased level of complexity of the regulatory network that needs to be dissected and elucidated to fully utilize this model organism. Even though several reports have addressed the question of duplicated cytokines in zebrafish, many functional links are still missing - especially in cases, when the whole ligand-receptor signalosome has been duplicated (e.g. *kitlg*/*kit*, *csf1*/*csf1r*) and the ligand-receptor specificities are unclear. Moreover, also the functions of specific cytokines are in some cases yet to be defined. An example can be IL11, a cytokine essential for megakaryocyte maturation **(Paul et al. 1990)** that triggers the activation of JAK/STAT pathway via binding to IL11Rα and gp130 **(Heinrich et al. 2003)**. In teleost, two paralogs of *il11* have been identified **(Huising et al. 2005)** but data indicating their respective functions are not yet available.

To reinforce zebrafish as a relevant non-mammalian model organism to study hematopoietic cell maintenance and differentiation during developmental and adult hematopoiesis, it is essential to investigate functions of yet uncharacterized cytokines and to decipher specific

roles of the duplicated paralogs. Only then we can take the full advantage of the powerful *in vivo* and *ex vivo* tools available for the zebrafish model and use it for modelling of human hematopoietic defects and malignancies in simplified and evolutionary conserved settings.

The role of Kit ligands in erythropoiesis in *D. rerio*

The main goal of the experimental part of this project was to investigate the function of two retained zebrafish paralogs of a crucial hematopoietic cytokine, the KIT ligand (KITLG or Stem Cell Factor / SCF), designated as Kitlga and Kitlgb. The role of Kit signaling in erythropoiesis has not been reported in zebrafish so far **(Parichy et al. 1999, Hultman et al. 2007)**, which is in contrast to previous studies in human **(Broudy 1997, Panzenbock et al. 1998, von Lindern et al. 1999, Ding et al. 2012)**, mouse **(Chabot et al. 1988, Huang et al. 1990, Antonchuk et al. 2004)** and chicken **(Hayman et al. 1993, Dolznig et al. 1995, Bartunek et al. 1996)**, where the essential role of KITLG in proper erythroid development was demonstrated.

Here we employed *ex vivo* clonal **(Stachura et al. 2009, Stachura et al. 2011, Svoboda et al. 2016)** and suspension culture assays, as well as *in vivo* gain- and loss-of-function experiments to study the function of Kit ligands. Due to the fact that the reported cross-reactivity of mammalian hematopoietic cytokines in zebrafish is rather limited **(Svoboda et al. 2016)**, we first cloned and expressed recombinant proteins for *ex vivo* experiments and transcribed mRNAs of *bona fide* zebrafish Kit ligands. In a similar manner as described previously **(Andrews et al. 1991, Bartunek et al. 1996, Stachura et al. 2009, Svoboda et al. 2016)**, for the *ex vivo* experiments we cloned specifically the extracellular portion of the cDNA devoid of the cytosolic part and transmembrane domain, technically generating the soluble forms of Kit ligands that we later used for stimulation of kidney marrow progenitor cells. On the other hand, for mRNA injection, we cloned the sequence corresponding to the full-length kit ligands, including all the domains that are schematically depicted in **Figure 4**, in agreement with the previously published strategy **(Mahony et al. 2018)**.

Importantly, in this study, we observed and reported for the first time that Kit signaling can contribute to zebrafish erythroid progenitor cell expansion. We demonstrated that treatment with Kitlga, but not Kitlgb, in combination with Epo, master regulator of erythropoiesis **(Paffett-Lugassy et al. 2007, Stachura et al. 2011)**, enabled erythroid expansion in both suspension cultures

and clonal assays, which is in agreement with the results obtained in other vertebrates **(Krantz 1991, Broudy 1997, Panzenbock et al. 1998, von Lindern et al. 1999, Katakura et al. 2015)**. Next, we also tested the effect of of dexamethasone (Dex) treatment, which has been previously shown to prolong the proliferation and self-renewal of erythroid progenitors and reduce the rate of spontaneous differentiation **(Panzenbock et al. 1998, Bauer et al. 1999, von Lindern et al. 1999, Kolbus et al. 2003, Leberbauer et al. 2005, England et al. 2011)**. In addition, it was previously reported that in stress erythropoiesis (e.g. in response to hypoxia or anemia), defective glucocorticoid (GR) signaling can lead to the inability increase self-renewal of the erythroid progenitors **(Bauer et al. 1999)**. In agreement with these studies, the combination of Epo, Dex and Kitlga in the suspension media led to synergistic erythroid expansion of kidney marrow cells; however, without Kitlga, Dex was not sufficient to trigger substantial expansion of the erythroid progenitors in cooperation with Epo alone. These results suggest that the combination of all three factors – Epo, Kitlg and Dex - is required for self-renewal of adult erythroid progenitors also in zebrafish.

To understand the mechanism that ensures the erythroid expansion and specifically the role of Kitlga in this process, we performed an RNAseq analysis, where we compared the effect of **Epo, Dex** versus **Epo, Dex, Kitlga** treatment of kidney marrow cells isolated from adult animals. As we expected due to the fact that both conditions contained Epo, prominent expression of erythroid-specific genes was revealed in both conditions. Nevertheless, we observed changes in expression between both cultures. Compared to the distinct erythroid fingerprint of **Epo, Dex, Kitlga** culture, the character in **Epo, Dex**–treated cells was more mixed, with enhanced expression of myeloid-specific genes. This effect can be explained by the fact that the isolated kidney marrow contains, in addition to progenitor cells, also a myeloid cell fraction, which is able to survive in culture. However, during erythroid expansion of cells treated with Epo, Dex, and Kitlga, myeloid cells were overgrown by erythroid progenitors. Moreover, the gene ontology (GO terms) analysis of the upregulated genes revealed an increase in expression of translation and erythroid-specific genes in Epo, Kitlga, Dex cultures. These results indicate that Kiltga-enhanced erythroid expansion happens in a similar manner like in other vertebrate species - by induction of proliferation **(Dolznig et al. 1995, Leberbauer et al. 2005)**, as well as enhancing protein translation. This is in agreement with studies in other vertebrates showing

that translation is enhanced before and during the terminal erythroid cell differentiation **(Alvarez-Dominguez et al. 2017, Khajuria et al. 2018)**.

To further support out findings, we tested the role of Kit ligands in zebrafish erythropoiesis *in vivo*, using full-length cytokine mRNA injection. In contrast to *ex vivo* cultures, where only Kitlga was able to cooperate with Epo to promote erythroid expansion, both kit ligands were potent *in vivo* in the expansion of the erythroid cells in 72 hpf larvae, when injected together with *epo* mRNA into single cell stage embryos. Moreover, we were able to enhance this effect by additional dexamethasone treatment of the embryos; however, the increase in the number of erythrocytes was not as prominent as in *ex vivo* experiments. This might be due to the presence of endogenous GR-signaling in developing embryos that is already employed, and therefore the dexamethasone treatment is only providing an additional enhancement of the already present effect.

Next, we hypothesize that the discrepancy between the activity of Kitlgb in cultures versus in injected embryos is likely connected to the fact that we were using two different forms of both ligands – soluble for *ex vivo* experiments, and full-length for *in vivo* experiments, in line with previous studies **(Mahony et al. 2018)**. The function of both isoforms has proved to be different **(Lennartsson and Ronnstrand 2012)** – the soluble form, which has been shown to be sufficient for erythroid signaling in cultured cells **(Hayman et al. 1993)**, is transported in circulation and can affect distant tissues, whereas the transmembrane form acts predominantly in stem cell niches **(Lennartsson and Ronnstrand 2012)**. Our data also indicate that in addition to HSPCs expansion that was previously reported **(Mahony et al. 2018)**, the full-length Kitlgb can contribute to erythroid expansion *in vivo.* Kitlgb activity might require a specific tissue architecture that cannot be replicated *ex vivo*. Alternatively, since we have seen the effect of Kitlgb only in the course of development, it is possible that it does not play a role in adult organism. However, data supporting such a hypothesis are missing.

Lastly, we investigated if Kita receptor is dispensable for erythroid cell expansion mediated by Kitlg *in vivo* using *kita* receptor mutant (sparse or $kita^{b5}/^{b5}$) and we failed to observe the cooperation of *epo* with either of the *kit* ligands in erythroid expansion, which we have seen in wild-type larvae. That suggests that Kita receptor is indeed the main receptor mediating Kit signaling in zebrafish erythroid cells, and although Kitb might also be involved, it could not

fully compensate for *kita* deficiency in our experiments. Moreover, our RNAseq data show that in *ex vivo* cultures of adult erythroid kidney marrow cells, the expression of *kita* receptor was overall much higher than the one of *kitb*. Therefore, we conclude that zebrafish Kita receptor seems to be required for Kitlg-mediated erythroid expansion *in vivo*.

In summary, we used *in vivo* and *ex vivo* approaches to address the questions of the role of zebrafish kit ligands in erythropoiesis. Importantly, we optimized the culture conditions for the expansion of erythroid progenitors from kidney marrow and we believe that together with previously established colony assays, the suspension cultures we established will be particularly useful for hematopoietic research of both normal and aberrant hematopoiesis, especially utilizing the hematopoietic mutant strains (e.g. *moonshine*, *mindbomb*) **(Ransom et al. 1996)** or disease models available in zebrafish. Moreover, the approach we present will enable further proteomic, genomic and biochemical analysis of *ex vivo* cultured and expanded cells, which was previously not possible. Finally, we assume that by using different cytokine combinations, optimal conditions for the growth of other zebrafish hematopoietic cell types can be established.

To conclude, there is a partial functional redundancy between zebrafish Kitlga and Kitlgb: Kitlga has been repeatedly associated with roles in melanogenesis and pigmentation, which have been probably lost in the case of Kitlgb. However, in gain-of-function experiments, both ligands seem to contribute to the overall process of zebrafish erythroid commitment and development *in vivo* and although it is not yet clear whether this function is necessarily required for erythroid development in steady state, its significance can increase under stress conditions (e.g. anemia or hypoxia). Nevertheless, the exact mechanism by which the diversification is controlled is yet to be elucidated. Here, we demonstrated that to a certain extent, the role of Kit signaling with respect to erythroid development is conserved from human to fish, as previously unnoticed (**Figure 21**) and our findings provide the support for the use of zebrafish as a model to study normal and aberrant human hematopoiesis.

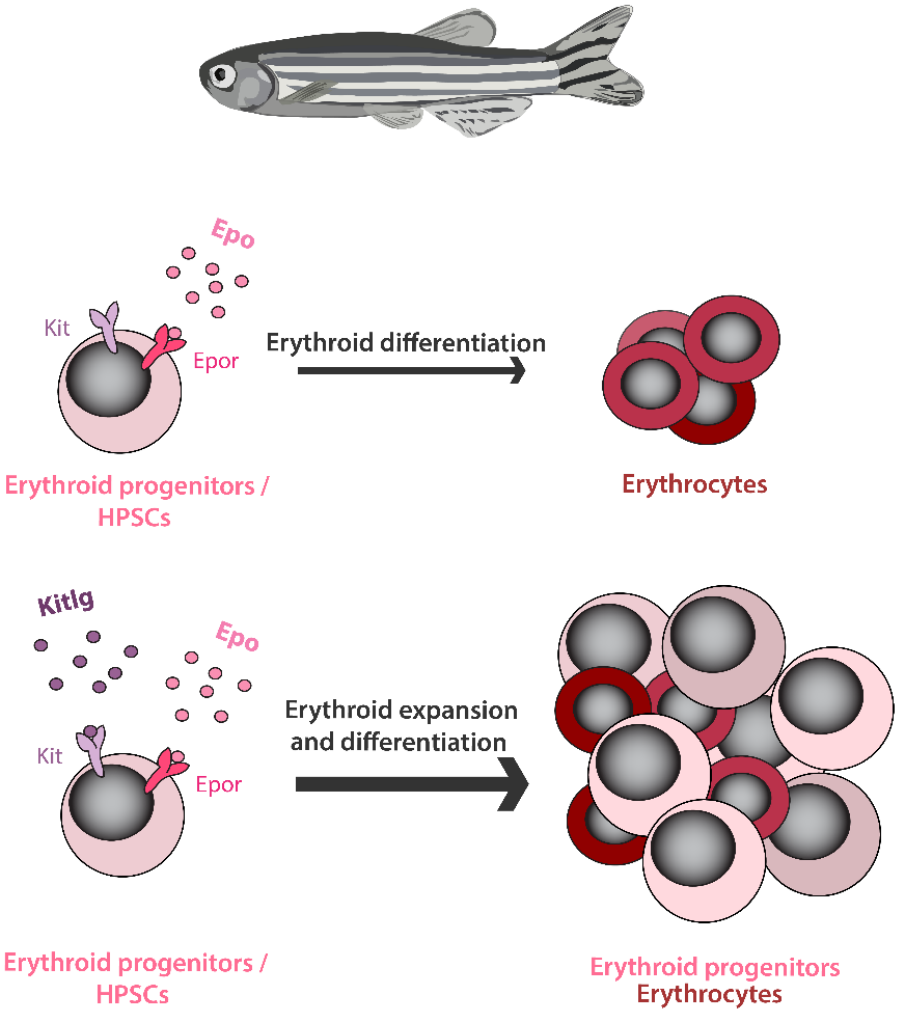

Figure 21 | Model of zebrafish Kit ligand cooperation with Epo in erythroid cell expansion. The proper balance between Epo and Kit signaling is essential to control erythroid progenitor self-renewal and proliferation versus terminal differentiation of erythrocytes. Zebrafish Kit ligands (Kitlg) cooperate with erythropoietin (Epo) to promote the expansion of erythroid progenitors. On the other hand, without the addition of Kitlg, cells differentiate into erythrocytes.

Zebrabase – the vision beyond husbandry and standardization

In the second part of this work I focused on another, more general aspect of animal research, which we soon found to be critical to make the use of the zebrafish model even possible. In addition to all the advantages zebrafish has to offer, the increasing popularity of small fish species in research might partially owe to the concept of 3R **(Russell and Burch 1959, Kirk 2018)** - especially to the principle of replacement, which states that using the lowest suitable species to answer a specific research question must be always preferred. Moreover, despite the strengths of the mouse as a mammalian model, there are experimental limitations that restrict its utility in certain research areas including large-scale studies and screens, where zebrafish can present a relevant alternative to rodents **(reviewed in Lieschke and Currie 2007, Ablain and Zon 2013, Rasighaemi et al. 2015)**.

For a long time, proper animal tracking has been neglected in the zebrafish field, but that has changed in the recent years. Even though zebrafish are non-mammalian vertebrates, their use is a subject of legal regulations by the EU Directive 2010/63 on the protection of animals for scientific purposes and the recommendations issued by FELASA and EuFishBioMed associations **(Alestrom et al. 2019)**, which require relatively high standards of animal identification, tracking and reporting. Moreover, also the emphasis on reproducibility and standardization of the experiments has become much more prominent in the last years in the zebrafish community. Finally, based on the recommendations by the Zebrafish Nomenclature committee (see zfin.org), all the names of zebrafish lines must follow a common naming standard that should be used consistently in reports, manuscripts and in the tracking system itself. All these demands make it practically impossible to conduct research on zebrafish without a detailed and purpose-designed database system.

Therefore, a zebrafish husbandry database, which would be compliant with these requirements, was critically missing back in 2014. Existing alternatives were displaying a number of shortcomings, including poor sustainability, limited exporting options or a single platform commitment, which allowed to use the database only from a particular type of a device (e.g. iPad). This situation prompted us to develop Zebrabase - a novel tracking solution for fish facilities optimized specifically for the use with small fish species or other aquatic animals housed in tanks. With Zebrabase, we aimed to address the aforementioned issues and

meet the needs of our modern zebrafish facility. Although our original plan was to develop Zebrabase solely for our own purposes, we were soon convinced by our collaborators and colleagues that the spread of this solution will lead to significant improvement in the workflow of both the researchers and zebrafish facility staff, and that we should contribute to the community by sharing this tool.

Zebrabase is a web-based solution, providing a cross-platform access and full support of mobile devices. For the users, the service is maintenance-free, and thanks to the hosted character of Zebrabase, we are able to provide automatic backup and recovery or instant version upgrades. Moreover, QR code functionalities including in-app camera integration are provided to ensure maximum versatility and data accessibility, which can be very beneficial for the real-life use of the application. To our knowledge, this set of features in unparalleled by any other solution.

The cornerstones of Zebrabase functionalities are comprehensive fish tracking, an interactive breeding history and advanced management features that allow users to keep animal-related records, actions and statistics efficiently organized within a single platform. We optimized the tracking logic to address the key specificities of fish tracking, especially following a group of the animals and its rearrangement, as opposed to individual animals, which, on the other hand, is the core of tracking solutions for non-aquatic models.

During the development of the application, we have also emphasized the reporting capabilities of the database, as this topic is gradually getting more important due to legal requirements associated with the use of laboratory animals. The export function of the database allows users to store fish census and usage reports for the whole facility or for a specific subset of the data (e.g. specific room, user, fishline or project license) in a standard spreadsheet file. This report provides an overview of all the animals that were born, died, euthanized or used for experiments in the facility. Moreover, it is also possible to export a full or any custom subset of fish stock records with a single click. Lastly, based on the feedback from the Zebrabase users, we implemented two modes in the Calendar interface – requests for the facility staff and requests for the user himself, which are comprehensibly visualized in the user interface and provide a platform for time-efficient planning of the animal-related actions (e.g. genotyping, breeding or transfers).

Although our initial mission was to provide an affordable but smart solution for small and starting facilities, soon we began to attract the larger ones, with the biggest facility currently housing 12,000 aquarium tanks spread between multiple rooms and buildings. Therefore, we were prompted to develop a set of features, which are particularly useful for large data handling. In large facilities, data separation and security is a necessity, because very often, many scientific groups share one animal facility but the records are not to be shared. For that reason, we developed Workgroups that allow to efficiently separate the data that should be only accessible to a specific subset of Zebrabase users. Another degree of separation is achieved by different various user rights (guest, standard user, administrator, facility staff). These two features can be combined to create a versatile system, where data are secured and cannot be mistakenly changed by users that should not have an access to it.

Also during the last year, we have significantly improved Zebrabase functionalities. First, based on the EU directive, we have implemented a dedicated Project function, which enables to enter Project licenses/IACUC codes for tracking of animals under a project license. We are currently working on enhancement of this system to enable also reporting of all the individual procedures under a specific project license. Second, we implemented batch actions, especially useful for big facilities with large datasets, which are currently available for counting, termination, basic record update and productivity changes that help to significantly speed up the otherwise tedious and repetitive tasks.

Initially, the development of a proper tracking database that would allow users to keep their animal-related records efficiently organized, seemed to be a straightforward assignment; however, as with time the significance and impact of the project was increasing, so was the complexity. An important question was how to ensure sustainability of the project, as both the technical and human resources that are used to develop Zebrabase and provide support to the users are not negligible and there are expenses associated with providing the service that have to be covered. Although Zebrabase is a non-profit project, we finally opted for a mixed model: To support small and starting facilities in using the zebrafish model and to motivate them to store the animal records systematically right from the beginning, we are providing Zebrabase in a free mode, which offers up to 150 tanks free of charge. After exceeding this limit, a yearly fee covering the initial setup, version updates, server

maintenance, daily data backup and recovery, and user support is charged according to the size of the facility (for details, see https://zebrabase.org/faq).

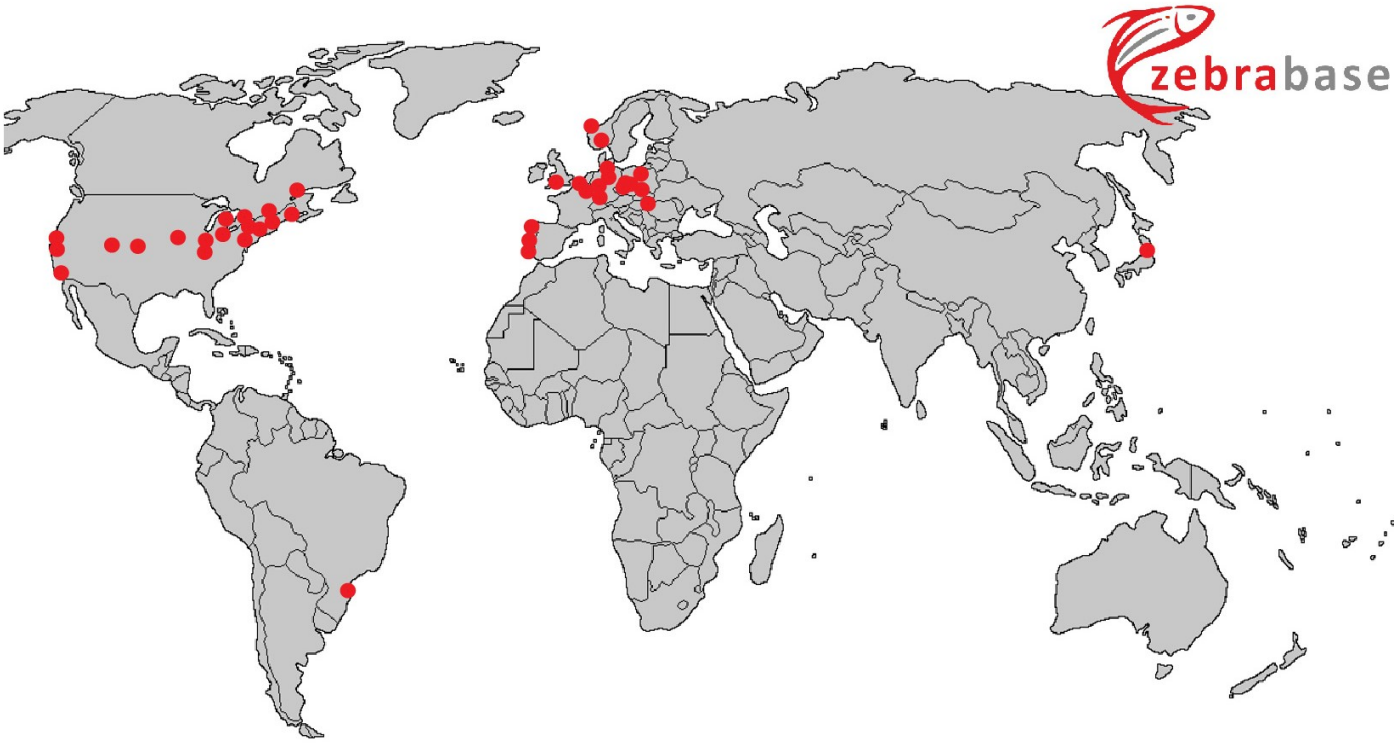

Figure 22 | An overview of zebrafish facilities using Zebrabase up to date. To date, more than 40 laboratories world-wide are using Zebrabase as their main fish tracking database (red dots) and over 100 more are testing it.

The direction of the development of the application is largely determined by a combination of our personal communication with the experts in the field of husbandry and animal welfare, as well as the feedback we get from researchers using Zebrabase. All the suggestions are regularly collected and assessed to prioritize the development of features which are most critical. In the near future, we plan to implement for instance the enterprise resource planning to streamline the workflow of researchers and facility managers, and to enable automated fee collection for the use of facility services. Moreover, currently the completely redesigned version of Zebrabase (version 3.0) is under intensive development and it should be released in summer 2020, which will include a handful of frequently requested functionalities as well as significant user interface improvements (e.g. drag and drop support). For the current information about new features, please visit our webpage (https://zebrabase.org/news).

Finally, we also believe that the concept of Zebrabase could be expanded to develop a common repository of shared fish stocks, where users would upload their stock information to the repository directly from their own Zebrabase database. The stock record in such a virtual stock center would then contain contact information and physical location of the stock and its status would be synchronized with the original database. That would greatly help to streamline the process of importing of genetically modified lines and would enhance collaboration in the community. We are convinced that such a practical tool, providing information about animals physically available, would be highly appreciated by the researchers, and together with the ZFIN database, which contains an complete virtual set of all the existing strains and alleles, it would provide a set of powerful tools that will help to efficiently select and manage genetically modified zebrafish lines.

To summarize, our general goal was to reinforce the zebrafish as a model of choice for hematopoietic research. The presented database solution, Zebrabase is a supportive tool for the community that can help to streamline the workflow of zebrafish experiments, record entering and reporting, and as such, it falls within the range of our initial objectives. Moreover, we are continuously developing the application so that it meets the requirements of both small and large facilities. As Zebrabase starts to be a predominant solution within the community, the responsibility for the future development and support of the project is high but with our growing team and more than 5 years of experience, we are ready to accept this challenge.

CONCLUSIONS

- **We established suspension culture conditions for *ex vivo* erythroid expansion of zebrafish kidney marrow cells.** Moreover, we assume that by using different cytokine combinations, optimal conditions for the growth of other hematopoietic cell types can be established. This new approach now available for the zebrafish model will be particularly useful for studies of normal and aberrant hematopoiesis (e.g. using hematopoietic mutant lines, disease models).

- **Kit signaling in hematopoiesis is conserved from human to zebrafish, making zebrafish a valid non-mammalian model to study self-renewal, proliferation and differentiation of hematopoietic cells**. These findings strengthen the zebrafish as a relevant non-mammalian model of human hematopoiesis and provide important insights for future studies of zebrafish hematopoietic development.

- **We developed an intuitive fish tracking database system, Zebrabase, and provided it as a hosted service to the zebrafish community.** We were able to fulfill our initial goals and implemented all the features we believed were essential for usefulness and usability of the application, while following conventions, nomenclature and husbandry requirements and recommendations. Zebrabase is currently used in more than 40 zebrafish facilities worldwide and is continuously gaining more popularity as a tracking solution of choice for both small and large facilities.

LIST OF PUBLICATIONS

Konířová, J, Oltová, J, Corlett, A, Kopycińska, J, Kolář, M, Bartůněk, P et al. **Modulated DISP3/PTCHD2 expression influences neural stem cell fate decisions.** Scientific Reports, 2017, 7: 41597 (10.1038/srep41597)

Oltova, J, Barton, C, Certal, AC, Argenton, F & Varga, ZM. **10th European Zebrafish Meeting 2017, Budapest: Husbandry Workshop Summary.** Zebrafish, 2018: **(workshop summary)** (10.1089/zeb.2017.1548)

Oltova, J*, Jindrich, J*, Skuta, C, Svoboda, O, Machonova, O & Bartunek, P. **Zebrabase: An Intuitive Tracking Solution for Aquatic Model Organisms.** Zebrafish, 2018, 15: 642-647 (10.1089/zeb.2018.1609)

*these authors contributed equally

Oltova, J, Svoboda, O & Bartunek, P. **Hematopoietic Cytokine Gene Duplication in Zebrafish Erythroid and Myeloid Lineages.** Frontiers in Cell and Developmental Biology, 2018, 6: **(review article)** (10.3389/fcell.2018.00174)

SUBMITTED MANUSCRIPTS:

Oltova, J, Svoboda, O, Machonova, O, Svatonova, P, Traver, D, Kolar, M, Bartunek, P. **Zebrafish Kit ligands cooperate with erythropoietin to promote erythroid cell expansion**, Blood Advances, 2020

A preprint version of the manuscript is available online (10.1101/2020.02.03.931634).

REFERENCES

Abbaspour Babaei, M., B. Kamalidehghan, M. Saleem, H. Z. Huri and F. Ahmadipour (2016). "Receptor tyrosine kinase (c-Kit) inhibitors: a potential therapeutic target in cancer cells." Drug Des Devel Ther **10**: 2443-2459.

Ablain, J., E. M. Durand, S. Yang, Y. Zhou and L. I. Zon (2015). "A CRISPR/Cas9 vector system for tissue-specific gene disruption in zebrafish." Dev Cell **32**(6): 756-764.

Ablain, J. and L. I. Zon (2013). "Of fish and men: using zebrafish to fight human diseases." Trends Cell Biol **23**(12): 584-586.

Akashi, K., D. Traver, T. Miyamoto and I. L. Weissman (2000). "A clonogenic common myeloid progenitor that gives rise to all myeloid lineages." Nature **404**(6774): 193-197.

Alestrom, P., L. D'Angelo, P. J. Midtlyng, D. F. Schorderet, S. Schulte-Merker, F. Sohm and S. Warner (2019). "Zebrafish: Housing and husbandry recommendations." Lab Anim: 23677219869037.

Alexander, W. S. (1999). "Thrombopoietin." Growth Factors **17**(1): 13-24.

Alexander, W. S. (1999). "Thrombopoietin and the c-Mpl receptor: insights from gene targeting." Int J Biochem Cell Biol **31**(10): 1027-1035.

Alexeev, V. and K. Yoon (2006). "Distinctive role of the cKit receptor tyrosine kinase signaling in mammalian melanocytes." J Invest Dermatol **126**(5): 1102-1110.

Alvarez-Dominguez, J. R., X. Zhang and W. Hu (2017). "Widespread and dynamic translational control of red blood cell development." Blood **129**(5): 619-629.

Amores, A., J. Catchen, A. Ferrara, Q. Fontenot and J. H. Postlethwait (2011). "Genome evolution and meiotic maps by massively parallel DNA sequencing: spotted gar, an outgroup for the teleost genome duplication." Genetics **188**(4): 799-808.

Anderson, J. L., M. L. Macurak, M. E. Halpern and S. A. Farber (2010). "A versatile aquatics facility inventory system with real-time barcode scan entry." Zebrafish **7**(3): 281-287.

Andrews, R. G., G. H. Knitter, S. H. Bartelmez, K. E. Langley, D. Farrar, R. W. Hendren, F. R. Appelbaum, I. D. Bernstein and K. M. Zsebo (1991). "Recombinant human stem cell factor, a c-kit ligand, stimulates hematopoiesis in primates." Blood **78**(8): 1975-1980.

Antonchuk, J., C. D. Hyland, D. J. Hilton and W. S. Alexander (2004). "Synergistic effects on erythropoiesis, thrombopoiesis, and stem cell competitiveness in mice deficient in thrombopoietin and steel factor receptors." Blood **104**(5): 1306-1313.

Ashman, L. K. (1999). "The biology of stem cell factor and its receptor C-kit." Int J Biochem Cell Biol **31**(10): 1037-1051.

Avery, S., L. Rothwell, W. D. Degen, V. E. Schijns, J. Young, J. Kaufman and P. Kaiser (2004). "Characterization of the first nonmammalian T2 cytokine gene cluster: the cluster contains functional single-copy genes for IL-3, IL-4, IL-13, and GM-CSF, a gene for IL-5 that appears to be a pseudogene, and a gene encoding another cytokinelike transcript, KK34." J Interferon Cytokine Res **24**(10): 600-610.

Bartunek, P., P. Pajer, V. Karafiat, G. Blendinger, M. Dvorak and M. Zenke (2002). "bFGF signaling and v-Myb cooperate in sustained growth of primitive erythroid progenitors." Oncogene **21**(3): 400-410.

Bartunek, P., L. Pichlikova, G. Stengl, G. Boehmelt, F. H. Martin, H. Beug, M. Dvorak and M. Zenke (1996). "Avian stem cell factor (SCF): production and characterization of the recombinant His-tagged SCF of chicken and its neutralizing antibody." Cytokine **8**(1): 14-20.

Bauer, A., F. Tronche, O. Wessely, C. Kellendonk, H. M. Reichardt, P. Steinlein, G. Schutz and H. Beug (1999). "The glucocorticoid receptor is required for stress erythropoiesis." Genes & Development **13**(22): 2996-3002.

Bertrand, J. Y., N. C. Chi, B. Santoso, S. Teng, D. Y. Stainier and D. Traver (2010). "Haematopoietic stem cells derive directly from aortic endothelium during development." Nature **464**(7285): 108-111.

Bertrand, J. Y., J. L. Cisson, D. L. Stachura and D. Traver (2010). "Notch signaling distinguishes 2 waves of definitive hematopoiesis in the zebrafish embryo." Blood **115**(14): 2777-2783.

Bertrand, J. Y., A. D. Kim, S. Teng and D. Traver (2008). "CD41+ cmyb+ precursors colonize the zebrafish pronephros by a novel migration route to initiate adult hematopoiesis." Development **135**(10): 1853-1862.

Bertrand, J. Y., A. D. Kim, E. P. Violette, D. L. Stachura, J. L. Cisson and D. Traver (2007). "Definitive hematopoiesis initiates through a committed erythromyeloid progenitor in the zebrafish embryo." Development **134**(23): 4147-4156.

Boatman, S., F. Barrett, S. Satishchandran, L. Jing, I. Shestopalov and L. I. Zon (2013). "Assaying hematopoiesis using zebrafish." Blood Cells Mol Dis **51**(4): 271-276.

Braasch, I., W. Salzburger and A. Meyer (2006). "Asymmetric evolution in two fish-specifically duplicated receptor tyrosine kinase paralogons involved in teleost coloration." Mol Biol Evol **23**(6): 1192-1202.

Broudy, V. C. (1997). "Stem cell factor and hematopoiesis." Blood **90**(4): 1345-1364.

Burger, A., H. Lindsay, J. Zaugg, A. Felker, C. Hess, C. Anders, L. M. Weber, R. Catena, N. E. Samson, I. Meyer, M. D. Robinson, M. Jinek and C. Mosimann (2015). Crispants: somatic mutagenesis with active CRISPR-Cas9 ribonucleoprotein complexes in zebrafish.

Butko, E., M. Distel, C. Pouget, B. Weijts, I. Kobayashi, K. Ng, C. Mosimann, F. E. Poulain, A. McPherson, C. W. Ni, D. L. Stachura, N. Del Cid, R. Espin-Palazon, N. D. Lawson, R. Dorsky, W. K. Clements and D. Traver (2015). "Gata2b is a restricted early regulator of hemogenic endothelium in the zebrafish embryo." Development **142**(6): 1050-1061.

Carroll, K. J. and T. E. North (2014). "Oceans of opportunity: exploring vertebrate hematopoiesis in zebrafish." Exp Hematol **42**(8): 684-696.

Castranova, D., A. Lawton, C. Lawrence, D. P. Baumann, J. Best, J. Coscolla, A. Doherty, J. Ramos, J. Hakkesteeg, C. Wang, C. Wilson, J. Malley and B. M. Weinstein (2011). "The effect of stocking densities on reproductive performance in laboratory zebrafish (Danio rerio)." Zebrafish **8**(3): 141-146.

Chabot, B., D. A. Stephenson, V. M. Chapman, P. Besmer and A. Bernstein (1988). "The proto-oncogene c-kit encoding a transmembrane tyrosine kinase receptor maps to the mouse W locus." Nature **335**(6185): 88-89.

Constantinescu, S. N., S. Ghaffari and H. F. Lodish (1999). "The Erythropoietin Receptor: Structure, Activation and Intracellular Signal Transduction." Trends Endocrinol Metab **10**(1): 18-23.

Cousin, X., T. Daouk, S. Pean, L. Lyphout, M. E. Schwartz and M. L. Begout (2012). "Electronic individual identification of zebrafish using radio frequency identification (RFID) microtags." J Exp Biol **215**(Pt 16): 2729-2734.

Crispino, J. D. and M. J. Weiss (2014). "Erythro-megakaryocytic transcription factors associated with hereditary anemia." Blood **123**(20): 3080-3088.

Davidson, A. J. and L. I. Zon (2004). "The 'definitive' (and 'primitive') guide to zebrafish hematopoiesis." Oncogene **23**(43): 7233-7246.

de Jong, J. L. and L. I. Zon (2005). "Use of the zebrafish system to study primitive and definitive hematopoiesis." Annu Rev Genet **39**: 481-501.

De Miguel, M. P., L. Cheng, E. C. Holland, M. J. Federspiel and P. J. Donovan (2002). "Dissection of the c-Kit signaling pathway in mouse primordial germ cells by retroviral-mediated gene transfer." Proc Natl Acad Sci U S A **99**(16): 10458-10463.

de Sauvage, F. J., P. E. Hass, S. D. Spencer, B. E. Malloy, A. L. Gurney, S. A. Spencer, W. C. Darbonne, W. J. Henzel, S. C. Wong, W. J. Kuang and et al. (1994). "Stimulation of megakaryocytopoiesis and thrombopoiesis by the c-Mpl ligand." Nature **369**(6481): 533-538.

Ding, K., K. Shameer, H. Jouni, D. R. Masys, G. P. Jarvik, A. N. Kho, M. D. Ritchie, C. A. McCarty, C. G. Chute, T. A. Manolio and I. J. Kullo (2012). "Genetic Loci implicated in erythroid differentiation and cell cycle regulation are associated with red blood cell traits." Mayo Clin Proc **87**(5): 461-474.

Ding, L., T. L. Saunders, G. Enikolopov and S. J. Morrison (2012). "Endothelial and perivascular cells maintain haematopoietic stem cells." Nature **481**(7382): 457-462.

Dolznig, H., P. Bartunek, K. Nasmyth, E. W. Mullner and H. Beug (1995). "Terminal differentiation of normal chicken erythroid progenitors: shortening of G1 correlates with loss of D-cyclin/cdk4 expression and altered cell size control." Cell Growth Differ **6**(11): 1341-1352.

Donnelly, C. J., M. McFarland, A. Ames, B. Sundberg, D. Springer, P. Blauth and C. J. Bult (2010). "JAX Colony Management System (JCMS): an extensible colony and phenotype data management system." Mamm Genome **21**(3-4): 205-215.

Drachman, J. G. and K. Kaushansky (1997). "Dissecting the thrombopoietin receptor: functional elements of the Mpl cytoplasmic domain." Proc Natl Acad Sci U S A **94**(6): 2350-2355.

Dzierzak, E. and S. Philipsen (2013). "Erythropoiesis: development and differentiation." Cold Spring Harb Perspect Med **3**(4): a011601.

England, S. J., K. E. McGrath, J. M. Frame and J. Palis (2011). "Immature erythroblasts with extensive ex vivo self-renewal capacity emerge from the early mammalian fetus." Blood **117**(9): 2708-2717.

Felker, A. and C. Mosimann (2016). "Contemporary zebrafish transgenesis with Tol2 and application for Cre/lox recombination experiments."

Force, A., M. Lynch, F. B. Pickett, A. Amores, Y. L. Yan and J. Postlethwait (1999). "Preservation of duplicate genes by complementary, degenerative mutations." Genetics **151**(4): 1531-1545.

Fuchs, O., O. Simakova, P. Klener, J. Cmejlova, J. Zivny, J. Zavadil and T. Stopka (2002). "Inhibition of Smad5 in Human Hematopoietic Progenitors Blocks Erythroid Differentiation Induced by BMP4." Blood Cells, Molecules, and Diseases **28**(2): 221-233.

Galloway, J. L. and L. I. Zon (2003). "Ontogeny of hematopoiesis: examining the emergence of hematopoietic cells in the vertebrate embryo." Curr Top Dev Biol **53**: 139-158.

Gandrillon, O., U. Schmidt, H. Beug and J. Samarut (1999). "TGF-beta cooperates with TGF-alpha to induce the self-renewal of normal erythrocytic progenitors: evidence for an autocrine mechanism." EMBO J **18**(10): 2764-2781.

Ganis, J. J., N. Hsia, E. Trompouki, J. L. de Jong, A. DiBiase, J. S. Lambert, Z. Jia, P. J. Sabo, M. Weaver, R. Sandstrom, J. A. Stamatoyannopoulos, Y. Zhou and L. I. Zon (2012). "Zebrafish globin switching occurs in two developmental stages and is controlled by the LCR." Dev Biol **366**(2): 185-194.

Geissler, E. N., M. A. Ryan and D. E. Housman (1988). "The dominant-white spotting (W) locus of the mouse encodes the c-kit proto-oncogene." Cell **55**(1): 185-192.

Ginhoux, F., M. Greter, M. Leboeuf, S. Nandi, P. See, S. Gokhan, M. F. Mehler, S. J. Conway, L. G. Ng, E. R. Stanley, I. M. Samokhvalov and M. Merad (2010). "Fate mapping analysis reveals that adult microglia derive from primitive macrophages." Science **330**(6005): 841-845.

Gong, Y., X. He, Q. Li, J. He, B. Bian, Y. Li, L. Ge, Y. Zeng, H. Xu and Z. Q. Yin (2019). "SCF/SCFR signaling plays an important role in the early morphogenesis and neurogenesis of human embryonic neural retina." Development **146**(20).

Gordon, M. S. and R. Hoffman (1992). "Growth factors affecting human thrombocytopoiesis: potential agents for the treatment of thrombocytopenia." Blood **80**(2): 302-307.

Grabbe, J., P. Welker, E. Dippel and B. M. Czarnetzki (1994). "Stem cell factor, a novel cutaneous growth factor for mast cells and melanocytes." Arch Dermatol Res **287**(1): 78-84.

Greter, M., I. Lelios, P. Pelczar, G. Hoeffel, J. Price, M. Leboeuf, T. M. Kundig, K. Frei, F. Ginhoux, M. Merad and B. Becher (2012). "Stroma-derived interleukin-34 controls the development and maintenance of langerhans cells and the maintenance of microglia." Immunity **37**(6): 1050-1060.

Guermonprez, P., J. Helft, C. Claser, S. Deroubaix, H. Karanje, A. Gazumyan, G. Darasse-Jeze, S. B. Telerman, G. Breton, H. A. Schreiber, N. Frias-Staheli, E. Billerbeck, M. Dorner, C. M. Rice, A. Ploss, F. Klein, M. Swiecki, M. Colonna, A. O. Kamphorst, M. Meredith, R. Niec, C. Takacs, F. Mikhail, A. Hari, D. Bosque, T. Eisenreich, M. Merad, Y. Shi, F. Ginhoux, L. Renia, B. C. Urban and M. C. Nussenzweig (2013). "Inflammatory Flt3l is essential to mobilize dendritic cells and for T cell responses during Plasmodium infection." Nat Med **19**(6): 730-738.

Hamilton, J. A. (2008). "Colony-stimulating factors in inflammation and autoimmunity." Nat Rev Immunol **8**(7): 533-544.

Hamilton, J. A. and A. Achuthan (2013). "Colony stimulating factors and myeloid cell biology in health and disease." Trends Immunol **34**(2): 81-89.

Harandi, O. F., S. Hedge, D. C. Wu, D. McKeone and R. F. Paulson (2010). "Murine erythroid short-term radioprotection requires a BMP4-dependent, self-renewing population of stress erythroid progenitors." J Clin Invest **120**(12): 4507-4519.

Hayman, M. J., S. Meyer, F. Martin, P. Steinlein and H. Beug (1993). "Self-renewal and differentiation of normal avian erythroid progenitor cells: regulatory roles of the TGF alpha/c-ErbB and SCF/c-kit receptors." Cell **74**(1): 157-169.

He, B. L., X. Shi, C. H. Man, A. C. Ma, S. C. Ekker, H. C. Chow, C. W. So, W. W. Choi, W. Zhang, Y. Zhang and A. Y. Leung (2014). "Functions of flt3 in zebrafish hematopoiesis and its relevance to human acute myeloid leukemia." Blood **123**(16): 2518-2529.

Heinrich, P. C., I. Behrmann, S. Haan, H. M. Hermanns, G. Muller-Newen and F. Schaper (2003). "Principles of interleukin (IL)-6-type cytokine signalling and its regulation." Biochem J **374**(Pt 1): 1-20.

Hensley, M. R., E. Hassenplug, R. McPhail and Y. F. Leung (2012). "ZeBase: an open-source relational database for zebrafish laboratories." Zebrafish **9**(1): 44-49.

Herbomel, P., B. Thisse and C. Thisse (1999). "Ontogeny and behaviour of early macrophages in the zebrafish embryo." Development **126**(17): 3735-3745.

Hoegg, S., H. Brinkmann, J. S. Taylor and A. Meyer (2004). "Phylogenetic timing of the fish-specific genome duplication correlates with the diversification of teleost fish." J Mol Evol **59**(2): 190-203.

Huang, E., K. Nocka, D. R. Beier, T. Y. Chu, J. Buck, H. W. Lahm, D. Wellner, P. Leder and P. Besmer (1990). "The hematopoietic growth factor KL is encoded by the Sl locus and is the ligand of the c-kit receptor, the gene product of the W locus." Cell **63**(1): 225-233.

Huang, T., J. Cui, L. Li, P. F. Hitchcock and Y. Li (2012). "The role of microglia in the neurogenesis of zebrafish retina." Biochem Biophys Res Commun **421**(2): 214-220.

Huber, T. L., Y. Zhou, P. E. Mead and L. I. Zon (1998). "Cooperative effects of growth factors involved in the induction of hematopoietic mesoderm." Blood **92**(11): 4128-4137.

Huising, M. O., C. P. Kruiswijk and G. Flik (2006). "Phylogeny and evolution of class-I helical cytokines." J Endocrinol **189**(1): 1-25.

Huising, M. O., C. P. Kruiswijk, J. E. van Schijndel, H. F. Savelkoul, G. Flik and B. M. Verburg-van Kemenade (2005). "Multiple and highly divergent IL-11 genes in teleost fish." Immunogenetics **57**(6): 432-443.

Hultman, K. A., N. Bahary, L. I. Zon and S. L. Johnson (2007). "Gene Duplication of the zebrafish kit ligand and partitioning of melanocyte development functions to kit ligand a." PLoS Genet **3**(1): e17.

Jacobsen, R. N., B. Nowlan, M. E. Brunck, V. Barbier, I. G. Winkler and J. P. Levesque (2016). "Fms-like tyrosine kinase 3 (Flt3) ligand depletes erythroid island macrophages and blocks medullar erythropoiesis in the mouse." Exp Hematol **44**(3): 207-212 e204.

Katakura, F., T. Yabu, T. Yamaguchi, J. Miyamae, Y. Shirinashihama, T. Nakanishi and T. Moritomo (2015). "Exploring erythropoiesis of common carp (Cyprinus carpio) using an in vitro colony assay in the presence of recombinant carp kit ligand A and erythropoietin." Dev Comp Immunol **53**(1): 13-22.

Kato, T., A. Matsumoto, K. Ogami, T. Tahara, H. Morita and H. Miyazaki (1998). "Native thrombopoietin: structure and function." Stem Cells **16 Suppl 2**: 11-19.

Kaushansky, K. (2006). "Lineage-specific hematopoietic growth factors." N Engl J Med **354**(19): 2034-2045.

Kaushansky, K., V. C. Broudy, A. Grossmann, J. Humes, N. Lin, H. P. Ren, M. C. Bailey, T. Papayannopoulou, J. W. Forstrom and K. H. Sprugel (1995). "Thrombopoietin expands erythroid progenitors, increases red cell production, and enhances erythroid recovery after myelosuppressive therapy." J Clin Invest **96**(3): 1683-1687.

Khajuria, R. K., M. Munschauer, J. C. Ulirsch, C. Fiorini, L. S. Ludwig, S. K. McFarland, N. J. Abdulhay, H. Specht, H. Keshishian, D. R. Mani, M. Jovanovic, S. R. Ellis, C. P. Fulco, J. M. Engreitz, S. Schutz, J. Lian, K. W. Gripp, O. K. Weinberg, G. S. Pinkus, L. Gehrke, A. Regev, E. S. Lander, H. T. Gazda, W. Y. Lee, V. G. Panse, S. A. Carr and V. G. Sankaran (2018). "Ribosome Levels Selectively Regulate Translation and Lineage Commitment in Human Hematopoiesis." Cell **173**(1): 90-103 e119.

Kirk, R. G. W. (2018). "Recovering The Principles of Humane Experimental Technique: The 3Rs and the Human Essence of Animal Research." Science Technology & Human Values **43**(4): 622-648.

Kissa, K., E. Murayama, A. Zapata, A. Cortes, E. Perret, C. Machu and P. Herbomel (2008). "Live imaging of emerging hematopoietic stem cells and early thymus colonization." Blood **111**(3): 1147-1156.

Kolbus, A., M. Blazquez-Domingo, S. Carotta, W. Bakker, S. Luedemann, M. von Lindern, P. Steinlein and H. Beug (2003). "Cooperative signaling between cytokine receptors and the

glucocorticoid receptor in the expansion of erythroid progenitors: molecular analysis by expression profiling." Blood **102**(9): 3136-3146.

Krantz, S. B. (1991). "Erythropoietin." Blood **77**(3): 419-434.

Krystal, G. (1994). "Transforming growth factor beta 1 is an inducer of erythroid differentiation." Journal of Experimental Medicine **180**(3): 851-860.

Kuil, L. E., N. Oosterhof, S. N. Geurts, H. C. van der Linde, E. Meijering and T. J. van Ham (2018).

Le Guyader, D., M. J. Redd, E. Colucci-Guyon, E. Murayama, K. Kissa, V. Briolat, E. Mordelet, A. Zapata, H. Shinomiya and P. Herbomel (2008). "Origins and unconventional behavior of neutrophils in developing zebrafish." Blood **111**(1): 132-141.

Leberbauer, C., F. Boulme, G. Unfried, J. Huber, H. Beug and E. W. Mullner (2005). "Different steroids co-regulate long-term expansion versus terminal differentiation in primary human erythroid progenitors." Blood **105**(1): 85-94.

Lennartsson, J. and L. Ronnstrand (2012). "Stem cell factor receptor/c-Kit: from basic science to clinical implications." Physiol Rev **92**(4): 1619-1649.

Lieschke, G. J. and P. D. Currie (2007). "Animal models of human disease: zebrafish swim into view." Nat Rev Genet **8**(5): 353-367.

Lieschke, G. J., D. Grail, G. Hodgson, D. Metcalf, E. Stanley, C. Cheers, K. J. Fowler, S. Basu, Y. F. Zhan and A. R. Dunn (1994). "Mice lacking granulocyte colony-stimulating factor have chronic neutropenia, granulocyte and macrophage progenitor cell deficiency, and impaired neutrophil mobilization." Blood **84**(6): 1737-1746.

Lieschke, G. J., E. Stanley, D. Grail, G. Hodgson, V. Sinickas, J. A. Gall, R. A. Sinclair and A. R. Dunn (1994). "Mice lacking both macrophage- and granulocyte-macrophage colony-stimulating factor have macrophages and coexistent osteopetrosis and severe lung disease." Blood **84**(1): 27-35.

Liongue, C. and A. C. Ward (2007). "Evolution of Class I cytokine receptors." BMC Evol Biol **7**: 120.

Liu, F., H. Y. Wu, R. Wesselschmidt, T. Kornaga and D. C. Link (1996). "Impaired production and increased apoptosis of neutrophils in granulocyte colony-stimulating factor receptor-deficient mice." Immunity **5**(5): 491-501.

Long, Q. M., A. M. Meng, H. Wang, J. R. Jessen, M. J. Farrell and S. Lin (1997). "GATA-1 expression pattern can be recapitulated in living transgenic zebrafish using GFP reporter gene." Development **124**(20): 4105-4111.

Macaulay, I. C., V. Svensson, C. Labalette, L. Ferreira, F. Hamey, T. Voet, S. A. Teichmann and A. Cvejic (2016). "Single-Cell RNA-Sequencing Reveals a Continuous Spectrum of Differentiation in Hematopoietic Cells." Cell Rep **14**(4): 966-977.

Mahony, C. B., R. J. Fish, C. Pasche and J. Y. Bertrand (2016). "tfec controls the hematopoietic stem cell vascular niche during zebrafish embryogenesis." Blood **128**(10): 1336-1345.

Mahony, C. B., C. Pasche and J. Y. Bertrand (2018). "Oncostatin M and Kit-Ligand Control Hematopoietic Stem Cell Fate during Zebrafish Embryogenesis." Stem Cell Reports **10**(6): 1920-1934.

Martinez, F. O. and S. Gordon (2014). "The M1 and M2 paradigm of macrophage activation: time for reassessment." F1000Prime Rep **6**: 13.

McNiece, I. K., K. E. Langley and K. M. Zsebo (1991). "Recombinant human stem cell factor synergises with GM-CSF, G-CSF, IL-3 and epo to stimulate human progenitor cells of the myeloid and erythroid lineages." Exp Hematol **19**(3): 226-231.

Mellgren, E. M. and S. L. Johnson (2005). "kitb, a second zebrafish ortholog of mouse Kit." Development Genes and Evolution **215**(9): 470-477.

Metcalf, D. (1985). "The granulocyte-macrophage colony-stimulating factors." Science **229**(4708): 16-22.

Metcalf, D. and N. A. Nicola (1983). "Proliferative effects of purified granulocyte colony-stimulating factor (G-CSF) on normal mouse hemopoietic cells." J Cell Physiol **116**(2): 198-206.

Migliaccio, A. R. and G. Migliaccio (1988). "Human embryonic hemopoiesis: control mechanisms underlying progenitor differentiation in vitro." Dev Biol **125**(1): 127-134.

Migliaccio, A. R., G. Migliaccio, A. D'Andrea, M. Baiocchi, S. Crotta, S. Nicolis, S. Ottolenghi and J. W. Adamson (1991). "Response to erythropoietin in erythroid subclones of the factor-dependent cell line 32D is determined by translocation of the erythropoietin receptor to the cell surface." Proc Natl Acad Sci U S A **88**(24): 11086-11090.

Miyagawa, S., M. Kobayashi, N. Konishi, T. Sato and K. Ueda (2000). "Insulin and insulin-like growth factor I support the proliferation of erythroid progenitor cells in bone marrow through the sharing of receptors." Br J Haematol **109**(3): 555-562.

Monson, C. A. and K. C. Sadler (2010). "Inbreeding Depression and Outbreeding Depression Are Evident in Wild-Type Zebrafish Lines." Zebrafish **7**(2): 189-197.

Mosimann, C., A. C. Puller, K. L. Lawson, P. Tschopp, A. Amsterdam and L. I. Zon (2013). "Site-directed zebrafish transgenesis into single landing sites with the phiC31 integrase system." Dev Dyn **242**(8): 949-963.

Mosimann, C. and L. I. Zon (2011). "Advanced zebrafish transgenesis with Tol2 and application for Cre/lox recombination experiments." Methods Cell Biol **104**: 173-194.

Muir, A. R. and D. N. Kerr (1958). "Erythropoiesis: an electron microscopical study." Q J Exp Physiol Cogn Med Sci **43**(1): 106-114.

Munugalavadla, V. and R. Kapur (2005). "Role of c-Kit and erythropoietin receptor in erythropoiesis." Crit Rev Oncol Hematol **54**(1): 63-75.

Nei, M. and A. K. Roychoudhury (1973). "Probability of fixation and mean fixation time of an overdominant mutation." Genetics **74**(2): 371-380.

Nicola, N. A. (1994). "Cytokine pleiotropy and redundancy: a view from the receptor." Stem Cells **12 Suppl 1**: 3-12; discussion 12-14.

Nicola, N. A., C. G. Begley and D. Metcalf (1985). "Identification of the human analogue of a regulator that induces differentiation in murine leukaemic cells." Nature **314**(6012): 625-628.

Nicola, N. A., D. Metcalf, M. Matsumoto and G. R. Johnson (1983). "Purification of a factor inducing differentiation in murine myelomonocytic leukemia cells. Identification as granulocyte colony-stimulating factor." J Biol Chem **258**(14): 9017-9023.

North, T. E., W. Goessling, C. R. Walkley, C. Lengerke, K. R. Kopani, A. M. Lord, G. J. Weber, T. V. Bowman, I. H. Jang, T. Grosser, G. A. Fitzgerald, G. Q. Daley, S. H. Orkin and L. I. Zon (2007). "Prostaglandin E2 regulates vertebrate haematopoietic stem cell homeostasis." Nature **447**(7147): 1007-1011.

Oltova, J., J. Jindrich, C. Skuta, O. Svoboda, O. Machonova and P. Bartunek (2018). "Zebrabase: An Intuitive Tracking Solution for Aquatic Model Organisms." Zebrafish **15**(6): 642-647.

Oltova, J., Svoboda, O., Machonova, O., Svatonova, P., Traver, D., Kolar, M., Bartunek, P. (submitted manuscript, 2020). "Zebrafish Kit ligands cooperate with erythropoietin to promote erythroid cell expansion."

Orkin, S. H. and K. Hochedlinger (2011). "Chromatin connections to pluripotency and cellular reprogramming." Cell **145**(6): 835-850.

Paffett-Lugassy, N., N. Hsia, P. G. Fraenkel, B. Paw, I. Leshinsky, B. Barut, N. Bahary, J. Caro, R. Handin and L. I. Zon (2007). "Functional conservation of erythropoietin signaling in zebrafish." Blood **110**(7): 2718-2726.

Pagan, A. J., C. T. Yang, J. Cameron, L. E. Swaim, F. Ellett, G. J. Lieschke and L. Ramakrishnan (2015). "Myeloid Growth Factors Promote Resistance to Mycobacterial Infection by Curtailing Granuloma Necrosis through Macrophage Replenishment." Cell Host Microbe **18**(1): 15-26.

Panzenbock, B., P. Bartunek, M. Y. Mapara and M. Zenke (1998). "Growth and differentiation of human stem cell factor/erythropoietin-dependent erythroid progenitor cells in vitro." Blood **92**(10): 3658-3668.

Parichy, D. M., J. F. Rawls, S. J. Pratt, T. T. Whitfield and S. L. Johnson (1999). "Zebrafish sparse corresponds to an orthologue of c-kit and is required for the morphogenesis of a subpopulation of melanocytes, but is not essential for hematopoiesis or primordial germ cell development." Development **126**(15): 3425-3436.

Patterson, L. B., E. J. Bain and D. M. Parichy (2014). "Pigment cell interactions and differential xanthophore recruitment underlying zebrafish stripe reiteration and Danio pattern evolution." Nat Commun **5**: 5299.

Paul, S. R., F. Bennett, J. A. Calvetti, K. Kelleher, C. R. Wood, R. M. O'Hara, Jr., A. C. Leary, B. Sibley, S. C. Clark, D. A. Williams and et al. (1990). "Molecular cloning of a cDNA encoding interleukin 11, a stromal cell-derived lymphopoietic and hematopoietic cytokine." Proc Natl Acad Sci U S A **87**(19): 7512-7516.

Pixley, F. J. and E. R. Stanley (2004). "CSF-1 regulation of the wandering macrophage: complexity in action." Trends Cell Biol **14**(11): 628-638.

Ransom, D. G., P. Haffter, J. Odenthal, A. Brownlie, E. Vogelsang, R. N. Kelsh, M. Brand, F. J. van Eeden, M. Furutani-Seiki, M. Granato, M. Hammerschmidt, C. P. Heisenberg, Y. J. Jiang, D. A. Kane, M. C. Mullins and C. Nusslein-Volhard (1996). "Characterization of zebrafish mutants with defects in embryonic hematopoiesis." Development **123**: 311-319.

Rasighaemi, P., F. Basheer, C. Liongue and A. C. Ward (2015). "Zebrafish as a model for leukemia and other hematopoietic disorders." J Hematol Oncol **8**: 29.

Ratnoff, O. D. (1987). "The evolution of hemostatic mechanisms." Perspect Biol Med **31**(1): 4-33.

Reya, T., S. J. Morrison, M. F. Clarke and I. L. Weissman (2001). "Stem cells, cancer, and cancer stem cells." Nature **414**(6859): 105-111.

Ribas, L., A. Valdivieso, N. Diaz and F. Piferrer (2017). "Appropriate rearing density in domesticated zebrafish to avoid masculinization: links with the stress response." J Exp Biol **220**(Pt 6): 1056-1064.

Russell, W. M. S. and R. L. Burch (1959). "The principles of humane experimental technique."

Schneider, W. and N. Gattermann (1994). "Megakaryocytes: origin of bleeding and thrombotic disorders." Eur J Clin Invest **24 Suppl 1**: 16-20.

Schroeder, C., L. Gibson, C. Nordstrom and H. Beug (1993). "The estrogen receptor cooperates with the TGF alpha receptor (c-erbB) in regulation of chicken erythroid progenitor self-renewal." EMBO J **12**(3): 951-960.

Simpson, C. F. (1967). "The Mechanism of Denucleation in Circulating Erythroblasts." The Journal of Cell Biology **35**(1): 237-245.

Spence, R., G. Gerlach, C. Lawrence and C. Smith (2008). "The behaviour and ecology of the zebrafish, Danio rerio." Biol Rev Camb Philos Soc **83**(1): 13-34.

Stachura, D. L., J. R. Reyes, P. Bartunek, B. H. Paw, L. I. Zon and D. Traver (2009). "Zebrafish kidney stromal cell lines support multilineage hematopoiesis." Blood **114**(2): 279-289.

Stachura, D. L., O. Svoboda, C. A. Campbell, R. Espin-Palazon, R. P. Lau, L. I. Zon, P. Bartunek and D. Traver (2013). "The zebrafish granulocyte colony-stimulating factors (Gcsfs): 2 paralogous cytokines and their roles in hematopoietic development and maintenance." Blood **122**(24): 3918-3928.

Stachura, D. L., O. Svoboda, R. P. Lau, K. M. Balla, L. I. Zon, P. Bartunek and D. Traver (2011). "Clonal analysis of hematopoietic progenitor cells in the zebrafish." Blood **118**(5): 1274-1282.

Steinlein, P., O. Wessely, S. Meyer, E. M. Deiner, M. J. Hayman and H. Beug (1995). "Primary, self-renewing erythroid progenitors develop through activation of both tyrosine kinase and steroid hormone receptors." Curr Biol **5**(2): 191-204.

Svoboda, O. and P. Bartunek (2015). "Origins of the Vertebrate Erythro/Megakaryocytic System." Biomed Res Int **2015**: 632171.

Svoboda, O., D. L. Stachura, O. Machonova, P. Pajer, J. Brynda, L. I. Zon, D. Traver and P. Bartunek (2014). "Dissection of vertebrate hematopoiesis using zebrafish thrombopoietin." Blood **124**(2): 220-228.

Svoboda, O., D. L. Stachura, O. Machonova, L. I. Zon, D. Traver and P. Bartunek (2016). "Ex vivo tools for the clonal analysis of zebrafish hematopoiesis." Nat Protoc **11**(5): 1007-1020.

Takahata, N. and T. Maruyama (1979). "Polymorphism and loss of duplicate gene expression: a theoretical study with application of tetraploid fish." Proc Natl Acad Sci U S A **76**(9): 4521-4525.

Tang, Q., S. Iyer, R. Lobbardi, J. C. Moore, H. Chen, C. Lareau, C. Hebert, M. L. Shaw, C. Neftel, M. L. Suva, C. J. Ceol, A. Bernards, M. Aryee, L. Pinello, I. A. Drummond and D. M. Langenau

(2017). "Dissecting hematopoietic and renal cell heterogeneity in adult zebrafish at single-cell resolution using RNA sequencing." J Exp Med **214**(10): 2875-2887.

Tornack, J., Y. Kawano, N. Garbi, G. J. Hammerling, F. Melchers and M. Tsuneto (2017). "Flt3 ligand-eGFP-reporter expression characterizes functionally distinct subpopulations of CD150(+) long-term repopulating murine hematopoietic stem cells." Eur J Immunol **47**(9): 1477-1487.

Touw, I. P. and G. J. van de Geijn (2007). "Granulocyte colony-stimulating factor and its receptor in normal myeloid cell development, leukemia and related blood cell disorders." Front Biosci **12**: 800-815.

Traver, D., B. H. Paw, K. D. Poss, W. T. Penberthy, S. Lin and L. I. Zon (2003). "Transplantation and in vivo imaging of multilineage engraftment in zebrafish bloodless mutants." Nat Immunol **4**(12): 1238-1246.

von Lindern, M., W. Zauner, G. Mellitzer, P. Steinlein, G. Fritsch, K. Huber, B. Lowenberg and H. Beug (1999). "The glucocorticoid receptor cooperates with the erythropoietin receptor and c-Kit to enhance and sustain proliferation of erythroid progenitors in vitro." Blood **94**(2): 550-559.

Wang, T., P. C. Hanington, M. Belosevic and C. J. Secombes (2008). "Two Macrophage Colony-Stimulating Factor Genes Exist in Fish That Differ in Gene Organization and Are Differentially Expressed." The Journal of Immunology **181**(5): 3310-3322.

Wang, Y., K. J. Szretter, W. Vermi, S. Gilfillan, C. Rossini, M. Cella, A. D. Barrow, M. S. Diamond and M. Colonna (2012). "IL-34 is a tissue-restricted ligand of CSF1R required for the development of Langerhans cells and microglia." Nat Immunol **13**(8): 753-760.

Watterson, G. A. (1983). "On the time for gene silencing at duplicate Loci." Genetics **105**(3): 745-766.

Wessely, O., A. Bauer, C. T. Quang, E. M. Deiner, M. von Lindern, G. Mellitzer, P. Steinlein, J. Ghysdael and H. Beug (1999). "A novel way to induce erythroid progenitor self renewal: cooperation of c-Kit with the erythropoietin receptor." Biol Chem **380**(2): 187-202.

Westerfield, M. (2000). A guide for the laboratory use of zebrafish (Danio rerio). 4th ed., Univ. of Oregon Press, Eugene.

Wickrema, A. and J. D. Crispino (2007). "Erythroid and megakaryocytic transformation." Oncogene **26**(47): 6803-6815.

Wu, S., R. Xue, S. Hassan, T. M. L. Nguyen, T. Wang, H. Pan, J. Xu, Q. Liu, W. Zhang and Z. Wen (2018). "Il34-Csf1r Pathway Regulates the Migration and Colonization of Microglial Precursors." Dev Cell **46**(5): 552-563 e554.

Yakulov, T. A. and G. Walz (2015). "Zebrafish Database: Customizable, Free, and Open-Source Solution for Facility Management." Zebrafish **12**(6): 462-469.

SUPPLEMENTARY DATA

Supplementary Table 1 | Statistics of differentially expressed genes in cells treated with Epo, Dex and Kitlga compared to cells treated with Epo, Dex only.

Ensembl Accession ID	symbol	log_2FoldChange	p-adjusted
ENSDARG00000114387	CU499336.2	-2.46	1.40E-25
ENSDARG00000098680	si:zfos-2326c3.2	-3.61	6.26E-23
ENSDARG00000044694	fybb	-2.36	4.25E-19
ENSDARG00000069542	si:dkey-8e10.2	3.01	5.19E-17
ENSDARG00000042722	blnk	-4.77	9.04E-16
ENSDARG00000101641	trpm2	-2.35	1.77E-14
ENSDARG00000102389	ved	-2.50	6.59E-14
ENSDARG00000060871	mctp1b	-3.31	6.27E-13
ENSDARG00000058476	stc1l	-3.10	3.74E-12
ENSDARG00000074283	inpp5d	-2.44	4.71E-12
ENSDARG00000069966	alox5b.3	1.30	8.62E-12
ENSDARG00000052826	runx3	-2.41	7.49E-11
ENSDARG00000037861	slc2a3b	-2.34	1.94E-10
ENSDARG00000104820	psd3l	-2.42	1.18E-09
ENSDARG00000076534	si:ch211-14a17.10	-3.59	1.28E-08
ENSDARG00000018263	pdia2	2.73	1.05E-07
ENSDARG00000057273	alox5a	-2.37	3.96E-07
ENSDARG00000077673	nlrp16	-6.32	9.60E-07
ENSDARG00000073686	heatr6	2.17	2.55E-06
ENSDARG00000068745	map4l	-2.40	8.18E-06
ENSDARG00000092862	si:ch211-260p9.3	-2.35	9.11E-06
ENSDARG00000022845	lias	3.25	9.80E-06
ENSDARG00000067672	card9	-3.64	1.02E-05
ENSDARG00000056258	cdc27	1.24	3.74E-05
ENSDARG00000094732	mical3b	-2.85	3.88E-05
ENSDARG00000045230	cox6b1	1.12	7.34E-05
ENSDARG00000100809	g6fl	1.58	8.46E-05
ENSDARG00000059933	plpp3	1.03	1.30E-04
ENSDARG00000062956	dagla	-2.59	2.12E-04
ENSDARG00000059925	usp24	1.01	2.12E-04
ENSDARG00000089582	si:dkey-265e15.2	-2.93	2.31E-04
ENSDARG00000013838	sulf2b	-2.95	4.49E-04
ENSDARG00000116660	pigrl2.3	-2.35	5.11E-04
ENSDARG00000042641	cyp51	1.48	5.66E-04
ENSDARG00000063527	elmo2	-4.40	6.38E-04
ENSDARG00000036776	aldh8a1	-2.75	9.79E-04
ENSDARG00000102097	nfkbiz	-2.42	1.13E-03
ENSDARG00000044774	pou5f3	-2.77	1.44E-03

ENSDARG00000018206	nck2a	2.55	1.56E-03
ENSDARG00000036728	si:dkey-211g8.1	-4.17	2.02E-03
ENSDARG00000021948	tnc	-2.70	2.62E-03
ENSDARG00000014386	galnt6	-2.47	2.68E-03
ENSDARG00000104890	si:ch211-76m11.3	6.07	5.99E-03
ENSDARG00000090038	BX248410.1	-2.72	6.08E-03
ENSDARG00000059832	adgrb3	-2.76	6.48E-03
ENSDARG00000077710	nlgn1	-3.42	8.15E-03
ENSDARG00000090164	si:ch73-362m14.2	-2.90	8.32E-03
ENSDARG00000057378	selenou1a	1.25	9.60E-03
ENSDARG00000060631	GARNL3	3.66	1.18E-02
ENSDARG00000062370	bcl2l13	1.02	1.40E-02
ENSDARG00000016470	anxa5b	-2.52	1.49E-02
ENSDARG00000099470	muc5.3	1.57	1.70E-02
ENSDARG00000003635	mogat3b	-2.32	1.71E-02
ENSDARG00000074590	wdpcp	2.36	1.86E-02
ENSDARG00000102395	CABZ01063602.1	3.48	2.07E-02
ENSDARG00000095142	si:ch211-208h16.4	2.63	2.27E-02
ENSDARG00000004318	cbwd	1.30	2.31E-02
ENSDARG00000044688	dusp4	1.03	2.32E-02
ENSDARG00000090369	zgc:86896	1.12	3.17E-02
ENSDARG00000079900	shroom4	1.12	3.62E-02
ENSDARG00000101214	pkd1l2b	1.21	3.81E-02
ENSDARG00000068400	znf131	1.72	4.40E-02
ENSDARG00000079946	sqlea	1.09	4.56E-02
ENSDARG00000058557	il11b	1.05	5.54E-02
ENSDARG00000008278	rcor2	1.47	6.54E-02
ENSDARG00000096849	si:dkey-16p21.8	1.13	6.64E-02

Supplementary Table 2 | Statistics of the difference in expression of selected erythroid genes in cells treated with Epo, Dex, Kitlga compared to cells treated with Epo, Dex only.

Ensembl Accession ID	symbol	log_2FoldChange	p-adjusted
ENSDARG00000002194	bcl2l13	1.02	1.40E-02
ENSDARG00000003462	rhd	0.84	5.84E-03
ENSDARG00000006818	tfr1a	0.55	1.06E-02
ENSDARG00000008840	hbae1.1	0.54	1.77E-01
ENSDARG00000010252	gata1a	0.52	5.65E-02
ENSDARG00000013477	bcl2l10	0.52	1.18E-01
ENSDARG00000017400	epb41b	0.49	3.78E-02
ENSDARG00000019930	hmbsa	0.48	6.30E-02
ENSDARG00000024295	slc11a2	0.45	9.81E-02
ENSDARG00000026766	hbaa1	0.38	3.55E-01
ENSDARG00000029019	ppox	0.38	1.89E-01
ENSDARG00000030490	klf1	0.37	2.68E-01
ENSDARG00000062370	sptb	0.35	1.71E-01
ENSDARG00000075641	urod	0.35	2.19E-01
ENSDARG00000088330	jak3	0.33	4.21E-01
ENSDARG00000097011	fech	0.32	2.76E-01
ENSDARG00000101322	steap3	0.32	4.57E-01
ENSDARG00000102167	tal1	0.32	3.54E-01

Supplementary Table 3 | GO enrichment analysis in in cells treated with Epo, Dex, Kitlga compared to cells treated with Epo, Dex only.

BIOLOGICAL PROCESSES

Accession	GO.Term	Odds.Ratio	P.value
GO:0000028	ribosomal small subunit assembly	60	6.34E-12
GO:0002181	cytoplasmic translation	53.8	2.63E-18
GO:0000027	ribosomal large subunit assembly	50	1.38E-12
GO:0042541	hemoglobin biosynthetic process	38.4	4.01E-07
GO:0030218	erythrocyte differentiation	31.1	3.08E-15
GO:0006412	translation	30.8	1.61E-73
GO:0048821	erythrocyte development	22.7	9.68E-06
GO:0043009	chordate embryonic development	18.7	1.55E-18
GO:0006414	translational elongation	17.8	2.65E-05
GO:0035162	embryonic hemopoiesis	15.1	2.91E-05
GO:0051726	regulation of cell cycle	12	1.42E-06

CELLULAR COMPARTMENT

Accession	GO.Term	Odds.Ratio	P.value
GO:0022625	cytosolic large ribosomal subunit	77	1.22E-52
GO:0022627	cytosolic small ribosomal subunit	72.9	9.55E-37
GO:0015935	small ribosomal subunit	70	1.05E-10
GO:0005840	ribosome	47.7	7.56E-82
GO:0015934	large ribosomal subunit	41.6	3.67E-06

MOLECULAR FUNCTION

Accession	GO.Term	Odds.Ratio	P.value
GO:0003735	structural constituent of ribosome	46.7	9.27E-80
GO:0019843	rRNA binding	31.8	1.67E-07
GO:0003723	RNA binding	5.14	5.75E-11

Script 1 | Optimized FiJi image analysis script for batch analysis of zebrafish benzidine staining in the tails. The script (IJ1 macro) was specifically optimized to distinguish brown benzidine staining from the black pigment cells, which were enhanced in some injection conditions. The Lab stack algorithm has been used for color thresholding. The properties the analysis can be finetuned by binary adjustments (e.g. Dilate, Erode, or Fill Holes).

```
input = getDirectory("Input directory");
output = getDirectory("Output directory");

Dialog.create("File type");
Dialog.addString("File suffix: ", ".jpg", 5);
Dialog.show();
suffix = Dialog.getString();
processFolder(input);

function processFolder(input) {
list = getFileList(input);
for (i = 0; i < list.length; i++) {
if(File.isDirectory(input + list[i]))
processFolder("" + input + list[i]);
if(endsWith(list[i], suffix))
processFile(input, output, list[i]);
}
}

function processFile(input, output, file) {
open(input + file);

name = getTitle;
dotIndex = indexOf(name, ".");
title = substring(name, 0, dotIndex);
selectWindow(name);
run("Duplicate...", "title = copy_" + name);
close(name);
selectWindow(title + "-1" + ".jpg");

min=newArray(3);
max=newArray(3);
filter=newArray(3);
a=getTitle();
run("Lab Stack");
run("Convert Stack to Images");
selectWindow("L*");
rename("0");
selectWindow("a*");
rename("1");
selectWindow("b*");
rename("2");
min[0]=6;
max[0]=255;
filter[0]="pass";
min[1]=6;
max[1]=166;
filter[1]="pass";
```

```
min[2]=0;
max[2]=162;
filter[2]="pass";
for (i=0;i<3;i++){
selectWindow(""+i);
setThreshold(min[i], max[i]);
run("Convert to Mask");
if (filter[i]=="stop")  run("Invert");
}
imageCalculator("AND create", "0","1");
imageCalculator("AND create", "Result of 0","2");
for (i=0;i<3;i++){
selectWindow(""+i);
close();
}
selectWindow("Result of 0");
close();
selectWindow("Result of Result of 0");
rename(a);
//run("Erode");
//run("Dilate");
//run("Fill Holes");
run("Analyze Particles...", "pixel display summarize");
saveAs("Tiff",  output + title + "_mask.tif");
run("Measure");
selectWindow("Results");
saveAs("Results",  output + title + ".xls");
run("Close");
run("Close");
print("Processing: " + input + file);
print("Saving to: " + output);
}
selectWindow("Summary");
saveAs("Results", output + "Results.xls");
run("Close");
selectWindow("Log");
run("Close");
```

Script 2 | Optimized FiJi image analysis script for batch analysis of colony forming assays. This script (IJ1 macro) was specifically developed for batch quantification of fluorescent colonies acquired on an automated upright microscope, where removing light scattering artifacts as well as small autofluorescent objects present in the semisolid media was necessary. The script is using bandpass filtering and thresholding. The properties of the analysis can be further adjusted using binary operations (e.g. Dilate, Erode, or Fill Holes).

```
input = getDirectory("Input directory");
output = getDirectory("Output directory");

Dialog.create("File type");
Dialog.addString("File suffix: ", ".jpg", 5);
Dialog.show();
suffix = Dialog.getString();

processFolder(input);

function processFolder(input) {
list = getFileList(input);
for (i = 0; i < list.length; i++) {
if(File.isDirectory(input + list[i]))
processFolder("" + input + list[i]);
if(endsWith(list[i], suffix))
processFile(input, output, list[i]);
}
}
function processFile(input, output, file) {
open(input + file);
name = getTitle;
dotIndex = indexOf(name, ".");
title = substring(name, 0, dotIndex);
selectWindow(name);
run("Duplicate...", "title=kopie1");
close(title);
selectWindow("kopie1");
run("8-bit");
//Filtering
//run("Subtract Background...", "rolling=100");
run("Bandpass Filter...", "filter_large=25000 filter_small=10 suppress=None tolerance=5");
//Thresholding
setAutoThreshold("IJ_IsoData dark");
run("Threshold...");
setThreshold(25, 255);
setOption("BlackBackground", true);
//Binary adjustments
run("Convert to Mask");
run("Erode");
run("Watershed");
run("Dilate");
run("Watershed");
selectWindow("Threshold");
run("Close");
//Analysis and saving of the mask and .txt files
```

```
47 run("Analyze Particles...", "size=10-25000 circularity=0.7-1 show=Masks display exclude clear
   summarize");
48 saveAs("Jpeg",  output + title + "_mask.jpg");
49 run("Close");
50 selectWindow("Summary");
51 saveAs("Results",  output + title + "_summary.txt");
52 run("Close");
53 selectWindow("Results");
54 saveAs("Results",  output + title + "_particles.txt");
55 run("Close");
56 run("Close");
57 print("Processing: " + input + file);
58 print("Saving to: " + output);
59 run("Close");
60 }
61 selectWindow("Log");
62 run("Close");
```

APPENDIX

Zebrafish Kit ligands cooperate with erythropoietin to promote erythroid cell expansion

Jana Oltova[1], Ondrej Svoboda[1,2], Olga Machonova[1], Petra Svatonova[1], David Traver[2], Michal Kolar[1], and Petr Bartunek[1]

[1] Institute of Molecular Genetics of the Czech Academy of Sciences, Prague, Czech Republic
[2] Department of Cellular and Molecular Medicine, University of California at San Diego, La Jolla, CA, USA.

Correspondence should be addressed to P.B.
bartunek@img.cas.cz

Key points:

- Kit signaling contributes to erythroid cell development and is conserved from fish to man
- Ex vivo expansion and self-renewal of zebrafish erythroid progenitors requires addition of recombinant Kitlga

Abstract

Kit ligand (Kitlg) is pleiotropic cytokine with a prominent role in vertebrate erythropoiesis. Although the role of Kitlg in this process has not yet been reported in *Danio rerio* (zebrafish), in the present study, we show that its function is evolutionary conserved. Zebrafish possess two copies of Kitlg genes (Kitlga and Kitlgb) due to whole genome duplication. To determine the role of each ligand in zebrafish, we performed a series of *ex vivo* and *in vivo* gain- and loss-of-function experiments. First, we tested the biological activity of recombinant Kitlg proteins in suspension culture from zebrafish whole kidney marrow and we demonstrate that Kitlga is necessary for expansion of erythroid progenitors *ex vivo*. To further address the role of *kitlga* and *kitlgb* in hematopoietic development *in vivo*, we performed gain-of-function experiments in zebrafish embryos, showing that both ligands cooperate with erythropoietin (Epo) to promote erythroid cell expansion. Finally, using the *kita* mutant (*kita*$^{b5/b5}$ or *sparse*), we show that Kita receptor is crucial for Kitlga/b cooperation with Epo in erythroid cells. In summary, using optimized suspension culture conditions with recombinant cytokines (Epo, Kitlga), we are reporting for the first time *ex vivo* suspension cultures of zebrafish hematopoietic progenitor cells, which can serve as an indispensable tool to study normal and aberrant hematopoiesis in zebrafish. Furthermore, we conclude that although partial functional diversification of Kit ligands has been described in other processes, in erythroid development, both paralogs play a similar role and their function is evolutionary conserved.

blood advances

American Society of Hematology
2021 L Street NW, Suite 900,
Washington, DC 20036
Phone: 202-776-0544 | Fax 202-776-0545
bloodadvances@hematology.org

Zebrafish Kit ligands cooperate with erythropoietin to promote erythroid cell expansion

Tracking no: ADV-2020-001700

Jana Oltova (Institute of Molecular Genetics of the Czech Academy of Sciences, Czech Republic) Ondrej Svoboda (Department of Cellular and Molecular Medicine, University of California at San Diego, La Jolla, CA, United States) Olga Machonova (Institute of Molecular Genetics of the Czech Academy of Sciences, Czech Republic) Petra Svatonova (Institute of Molecular Genetics of the Czech Academy of Sciences, Czech Republic) David Traver (University of California, San Diego, United States) Michal Kolar (Institute of Molecular Genetics of the Czech Academy of Sciences, Czech Republic) Petr Bartunek (Institute of Molecular Genetics of the Czech Academy of Sciences, Czech Republic)

Abstract:
Kit ligand (Kitlg) is pleiotropic cytokine with a prominent role in vertebrate erythropoiesis. Although the role of Kitlg in this process has not yet been reported in Danio rerio (zebrafish), in the present study, we show that its function is evolutionary conserved. Zebrafish possess two copies of Kitlg genes (Kitlga and Kitlgb) due to whole genome duplication. To determine the role of each ligand in zebrafish, we performed a series of ex vivo and in vivo gain- and loss-of-function experiments. First, we tested the biological activity of recombinant Kitlg proteins in suspension culture from zebrafish whole kidney marrow and we demonstrate that Kitlga is necessary for expansion of erythroid progenitors ex vivo. To further address the role of kitlga and kitlgb in hematopoietic development in vivo, we performed gain of function experiments in zebrafish embryos, showing that both ligands cooperate with erythropoietin (Epo) to promote erythroid cell expansion. Finally, using the kita mutant (kitab5/b5 or sparse), we show that Kita receptor is crucial for Kitlga/b cooperation with Epo in erythroid cells. In summary, using optimized suspension culture conditions with recombinant cytokines (Epo, Kitlga), we are reporting for the first time ex vivo suspension cultures of zebrafish hematopoietic progenitor cells, which can serve as an indispensable tool to study normal and aberrant hematopoiesis in zebrafish. Furthermore, we conclude that although partial functional diversification of Kit ligands has been described in other processes, in erythroid development, both paralogs play a similar role and their function is evolutionary conserved.

Conflict of interest: No COI declared

COI notes:

Preprint server: Yes; bioRxiv 10.1101/2020.02.03.931634

Author contributions and disclosures: J.O., O.M., O.S. performed the experiments, J.O, O.S., P.S., D.T., M.K. and P.B. designed the experiments, analyzed the data and wrote the manuscript.

Non-author contributions and disclosures: Yes; Trevor Epp (Institute of Molecular Genetics, member of the Bartunek lab) edited the manuscript as native speaker for typos and grammar. He was funded from Ministry of Education, Youth and Sports - Program NPU I (LO1419) - the same source as the work performed in the manuscript.

Agreement to Share Publication-Related Data and Data Sharing Statement: RNAseq data are available in ArrayExpress under accession number E-MTAB-8800. Plasmids for cytokine expression are available via Addgene with the accession numbers 140292 (pAc-His-zfKitlga) and 140293 (pAc-His-zfKitlgb).

Clinical trial registration information (if any):

Zebrafish Kit ligands cooperate with erythropoietin to promote erythroid cell expansion

Jana Oltova[1], Ondrej Svoboda[1,2], Olga Machonova[1], Petra Svatonova[1], David Traver[2], Michal Kolar[1], and Petr Bartunek[1]

[1] Institute of Molecular Genetics of the Czech Academy of Sciences, Prague, Czech Republic
[2] Department of Cellular and Molecular Medicine, University of California at San Diego, La Jolla, CA, USA.

Corresponding author:

Petr Bartunek

Institute of Molecular Genetics of the Czech Academy of Sciences
Videnska 1083, 142 20 Prague 4, Czech Republic

+420 296 443 117
bartunek@img.cas.cz

Short title (max 50 characters): Kitlg and Epo cooperation in erythropoiesis

Word count - main text: 3922

Word count – supplemental information: 676

Word count - abstract: 244

Figure/table count: 4 figures, 3 supplemental figures, 6 supplemental tables

Reference count: 51

Key points:

- Kit signaling contributes to erythroid cell development and is conserved from fish to man
- Ex vivo expansion and self-renewal of zebrafish erythroid progenitors requires addition of recombinant Kitlga

Abstract

Kit ligand (Kitlg) is pleiotropic cytokine with a prominent role in vertebrate erythropoiesis. Although the role of Kitlg in this process has not yet been reported in *Danio rerio* (zebrafish), in the present study, we show that its function is evolutionary conserved. Zebrafish possess two copies of Kitlg genes (Kitlga and Kitlgb) due to whole genome duplication. To determine the role of each ligand in zebrafish, we performed a series of *ex vivo* and *in vivo* gain- and loss-of-function experiments. First, we tested the biological activity of recombinant Kitlg proteins in suspension culture from zebrafish whole kidney marrow and we demonstrate that Kitlga is necessary for expansion of erythroid progenitors *ex vivo*. To further address the role of *kitlga* and *kitlgb* in hematopoietic development *in vivo*, we performed gain-of-function experiments in zebrafish embryos, showing that both ligands cooperate with erythropoietin (Epo) to promote erythroid cell expansion. Finally, using the *kita* mutant (*kita*$^{b5/b5}$ or *sparse*), we show that Kita receptor is crucial for Kitlga/b cooperation with Epo in erythroid cells. In summary, using optimized suspension culture conditions with recombinant cytokines (Epo, Kitlga), we are reporting for the first time *ex vivo* suspension cultures of zebrafish hematopoietic progenitor cells, which can serve as an indispensable tool to study normal and aberrant hematopoiesis in zebrafish. Furthermore, we conclude that although partial functional diversification of Kit ligands has been described in other processes, in erythroid development, both paralogs play a similar role and their function is evolutionary conserved.

Introduction

The most prominent cytokines that regulate proliferation and differentiation of erythroid cells in vertebrates are erythropoietin (EPO)[1-3] and Kit ligand (KITLG or stem cell factor, SCF)[4-9]. As was described in other vertebrates but not in zebrafish, binding of EPO and KITLG to their cognate receptors ensures erythroid lineage commitment by triggering specific signaling events[1,8,10,11].

Besides its role in erythropoiesis, KITLG acts pleiotropically, affecting a wide range of tissues and cells, including hematopoietic (HSCs) and germ stem cells [12-14]. It is an important regulator that plays a role in many processes, both during ontogenesis and in the adult organism[13,15]. In mammals, KIT signaling is associated with erythro-myelopoiesis[16], as well as neurogenesis and pigmentation[13,17-19]. Interestingly, there are two forms of KITLG occurring *in vivo* – transmembrane, important for the regulation of stem cells in their niches, and soluble, affecting more distant tissues[13,20]. Binding of KITLG to its receptor KIT, a member of receptor tyrosine kinase type-III family, leads to its autophosphorylation, further triggering various signaling cascades, including PI-3K, MAPK, SRC and JAK kinase pathways[20,21].

In teleost species that include zebrafish, this scenario is more complex due to the fact that the whole ligand-receptor signalosome has been duplicated as a result of an extra round of whole genome duplication. Future studies are therefore dependent on the understanding of diversification of the functions of both ligands (Kitlga, Kitlgb) and receptors (Kita, Kitb) and their binding specificities. Similarly, there are also two copies of the *epo* gene present in the zebrafish genome - *epoa* and *epob*. The zebrafish *epoa* seems to play a similar role as its mammalian ortholog[22,23] but no role in hematopoiesis has been so far reported for *epob (OS, PB, unpublished).* For simplicity, we will use the designation Epo/*epo* for Epoa/*epoa* in this study.

Current data support the hypothesis that Kit receptor and Kit ligand paralogs have subspecialized during evolution. Kita is expressed in the neural crest, lateral line and notochord[24]. Overexpression of Kitlga results in hyper-pigmentation[25] and *kita* receptor mutants (*kita*$^{b5/b5}$ or *sparse*) have defective pigmentation[24]. On the other hand, the second zebrafish Kit paralog, Kitb, is expressed in neural tube and otic vesicles and likely does not play a role in melanogenesis[26,27]. Neither has a role in melanogenesis been reported for Kitlgb[27].

Although studied extensively, the role of Kit signaling in zebrafish hematopoiesis has remained unknown for a long time. So far, there are only two studies that suggest potential roles of Kitlg in hematopoiesis in *D. rerio*. The first shows a mild increase of HSCs upon overexpression of Kitlgb[28], the second reports a decrease in the number of HSCs upon downregulation of Kitb; however, no such phenotype was observed

for Kita or Kitlga. Based on that, the authors concluded that neither Kita nor Kitlga are involved in hematopoiesis, but only in melanocyte formation, as suggested by previous studies[27]. Contradictory to the findings in other vertebrate models, and despite the fact that Kit receptors are expressed in hematopoietic tissues[24,27], hematopoiesis is not affected in the adult *kita* mutants (*kita*$^{b5/b5}$ or *sparse*)[24] under steady-state conditions.

The utilization of zebrafish as a model organism requires understanding of the regulatory mechanisms of hematopoietic lineage development and their evolutionary conservation, as well as proper approaches to study blood development and disease. The objective of this study is to better understand the importance of Kit ligands in zebrafish hematopoiesis, and thus providing important insights for further research of hematopoietic development. Although *ex vivo* expansion of erythroid progenitors has been reported in different vertebrate organisms[29], a similar approach that would enable analysis of normal and aberrant hematopoiesis in zebrafish is not yet available. Here, we establish suspension culture conditions for the expansion of zebrafish erythroid progenitors and we investigate the role of the two zebrafish paralogs of Kit ligands (Kitlg) in zebrafish hematopoiesis using *in vivo* and *ex vivo* experimental approaches.

Methods

Animal stocks and embryos

Fish were mated, raised and staged according to "The zebrafish book. A guide for the laboratory use of zebrafish (*Danio rerio*)"[30] and the recommendations for zebrafish husbandry and housing[31]. For tracking the animals (age, number, health, genotype), we used an in-house developed dedicated database solution called Zebrabase[32]. Fish were kept in ZebTEC aquatic system (Tecniplast). Transgenic reporter lines expressing fluorescent genes under the control of tissue specific promoters (*gata1*:*DsRed*[33] and *LCR:GFP*[34], as well as mutant lines (kita$^{b5/b5}$ or *sparse*)[24] and wild-type animals WT(AB) were used in this study. For *ex vivo* experiments, 6-month old fish were used to ensure optimal number and state of whole kidney marrow cells. Animal care and experiments were approved by the Animal Care Committee of the Institute of Molecular Genetics, Czech Academy of Sciences (13/2016 and 96/2018) in compliance with national and institutional guidelines.

Ex vivo cultures

Zebrafish whole kidney marrow cells were isolated as previously described[35]. Cells were plated and cultivated in zfS13 medium (for composition see Supplemental Table 3). Carp serum was obtained by the procedure described and published previously[35]. Specific cytokines and growth factors were added at final

concentrations of (100 ng/ml), dexamethasone was added at final 1µM. One third of the medium was exchanged every other day to ensure optimal growth of the cells. To study the clonogenic potential of the whole kidney marrow cells after addition of different cytokines, we performed clonal assays in semisolid media (methylcellulose), which prevents movement of the single cells plated in it. For the detailed protocol for these assays, please refer to Svoboda et al., 2016[35].

Cytokine cloning and expression

First, the amino acid sequence of zebrafish Kitlga/b, was subjected to protein structure prediction and hydrophobicity analysis using Phobius tool (http://phobius.sbc.su.se/). Two large hydrophobic regions (amino acid positions 1 to 24 and 206 to 224 for Kitlga, and amino acid positions 1 to 31 and 185 to 209 for Kitlgb) corresponding to the putative signal peptide (SP) and transmembrane (TM) domains, respectively, were identified (Supplemental Figure 1A). To generate a Kitlga/b version devoid of both domains, sequence specific primers (Supplemental Table 1) were used for PCR amplification of each Kitlg cDNA fragment corresponding to amino acid 25 to 182 (Kitlga) and 31 to 187 (Kitlgb) from adult zebrafish retina. We used the baculovirus expression system to produce soluble Kitlga/b in large quantities. We cloned the amplified fragment into modified pAc-GP67-B vector containing 6xHis and generated the recombinant baculovirus by co-transfection of pAc-His-Kitlga/b and BaculoGold Bright Baculovirus DNA into sf21 insect cells. Virus-infected cells expressed GFP and secrete recombinant His-Kitlga/b extracellularly. Finally, we purified the secreted proteins on a Ni2+-NTA agarose column and used them for the following experiments (Supplemental Figure 2B). To generate Kitlga/b the construct for mRNA injection experiments, the full length cDNA fragment was amplified using RT-PCR using sequence specific primers (Supplemental Table 1). Erythropoietin protein and mRNA has been prepared as previously described[22,35,36].

Additional methods

For experimental details on the generation of recombinant cytokines, mRNA microinjection, benzidine staining, image analysis, qPCR, FACS-sorting, RNAseq and transcriptomics, please refer to supplemental methods.

Data sharing statement

RNAseq data are available in ArrayExpress under accession number E-MTAB-8800. Plasmids for cytokine expression are available via Addgene with the accession numbers 140292 (pAc-His-zfKitlga) and 140293 (pAc-His-zfKitlgb).

Results

Kit ligands promote erythroid and myeloid expansion of whole kidney marrow cells.

First, we cloned and expressed recombinant zebrafish Kitlga and Kitlgb. We amplified the mature form of zebrafish *kitlga* and *kitlgb* lacking the signal peptide-encoding region, intracellular and transmembrane region (Supplemental Figure 1A) from adult retina and we produced recombinant Kitlga and Kitlgb in sf21 insect cells (Supplemental Figure 1B). His-tagged purified proteins were used in the following experiments.

To test the biological activity of Kitlg proteins, we designed an experiment using whole kidney marrow cells isolated from adult, 6-month old zebrafish. To reveal differences that would suggest biological activity and potential cooperation of Kitlg proteins with other recombinant cytokines, we treated the cells with various factors, or their combination, and subsequently counted them at specific time points. After 3 days in culture, the potential enhancement in the myeloid lineage was assessed. We added both Kit ligands, either separately or combined with Gcsfa, which has been previously shown to support myeloid cell fate[37]. Interestingly, we observed an increase in the number of cells in all the conditions tested when compared to untreated control. In agreement with previously published studies, Gcsfa promoted significantly the growth of whole kidney marrow cells, and the effect was further potentiated by the addition of either of the Kit ligands. The Kit ligands alone exhibited reproducible mild activity that was, however, statistically not significant (Figure 1A).

Next, we tested the activity of Kit ligands during erythroid cell expansion. Cells were treated with both Kitlga and Kitlgb, either separately or combined with Epo. The increase in cell number was quantified after 7 days in culture. In agreement with previously published studies[22,36], Epo boosted cell growth significantly and again, there was a mild increase in the number of the cells when treated with any of the Kit ligands alone. Strikingly, when Epo was combined with Kitlga, we measured a significant increase in the number of cells at 7 days in culture compared to Epo alone (Figure 1B).

With the aim of maximum expansion of erythroid progenitors, we decided to improve the conditions for suspension culture of whole kidney marrow cells. Although there were no existing reports of suspension culture of zebrafish or hematopoietic progenitor cells, we supposed that similar conditions might be effective in suspension cultures as was shown in human and mouse [10,38]. As different steroids were reported as important players in the maintenance of self-renewal and proliferation of erythroid progenitors in chicken, mouse and human [38-41], we included dexamethasone and tested different concentrations and combinations of all three factors.

We found that, in line with previous findings in other vertebrates, Kitlga, Epo and Dex act synergistically in *ex vivo* cultures, enabling erythroid expansion (Figure 1C, left). When compared to the cells treated with Epo and Dex, cells treated with Epo, Dex and Kitlga formed islets of round, highly *gata1:DsRed*-positive cells, corresponding to erythroid progenitors (Figure 1C, right). Additionally, we observed that Epo can cooperate with Kitlga to promote the growth of large erythroid colonies in colony forming assays in methylcellulose (Supplemental Figure 2C). When Kitlga was combined with Epo in kidney marrow culture from *gata1:DsRed* transgenic fish, we observed significantly more, highly *gata1*:DsRed positive colonies that were also significantly larger (Supplemental Figure 2A,B) However, no similar effect was observed after the addition of Kitlgb in either liquid or semisolid media (data not shown).

Kitlga treatment, when combined with Epo and dexamethasone, leads to upregulation of erythroid-, translation- and cell cycle-related gene expression

To gain deeper insight into the mechanism of Kitlga action when combined with Epo and Dex in kidney marrow suspension cultures, we performed an RNAseq experiment, comparing samples from Epo, Dex, Kitlga and Epo, Dex-treated cells. Samples were collected after 8 days in culture. This was the first time-point where we could observe a significant increase in proliferation of erythroid cells in the presence of Epo, Dex and Kitlga, as shown in the growth curve (Figure 1C, left).

RNAseq analysis revealed that both culture conditions resulted in high expression of erythroid marker genes (data not shown). However, addition of Kitlga to the Epo, Dex combination caused an additional increase in expression of erythroid genes. Among the upregulated differentially expressed genes (see heatmap in Figure 1D and Supplemental Table 4), we identified several erythroid (*g6fl*, *lias*) and cell cycle (*cdc27*) specific genes, confirming additional Kitlga-mediated erythroid cell expansion over Epo and Dex treatment alone. On the contrary, downregulated genes were mostly linked to the myeloid cell lineage (*pigrl2*.3, *blnk*, *nfkbiz*, *alox5a*, *inpp5d*), providing further evidence that Epo, Dex, Kitlga-induced expansion led to a more enriched erythroid cell population as compared to Epo, Dex culture alone. Next, we examined the expression of both kit receptor and revealed that the expression of kita is predominant in adult erythroid progenitor cells (average raw counts 285 (kita) vs. 3 (kitb)).

Finally, we were interested specifically in changes in expression of erythroid-specific genes. The analysis of RNAseq data reveled that, compared to cells treated with Epo and Dex, cells treated with Epo, Dex and Kitlga display higher expression of many of the important erythroid genes – namely globins (*hbae1.1*, *hbaa1*), genes involved in heme and iron metabolism (e.g. *urod*, *slc11a2*, *steap3*), erythroid cytoskeleton (e.g. *rhd*, *sptb*, *eph41b*) and signaling (*gata1a*, *jak3*) (Figure 1E, Supplemental Table 5). Based on GO

prediction, we revealed an enrichment in specific categories of biological processes – namely in translation (GO:0006412, GO:0002181, GO:0000028, GO:0000027), erythropoiesis (GO:0042541, GO:0030218, GO:0048821) and cell cycle regulation (GO:0051726). For a full list of enriched GO terms in all three standard GO term categories, refer to Supplemental Table 6.

Both Kit ligands cooperate with Epo to promote erythroid expansion in zebrafish embryos

To test the function of both Kit ligands *in vivo*, we microinjected cytokine mRNA(s) into 1-cell stage embryos. When combined with *epo*, both *kitlga* and *kitlgb* showed an enhancement in *gata1*:*DsRed* expression (Figure 2A) and hemoglobinization (Figure 2B) at 72 hpf compared to *epo* alone. Quantification of benzidine staining in the tails of 72 hpf embryos confirmed the observed trend. Quantitative PCR (qPCR) analysis from whole injected embryos also showed an increase in the expression of erythroid markers at 72 hpf (Figure 2D) when *epo* was combined with either of the ligands, however, these changes were rather subtle. Finally, in agreement with previous studies, we observed increased number of melanocytes after the overexpression of Kitlga but not Kitlgb (Figure 2B).

The expression of both kit receptors is gradually increasing during embryonic development

To better understand the mechanism of cooperation of Epo with Kit ligands, we first analyzed the expression of both kit receptors in tissues and during the development by qPCR. Among all the tissues analyzed, the highest *kita* expression was observed in kidney (Supplemental Figure 3A) while the highest kitb expression was observed in the retina (Supplemental Figure 3B). During embryonic zebrafish development, the highest relative expression was observed at 72 hpf for both *kita* and *kitb* (Figure 3A). As we saw a significant expansion of erythroid, *gata1:DsRed*+ cells in *ex vivo* cultures, we aimed to analyze the dynamics of the receptor expression in erythroid cells during development. Therefore, we collected samples from 24 hpf, 48 hpf and 72 hpf *gata1:DsRed* and *LCR:GFP* embryos and FACS-sorted *gata1*:*DsRed*-positive cells (Figure 3B) or *LCR*:*GFP*-positive cells (Figure 3C), respectively. In both cases, we found that there is a gradually increasing expression of both receptors in erythroid cells during the course of early development (Figure 3D).

Kita mediates Kitlg-dependent erythroid expansion in vivo

To understand the molecular basis of the effect we observed on erythroid cells, we used the *sparse* mutant (*kita*$^{b5/b5}$) zebrafish, lacking the functional Kita receptor. In general, we noticed slightly decreased number of erythrocytes in the uninjected mutants compared to wild-type embryos (data not shown). Next, we injected mRNA for *epo*, *kitlga* and *kitlgb* and we observed that in *sparse* mutants, the effect of cooperation

between any of the *kitlg* and *epo* is lost; however, the effect of *epo* alone was comparable to the wild-type animals (Figure 4A). These findings are also supported by qPCR data showing that the expression of β-globin (*hbbe1*) and *gata1a* is not increased after the injection of *epo* with either of the kit ligands, as is the case in wild-type embryos (Figure 4B).

To summarize, we have cloned and expressed both Kit ligand zebrafish paralogs. Using the purified recombinant proteins, we tested various cytokine combinations in suspension culture of whole kidney marrow cells and defined an optimal factor combination, composed of Epo, Kitlga and dexamethasone, which enables efficient expansion of erythroid progenitors. Also, we tested gain of function effect of both *kitlga and kitlgb* in embryonic hematopoiesis and observed an increase in the number of erythroid cells in *epo, kitlgb* and *epo, kitlgb* mRNA-injected fish compared to *epo* alone. Finally, by employing the *kita* (*sparse*) mutants, we showed that Kita is mediating Kitlg-dependent erythroid expansion *in vivo*.

Discussion

In this study, we explored the role of zebrafish Kit ligands in hematopoiesis. In zebrafish, multiple paralogs of many important genes resulted from an extra round of whole genome duplication 250-350 million years ago[42,43], including hematopoietic cytokines. After such an event, the process of pseudogenization often leads to a loss of function of one of the paralogs[44-46]. Alternatively, paralogs of an ancestral gene can either remain functionally redundant, split the original function between the two (subfunctionalization), or acquire completely new functions (neofunctionalization)[47]. Here, we studied the hematopoietic function of two retained zebrafish paralogs of a crucial hematopoietic cytokine, the Kit ligand (KITL or Stem Cell Factor – SCF), designated as Kitlga and Kitlgb.

So far, KIT signaling has not been associated with erythropoiesis in zebrafish [24,25]. This is in contrast with previous studies in human[8], mouse[4] and chicken[9,16,48], where it has been shown that KITL is critical for proper erythroid development[5,15,49]. By focusing on Kit function during erythropoiesis in zebrafish, we were able to prove for the first time, using *ex vivo* and *in vivo* gain- and loss-of-function experiments, that Kit signaling does indeed play a role in zebrafish erythroid differentiation. Based on RNAseq and GO analysis, this likely happens in a similar manner as in other vertebrate species / via induction of cell proliferation coupled with differentiation[40,48], promoting cell cycle progression and enhancing protein translation in differentiating cells.

To examine the role of Kit ligands *ex vivo*, we used clonal assays and liquid culture experiments[23,36,37,50]. Since the reported cross-reactivity of mammalian hematopoietic cytokines in zebrafish is very limited[35], it was essential to use *bona fide* zebrafish Kit ligands as recombinant proteins. Similarly as described for other cytokines[7,9,35,36], we cloned the extracellular portion of the corresponding cDNAs, lacking the N-terminal signal peptide, transmembrane domain and cytosolic part of both cytokines. This approach allowed us to generate soluble form of Kit ligands to stimulate kidney marrow progenitor cells *ex vivo*[8,13].

As a result, treatment of hematopoietic progenitor cells isolated from kidney marrow with Kitlga, but not Kitlgb, in combination with the other master regulator of erythroid lineage commitment, Epo[22,23], enabled erythroid expansion of cells in suspension cultures and clonal assays, as in other vertebrates[1,8,10,11]. Next, we also tested the activity of dexamethasone (Dex) in addition to Epo and Kitlga. Dex is a glucocorticoid receptor agonist that has been reported to support self-renewal and differentiation of erythroid progenitors[10,38-40] and indeed, addition of Dex to Kitlga and Epo led to synergistic erythroid expansion in suspension cultures.

To understand the mechanism triggering this substantial cell expansion, we performed an RNAseq experiment. We decided to compare the effect of Epo and Dex versus Epo, Dex, and Kitlga treatment on adult kidney marrow cells. Transcriptional profiling showed expression of erythroid specific genes in both conditions, as expected due to Epo-mediated signaling. However, we observed relatively subtle changes in expression between the Epo and Dex and the Epo, Dex, and Kitlga cultures. The trends of expression changes showed a distinct erythroid fingerprint in cells treated with Epo, Dex and Kitlga, compared to a more mixed/myeloid one in cells treated with Epo and Dex alone, as suggested by the increased expression of myeloid-specific genes. In addition, we found that the prominent receptor expressed in adult erythroid progenitor cells is kita, indicating that the effect of erythroid expansion is mediated by this receptor. This corresponds to the fact that isolation of kidney marrow cells yields, in addition to progenitor cells, also a fraction of myeloid cells with the ability to survive in the culture. However, this effect becomes negligible during erythroid expansion of cells treated with Epo, Dex, and Kitlga, when myeloid cells are overgrown by expanding erythroid progenitors. Importantly, gene ontology analysis revealed an enrichment especially in translation and expression of erythroid-specific genes in Epo, Dex and Kitlga cultures. Therefore, we hypothesize that Kitlga might enhance erythroid cell development and cell proliferation potentially through upregulation of genes related to protein translation and cell cycle progression.

To confirm these findings, we decided to test whether Kit signaling is involved also in zebrafish erythropoiesis *in vivo* using full length form of both kit ligands. Surprisingly, and in contrast to *ex vivo*

cultures, we found that in addition to *kitlga*, also *kitlgb* was potent in expansion of erythroid cells at 72 hpf when injected together with *epo* mRNA (Figure 2D). We hypothesize that the discrepancy between *ex vivo* and *in vivo* results in respect to Kitlgb activity might be explained by usage of different forms of kit ligands. For *ex vivo* experiments, we used soluble forms, whereas for *in vivo* experiments, we used the full-length coding sequence, including transmembrane and cytosolic domains, as used in previous reports[27]. It has been shown that the function of soluble and trans-membrane forms under physiological conditions is different[13]. The soluble form is distributed throughout the whole organism via circulation and affect distant tissues. It has been shown that this form is required and sufficient for proper erythroid signaling in cultured cells[16]. On the other hand, according to previous studies, the major site of action of the transmembrane form of Kit ligand might be in stem cell niches[13]. We hypothesize that full length Kitlgb can contribute, in addition to HSPCs[27], also to erythroid expansion *in vivo*.

Finally, we investigated, if Kita receptor is dispensable in Kitlg-mediated erythroid cell expansion *in vivo*. As a result, we did not observe the cooperation of *epo* with either of the *kit* ligands in erythroid differentiation in *kita* (*sparse*) mutant fish. These data suggest that Kita is responsible for Kit signal transduction in erythroid cells. Although Kitb might also be involved in this process, it couldn't compensate for missing Kita, and Kita seems to be required for Kit signaling in zebrafish erythroid cells.

To summarize, in this study we have addressed the question of the role of Kitlg in hematopoiesis in zebrafish using both *in vivo* and *ex vivo* approaches. Importantly, we established optimized liquid culture conditions for erythroid expansion of kidney marrow progenitor cells that require the addition of Kitlga. Together with colony forming assays, suspension cultures might serve as indispensable tools in disease modelling, allowing analysis of normal and aberrant hematopoiesis in zebrafish blood mutants (*vlade*, *moonshine*, *mindbomb* etc.)[51]. This will enable further biochemical, genomic and proteomic analysis of *ex vivo* cultured and expanded cells.

Interestingly, zebrafish Kitlga and Kitlgb seem to possess only partial redundancy in its function: Kitlga retains the role in melanogenesis and pigmentation, which is lost in the case of Kitlgb, but both ligands potentially contribute to the overall process of erythroid commitment and development in zebrafish *in vivo*. Although this function is not required in steady state erythroid development, it might become important in stress conditions. The exact mechanism of functional diversification of Kit ligands has yet to be investigated but altogether, we demonstrate that role of Kit signaling is evolutionarily conserved with respect to erythroid development as previously unnoticed[24], and therefore it strengthens the use of zebrafish as a model to study normal and aberrant human hematopoiesis.

Acknowledgements

We thank Nikol Pavlu,Tereza Hojerova and Tereza Hingarova for animal care, Tereza Mikulasova and Martina Hason, for graphical work and cDNA samples, Trevor Epp for editing the manuscript and Leonard Zon for providing *gata1:DsRed* and *LCR:GFP* reporter fish lines. Supported by the Czech Science Foundation (16-21024S), Ministry of Health (NV19-07-00412), Ministry of Education, Youth and Sports - Program NPU I (LO1419) to PB. OS was partially funded by American Heart Association (19POST34380328).

Authorship contribution

J.O., O.M., O.S. performed the experiments, J.O, O.S., P.S., D.T., M.K., and P.B. designed the experiments, analyzed the data and wrote the manuscript.

Conflict of interest

The authors declare no conflict of interest.

References

1 Krantz, S. B. Erythropoietin. *Blood* **77**, 419-434 (1991).

2 Goldwasser, E., Krantz, S. B. & Wang, F. F. Erythropoietin and erythroid differentiation. *Symposium on Fundamental Cancer Research* **37**, 103-107 (1984).

3 Graber, S. E. & Krantz, S. B. Erythropoietin and the control of red cell production. *Annual review of medicine* **29**, 51-66, doi:10.1146/annurev.me.29.020178.000411 (1978).

4 Antonchuk, J., Hyland, C. D., Hilton, D. J. & Alexander, W. S. Synergistic effects on erythropoiesis, thrombopoiesis, and stem cell competitiveness in mice deficient in thrombopoietin and steel factor receptors. *Blood* **104**, 1306-1313, doi:10.1182/blood-2004-04-1522 (2004).

5 Huang, E. *et al.* The hematopoietic growth factor KL is encoded by the Sl locus and is the ligand of the c-kit receptor, the gene product of the W locus. *Cell* **63**, 225-233, doi:10.1016/0092-8674(90)90303-v (1990).

6 Toksoz, D. *et al.* Support of human hematopoiesis in long-term bone marrow cultures by murine stromal cells selectively expressing the membrane-bound and secreted forms of the human homolog of the steel gene product, stem cell factor. *Proceedings of the National Academy of Sciences of the United States of America* **89**, 7350-7354 (1992).

7 Andrews, R. G. *et al.* Recombinant human stem cell factor, a c-kit ligand, stimulates hematopoiesis in primates. *Blood* **78**, 1975-1980 (1991).

8 Broudy, V. C. Stem cell factor and hematopoiesis. *Blood* **90**, 1345-1364 (1997).

9 Bartunek, P. *et al.* Avian stem cell factor (SCF): production and characterization of the recombinant His-tagged SCF of chicken and its neutralizing antibody. *Cytokine* **8**, 14-20, doi:10.1006/cyto.1996.0003 (1996).

10 Panzenbock, B., Bartunek, P., Mapara, M. Y. & Zenke, M. Growth and differentiation of human stem cell factor/erythropoietin-dependent erythroid progenitor cells in vitro. *Blood* **92**, 3658-3668 (1998).

11 Katakura, F. *et al.* Exploring erythropoiesis of common carp (Cyprinus carpio) using an in vitro colony assay in the presence of recombinant carp kit ligand A and erythropoietin. *Developmental and comparative immunology* **53**, 13-22, doi:10.1016/j.dci.2015.06.006 (2015).

12 Bokemeyer, C. *et al.* Expression of stem-cell factor and its receptor c-kit protein in normal testicular tissue and malignant germ-cell tumours. *J Cancer Res Clin Oncol* **122**, 301-306, doi:10.1007/bf01261407 (1996).

13 Lennartsson, J. & Ronnstrand, L. Stem cell factor receptor/c-Kit: from basic science to clinical implications. *Physiol Rev* **92**, 1619-1649, doi:10.1152/physrev.00046.2011 (2012).

14 Pesce, M., Di Carlo, A. & De Felici, M. The c-kit receptor is involved in the adhesion of mouse primordial germ cells to somatic cells in culture. *Mechanisms of development* **68**, 37-44, doi:10.1016/s0925-4773(97)00120-2 (1997).

15 Ding, L., Saunders, T. L., Enikolopov, G. & Morrison, S. J. Endothelial and perivascular cells maintain haematopoietic stem cells. *Nature* **481**, 457-462, doi:10.1038/nature10783 (2012).

16 Hayman, M. J., Meyer, S., Martin, F., Steinlein, P. & Beug, H. Self-renewal and differentiation of normal avian erythroid progenitor cells: regulatory roles of the TGF alpha/c-ErbB and SCF/c-kit receptors. *Cell* **74**, 157-169 (1993).

17 Grabbe, J., Welker, P., Dippel, E. & Czarnetzki, B. M. Stem cell factor, a novel cutaneous growth factor for mast cells and melanocytes. *Arch Dermatol Res* **287**, 78-84, doi:10.1007/bf00370723 (1994).

18 Alexeev, V. & Yoon, K. Distinctive role of the cKit receptor tyrosine kinase signaling in mammalian melanocytes. *J Invest Dermatol* **126**, 1102-1110, doi:10.1038/sj.jid.5700125 (2006).

19 Gong, Y. *et al.* SCF/SCFR signaling plays an important role in the early morphogenesis and neurogenesis of human embryonic neural retina. *Development* **146**, doi:10.1242/dev.174409 (2019).

20 Ashman, L. K. The biology of stem cell factor and its receptor C-kit. *The international journal of biochemistry & cell biology* **31**, 1037-1051, doi:10.1016/s1357-2725(99)00076-x (1999).

21 Abbaspour Babaei, M., Kamalidehghan, B., Saleem, M., Huri, H. Z. & Ahmadipour, F. Receptor tyrosine kinase (c-Kit) inhibitors: a potential therapeutic target in cancer cells. *Drug Des Devel Ther* **10**, 2443-2459, doi:10.2147/DDDT.S89114 (2016).

22 Paffett-Lugassy, N. *et al.* Functional conservation of erythropoietin signaling in zebrafish. *Blood* **110**, 2718-2726, doi:10.1182/blood-2006-04-016535 (2007).

23 Stachura, D. L. *et al.* Clonal analysis of hematopoietic progenitor cells in the zebrafish. *Blood* **118**, 1274-1282, doi:10.1182/blood-2011-01-331199 (2011).

24 Parichy, D. M., Rawls, J. F., Pratt, S. J., Whitfield, T. T. & Johnson, S. L. Zebrafish sparse corresponds to an orthologue of c-kit and is required for the morphogenesis of a subpopulation of melanocytes, but is not essential for hematopoiesis or primordial germ cell development. *Development* **126**, 3425-3436 (1999).

25 Hultman, K. A., Bahary, N., Zon, L. I. & Johnson, S. L. Gene Duplication of the zebrafish kit ligand and partitioning of melanocyte development functions to kit ligand a. *PLoS genetics* **3**, e17, doi:10.1371/journal.pgen.0030017 (2007).

26 Mellgren, E. M. & Johnson, S. L. kitb, a second zebrafish ortholog of mouse Kit. *Development Genes and Evolution* **215**, 470-477, doi:10.1007/s00427-005-0001-3 (2005).

27 Mahony, C. B., Pasche, C. & Bertrand, J. Y. Oncostatin M and Kit-Ligand Control Hematopoietic Stem Cell Fate during Zebrafish Embryogenesis. *Stem cell reports* **10**, 1920-1934, doi:10.1016/j.stemcr.2018.04.016 (2018).

28 Mahony, C. B., Fish, R. J., Pasche, C. & Bertrand, J. Y. tfec controls the hematopoietic stem cell vascular niche during zebrafish embryogenesis. *Blood* **128**, 1336-1345, doi:10.1182/blood-2016-04-710137 (2016).

29 von Lindern, M. *et al.* The glucocorticoid receptor cooperates with the erythropoietin receptor and c-Kit to enhance and sustain proliferation of erythroid progenitors in vitro. *Blood* **94**, 550-559 (1999).

30 Westerfield, M. *A guide for the laboratory use of zebrafish (Danio rerio). 4th ed.*, (Univ. of Oregon Press, Eugene, 2000).

31 Alestrom, P. *et al.* Zebrafish: Housing and husbandry recommendations. *Lab Anim*, 23677219869037, doi:10.1177/0023677219869037 (2019).

32 Oltova, J. *et al.* Zebrabase: An Intuitive Tracking Solution for Aquatic Model Organisms. *Zebrafish* **15**, 642-647, doi:10.1089/zeb.2018.1609 (2018).

33 Traver, D. *et al.* Transplantation and in vivo imaging of multilineage engraftment in zebrafish bloodless mutants. *Nature immunology* **4**, 1238-1246, doi:10.1038/ni1007 (2003).

34 Ganis, J. J. *et al.* Zebrafish globin switching occurs in two developmental stages and is controlled by the LCR. *Developmental biology* **366**, 185-194, doi:10.1016/j.ydbio.2012.03.021 (2012).

35 Svoboda, O. *et al.* Ex vivo tools for the clonal analysis of zebrafish hematopoiesis. *Nature protocols* **11**, 1007-1020, doi:10.1038/nprot.2016.053 (2016).

36 Stachura, D. L. *et al.* Zebrafish kidney stromal cell lines support multilineage hematopoiesis. *Blood* **114**, 279-289, doi:10.1182/blood-2009-02-203638 (2009).

37 Stachura, D. L. *et al.* The zebrafish granulocyte colony-stimulating factors (Gcsfs): 2 paralogous cytokines and their roles in hematopoietic development and maintenance. *Blood* **122**, 3918-3928, doi:10.1182/blood-2012-12-475392 (2013).

38 Kolbus, A. *et al.* Cooperative signaling between cytokine receptors and the glucocorticoid receptor in the expansion of erythroid progenitors: molecular analysis by expression profiling. *Blood* **102**, 3136-3146, doi:10.1182/blood-2003-03-0923 (2003).

39 England, S. J., McGrath, K. E., Frame, J. M. & Palis, J. Immature erythroblasts with extensive ex vivo self-renewal capacity emerge from the early mammalian fetus. *Blood* **117**, 2708-2717, doi:10.1182/blood-2010-07-299743 (2011).

40 Leberbauer, C. *et al.* Different steroids co-regulate long-term expansion versus terminal differentiation in primary human erythroid progenitors. *Blood* **105**, 85-94, doi:10.1182/blood-2004-03-1002 (2005).

41 Schroeder, C., Gibson, L., Nordstrom, C. & Beug, H. The estrogen receptor cooperates with the TGF alpha receptor (c-erbB) in regulation of chicken erythroid progenitor self-renewal. *EMBO J* **12**, 951-960 (1993).

42 Hoegg, S., Brinkmann, H., Taylor, J. S. & Meyer, A. Phylogenetic timing of the fish-specific genome duplication correlates with the diversification of teleost fish. *J Mol Evol* **59**, 190-203, doi:10.1007/s00239-004-2613-z (2004).

43 Amores, A., Catchen, J., Ferrara, A., Fontenot, Q. & Postlethwait, J. H. Genome evolution and meiotic maps by massively parallel DNA sequencing: spotted gar, an outgroup for the teleost genome duplication. *Genetics* **188**, 799-808, doi:10.1534/genetics.111.127324 (2011).

44 Nei, M. & Roychoudhury, A. K. Probability of fixation and mean fixation time of an overdominant mutation. *Genetics* **74**, 371-380 (1973).

45 Takahata, N. & Maruyama, T. Polymorphism and loss of duplicate gene expression: a theoretical study with application of tetraploid fish. *Proceedings of the National Academy of Sciences of the United States of America* **76**, 4521-4525 (1979).

46 Watterson, G. A. On the time for gene silencing at duplicate Loci. *Genetics* **105**, 745-766 (1983).

47 Force, A. *et al.* Preservation of duplicate genes by complementary, degenerative mutations. *Genetics* **151**, 1531-1545 (1999).

48 Dolznig, H., Bartunek, P., Nasmyth, K., Mullner, E. W. & Beug, H. Terminal differentiation of normal chicken erythroid progenitors: shortening of G1 correlates with loss of D-cyclin/cdk4 expression and altered cell size control. *Cell Growth Differ* **6**, 1341-1352 (1995).

49 Chabot, B., Stephenson, D. A., Chapman, V. M., Besmer, P. & Bernstein, A. The proto-oncogene c-kit encoding a transmembrane tyrosine kinase receptor maps to the mouse W locus. *Nature* **335**, 88-89, doi:10.1038/335088a0 (1988).

50 Svoboda, O. *et al.* Dissection of vertebrate hematopoiesis using zebrafish thrombopoietin. *Blood* **124**, 220-228, doi:10.1182/blood-2014-03-564682 (2014).

51 Ransom, D. G. *et al.* Characterization of zebrafish mutants with defects in embryonic hematopoiesis. *Development* **123**, 311-319 (1996).

Figure legends

Figure 1. The effect of zebrafish Kitlga and Kitlgb on self-renewal and proliferation of hematopoietic cells *ex vivo*.

(A, B) Quantification of the number of whole kidney marrow cells after treatment with PBS (control) or specific cytokine combinations for 3 days (A) and 7 days (B). Statistical significance was assessed using standard one-way ANOVA.

(C) Growth curve for *ex vivo* culture of whole kidney marrow cells with different cytokine combinations. Biological duplicates for every condition and timepoint are shown. Representative photomicrographs (right) of whole kidney marrow cells isolated from transgenic *gata1:DsRed* fish treated with Epo, Dex and Kitlga and cultivated for 8 days. Images were acquired on Olympus IX70 inverted microscope equipped with the Olympus DP72 camera using a 20x objective. Scale bar represents 100 um.

(D, E) An expression heatmap of Epo, Dex and Epo, Dex, Kitlga treated cells showing the top predicted differentially expressed genes (D) and representative markers of erythroid differentiation (E). Color coding by z-score for heatmaps in E and F.

Figure 2. *In vivo* effects of *kitlga* and *kitlgb* at 72 hpf.

(A) Representative micrographs of *gata1:DsRed* transgenic reporter larvae at 72 hpf after injection of corresponding mRNAs. Control represents uninjected larvae. Images were acquired on Zeiss Axio Zoom.V16 with Zeiss Axiocam 506 mono camera and ZEN Blue software.

(B) Representative micrographs of benzidine stained embryonic tails at 72 hpf after injection of corresponding mRNAs. Control represents uninjected embryos. NOTE increase in pigmentation in the dorsal part of *kitlga*-injected embryos. Z-stacks were acquired on Zeiss Axio Zoom.V16 with Zeiss Axiocam 105 color camera and processed using Extended Depth of Focus module in the ZEN blue software.

(C) Quantification of the benzidine stained embryonic tails in (B). Values were plotted using the mean of *epo* as the relative expression fold 1.

(D) qPCR expression analysis of *gata1a* and *hbbe1* from whole injected embryos at 72 hpf. Data have been normalized using *mob4* as the housekeeping gene and using uninjected control as the relative expression fold 1. Bars represent a mean of three triplicates with SD.

Figure 3. Expression of *kit* receptors in the development.

(A) qPCR expression analysis of *kita* (left) and *kitb* (right) at different developmental stages. Data was normalized using *ef1a* as the housekeeping gene and using the 24 hpf sample as relative expression fold 1.

(B) Sorting strategy used for FACS isolation of *gata1:DsRed* positive cells (top left) from transgenic zebrafish at 24 hpf stage. qPCR expression analysis of *gata1* (top right), *kita* (bottom left) and *kitb* (bottom right) in *gata1:DsRed* negative and positive cells. Data was normalized using *ef1a* as the housekeeping gene and using the *gata1:DsRed* positive 24 hpf sample as relative expression fold 1.

(C) Sorting strategy used for FACS isolation of *LCR:GFP* positive cells (top left) from transgenic zebrafish at 24 hpf stage. qPCR expression analysis of *gata1* (top right), *kita* (bottom left) and *kitb* (bottom right) in *LCR:GFP* negative and positive cells. Data was normalized using *ef1a* as the housekeeping gene and using the *LCR:GFP* positive 24 hpf sample as relative expression fold 1.

Figure 4. The effect of *kitlga* and *kitlgb* in *sparse* mutants.

(A) Quantification of the benzidine staining in the tail region of control (uninjected) or *epo*, *kitlga* and *kitlgb* mRNA injected wild-type or *kita* mutant embryos (*sparse*). Values were plotted relatively to the mean of *epo* (=1). NOTE that for demonstrative purposes, Figure 4A left is re-used from Figure 2C.

(B) qPCR expression analysis of *gata1a* and *hbbe1* from whole injected *kita* mutant embryos (*sparse*) at 72 hpf. Data was normalized using *mob4* as the housekeeping gene and uninjected control as the relative expression fold 1. Bars represent mean of three triplicates with SD.

Figure 1

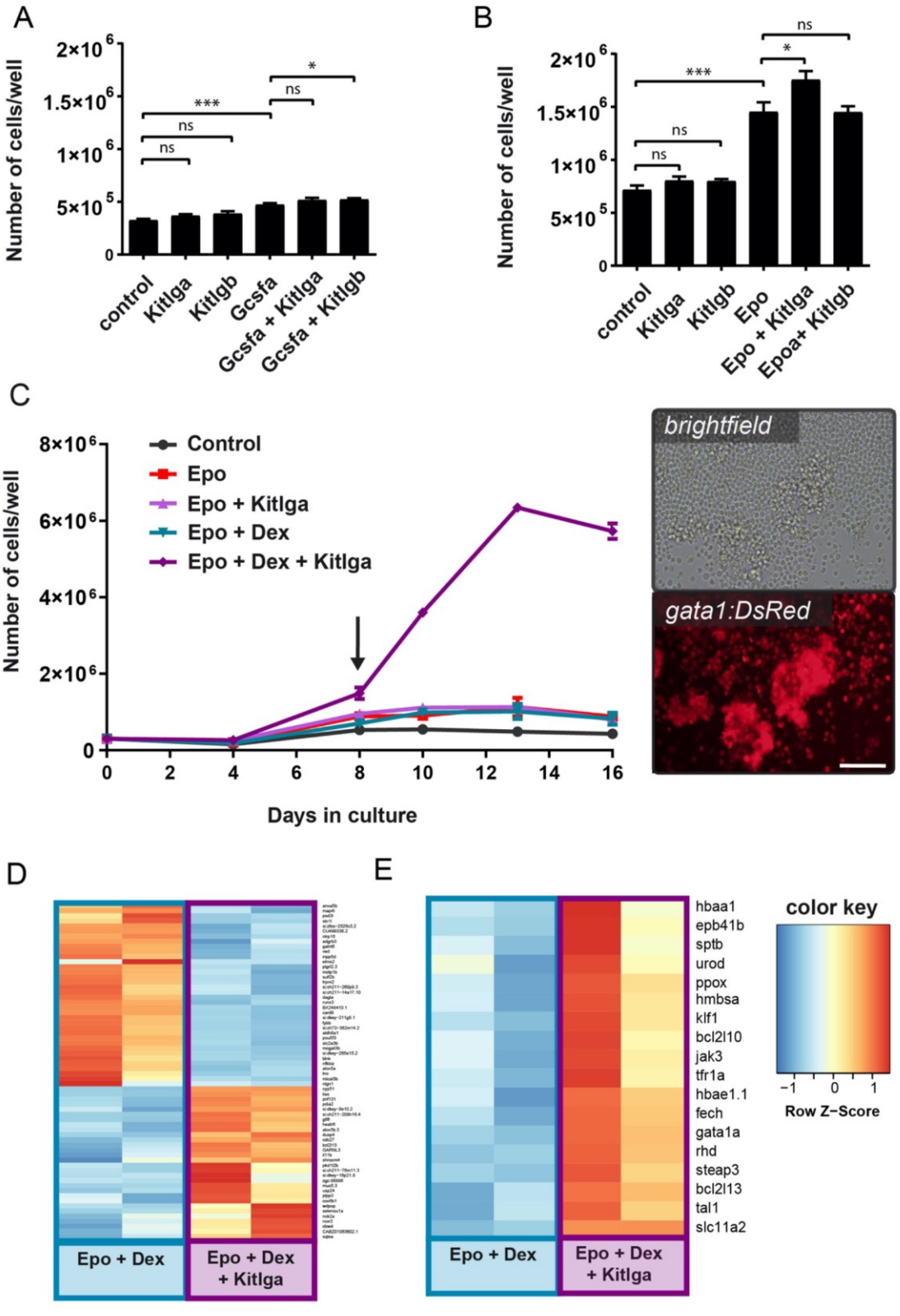
A
Number of cells/well
2×10^6
1.5×10^6
1×10^6
5×10^5
0
ns
ns
***
ns
*
control
Kitlga
Kitlgb
Gcsfa
Gcsfa + Kitlga
Gcsfa + Kitlgb
B
Number of cells/well
2×10^6
1.5×10^6
1×10^6
5×10^5
0
ns
ns
***
ns
*
control
Kitlga
Kitlgb
Epo
Epo + Kitlga
Epoa+ Kitlgb
C
Number of cells/well
8×10^6
6×10^6
4×10^6
2×10^6
0
Control
Epo
Epo + Kitlga
Epo + Dex
Epo + Dex + Kitlga
0
2
4
6
8
10
12
14
16
Days in culture
brightfield
gata1:DsRed
D
Epo + Dex
Epo + Dex + Kitlga
E
hbaa1
epb41b
sptb
urod
ppox
hmbsa
klf1
bcl2l10
jak3
tfr1a
hbae1.1
fech
gata1a
rhd
steap3
bcl2l13
tal1
slc11a2
Epo + Dex
Epo + Dex + Kitlga
color key
−1
0
1
Row Z−Score

Figure 2

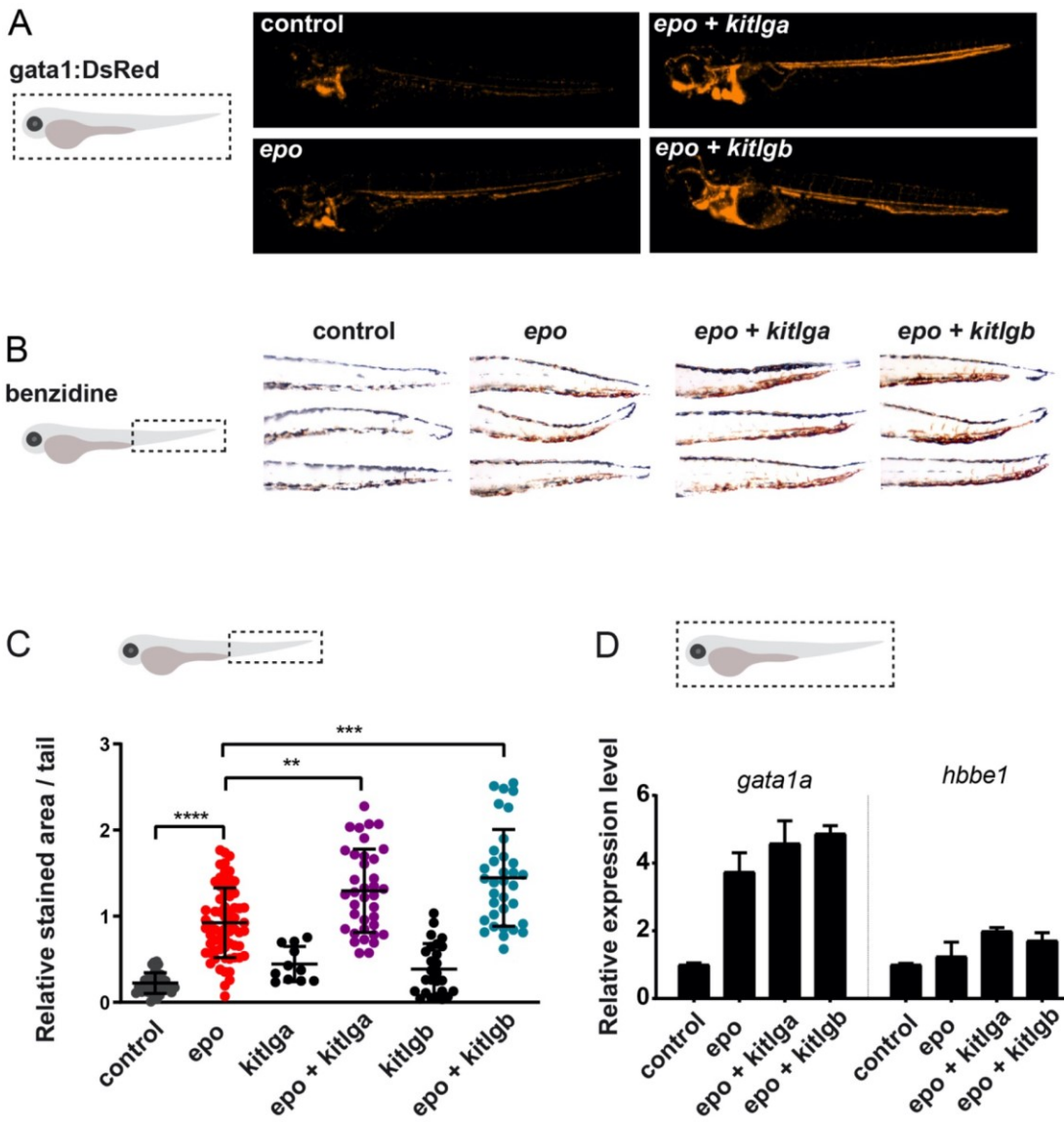
A
gata1:DsRed
control
epo + kitlga
epo
epo + kitlgb
B
benzidine
control
epo
epo + kitlga
epo + kitlgb
C
Relative stained area / tail
****
**
***
control
epo
kitlga
epo + kitlga
kitlgb
epo + kitlgb
D
Relative expression level
gata1a
hbbe1
control
epo
epo + kitlga
epo + kitlgb

Figure 3

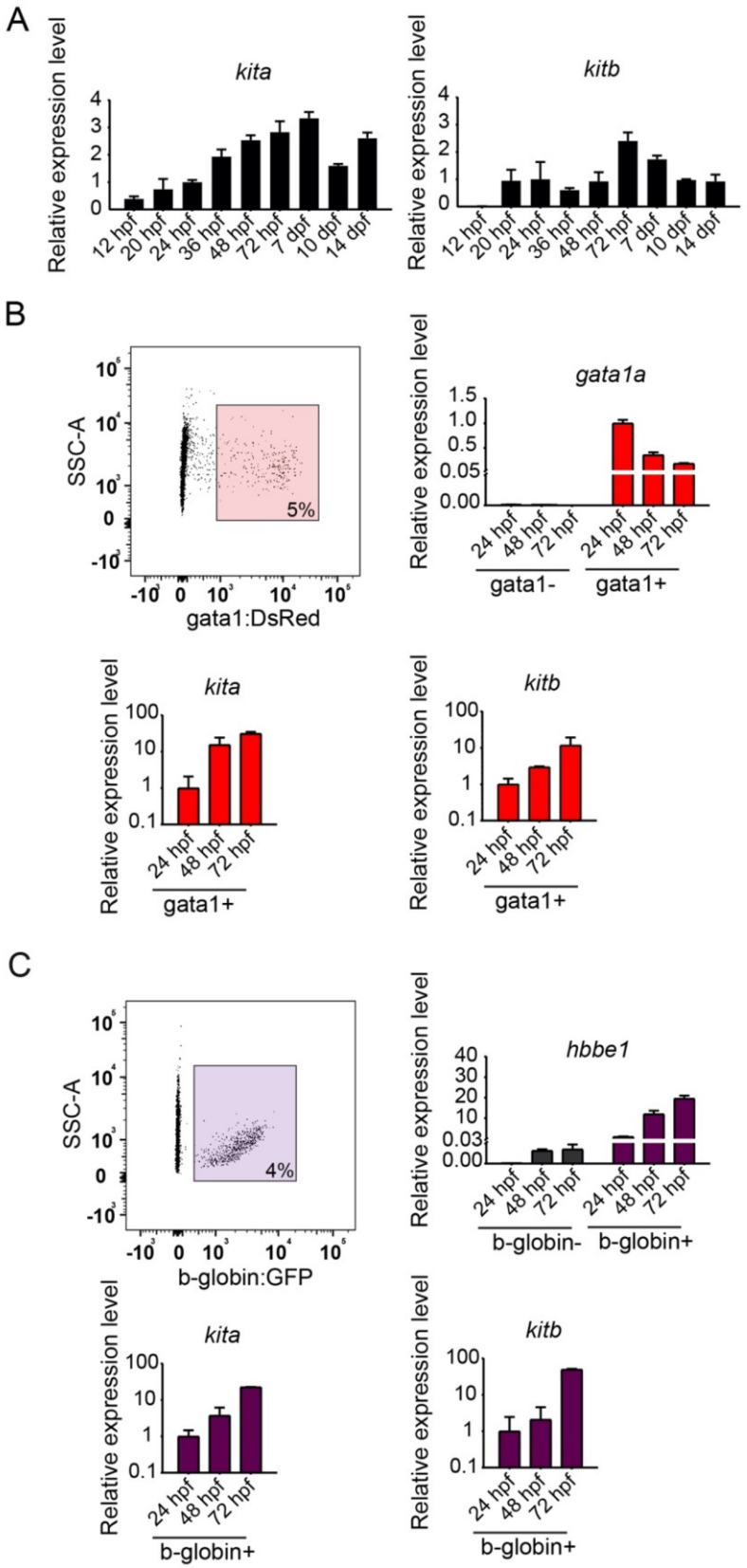
A
kita
kitb
Relative expression level
12 hpf
20 hpf
24 hpf
36 hpf
48 hpf
72 hpf
7 dpf
10 dpf
14 dpf
B
SSC-A
5%
gata1:DsRed
gata1a
gata1-
gata1+
24 hpf
48 hpf
72 hpf
C
4%
b-globin:GFP
hbbe1
b-globin-
b-globin+

Figure 4

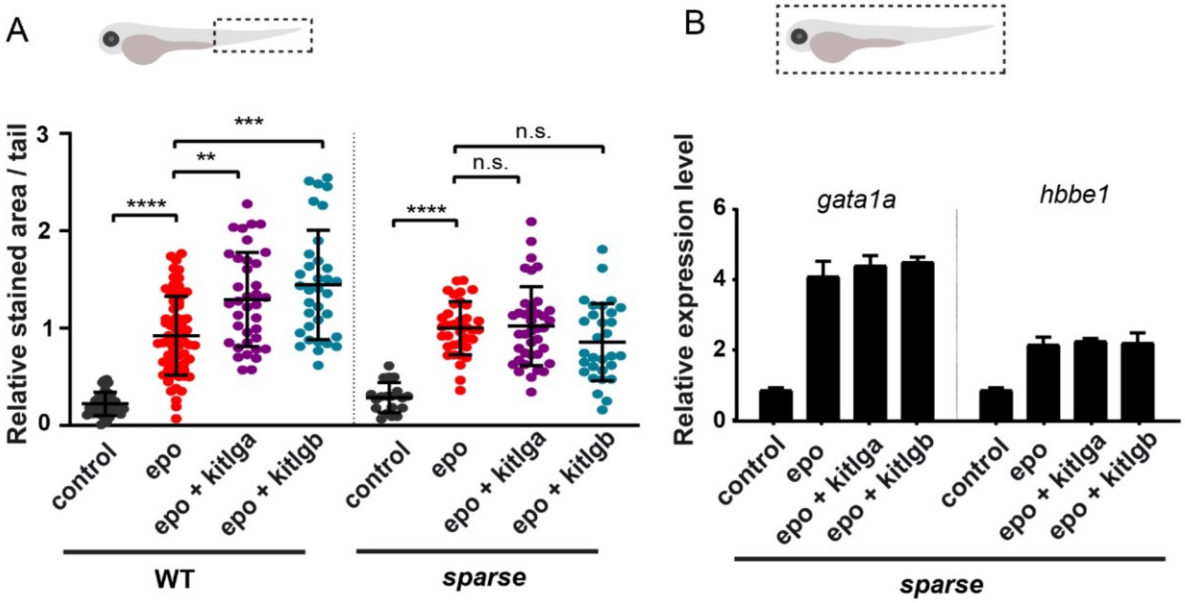
A
B
Relative stained area / tail
3
2
1
0
****
**
***
n.s.
n.s.
****
control
epo
epo + kitlga
epo + kitlgb
control
epo
epo + kitlga
epo + kitlgb
WT
sparse
Relative expression level
6
4
2
0
gata1a
hbbe1
control
epo
epo + kitlga
epo + kitlgb
control
epo
epo + kitlga
epo + kitlgb
sparse

Supplemental methods

mRNA microinjections

mRNAs were transcribed *in vitro* using mMessage mMachine SP6 kit (Roche) from a linearized pCS2+ vector containing PCR-amplified product and purified by lithium chloride extraction. 1-cell stage embryos were injected with 2 nl of the injection mix. The concentration of mRNA was 300 ng/ul for each cytokine, which equals to 600 pg of each mRNA per embryo.

Benzidine staining and image analysis

72 hpf embryos were anesthetized by Tricaine (MS-222) and incubated for 5 minutes on ice. Next, embryos were washed with cold PBS and fresh benzidine solution composed of o-dianisidine (Sigma-Aldrich, D9143) (0.6 mg/ml), sodium acetate pH 4.5 (0.01 M), hydrogen peroxide (0.65%) and ethanol (40%). Fish were incubated for 10 mins in dark, followed by wash with PBS. Fish were imaged using Zeiss Axio Zoom.V16 with Plan Neofluar Z 1.0x objective (total magnification 125x) and Zeiss Axiocam 105 mono camera. Acquired brightfield z-stacks were processed using the Extended Depth of Focus module in ZEN blue 2.3 software and images were quantified in Fiji.

FACS Sorting of embryos

24 hpf, 48 hpf and 72 hpf embryos were treated with Liberase TM (Roche, 05401119001), diluted 100x in PBS and incubated at 37°C for 1, 1.5 or 2.5 hours, respectively for each stage. Suspension was filtered using a 30µm filter, centrifuged and resuspended in PBS. Sorted cells were collected into TRI Reagent (Sigma, T3934) and isolated with RNeasy Plus Mini Kit (Qiagen, 74136).

RNA isolation from embryos and qPCR

RNA was collected from whole injected embryos using PureLink Micro Kit (Invitrogen, 12183-016) according to the manufacturer's instruction that include DNase I treatment and cDNA was synthesized using iScript™ cDNA Synthesis Kit (Bio-Rad). qPCR analysis was performed in triplicate with the LightCycler

480 and SYBR Green I (Roche). *ef1a* or *mob4* housekeeping genes were used to normalize the RNA content of samples, and data were calculated with the ΔΔCt method. The qPCR primers are listed in Supplemental Table 2.

RNAseq and transcriptomics

Total RNA was isolated from 6-7×10^6 WKM cells cultivated in the presence of Epo, Dex or Epo, Dex and Kitlga in biological duplicates, according to the PureLink Micro Kit (Invitrogen) manufacturer's protocol that includes DNase I treatment. The quantity of isolated RNA was measured spectrophotometrically using NanoDrop ND-1000 (Thermo Fisher Scientific) and its quality was analyzed by Agilent 2100 Bioanalyser (Agilent Technologies). RNA integrity number, which is regarded as criteria for high-quality total RNA, ranged between 9.5 and 10. Takara SMARTer Stranded Total RNA-Seq Kit v2 (Takara Bio) was used for cDNA library preparation starting with 3.5 ng of total RNA. Library size distribution was evaluated on the Agilent 2100 Bioanalyzer using the High Sensitivity DNA Kit (Agilent Technologies). Libraries were sequenced on the Illumina NextSeq® 500 instrument (Illumina) using 75bp single-end configuration yielding on average 47 million reads per sample.

Read quality was assessed by FastQC[1.] Individual steps of read processing were removing of sequencing adaptors with Trimmomatic (v0.36)[1], removing of ribosomal RNA with SortMeRna (v2.1)[2], mapping to reference transcriptome GRCz11[3] (Ensembl assembly version 98) and quantifying with Salmon[4]. Aggregation of transcript-level quantification to the gene level was performed with tximport[5] and served as input for differential expression analysis using DESeq2 R (v3.6.0) Bioconductor (v3.9) package[6]. Prior to the analysis, genes not expressed in at least two samples were discarded. Shrunken log2-fold changes using the adaptive shrinkage estimator[7] were used for differential expression analysis. Genes exhibiting minimal absolute log2-fold change value of 1 (for the genes that were upregulated in Epo, Dex, Kitla condition) or -2.32 (for the genes that were downregulated in Epo, Dex, Kitla condition) and statistical significance (adjusted p-value) of <0.1 between compared groups of samples were considered as differentially expressed for subsequent interpretation and visualization. Gene ontology (GO) enrichment analysis was done using gene length bias aware algorithm implemented in goseq R Bioconductor package[8]. The thresholds for up and down regulated genes entering the GO term analysis were log2-fold change > 0.415 and adjusted p-value < 0.1. Supplementary Table S6 shows GO terms with the cutoff of log2-fold change > 0.3 and p<0.0001 sorted by Odds ratio.

References

1 http://www.bioinformatics.babraham.ac.uk/projects/fastqc.

2 https://bioinfo.lifl.fr/RNA/sortmerna/.

3 http://www.ensembl.org/Danio_rerio/Info/Annotation.

4 Patro, R., Duggal, G., Love, M. I., Irizarry, R. A. & Kingsford, C. Salmon provides fast and bias-aware quantification of transcript expression. *Nature methods* **14**, 417-419, doi:10.1038/nmeth.4197 (2017).

5 Soneson, C., Love, M. I. & Robinson, M. D. Differential analyses for RNA-seq: transcript-level estimates improve gene-level inferences. *F1000Res* **4**, 1521, doi:10.12688/f1000research.7563.2 (2015).

6 Love, M. I., Huber, W. & Anders, S. Moderated estimation of fold change and dispersion for RNA-seq data with DESeq2. *Genome Biol* **15**, 550, doi:10.1186/s13059-014-0550-8 (2014).

7 Stephens, M. False discovery rates: a new deal. *Biostatistics* **18**, 275-294, doi:10.1093/biostatistics/kxw041 (2017).

8 Young, M. D., Wakefield, M. J., Smyth, G. K. & Oshlack, A. Gene ontology analysis for RNA-seq: accounting for selection bias. *Genome Biol* **11**, R14, doi:10.1186/gb-2010-11-2-r14 (2010).

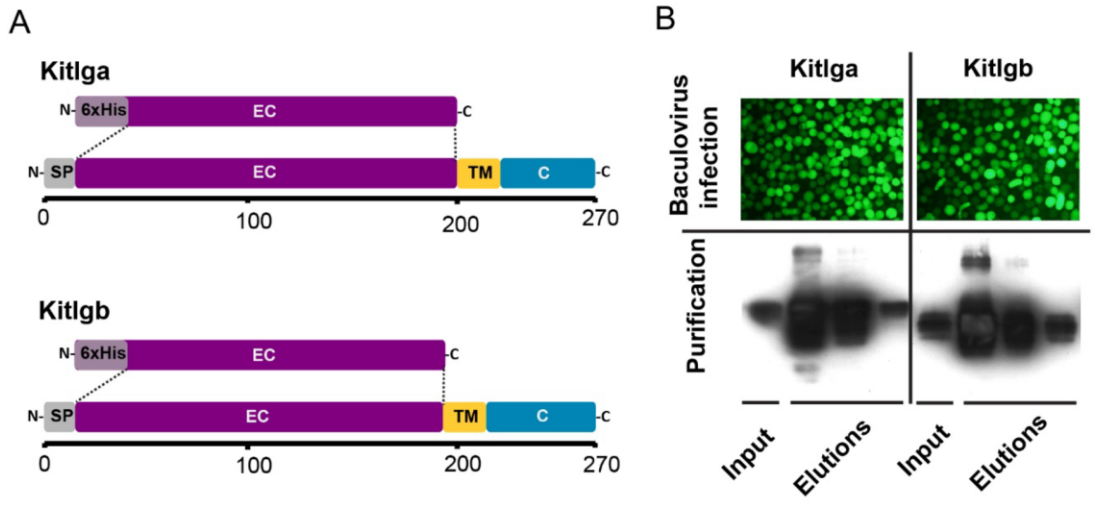

Figure S1. Cloning and expression of zebrafish Kitlga and Kitlgb.

(A) Sequence encoding the mature extracellular form (without the signaling peptide, transmembrane domain and cytosolic part) of each of the Kit ligands was amplified using RT-PCR from adult zebrafish retina and cloned into modified pAc-GP67-B vector containing 6xHis to generate recombinant His-tagged Kitlga and kitlgb proteins. SP - signaling peptide, EC – extracellular part, TM – transmembrane domain, C – cytosolic part, 6xHis - 6x histidine tag. Scale represents the number of amino acids.

(B) sf21 insect cells were co-transfected with BaculoGold Bright DNA (BD Biosciences) and Kitlga/b transfer vector leading to the production of a recombinant virus. Virus-infected cells were GFP-positive (top). Recombinant proteins were secreted from infected cells, purified using affinity chromatography and detected using anti-His antibody (bottom).

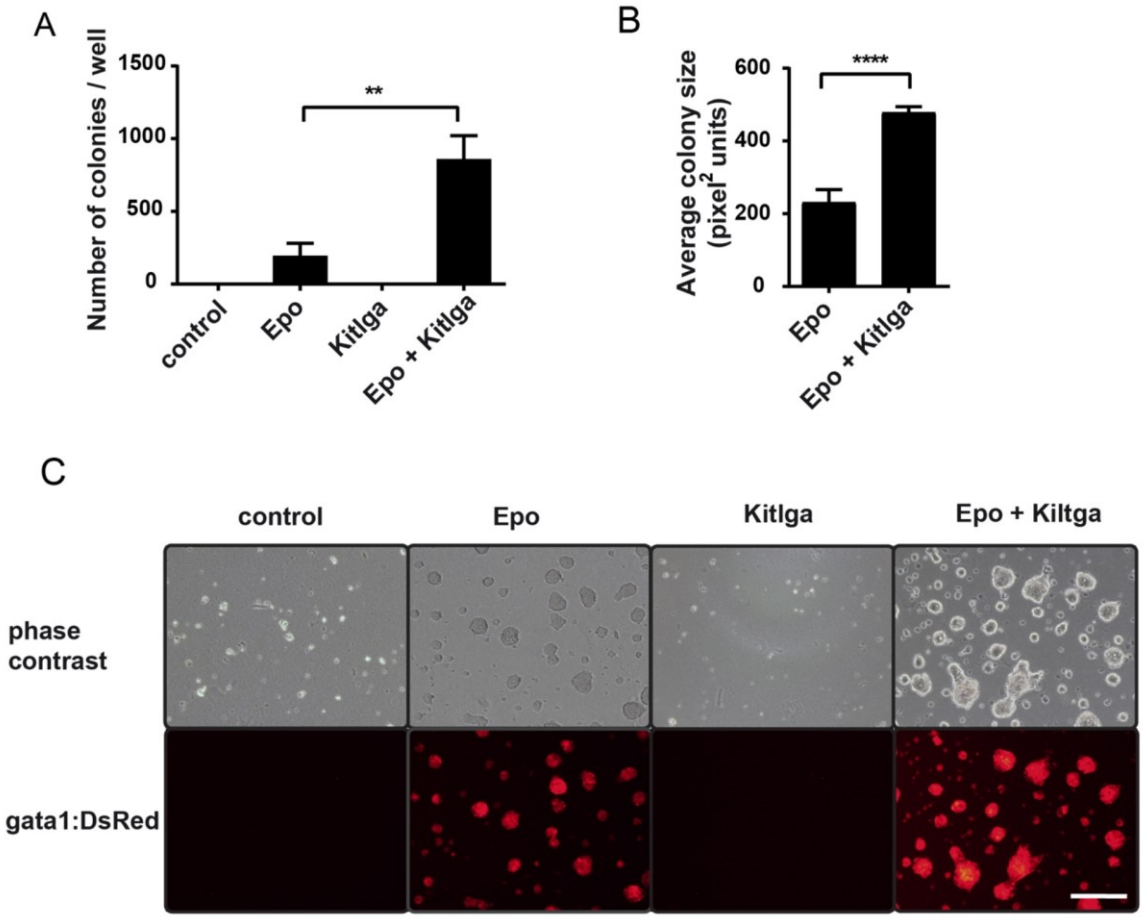

Figure S2. The effect of Kitlga in colony forming assays.

(A) Quantification of the number of colonies that formed from whole kidney marrow cells after treatment with PBS (control) or specific cytokine combinations for 7 days. Each condition was counted for three separate wells of a 12-well plate from images acquired on Zeiss Axio Zoom.V16. Each bar represents mean with SD. Statistical significance was determined by one-way ANOVA.

(B) Quantification of the difference in the size of the colonies in (A). Each bar represents a triplicate mean with SD. Statistical significance has been determined by t-test.

(C) Representative brightfield (top) and fluorescent (bottom) micrograph of *gata1*:DsRed positive colonies for each cytokine and their combination. Images were acquired on Olympus IX70 inverted microscope equipped with the Olympus DP72 camera, using a 10x objective. Scale bar represents 200 um.

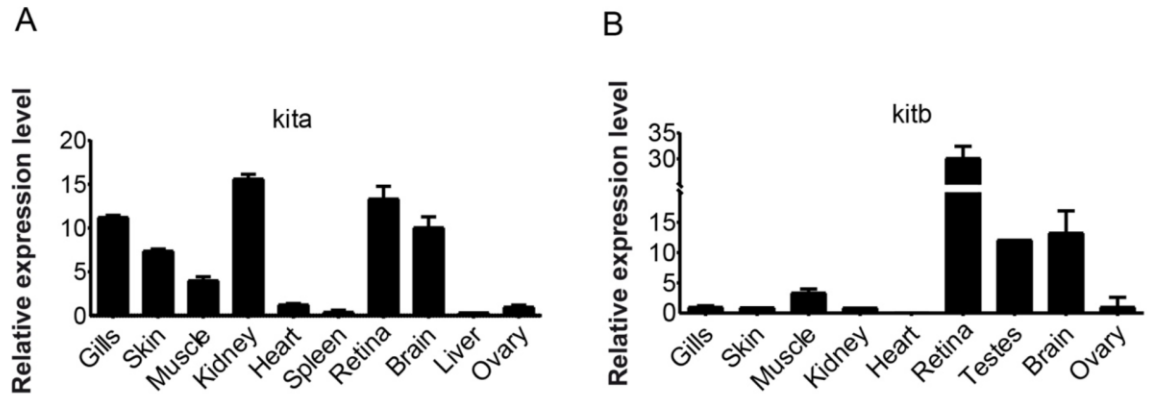

Figure S3. Expression of kit receptors in tissues.

qPCR expression analysis of *kita* (A) and *kitb* (B) in various adult tissues. Data were normalized using ef1a as the housekeeping gene and using ovary sample as relative expression fold 1.

Supplemental Table 1. Primers for cloning kit ligands.

	Forward primer	Reverse primer
Protein		
kitlga	CGGGATCCATTGAAATAGGAAATCCCAT	GCGGATCCTTACTCATTTGTACTATGTTGCGC
kitlgb	GCGGATCCGGGAGCCCTTTAACAGATGA	GCGGATCCTTAATGAACCGCAGAGTTCATGCC
mRNA		
kitlga	GCGGATCCGGTTTCGCTGACATTGGAGT	GCGGATCCTTTGTTCCTGTAGGTTGGGC
kitlgb	GCGGATCCGGAGACACGGCTGATTTGTT	GCGGATCCATCCCGTTCTGGATATTCCC

Supplemental Table 2. Primers for qPCR.

	Forward primer	Reverse primer
gata1a	GTTTACGGCCCTTCTCCACA	CACATTCACGAGCCTCAGGT
hbbe1	CTTGACCATCGTTGTTG	GATGAATTTCTGGAAAGC
kita	CTATGTTGTCAAAGGCAATGCT	CCAGACGTCACTCTCAAAGGT
kitb	GGATACAGAATGAGTGAGCCTGA	CTCCAGCACCATCTCATCAC
efa1	GAGAAGTTCGAGAAGGAAGC	CGTAGTATTTGCTGGTCTCG
mob4	CACCCGTTTCGTGATGAAGTACAA	GTTAAGCAGGATTTACAATGGAG

Supplemental Table 3. Composition of zebrafish S13 medium.

zf S13 medium	final concentration
DMEM (Gibco, cat. no. 41966-029)	
Distilled Water (Gibco, cat. no. 15230-089)	
FBS, embryonic-stem-cell qualified (Biosera, cat. no. FB-1001S/500)	10%
Carp Serum	2%
BSA 10% (StemCell Technologies, cat. no. 09300)	0.5%
NaHCO3, 7.5%	0.2%
beta-Mercaptoethanol (Sigma-Aldrich, cat. no. M6250)	0.1 mM
L-Glutamine, 0.2 M (Gibco, cat. no. 25030-081)	4 mM
Hypoxanthine (Sigma-Aldrich, cat. no. H9636)	200mg/100ml
FE-SIH iron supplement, 1000x (Sigma-Aldrich, cat. no. I3153)	
Penicillin-streptomycin, 100× (Gibco, cat. no. 15140122)	
solution A (1000x)	
solution B (50x)	

solution B in water	final concentration
L-Methionine	10 mM
L-Phenylalanine	20 mM
L-Alanine	10 mM
Glycine	50 mM
L-Threonine	40 mM
L-Isoleucine	40 mM
L-Proline	10 mM
L-Valine	40 mM
L-Aspartic Acid	10 mM
L-Glutamic Acid	25 mM

solution A in water	final concentration
Biotin (Sigma B4639)	0.1%

Supplemental Table 4. Statistics of differentially expressed genes in cells treated with Epo, Dex, Kitlga compared to cells treated with Epo, Dex only.

Ensembl Accession ID	symbol	log_2FoldChange	p-adjusted
ENSDARG00000114387	CU499336.2	-2.46	1.40E-25
ENSDARG00000098680	si:zfos-2326c3.2	-3.61	6.26E-23
ENSDARG00000044694	fybb	-2.36	4.25E-19
ENSDARG00000069542	si:dkey-8e10.2	3.01	5.19E-17
ENSDARG00000042722	blnk	-4.77	9.04E-16
ENSDARG00000101641	trpm2	-2.35	1.77E-14
ENSDARG00000102389	ved	-2.50	6.59E-14
ENSDARG00000060871	mctp1b	-3.31	6.27E-13
ENSDARG00000058476	stc1l	-3.10	3.74E-12
ENSDARG00000074283	inpp5d	-2.44	4.71E-12
ENSDARG00000069966	alox5b.3	1.30	8.62E-12
ENSDARG00000052826	runx3	-2.41	7.49E-11
ENSDARG00000037861	slc2a3b	-2.34	1.94E-10
ENSDARG00000104820	psd3l	-2.42	1.18E-09
ENSDARG00000076534	si:ch211-14a17.10	-3.59	1.28E-08
ENSDARG00000018263	pdia2	2.73	1.05E-07
ENSDARG00000057273	alox5a	-2.37	3.96E-07
ENSDARG00000077673	nlrp16	-6.32	9.60E-07
ENSDARG00000073686	heatr6	2.17	2.55E-06
ENSDARG00000068745	map4l	-2.40	8.18E-06
ENSDARG00000092862	si:ch211-260p9.3	-2.35	9.11E-06
ENSDARG00000022845	lias	3.25	9.80E-06
ENSDARG00000067672	card9	-3.64	1.02E-05
ENSDARG00000056258	cdc27	1.24	3.74E-05
ENSDARG00000094732	mical3b	-2.85	3.88E-05
ENSDARG00000045230	cox6b1	1.12	7.34E-05
ENSDARG00000100809	g6fl	1.58	8.46E-05
ENSDARG00000059933	plpp3	1.03	1.30E-04
ENSDARG00000062956	dagla	-2.59	2.12E-04
ENSDARG00000059925	usp24	1.01	2.12E-04
ENSDARG00000089582	si:dkey-265e15.2	-2.93	2.31E-04
ENSDARG00000013838	sulf2b	-2.95	4.49E-04
ENSDARG00000116660	pigrl2.3	-2.35	5.11E-04
ENSDARG00000042641	cyp51	1.48	5.66E-04
ENSDARG00000063527	elmo2	-4.40	6.38E-04
ENSDARG00000036776	aldh8a1	-2.75	9.79E-04
ENSDARG00000102097	nfkbiz	-2.42	1.13E-03

ENSDARG00000044774	pou5f3	-2.77	1.44E-03
ENSDARG00000018206	nck2a	2.55	1.56E-03
ENSDARG00000036728	si:dkey-211g8.1	-4.17	2.02E-03
ENSDARG00000021948	tnc	-2.70	2.62E-03
ENSDARG00000014386	galnt6	-2.47	2.68E-03
ENSDARG00000104890	si:ch211-76m11.3	6.07	5.99E-03
ENSDARG00000090038	BX248410.1	-2.72	6.08E-03
ENSDARG00000059832	adgrb3	-2.76	6.48E-03
ENSDARG00000077710	nlgn1	-3.42	8.15E-03
ENSDARG00000090164	si:ch73-362m14.2	-2.90	8.32E-03
ENSDARG00000057378	selenou1a	1.25	9.60E-03
ENSDARG00000060631	GARNL3	3.66	1.18E-02
ENSDARG00000062370	bcl2l13	1.02	1.40E-02
ENSDARG00000016470	anxa5b	-2.52	1.49E-02
ENSDARG00000099470	muc5.3	1.57	1.70E-02
ENSDARG00000003635	mogat3b	-2.32	1.71E-02
ENSDARG00000074590	wdpcp	2.36	1.86E-02
ENSDARG00000102395	CABZ01063602.1	3.48	2.07E-02
ENSDARG00000095142	si:ch211-208h16.4	2.63	2.27E-02
ENSDARG00000004318	cbwd	1.30	2.31E-02
ENSDARG00000044688	dusp4	1.03	2.32E-02
ENSDARG00000090369	zgc:86896	1.12	3.17E-02
ENSDARG00000079900	shroom4	1.12	3.62E-02
ENSDARG00000101214	pkd1l2b	1.21	3.81E-02
ENSDARG00000068400	znf131	1.72	4.40E-02
ENSDARG00000079946	sqlea	1.09	4.56E-02
ENSDARG00000058557	il11b	1.05	5.54E-02
ENSDARG00000008278	rcor2	1.47	6.54E-02
ENSDARG00000096849	si:dkey-16p21.8	1.13	6.64E-02

Supplemental Table 5 – Statistics of the difference in expression of selected erythroid genes in cells treated with Epo, Dex, Kitlga compared to cells treated with Epo, Dex only.

Ensembl Accession ID	symbol	log_2FoldChange	p-adjusted
ENSDARG00000002194	bcl2l13	1.02	1.40E-02
ENSDARG00000003462	rhd	0.84	5.84E-03
ENSDARG00000006818	tfr1a	0.55	1.06E-02
ENSDARG00000008840	hbae1.1	0.54	1.77E-01
ENSDARG00000010252	gata1a	0.52	5.65E-02
ENSDARG00000013477	bcl2l10	0.52	1.18E-01
ENSDARG00000017400	epb41b	0.49	3.78E-02
ENSDARG00000019930	hmbsa	0.48	6.30E-02
ENSDARG00000024295	slc11a2	0.45	9.81E-02
ENSDARG00000026766	hbaa1	0.38	3.55E-01
ENSDARG00000029019	ppox	0.38	1.89E-01
ENSDARG00000030490	klf1	0.37	2.68E-01
ENSDARG00000062370	sptb	0.35	1.71E-01
ENSDARG00000075641	urod	0.35	2.19E-01
ENSDARG00000088330	jak3	0.33	4.21E-01
ENSDARG00000097011	fech	0.32	2.76E-01
ENSDARG00000101322	steap3	0.32	4.57E-01
ENSDARG00000102167	tal1	0.32	3.54E-01

Supplemental Table 6. GO enrichment analysis in in cells treated with Epo, Dex, Kitlga compared to cells treated with Epo, Dex only.

Biological processes

Accession	GO.Term	Odds.Ratio	P.value
GO:0000028	ribosomal small subunit assembly	60	6.34E-12
GO:0002181	cytoplasmic translation	53.8	2.63E-18
GO:0000027	ribosomal large subunit assembly	50	1.38E-12
GO:0042541	hemoglobin biosynthetic process	38.4	4.01E-07
GO:0030218	erythrocyte differentiation	31.1	3.08E-15
GO:0006412	translation	30.8	1.61E-73
GO:0048821	erythrocyte development	22.7	9.68E-06
GO:0043009	chordate embryonic development	18.7	1.55E-18
GO:0006414	translational elongation	17.8	2.65E-05
GO:0035162	embryonic hemopoiesis	15.1	2.91E-05
GO:0051726	regulation of cell cycle	12	1.42E-06

Cellular compartment

Accession	GO.Term	Odds.Ratio	P.value
GO:0022625	cytosolic large ribosomal subunit	77	1.22E-52
GO:0022627	cytosolic small ribosomal subunit	72.9	9.55E-37
GO:0015935	small ribosomal subunit	70	1.05E-10
GO:0005840	ribosome	47.7	7.56E-82
GO:0015934	large ribosomal subunit	41.6	3.67E-06

Molecular function

Accession	GO.Term	Odds.Ratio	P.value
GO:0003735	structural constituent of ribosome	46.7	9.27E-80
GO:0019843	rRNA binding	31.8	1.67E-07
GO:0003723	RNA binding	5.14	5.75E-11

frontiers in Cell and Developmental Biology

MINI REVIEW
published: 20 December 2018
doi: 10.3389/fcell.2018.00174

Hematopoietic Cytokine Gene Duplication in Zebrafish Erythroid and Myeloid Lineages

*Jana Oltova[1], Ondrej Svoboda[1,2] and Petr Bartunek[1]**

[1] Department of Cell Differentiation, Institute of Molecular Genetics of the ASCR, v.v.i., Prague, Czechia, [2] Department of Cellular and Molecular Medicine, University of California, San Diego, La Jolla, CA, United States

Hematopoiesis is a precisely orchestrated process regulated by the activity of hematopoietic cytokines and their respective receptors. Due to an extra round of whole genome duplication during vertebrate evolution in teleost fish, zebrafish have two paralogs of many important genes, including genes involved in hematopoiesis. Importantly, these duplication events brought increased level of complexity in such cases, where both ligands and receptors have been duplicated in parallel. Therefore, precise understanding of binding specificities between duplicated ligand-receptor signalosomes as well as understanding of their differential expression provide an important basis for future studies to better understand the role of duplication of these genes. However, although many recent studies in the field have partly addressed functional redundancy or sub-specialization of some of those duplicated paralogs, this information remains to be scattered over many publications and unpublished data. Therefore, the focus of this review is to provide an overview of recent findings in the zebrafish hematopoietic field regarding activity, role and specificity of some of the hematopoietic cytokines with emphasis on crucial regulators of the erythro-myeloid lineages.

Keywords: zebrafish, hematopoiesis, cytokine, genome duplication, myelopoiesis, erythropoiesis

OPEN ACCESS

Edited by:
Eirini Trompouki,
Max-Planck-Institut für Immunbiologie und Epigenetik, Germany

Reviewed by:
Valerie Wittamer,
Free University of Brussels, Belgium
Jill de Jong,
University of Chicago, United States

***Correspondence:**
Petr Bartunek
bartunek@img.cas.cz

Specialty section:
This article was submitted to Cell Growth and Division, a section of the journal Frontiers in Cell and Developmental Biology

Received: *26 September 2018*
Accepted: *06 December 2018*
Published: *20 December 2018*

Citation:
Oltova J, Svoboda O and Bartunek P (2018) Hematopoietic Cytokine Gene Duplication in Zebrafish Erythroid and Myeloid Lineages. Front. Cell Dev. Biol. 6:174. doi: 10.3389/fcell.2018.00174

INTRODUCTION

Hematopoiesis, the multistep process of formation and turnover of blood cells, is precisely regulated by an array of extrinsic and intrinsic factors (Kaushansky, 2006). Extrinsic factors include cytokines and growth factors that bind to their corresponding receptors and in turn activate intracellular signaling molecules that further modulate cellular responses, mainly by controlling activity of different transcriptional activators or repressors. The process of hematopoiesis begins already in early development, where red blood cells and macrophages are formed in a primitive wave to provide necessary support for the developing embryo. Later in development, the whole system is largely driven by proliferation, self-renewal, and differentiation of lineage restricted progenitors as well as hematopoietic stem cells (HSCs) and hematopoietic multipotent progenitor cells (MPPs) with reduced self-renewal capabilities. All erythroid and myeloid cells derive from HSCs with the exception of some tissue resident macrophages which are independent on HSC input (Ginhoux et al., 2010).

According to the classical hierarchical model of definitive vertebrate hematopoiesis (Akashi et al., 2000), the HSCs asymmetrically lose their long term self-renewing capabilities to form MPPs that further give rise to common lymphoid and common myeloid progenitors. The common myeloid progenitors afterward differentiate into bipotent megakaryocyte-erythrocyte progenitors (MEPs) and restricted common myelo-monocytic progenitors (CMPs). In this review, we will focus on cytokines that regulate formation and maintenance of these erythro-myeloid hematopoietic lineages.

Hematopoiesis is well conserved throughout the vertebrates, with all the major blood lineages – myeloid, erythroid and lymphoid – conserved from fish to men. Importantly, also the sequential waves of developing blood cells during ontogenesis are present during the development of the zebrafish embryo, leading finally to a fully fledged adult hematopoietic system, as has been described in other vertebrates. However, some differences between mammalian and non-mammalian hematopoiesis do exist (Svoboda and Bartunek, 2015), particularly in erythro-megakaryocytic lineages. In mammals, bi-potent cells termed megakaryocyte-erythrocyte progenitors (MEPs) give rise to either endoreduplicated megakaryocytes (Svoboda et al., 2014) that serve as a precursor for platelet biogenesis, or to enucleated erythrocytes (Muir and Kerr, 1958; Simpson, 1967). On the other hand, non-mammalian vertebrates possess bi-potent thrombocyte-erythrocyte progenitors (TEPs) instead that differentiate into functional homologs of platelets, termed thrombocytes or to nucleated erythrocytes (**Figure 1**; Ratnoff, 1987; Schneider and Gattermann, 1994; Svoboda et al., 2014). Besides these differences, the rest of the hematopoietic differentiation tree is well conserved in all vertebrate animals.

Hematopoietic cytokines signal via their cognate receptors to drive target cell proliferation and/or differentiation. In general, cytokines are pleiotropic in their function and for this reason also many factors regulating erythro-thrombocytic differentiation have broader effect on all hematopoietic lineages (Nicola, 1994).

In vertebrates, the major cytokines regulating red blood cell development from bipotent TEPs or MEPs through committed burst forming units-erythroid (BFU-E), colony forming units-erythroid (CFU-E) and erythroblasts, are erythropoietin (EPO) and stem cell factor (SCF, or KIT ligand, KITLG). On the other hand, thrombopoietin (TPO) is the key mediator of thrombocyte or platelet formation from TEPs/MEPs and is also responsible for platelet formation from polyploid megakaryocytes (Kaushansky et al., 1995; Kato et al., 1998). Other important erythro/thrombocytic regulators that promote self-renewal of erythroid progenitors or their differentiation include insulin (INS) and insulin-like growth factor (IGF1) (Miyagawa et al., 2000). Moreover, transforming growth factor α (TGFα) and TGFβ family members (Krystal, 1994; Huber et al., 1998; Gandrillon et al., 1999; Fuchs et al., 2002; Harandi et al., 2010), interleukin 3 (IL3), and fibroblast growth factor 2 (FGF2) (Bartunek et al., 2002) also play a crucial role in this process.

In thrombocytic differentiation, TPO interacts with and activates its cognate receptor, TPOR (c-MPL) (de Sauvage et al., 1994; Alexander, 1999b) and this signaling has been shown to be necessary for proper thrombopoiesis (Alexander, 1999a). This signaling is complemented by IL12 and SDF1, necessary for proper megakaryocytic maturation and proper platelet formation (Gordon and Hoffman, 1992). Function of these lineage-restricted factors is complemented by other regulators, especially interleukins (IL3, IL6, IL11), G-CSF, GM-CSF (McNiece et al., 1991; Gordon and Hoffman, 1992) and SCF (Steinlein et al., 1995; Broudy, 1997) that can enhance both erythroid and thrombocytic differentiation.

The CMPs also give rise to other substantial myelo-monocytic cell types – granulocytes, monocytes/macrophages and dendritic cells (Akashi et al., 2000), whose proliferation and differentiation from hematopoietic stem and progenitor cells (HSPCs) is regulated by macrophage colony-stimulating factor (M-CSF, or CSF1), granulocyte-macrophage CSF (GM-CSF, or CSF2), granulocyte CSF (G-CSF, or CSF3) and interleukin 3 (IL3) (Metcalf and Nicola, 1983; Metcalf, 1985; Migliaccio et al., 1991; Lieschke et al., 1994; Liu et al., 1996). These cytokines act via their cognate receptors – M-CSF receptor (M-CSFR, or CSF1R), G-CSF receptor (G-CSFR, or CSF3R), GM-CSF receptor (GM-CSFR, or CSF2RA) and interleukin 3 receptor (IL3RA), respectively.

Due to poor sequence homology between teleost and mammalian cytokines, the mammalian cytokines generally do not cross-react with zebrafish hematopoietic cells (Stachura et al., 2009, 2011, 2013; Svoboda et al., 2014) and for the same reason, the identification of zebrafish cytokine orthologs has been challenging. However, many successful attempts of identifying, generating and using recombinant zebrafish cytokines have been reported in recent years (Stachura et al., 2009, 2011, 2013; Svoboda et al., 2014).

Due to an extra round of whole genome duplication (WGD) during the evolution of teleost fish, which occurred 320–350 million years ago (Hoegg et al., 2004; Amores et al., 2011), zebrafish possess multiple paralogs of many important genes. After WGD, duplicated paralogs are often lost through a process of pseudogenization, where detrimental mutations accumulate in the duplicated gene (Nei and Roychoudhury, 1973; Takahata and Maruyama, 1979; Watterson, 1983). Alternatively, the two paralogs of the ancestral gene can be retained and either acquire new functions (i.e., neofunctionalization) or split the original function between the two paralogs (i.e., subfunctionalization) (Force et al., 1999).

Importantly, the event of duplication brought an increased level of complexity in such cases when both ligands and receptors have been duplicated (and retained) in parallel. Therefore, precise understanding of binding specificities between duplicated ligand-receptor signalosomes, as well as an understanding of their differential expression, will provide an important basis for future studies to better understand evolution of the vertebrate genome. Although many recent studies in the field have partly addressed functional redundancy or sub-specialization of some of these duplicated paralogs (Hultman et al., 2007; Wang et al., 2008; Stachura et al., 2013; Butko et al., 2015), there are still many unknowns.

Understanding the precise relationship between mammalian and non-mammalian hematopoiesis may have an important

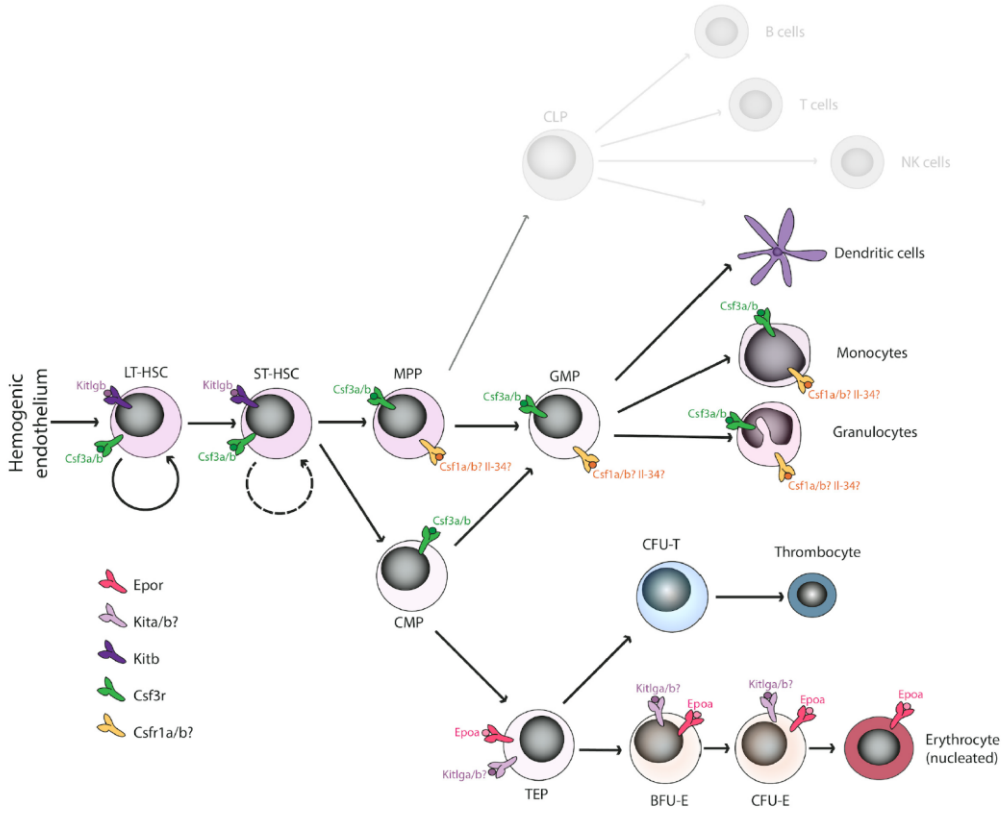

FIGURE 1 | Overview of duplicated hematopoietic cytokines and receptors regulating the erythro-myeloid lineage in *Danio rerio*. Various cytokine receptors have been proposed to act at the level of hematopoietic stem cells (Kitb, Csf3r), the myeloid lineage (Csf1ra/b, Csf3r), or the erythroid lineage (Epor, Kita/b) in *D. rerio* binding the corresponding ligands. The function of missing cytokines (Il-3, Il-5, GM-CSF, Fli3) is most likely compensated by other factors. Some duplicated paralogs have undergone sub-specification (e.g., Kitlga/b), whereas some other seem to have lost their function in hematopoiesis (e.g., Epob). LT-HSC, long-term hematopoietic stem cells; ST-HSC, short-term hematopoietic stem cells; MPP, multipotent progenitor cells; GMP, granulocyte-macrophage progenitors; CMP, common myeloid progenitors; TEP, thrombo-erythroid progenitors; BFU-E, burst forming units-erythroid; CFU-E, colony forming units-erythroid.

impact on general hematopoiesis research. Due to the interference with sophisticated mammalian megakaryocytic and erythroid enhancements, the employment of mammalian model organisms brings only partial success in the quest of identifying novel key regulators of cell fate determination. Once we have detailed understanding of cytokines and the receptors driving hematopoiesis in zebrafish, we can overcome these obstacles and efficiently utilize this non-mammalian model organism, instead.

DUPLICATED ERYTHRO-MYELOID CYTOKINE GENES IN ZEBRAFISH

Epoa/b

Erythropoietin (EPO) is the major regulator of erythropoiesis, mediating self-renewal, survival and differentiation via the Epo receptor (EPOR) (Krantz, 1991). EPOR homodimerization mediated by EPO binding leads to auto-phosphorylation of JAK2 that is bound to Box1/2 and that in turn phosphorylates the receptor itself as well as other signaling molecules such as STAT5 (signal transducers and activators of transcription) transcription factor, PI-3K (phosphatidylinositol 3-kinase) and mitogen-activated protein kinase (MAPK) (Drachman and Kaushansky, 1997; Constantinescu et al., 1999).

We previously identified two copies of the epo gene in zebrafish, termed epoa and epob. Although zebrafish epoa probably plays a similar role as its mammalian ortholog, the epob has not been studied so far and it is likely that it formed a pseudo-gene without having any biological role. Zebrafish erythropoietin encoded by the epoa gene is a crucial cytokine for erythroid cell development and maintenance (Krystal, 1994) and it has been shown to stimulate proliferation, and differentiation of erythroid cells (Paffett-Lugassy et al., 2007; Stachura et al., 2011). Moreover, recombinant zebrafish Epoa has been shown to expand and differentiate erythroid cells *ex vivo* (Stachura et al., 2009) and in combination with other factors such as Gcsfa or Tpo, and it promotes multilineage erythro-myeloid hematopoiesis in semisolid media (Stachura et al., 2011; Svoboda et al., 2014). To date, a single erythropoietin receptor has been identified in zebrafish (Paffett-Lugassy et al., 2007).

Kitlga/b

KIT ligand (KITLG) is a classic example of a cytokine acting on many different levels. KIT signaling plays an important role in a variety of tissues and cells, such as HSCs and germ stem cells. Moreover, KIT also plays a significant role during erythro-myelopoiesis (Hayman et al., 1993), neurogenesis and pigmentation, and mutations in this gene have been reported in many types of cancers including erythroleukemia (Kosmider et al., 2005; Abbaspour Babaei et al., 2016). Binding of KITLG to its cognate receptor (KIT) – member of the receptor tyrosine kinase type III family (RTKIII) – promotes various signaling cascades. Ligand-based activation of Kit triggers auto-phosphorylation and activation of PI-3K, MAPK, SRC, but also JAK kinase pathways (Ashman, 1999; Abbaspour Babaei et al., 2016). Notably, KITLG exists in two forms *in vivo* – transmembrane, which seems to be important to regulate stem cells in their niches, and soluble, that affects distant tissues (Ashman, 1999).

Interestingly, both Kit and Kitlg have been duplicated in teleost to form two receptors (Kita and Kitb) and two ligands (Kitlga and Kitlgb). This duplication of the whole ligand-receptor signalosome is relatively uncommon and raises many questions about diversification of both ligands and receptors as well as their binding specificities for each other. These questions have been poorly studied so far and very little is known about Kit involvement during zebrafish hematopoiesis. So far, it has been shown that both kitlg paralogs might have subspecialized during teleost phylogenesis. Kita is expressed in neural crest, lateral line or in the notochord. Similar to their mammalian counterparts, both Kitlga as well as Kita are involved in melanogenesis, since overexpression of kitlga results in a hyper pigmentation phenotype (Hultman et al., 2007), whereas kita receptor mutants (sparse) show severe pigmentation defects (Parichy et al., 1999). On the contrary, the second zebrafish Kit paralog, Kitb, does not seem to play a role during melanogenesis. It has been shown to be expressed in neural tube and otic vesicles (Mellgren and Johnson, 2005).

As mentioned above, Kit signaling has been poorly studied in the hematopoietic context and there are only two studies that present any possible Kit involvement in these processes. It has been shown that even though the kita is expressed in hematopoietic tissues, surprisingly and in contradiction to the other vertebrate models, hematopoiesis does not seem to be affected in the kita receptor (sparse) mutants (Parichy et al., 1999). So far, the only studies demonstrating any potential importance of Kit signaling during hematopoiesis in zebrafish at present are a mild increase of HSCs upon overexpression of kitlgb (Mahony et al., 2016) and decrease of HSCs upon downregulation of kitb (Mahony et al., 2018).

Csf3a/b

Colony stimulating factor 3, CSF3, also known as granulocyte colony stimulating factor (GCSF), is a cytokine crucial for proliferation, differentiation and survival of monocytes, macrophages and neutrophilic granulocytes (Metcalf and Nicola, 1983; Nicola et al., 1983, 1985; Lieschke et al., 1994; Liu et al., 1996). CSF3 binds to its cognate receptor, CSF3R, activating signaling cascades including JAK2/STAT5 and MAPK pathway, important for neutrophil production during both steady state and emergency hematopoiesis (Touw and van de Geijn, 2007).

Two paralogs of Csf3, the major regulator of granulocytic, monocytic and megakaryocytic differentiation, have been reported in zebrafish with a slightly diverged function. Based on extensive synteny analysis, it has been suggested that chromosomal regions harboring Csf3a/b share common ancestral origin and probably emerged from a chromosome/genome duplication event (Stachura et al., 2013). Although like in mammals, both zebrafish Csf3 paralogs stimulate granulocytic differentiation (Nicola et al., 1983, 1985) and monocyte/macrophage differentiation (Migliaccio et al., 1988), they appear to play a broader role in hematopoiesis, including HSCs specification and expansion. Both paralogs differ in the levels of spatio-temporal expression during development and in the adult animals. Csf3a expression is low in early development, rising gradually over time, whereas Csf3b is highly expressed starting from 6 hpf but its levels decrease over time. Despite these differences, overexpression of both ligands during development indicates redundant functions. Slight differences in binding kinetics to Csf3r, indicate another possible mechanism that controls spatio-temporal activity of both zebrafish Csf3 paralogs (Stachura et al., 2013).

High csf3b expression has been detected in the kidney, the main site of hematopoiesis in zebrafish, as well as testes, skin and gills. Csf3a has been detected at lower levels in these tissues, with high expression in heart and spleen. Although the differences in tissue expression might indicate that the major player could be csf3b, both of these ligands retain the ability to differentiate myeloid progenitors. As in mammals, Csf3 is important for both primitive and definitive waves of generation of myelomonocytic cells (Stachura et al., 2013).

These findings suggest that during vertebrate evolution, Csf3 was involved in many levels of hematopoiesis, but after the radiation of mammals other specialized cytokines evolved and have likely taken over the function of Csf3 (Avery et al., 2004; Huising et al., 2006). Csf3 probably represents an ancient cytokine whose functions were diversified in evolution following duplication events (Stachura et al., 2013).

Csf1a/b and IL34

In mammals, CSF1 is the major regulator of many myeloid cells, such as monocytes, macrophages, dendritic cells, microglia, osteoclasts, or Langerhans and Kupffer cells, and it also plays an important role in disease development (Hamilton, 2008; Hamilton and Achuthan, 2013). The ligand binds to its specific receptor (CSF1R), which is another member of RTKIII family, and activated CSF1R further promotes JAK2/STAT5, PI3K, and MEK signaling (Pixley and Stanley, 2004; Martinez and Gordon, 2014). It has been shown that CSF1 is not the only ligand to bind and activate this receptor. Alternatively, it can be activated also by IL34 in certain tissues – Langerhans cells and microglia inside mouse brain (Greter et al., 2012; Wang et al., 2012).

Similarly to other cytokines described, the CSF1 has been identified in the form of two paralogs in zebrafish (csf1a/b) (Wang et al., 2008). Along with two csf1 receptors (csf1ra/b) found in fish, this provides another relatively unique example of duplication of the whole receptor-ligand signalosome (Braasch et al., 2006). Regarding the IL34 that has been similarly reported to exist in two copies in salmon (Pagan et al., 2015), only a single il34 gene has been identified in zebrafish so far.

Zebrafish Csf1a and Il34 signaling has been shown to play a role in microglia development in the retina (Huang et al., 2012) as well as in pigment pattern formation during development (Patterson et al., 2014) (Csf1a only). Supporting this, the csf1ra mutant fish (panther) have decreased numbers of microglia and macrophages (Herbomel et al., 1999; Pagan et al., 2015). Il34 has recently been shown to regulate distribution of yolk sac macrophages and microglial precursors and seeding of the brain in zebrafish embryos (van Ham et al., 2018; Wu et al., 2018). On the other hand, any information about the functional role of csf1rb are missing.

Examples of Potentially Missing Cytokine Genes

Genome evolution in the teleost fish did not only bring another rounds of duplication, but it also brought many losses of individual genes or clusters of genes including some of the class I cytokine family members (Liongue and Ward, 2007). This includes a missing cluster of il3 family genes with the disappearance of ligands and receptors for il3, il5, and gmcsf. In mammals and birds, these factors are responsible for the maintenance of myelo-monocytic lineages and their loss in teleost indicates that they were possibly substituted by other newly duplicated genes (Stachura et al., 2013).

Another example of a cytokine potentially missing in the zebrafish genome is flt3l, an important regulator of HSCs and myeloid cells (Guermonprez et al., 2013; Jacobsen et al., 2016; Tornack et al., 2017). However, the possibility exists that it has not yet been identified due to sequence divergence. This hypothesis is supported by the fact that flt3l is present both in mammals and even some lower vertebrates including *Latimeria* and elephant shark (Tan et al., 2012) and its cognate receptor, Flt3, is expressed in the developing zebrafish embryo and adult HSCs and monocytes (He et al., 2014; Macaulay et al., 2016; Tang et al., 2017).

CONCLUSION

The whole-genome duplication in teleost fish raises interesting questions regarding hematopoietic cytokine sub-specialization, redundancy and gain/loss of function. In this review, we have reviewed particular examples of all of these events, discussing epob loss of function, sub-specialization of kitlga/b, or the redundancy between csf3a/b (**Figure 1**). We hypothesize that some specific gene duplications might even have enabled or compensated for the loss of some specific genes in the zebrafish genome (GM-CSF/IL3 cluster).

Although several reports have addressed the question of duplicated cytokines in zebrafish, many functional links are still missing, especially the ligand receptor specificities in cases, when the whole ligand-receptor signalosome has been duplicated (e.g., Kitlg/Kit, Csf1/Csf1r). Moreover, functions of many hematopoietic cytokines have yet not been elucidated. One example is IL11, a crucial regulator of megakaryocyte maturation (Paul et al., 1990) that binds to IL11Rα and gp130, activating the JAK/STAT pathway (Heinrich et al., 2003). Two paralogs of il11 have been identified in teleost (Huising et al., 2005); however, data indicating respective functions of each of the paralogs are still missing.

Zebrafish is a powerful model organism for studies of hematopoietic cell maintenance and differentiation both in the course of development and in the adult animal using the wide range of available *in vivo* and *ex vivo* tools. Therefore, it is very important to understand the precise function of each of the paralogs and elucidate the functions of the yet uncharacterized cytokines that would enable more complex experiments elucidating the fine details of hematopoietic regulatory mechanisms.

AUTHOR CONTRIBUTIONS

All authors listed have made a substantial, direct and intellectual contribution to the work, and approved it for publication.

FUNDING

This work was supported by the Ministry of Education, Youth and Sports – Program NPU I (LO1419), and the Czech Science Foundation (16-21024S) to PB.

ACKNOWLEDGMENTS

We would like to thank Trevor Epp for proofreading the manuscript.

REFERENCES

Abbaspour Babaei, M., Kamalidehghan, B., Saleem, M., Huri, H. Z., and Ahmadipour, F. (2016). Receptor tyrosine kinase (c-Kit) inhibitors: a potential therapeutic target in cancer cells. *Drug Des. Dev. Ther.* 10, 2443–2459. doi: 10.2147/DDDT.S89114

Akashi, K., Traver, D., Miyamoto, T., and Weissman, I. L. (2000). A clonogenic common myeloid progenitor that gives rise to all myeloid lineages. *Nature* 404, 193–197. doi: 10.1038/35004599

Alexander, W. S. (1999a). Thrombopoietin and the c-Mpl receptor: insights from gene targeting. *Int. J. Biochem. Cell Biol.* 31, 1027–1035.

Alexander, W. S. (1999b). Thrombopoietin. *Growth Factors* 17, 13–24. doi: 10.3109/08977199909001059

Amores, A., Catchen, J., Ferrara, A., Fontenot, Q., and Postlethwait, J. H. (2011). Genome evolution and meiotic maps by massively parallel DNA sequencing: spotted gar, an outgroup for the teleost genome duplication. *Genetics* 188, 799–808. doi: 10.1534/genetics.111.127324

Ashman, L. K. (1999). The biology of stem cell factor and its receptor C-kit. *Int. J. Biochem. Cell Biol.* 31, 1037–1051. doi: 10.1016/S1357-2725(99)00076-X

Avery, S., Rothwell, L., Degen, W. D., Schijns, V. E., Young, J., Kaufman, J., et al. (2004). Characterization of the first nonmammalian T2 cytokine gene cluster: the cluster contains functional single-copy genes for IL-3, IL-4, IL-13, and GM-CSF, a gene for IL-5 that appears to be a pseudogene, and a gene encoding another cytokinelike transcript, KK34. *J. Interferon Cytokine Res.* 24, 600–610. doi: 10.1089/jir.2004.24.600

Bartunek, P., Pajer, P., Karafiat, V., Blendinger, G., and Dvorak, M. (2002). bFGF signaling and v-Myb cooperate in sustained growth of primitive erythroid progenitors. *Oncogene* 21, 400–410. doi: 10.1038/sj/onc/1205103

Braasch, I., Salzburger, W., and Meyer, A. (2006). Asymmetric evolution in two fish-specifically duplicated receptor tyrosine kinase paralogons involved in teleost coloration. *Mol. Biol. Evol.* 23, 1192–1202. doi: 10.1093/molbev/msk003

Broudy, V. C. (1997). Stem cell factor and hematopoiesis. *Blood* 90, 1345–1364.

Butko, E., Distel, M., Pouget, C., Weijts, B., Kobayashi, I., Ng, K., et al. (2015). Gata2b is a restricted early regulator of hemogenic endothelium in the zebrafish embryo. *Development* 142, 1050–1061. doi: 10.1242/dev.119180

Constantinescu, S. N., Ghaffari, S., and Lodish, H. F. (1999). The Erythropoietin receptor: structure. activation and intracellular signal transduction. *Trends Endocrinol. Metab.* 10, 18–23. doi: 10.1016/S1043-2760(98)00101-5

de Sauvage, F. J., Hass, P. E., Spencer, S. D., Malloy, B. E., Gurney, A. L., Spencer, S. A., et al. (1994). Stimulation of megakaryocytopoiesis and thrombopoiesis by the c-Mpl ligand. *Nature* 369, 533–538. doi: 10.1038/369533a0

Drachman, J. G., and Kaushansky, K. (1997). Dissecting the thrombopoietin receptor: functional elements of the Mpl cytoplasmic domain. *Proc. Natl. Acad. Sci. U.S.A.* 94, 2350–2355. doi: 10.1073/pnas.94.6.2350

Force, A., Lynch, M., Pickett, F. B., Amores, A., Yan, Y. L., and Postlethwait, J. (1999). Preservation of duplicate genes by complementary, degenerative mutations. *Genetics* 151, 1531–1545.

Fuchs, O., Simakova, O., Klener, P., Cmejlova, J., Zivny, J., Zavadil, J., et al. (2002). Inhibition of Smad5 in human hematopoietic progenitors blocks erythroid differentiation induced by BMP4. *Blood Cells Mol. Dis.* 28, 221–233. doi: 10.1006/bcmd.2002.0487

Gandrillon, O., Schmidt, U., Beug, H., and Samarut, J. (1999). TGF-beta cooperates with TGF-alpha to induce the self-renewal of normal erythrocytic progenitors: evidence for an autocrine mechanism. *EMBO J.* 18, 2764–2781. doi: 10.1093/emboj/18.10.2764

Ginhoux, F., Greter, M., Leboeuf, M., Nandi, S., See, P., Gokhan, S., et al. (2010). Fate mapping analysis reveals that adult microglia derive from primitive macrophages. *Science* 330, 841–845. doi: 10.1126/science.1194637

Gordon, M. S., and Hoffman, R. (1992). Growth factors affecting human thrombocytopoiesis: potential agents for the treatment of thrombocytopenia. *Blood* 80, 302–307.

Greter, M., Lelios, I., Pelczar, P., Hoeffel, G., Price, J., Leboeuf, M., et al. (2012). Stroma-derived interleukin-34 controls the development and maintenance of langerhans cells and the maintenance of microglia. *Immunity* 37, 1050–1060. doi: 10.1016/j.immuni.2012.11.001

Guermonprez, P., Helft, J., Claser, C., Deroubaix, S., Karanje, H., Gazumyan, A., et al. (2013). Inflammatory Flt3l is essential to mobilize dendritic cells and for T cell responses during Plasmodium infection. *Nat. Med.* 19, 730–738. doi: 10.1038/nm.3197

Hamilton, J. A. (2008). Colony-stimulating factors in inflammation and autoimmunity. *Nat. Rev. Immunol.* 8, 533–544. doi: 10.1038/nri2356

Hamilton, J. A., and Achuthan, A. (2013). Colony stimulating factors and myeloid cell biology in health and disease. *Trends Immunol.* 34, 81–89. doi: 10.1016/j.it.2012.08.006

Harandi, O. F., Hedge, S., Wu, D. C., McKeone, D., and Paulson, R. F. (2010). Murine erythroid short-term radioprotection requires a BMP4-dependent, self-renewing population of stress erythroid progenitors. *J. Clin. Invest.* 120, 4507–4519. doi: 10.1172/JCI41291

Hayman, M. J., Meyer, S., Martin, F., Steinlein, P., and Beug, H. (1993). Self-renewal and differentiation of normal avian erythroid progenitor cells: regulatory roles of the TGF alpha/c-ErbB and SCF/c-kit receptors. *Cell* 74, 157–169. doi: 10.1016/0092-8674(93)90303-8

He, B. L., Shi, X., Man, C. H., Ma, A. C., Ekker, S. C., Chow, H. C., et al. (2014). Functions of flt3 in zebrafish hematopoiesis and its relevance to human acute myeloid leukemia. *Blood* 123, 2518–2529. doi: 10.1182/blood-2013-02-486688

Heinrich, P. C., Behrmann, I., Haan, S., Hermanns, H. M., Muller-Newen, G., and Schaper, F. (2003). Principles of interleukin (IL)-6-type cytokine signalling and its regulation. *Biochem. J.* 374(Pt 1), 1–20. doi: 10.1042/bj20030407

Herbomel, P., Thisse, B., and Thisse, C. (1999). Ontogeny and behaviour of early macrophages in the zebrafish embryo. *Development* 126, 3735–3745.

Hoegg, S., Brinkmann, H., Taylor, J. S., and Meyer, A. (2004). Phylogenetic timing of the fish-specific genome duplication correlates with the diversification of teleost fish. *J. Mol. Evol.* 59, 190–203. doi: 10.1007/s00239-004-2613-z

Huang, T., Cui, J., Li, L., Hitchcock, P. F., and Li, Y. (2012). The role of microglia in the neurogenesis of zebrafish retina. *Biochem. Biophys. Res. Commun.* 421, 214–220. doi: 10.1016/j.bbrc.2012.03.139

Huber, T. L., Zhou, Y., Mead, P. E., and Zon, L. I. (1998). Cooperative effects of growth factors involved in the induction of hematopoietic mesoderm. *Blood* 92, 4128–4137.

Huising, M. O., Kruiswijk, C. P., and Flik, G. (2006). Phylogeny and evolution of class-I helical cytokines. *J. Endocrinol.* 189, 1–25. doi: 10.1677/joe.1.06591

Huising, M. O., Kruiswijk, C. P., van Schijndel, J. E., Savelkoul, H. F., Flik, G., and Verburg-van Kemenade, B. M. (2005). Multiple and highly divergent IL-11 genes in teleost fish. *Immunogenetics* 57, 432–443. doi: 10.1007/s00251-005-0012-2

Hultman, K. A., Bahary, N., Zon, L. I., and Johnson, S. L. (2007). Gene Duplication of the zebrafish kit ligand and partitioning of melanocyte development functions to kit ligand a. *PLoS Genet.* 3:e17. doi: 10.1371/journal.pgen.0030017

Jacobsen, R. N., Nowlan, B., Brunck, M. E., Barbier, V., Winkler, I. G., and Levesque, J. P. (2016). Fms-like tyrosine kinase 3 (Flt3) ligand depletes erythroid island macrophages and blocks medullar erythropoiesis in the mouse. *Exp. Hematol.* 44, 207–212e204. doi: 10.1016/j.exphem.2015.11.004

Kato, T., Matsumoto, A., Ogami, K., Tahara, T., Morita, H., and Miyazaki, H. (1998). Native thrombopoietin: structure and function. *Stem Cells* 16, 322–328. doi: 10.1002/stem.160322

Kaushansky, K. (2006). Lineage-specific hematopoietic growth factors. *N. Engl. J. Med.* 354, 2034–2045. doi: 10.1056/NEJMra052706

Kaushansky, K., Broudy, V. C., Grossmann, A., Humes, J., Lin, N., Ren, H. P., et al. (1995). Thrombopoietin expands erythroid progenitors, increases red cell production, and enhances erythroid recovery after myelosuppressive therapy. *J. Clin. Invest.* 96, 1683–1687. doi: 10.1172/JCI118210

Kosmider, O., Denis, N., Lacout, C., Vainchenker, W., Dubreuil, P., and Moreau-Gachelin, F. (2005). Kit-activating mutations cooperate with Spi-1/PU.1 overexpression to promote tumorigenic progression during erythroleukemia in mice. *Cancer Cell* 8, 467–478. doi: 10.1016/j.ccr.2005.11.009

Krantz, S. B. (1991). Erythropoietin. *Blood* 77, 419–434.

Krystal, G. (1994). Transforming growth factor beta 1 is an inducer of erythroid differentiation. *J. Exp. Med.* 180, 851–860. doi: 10.1084/jem.180.3.851

Lieschke, G. J., Grail, D., Hodgson, G., Metcalf, D., Stanley, E., Cheers, C., et al. (1994). Mice lacking granulocyte colony-stimulating factor have chronic neutropenia, granulocyte and macrophage progenitor cell deficiency, and impaired neutrophil mobilization. *Blood* 84, 1737–1746.

Liongue, C., and Ward, A. C. (2007). Evolution of Class I cytokine receptors. *BMC Evol. Biol.* 7:120. doi: 10.1186/1471-2148-7-120

Liu, F., Wu, H. Y., Wesselschmidt, R., Kornaga, T., and Link, D. C. (1996). Impaired production and increased apoptosis of neutrophils in granulocyte

colony-stimulating factor receptor-deficient mice. *Immunity* 5, 491–501. doi: 10.1016/S1074-7613(00)80504-X

Macaulay, I. C., Svensson, V., Labalette, C., Ferreira, L., Hamey, F., Voet, T., et al. (2016). Single-Cell RNA-Sequencing reveals a continuous spectrum of differentiation in hematopoietic cells. *Cell Rep.* 14, 966–977. doi: 10.1016/j.celrep.2015.12.082

Mahony, C. B., Fish, R. J., Pasche, C., and Bertrand, J. Y. (2016). tfec controls the hematopoietic stem cell vascular niche during zebrafish embryogenesis. *Blood* 128, 1336–1345. doi: 10.1182/blood-2016-04-710137

Mahony, C. B., Pasche, C., and Bertrand, J. Y. (2018). Oncostatin M and kit-ligand control hematopoietic stem cell fate during zebrafish embryogenesis. *Stem Cell Rep.* 10, 1920–1934. doi: 10.1016/j.stemcr.2018.04.016

Martinez, F. O., and Gordon, S. (2014). The M1 and M2 paradigm of macrophage activation: time for reassessment. *F1000Prime Rep.* 6:13. doi: 10.12703/P6-13

McNiece, I. K., Langley, K. E., and Zsebo, K. M. (1991). Recombinant human stem cell factor synergises with GM-CSF, G-CSF, IL-3 and epo to stimulate human progenitor cells of the myeloid and erythroid lineages. *Exp. Hematol.* 19, 226–231.

Mellgren, E. M., and Johnson, S. L. (2005). kitb, a second zebrafish ortholog of mouse Kit. *Dev. Genes Evol.* 215, 470–477. doi: 10.1007/s00427-005-0001-3

Metcalf, D. (1985). The granulocyte-macrophage colony-stimulating factors. *Science* 229, 16–22. doi: 10.1126/science.2990035

Metcalf, D., and Nicola, N. A. (1983). Proliferative effects of purified granulocyte colony-stimulating factor (G-CSF) on normal mouse hemopoietic cells. *J. Cell. Physiol.* 116, 198–206. doi: 10.1002/jcp.1041160211

Migliaccio, G., Migliaccio, A. R., and Adamson, J. W. (1988). In vitro differentiation of human granulocyte/macrophage and erythroid progenitors: comparative analysis of the influence of recombinant human erythropoietin, G-CSF, GM-CSF, and IL-3 in serum-supplemented and serum-deprived cultures. *Blood* 72, 248–256.

Migliaccio, G., Migliaccio, A. R., and Adamson, J. W. (1991). In vitro differentiation and proliferation of human hematopoietic progenitors: the effects of interleukins 1 and 6 are indirectly mediated by production of granulocyte-macrophage colony-stimulating factor and interleukin 3. *Exp. Hematol.* 19, 3–10.

Miyagawa, S., Kobayashi, M., Konishi, N., Sato, T., and Ueda, K. (2000). Insulin and insulin-like growth factor I support the proliferation of erythroid progenitor cells in bone marrow through the sharing of receptors. *Br. J. Haematol.* 109, 555–562. doi: 10.1046/j.1365-2141.2000.02047.x

Muir, A. R., and Kerr, D. N. (1958). Erythropoiesis: an electron microscopical study. *Q. J. Exp. Physiol. Cogn. Med. Sci.* 43, 106–114. doi: 10.1113/expphysiol.1958.sp001295

Nei, M., and Roychoudhury, A. K. (1973). Probability of fixation and mean fixation time of an overdominant mutation. *Genetics* 74, 371–380.

Nicola, N. A. (1994). Cytokine pleiotropy and redundancy: a view from the receptor. *Stem Cells* 12(Suppl. 1), 3–12; discussion 12–14.

Nicola, N. A., Begley, C. G., and Metcalf, D. (1985). Identification of the human analogue of a regulator that induces differentiation in murine leukaemic cells. *Nature* 314, 625–628. doi: 10.1038/314625a0

Nicola, N. A., Metcalf, D., Matsumoto, M., and Johnson, G. R. (1983). Purification of a factor inducing differentiation in murine myelomonocytic leukemia cells. Identification as granulocyte colony-stimulating factor. *J. Biol. Chem.* 258, 9017–9023.

Paffett-Lugassy, N., Hsia, N., Fraenkel, P. G., Paw, B., Leshinsky, I., Barut, B., et al. (2007). Functional conservation of erythropoietin signaling in zebrafish. *Blood* 110, 2718–2726. doi: 10.1182/blood-2006-04-016535

Pagan, A. J., Yang, C. T., Cameron, J., Swaim, L. E., Ellett, F., Lieschke, G. J., et al. (2015). Myeloid growth factors promote resistance to mycobacterial infection by curtailing Granuloma necrosis through macrophage replenishment. *Cell Host Microbe* 18, 15–26. doi: 10.1016/j.chom.2015.06.008

Parichy, D. M., Rawls, J. F., Pratt, S. J., Whitfield, T. T., and Johnson, S. L. (1999). Zebrafish sparse corresponds to an orthologue of c-kit and is required for the morphogenesis of a subpopulation of melanocytes, but is not essential for hematopoiesis or primordial germ cell development. *Development* 126, 3425–3436.

Patterson, L. B., Bain, E. J., and Parichy, D. M. (2014). Pigment cell interactions and differential xanthophore recruitment underlying zebrafish stripe reiteration and Danio pattern evolution. *Nat. Commun.* 5:5299. doi: 10.1038/ncomms6299

Paul, S. R., Bennett, F., Calvetti, J. A., Kelleher, K., Wood, C. R., O'Hara, R. M., et al. (1990). Molecular cloning of a cDNA encoding interleukin 11, a stromal cell-derived lymphopoietic and hematopoietic cytokine. *Proc. Natl. Acad. Sci. U.S.A.* 87, 7512–7516. doi: 10.1073/pnas.87.19.7512

Pixley, F. J., and Stanley, E. R. (2004). CSF-1 regulation of the wandering macrophage: complexity in action. *Trends Cell Biol.* 14, 628–638. doi: 10.1016/j.tcb.2004.09.016

Ratnoff, O. D. (1987). The evolution of hemostatic mechanisms. *Perspect. Biol. Med.* 31, 4–33. doi: 10.1353/pbm.1987.0003

Schneider, W., and Gattermann, N. (1994). Megakaryocytes: origin of bleeding and thrombotic disorders. *Eur. J. Clin. Invest.* 24(Suppl. 1), 16–20. doi: 10.1111/j.1365-2362.1994.tb02420.x

Simpson, C. F. (1967). The mechanism of denucleation in circulating erythroblasts. *J. Cell Biol.* 35, 237–245. doi: 10.1083/jcb.35.1.237

Stachura, D. L., Reyes, J. R., Bartunek, P., Paw, B. H., Zon, L. I., and Traver, D. (2009). Zebrafish kidney stromal cell lines support multilineage hematopoiesis. *Blood* 114, 279–289. doi: 10.1182/blood-2009-02-203638

Stachura, D. L., Svoboda, O., Campbell, C. A., Espin-Palazon, R., Lau, R. P., Zon, L. I., et al. (2013). The zebrafish granulocyte colony-stimulating factors (Gcsfs): 2 paralogous cytokines and their roles in hematopoietic development and maintenance. *Blood* 122, 3918–3928. doi: 10.1182/blood-2012-12-475392

Stachura, D. L., Svoboda, O., Lau, R. P., Balla, K. M., Zon, L. I., Bartunek, P., et al. (2011). Clonal analysis of hematopoietic progenitor cells in the zebrafish. *Blood* 118, 1274–1282. doi: 10.1182/blood-2011-01-331199

Steinlein, P., Wessely, O., Meyer, S., Deiner, E. M., Hayman, M. J., and Beug, H. (1995). Primary, self-renewing erythroid progenitors develop through activation of both tyrosine kinase and steroid hormone receptors. *Curr. Biol.* 5, 191–204. doi: 10.1016/S0960-9822(95)00040-6

Svoboda, O., and Bartunek, P. (2015). Origins of the vertebrate erythro/megakaryocytic system. *Biomed. Res. Int.* 2015:632171. doi: 10.1155/2015/632171

Svoboda, O., Stachura, D. L., Machonova, O., Pajer, P., Brynda, J., Zon, L. I., et al. (2014). Dissection of vertebrate hematopoiesis using zebrafish thrombopoietin. *Blood* 124, 220–228. doi: 10.1182/blood-2014-03-564682

Takahata, N., and Maruyama, T. (1979). Polymorphism and loss of duplicate gene expression: a theoretical study with application of tetraploid fish. *Proc. Natl. Acad. Sci. U.S.A.* 76, 4521–4525. doi: 10.1073/pnas.76.9.4521

Tan, Y. Y., Kodzius, R., Tay, B. H., Tay, A., Brenner, S., and Venkatesh, B. (2012). Sequencing and analysis of full-length cDNAs, 5′-ESTs and 3′-ESTs from a cartilaginous fish, the elephant shark (*Callorhinchus milii*). *PLoS One* 7:e47174. doi: 10.1371/journal.pone.0047174

Tang, Q., Iyer, S., Lobbardi, R., Moore, J. C., Chen, H., Lareau, C., et al. (2017). Dissecting hematopoietic and renal cell heterogeneity in adult zebrafish at single-cell resolution using RNA sequencing. *J. Exp. Med.* 214, 2875–2887. doi: 10.1084/jem.20170976

Tornack, J., Kawano, Y., Garbi, N., Hammerling, G. J., Melchers, F., and Tsuneto, M. (2017). Flt3 ligand-eGFP-reporter expression characterizes functionally distinct subpopulations of CD150(+) long-term repopulating murine hematopoietic stem cells. *Eur. J. Immunol.* 47, 1477–1487. doi: 10.1002/eji.201646730

Touw, I. P., and van de Geijn, G. J. (2007). Granulocyte colony-stimulating factor and its receptor in normal myeloid cell development, leukemia and related blood cell disorders. *Front. Biosci.* 12:800–815. doi: 10.2741/2103

van Ham, T. J., Oosterhof, N., Kuil, L. E., van der Linde, H. C., Geurts, S. N., and Meijering, E. (2018). Reverse genetic screen reveals that Il34 facilitates yolk sac macrophage distribution and seeding of the brain. *bioRxiv* [Preprint]. doi: 10.1101/406553

Wang, T., Hanington, P. C., Belosevic, M., and Secombes, C. J. (2008). Two macrophage colony-stimulating factor genes exist in fish that differ in gene

organization and are differentially expressed. *J. Immunol.* 181, 3310–3322. doi: 10.4049/jimmunol.181.5.3310

Wang, Y., Szretter, K. J., Vermi, W., Gilfillan, S., Rossini, C., Cella, M., et al. (2012). IL-34 is a tissue-restricted ligand of CSF1R required for the development of Langerhans cells and microglia. *Nat. Immunol.* 13, 753–760. doi: 10.1038/ni.2360

Watterson, G. A. (1983). On the time for gene silencing at duplicate Loci. *Genetics* 105, 745–766.

Wu, S., Xue, R., Hassan, S., Nguyen, T. M. L., Wang, T., Pan, H., et al. (2018). Il34-Csf1r pathway regulates the migration and colonization of microglial precursors. *Dev. Cell* 46, 552.e4–563.e4. doi: 10.1016/j.devcel.2018.08.005

Conflict of Interest Statement: The authors declare that the research was conducted in the absence of any commercial or financial relationships that could be construed as a potential conflict of interest.

ZEBRAFISH
Volume 00, Number 00, 2018
Mary Ann Liebert, Inc.
DOI: 10.1089/zeb.2018.1609

Zebrabase: An Intuitive Tracking Solution for Aquatic Model Organisms

Jana Oltova,[1,*] Jindrich Jindrich,[2,3,*] Ctibor Skuta,[2] Ondrej Svoboda,[1] Olga Machonova,[1] and Petr Bartunek[1,2]

Abstract

Small fish species, such as zebrafish and medaka, are increasingly gaining popularity in basic research and disease modeling as a useful alternative to rodent model organisms. However, the tracking options for fish within a facility are rather limited. In this study, we present an aquatic species tracking database, Zebrabase, developed in our zebrafish research and breeding facility that represents a practical and scalable solution and an intuitive platform for scientists, fish managers, and caretakers, in both small and large facilities. Zebrabase is a scalable, cross-platform fish tracking database developed especially for fish research facilities. Nevertheless, this platform can be easily adapted for a wide variety of aquatic model organisms housed in tanks. It provides sophisticated tracking, reporting, and management functions that help keep animal-related records well organized, including a QR code functionality for tank labeling. The implementation of various user roles ensures a functional hierarchy and customized access to specific functions and data. In addition, Zebrabase makes it easy to personalize rooms and racks, and its advanced statistics and reporting options make it an excellent tool for creating periodic reports of animal usage and productivity. Communication between the facility and the researchers can be streamlined by the database functions. Finally, Zebrabase also features an interactive breeding history and a smart interface with advanced visualizations and intuitive color coding that accelerate the processes.

Keywords: zebrafish, tracking, husbandry, facility database, Django, Python

Introduction

Zebrafish is a popular vertebrate model organism widely used in scientific research and a highly prized disease model. Thanks to its high fecundity, optical transparency, and rapid development, zebrafish is highly attractive model for live imaging and developmental studies. Especially the recent, rapid progress in the field of genome editing has prompted us to develop a database system that would facilitate fish tracking of the F0 and F1 generations of newly created, genetically modified lines, which is both highly laborious and space demanding and requires a high level of organization in the facility. Furthermore, proper outcrossing is required in zebrafish to prevent the inbreeding depression of fish stocks,[1] which is particularly prone to mix-ups.

Despite the increasing use of the zebrafish model in research, the currently available tracking options suitable for aquatic animals housed in tanks remain rather limited, and scientists often depend on outdated software solutions or simple spreadsheets. An explanation for this limitation could be that the requirements for aquatic organism tracking significantly differ from the rodent tracking, wherein systems such as PyRat (www.scionics.com/pyrat.html) or open-source JAX Colony Management System[2] (http://colonymanagement.jax.org) have long been established as a standard. The main specificity of aquatic animal tracking is group tracking, as opposed to tracking individual animals. One of the reasons for group tracking is that, up to date, there is no cost-effective system designed to distinguish single fish individuals in a tank. Technologies such as subdermal chipping are developing fast, but the technology is not yet sufficiently miniaturized to enable its routine use in tracking small fish species, although some significant advances have been reported using the radio frequency identification microtags.[3] In addition, due to the social requirements and bulk mating, zebrafish should be kept within a specific density range in the with both males and females.[4,5]

[1]Department of Cell Differentiation, Institute of Molecular Genetics AS CR v.v.i., Prague, Czech Republic.
[2]CZ-OPENSCREEN, Institute of Molecular Genetics AS CR v.v.i., Prague, Czech Republic.
[3]Department of Organic Chemistry, Faculty of Science, Charles University, Prague, Czech Republic.
*These authors contributed equally to this work.

Keeping individual fish in solitude adversely affects their development and health[6] and, moreover, is very space inefficient.

A handful of solutions, either commercial (e.g., www.daniodata.com, www.scionics.com/pyrat_aquatic.html) or open-source[7–9] (http://zebase.bio.purdue.edu, http://aqacs.uoregon.edu/zf/files, https://zebrafish.jimdo.com) are currently available. However, none of them is prevalent in the zebrafish community most likely because each of them is tailored to a slightly different set of requirements of the facilities. Two main drawbacks of the solutions currently available in the market are the price and dedication to a single platform, which can both be perceived as a limiting factor, especially for small facilities with a limited budget. The sustainability and implementation of new functions have been the bottleneck of some databases developed in the recent years, and this aspect should indeed be carefully considered because switching from one system to another can be rather tedious, especially when aiming to save the tracking history. Finally, as reporting requirements from local authorities are becoming increasingly rigorous in many countries, another feature missing in some of the existing solutions is a detailed fish usage and health reporting capability. In this study, we present Zebrabase, a novel tracking database for zebrafish housing facilities.

Results

General concept

Zebrabase is a web-based, cross-platform hosted zebrafish tracking solution supporting both desktop and mobile use on Mac, Linux, Windows, Android, and iOS. The database is accessible via an optimized user interface, which serves both for browsing fish stock records and creating new ones via the action menu. Moreover, Zebrabase has a built-in QR code generator and QR code reader functionality that provide instant access to all fish stock information and related actions on a mobile device.

Basic operation principles

Zebrabase enables users to track animals from birth to death and to store detailed records of all relevant events. Every action performed by the user creates a record in the database and can be later used for reporting purposes. Zebrabase is optimized for touch devices and supports the use of QR codes for tank labeling to efficiently track animals.

Fish characterization and grouping

The most important purpose of Zebrabase is the time-efficient and comprehensive tracking of fish stocks. Therefore, all animals in a facility are divided into fishlines specified by the database administrator, who defines their genotypes, the date of creation or import and other optional information (https://public.zebrabase.org/fishline/create). Fish corresponding to a single fishline are further organized into groups of siblings, stocks, sharing the same date of birth, and parents. Because the number of fish in some stocks might exceed the capacity of a single tank, we introduced another level of grouping animals, substocks, which refer to a defined stock subset in a single tank. Thus, substock is the basic unit tracked in the database consisting of a variable number of fish individuals.

Genotypes consist of a modification category (transgene, natural mutant, engineered mutant, or custom) and either of a driver, triggered gene, and an optional allele for transgenic genotypes or of an affected gene and allele/mutation for mutant genotypes. The Zebrabase name generation rules are based on the common ZFIN nomenclature (https://wiki.zfin.org/display/general/ZFIN+Zebrafish+Nomenclature+Guidelines). An alias can also be specified and used as a trivial name for substocks with very long generated names (e.g., in the case of multiple genotypes) or a suffix can be appended to the generated name.

Zebrabase enables users to store attachments for each fishline to effectively organize genotyping protocols, publications, and all visual content, for example, phenotypes of mutant lines or transgene expression patterns used as a sorting reference for reporter lines. To achieve an additional degree of organization of the fishlines, a responsible user, and a workgroup can be specified.

Spatial and temporal tracking

We have developed a system for tracking animals in laboratory, which uses the positional widget termed facility (Fig. 1A), a platform for user-defined rooms, racks, and tanks. In facility, the productivity of substocks is visualized by consistent color coding to provide a quick status reference for users. We have also optimized the QR code functionality to efficiently record the action history of each substock via any mobile device, as an alternative to the manual entering from a desktop computer. In addition, a list view of all substocks, regardless of their position in the facility, including deceased or terminated substocks, can be found under the fish tab (Fig. 1B).

An interactive breeding history diagram is shown at the substock record page (https://public.zebrabase.org/substock/1673), which provides links to all substocks in the whole pedigree. This diagram also shows the dates of crosses and splits and, when clicked, leads to the action detail page. Breeding history enables to efficiently track animals that may have shared the same housing or breeding tank (e.g., during outcrosses) when requiring to adopt a cautious approach upon disease outbreak or potential fish mix-ups, among others.

Zebrabase also features a number of actions—crossing, split, transfer, count, productivity, genotyping, add request, and print QR code. These actions can be fully tracked, browsed, or filtered at any time, when requiring to trace a specific event. Action history is also listed on the substock record page to provide a full overview of all actions performed with a particular substock.

Animal age and productivity

We have implemented statuses for each substock that are determined by productivity (the ability to spawn), age, and additional information inserted by facility staff or researchers. Each status is visualized in a specific color to highlight the problematic substocks and to avoid mistakenly using them in an experiment. These basic statuses are unproductive, productive, retired, deceased, and sorted out. Moreover, temporary statuses can be turned on and off to visualize temporary productivity or progeny survival issues. The specific reason for the temporary statuses can be independently defined by each facility, based on their standard operating procedures.

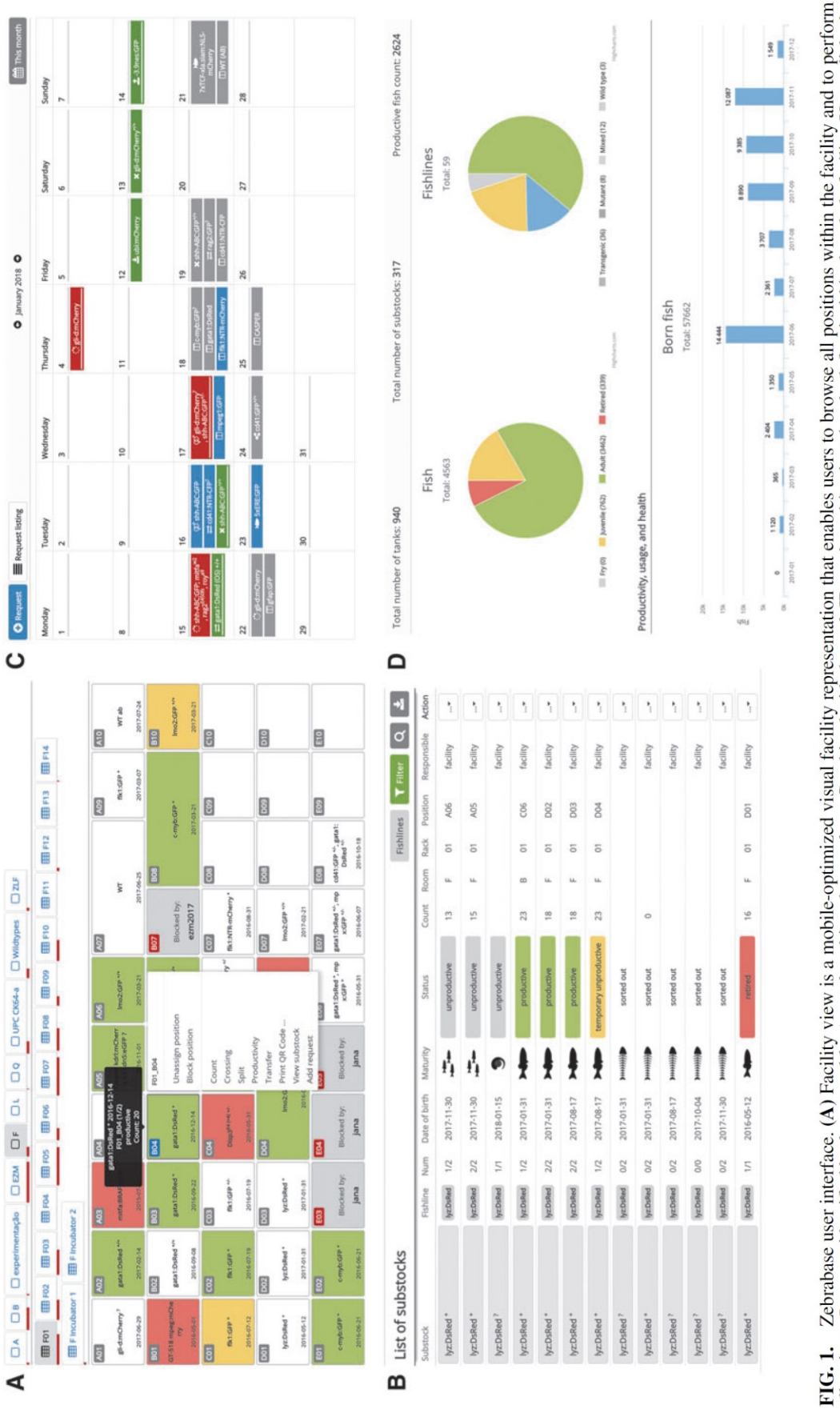

FIG. 1. Zebrabase user interface. **(A)** Facility view is a mobile-optimized visual facility representation that enables users to browse all positions within the facility and to perform all actions. *Rows* are identified by *letters* and *horizontal* positions by *numbers*. Combined with the rack ID, each position is uniquely defined within the whole facility. Upon click, the action menu appears and enables users to perform all actions available for a particular substock. **(B)** Fish list is a list of all records in the facility, regardless of whether they have a specific position in the facility or not. Records can be intuitively filtered, according to various parameters, to create a subset of fish of our interest. By default, only active (alive) fish are shown in the list, but that can be changed by adjusting the filter. Substocks are color-coded in the following manner: *green*—productive, *dark gray*—blocked, *light gray*—unproductive, *red*—retired, and *yellow*—temporary productivity issues. **(C)** Representation of various requests and self-requests in the calendar. Various icons are used for various types of requests (fish, setup fish, crossing, terminate, genotyping, mobilize fish, transfer, import, export). The requests are color-coded in the following manner: *gray*—new requests, *blue*—accepted requests, *green*—performed requests, and *red*—declined requests. **(D)** Zebrabase statistics enables users to store, visualize and export data for reporting purposes. The overview of facility statistics is presented as pie charts. *Left*—overview of the age distribution of the fish in the facility. *Right*—overview of the fishlines in the facility. *Bottom*—the bar charts are provided and plotted monthly for fish born, deceased, euthanized, and used for experiments in the facility (images not shown). Figure 1 can be viewed in greater detail online at www.liebertpub.com/zeb

Breeding management

The crossing action serves for incrossing and outcrossing substocks in the database. When outcrossing substocks of different fishlines, a new fishline with the corresponding genotype combination is automatically created, unless it is already present in the database. Similarly to all other actions, crossing can be initialized both from the fish list and from the facility view. Moreover, Zebrabase enables users to distinguish automatically whether fish are hetero- or homozygous or whether zygosity is unknown for a specific genotype based on the zygosities of the parents. To plan or request crosses, the requesting functionality is accessible via the calendar tab.

Genotyping

For the purposes of genotyping and sorting fish according to the transgene or mutation, two functionalities are available to improve the workflow. The action genotyping enables users to independently enter the zygosity of each genotype; if a more complex, physical rearrangement of the fish substocks is performed, a compound action split enables users to split the fish stock according to the genotypes, zygosities, or any other parameter, while they simultaneously enter the counts and positions.

Workgroups and user rights

In case more research groups are sharing the facility and wish to have their data separated, the workgroup functionality enables to setup multiple workgroups with defined administrators, whose data will be completely separated in the user interface, although they are using a single database instance. However, the facility members (e.g., caretakers) can still retain the right to see the data of all workgroups sharing the facility, if required. Within each workgroup, several permission groups—administrator, facility staff, standard user, or guest—can be assigned to users ensuring their different rights. The permission groups have assigned permissions ranging from view-only to the most advanced administrator rights. In addition, a single user can be assigned to more permission groups, and the permissions automatically combine with each other.

Calendar, requesting, and experiment planning

Submitting a request is a way to ask the facility staff for specific actions such as setting up fish for crossing, splitting, or terminating substocks and fishlines. Every request is then recorded in the database and shown in the calendar (Fig. 1C). E-mail notifications for new requests can be sent to the facility staff, if configured. The facility members are then able to accept the request, mark it as performed when the request is completed or decline it. Using the same functionality but assigning self-requests is a useful way to plan experiments. Self-requests are visible only to the user who created it. Generally, several request types can be entered: fish, setup fish, transfer substock, terminate substock, import, export, crossing, mobilize fish, and genotyping.

Statistics and reporting counts and usage of the animals

Zebrabase uses a comprehensive reporting system of animal usage or death via the action count. Initially, the start count must be specified, which is typically performed when the juvenile fish are introduced into the facility system, or at any earlier or later time. Once this figure is available for a particular substock, the used or deceased fish can be subtracted, and the purpose of their euthanasia can be specified, if appropriate (e.g., type of an experiment). These records are then visualized in the facility overview (Fig. 1D) and can be used to generate reports.

Data import and export

We provide a simple spreadsheet template that enables users to import a complete dataset, including the breeding history, to a new Zebrabase instance. Data exporting options include exporting statistics and full substock data (Supplementary Table S1; Supplementary Data are available online at www.liebertpub.com/zeb) into an .xls or .csv files and, upon request, complete database dumps can be provided.

Methods

System architecture

The Zebrabase system is operated with the utmost effort to ensure service availability. The system runs on a virtual server in an environment consisting of two clusters of hardware servers. Individual hardware components of the environment are redundant, and each cluster is housed in a different data center of the Institute of Molecular Genetics. The system is replicated from the primary to the secondary cluster every 30 min. In case the primary cluster becomes unavailable, the service can be restored in a short time on the secondary cluster by a system administrator. Due to rapid development of Zebrabase, a standalone version of the database where data would be stored at local servers is not available at the moment. However, we plan to provide such an option in the future under the condition of dedication to a single version of the database in the particular database instance.

Database development

For every instance of Zebrabase, a dedicated PostgreSQL database (www.postgresql.org) is created to ensure high data security and consistency. The code base (Zebrabase version), both back- and front-end, is the same for all Zebrabase instances. For the back-end part of the application, the Python programming language (www.python.org) is used with the Django web framework (www.djangoproject.com), which facilitates data exchange between a web browser and the database. The front-end part is implemented using the latest HTML5/CSS3 technologies that enable the interface to be responsive and interactive and to use data visualizations. Zebrabase is a multiplatform (Windows, Mac OS, Android, iOS, and Linux-based systems) web application that works in all modern Internet browsers (Google Chrome, Mozilla Firefox, Microsoft Edge, and Apple Safari, among others).

Data security and backup

All communication between users and the Zebrabase system is secured via Secure Sockets Layer (SSL), and a completely separate instance of Zebrabase is provided to each customer (e.g., facility or laboratory). Database dumps are performed four times a day and archived for 6 months when data restoration is necessary. In addition, fish stock records and statistics can be exported to an .xls or a .csv file directly from the user interface at any time to provide additional data backup.

User interface

Zebrabase user interface provides full touch support and cross-platform access via web browser. Zebrabase implements an intuitive and consistent color coding, icons, and visualization in the Graphical User Interphase (GUI) that enables easy orientation in the fish substocks. User support is reachable via the feedback link at the bottom of every Zebrabase instance, which also provides an interface for suggestions of new features or improvements.

Discussion

As the popularity of small fish species is increasing in research, the need for a proper tracking database that allows users to keep records of all animals, provides statistics and reporting capabilities, and enhances communication between users and caretakers at larger scale breeding facilities is critical. In this article, we propose a novel tracking database for aquatic model facilities, especially optimized for the use with small fish species such as zebrafish. Several major shortcomings of existing solutions have prompted us to develop Zebrabase, including commitment to a single platform, limited data export and transfer options, poor sustainability, and missing mobile device support. With Zebrabase, we tried to tackle these issues and to create a tracking solution that meets the needs of aquatic model facilities of any scale.

Zebrabase has been built around several key concepts that guarantee cross-platform operations, including full mobile device support and hosted maintenance-free service for users, unparalleled by any other solution. The cornerstones of Zebrabase are comprehensive animal tracking, interactive breeding history, and advanced management features. The animal tracking system of Zebrabase has been designed to carefully address the key specificities of the zebrafish tracking, primarily following a group of animals rather than tracking an individual animal, which substantially determines the data analysis and interpretation.

We have also focused on the reporting capabilities of the database, which allow users to store fish census and usage reports for the whole facility in a single excel file. This report provides a monthly overview of all fish born, deceased, euthanized, and used for experiments. We have also applied the suggestions of our beta testers and enhanced the requesting and experiment planning features of the database. The latest version now enables users to assign various types of requests either to the facility or to the users themselves so that all required actions in the fish facility are comprehensibly visualized. Advanced management features of Zebrabase, such as workgroups, user roles, responsible users, and QR code labeling will be a great benefit, especially for large facilities. Full touch and camera integration and QR code support are provided in the most recent Zebrabase version to ensure maximum system versatility and data accessibility from any device, which can be very beneficial for real-life use in fish facilities. In-App camera support is currently unavailable on Apple devices, but the substock records can be alternatively accessed via any mobile QR code reader application.

Zebrabase is a nonprofit project designed to support small and starting facilities by providing the service for free for up to 150 active substocks or 3 racks. After reaching this threshold, a yearly fee covering the initial setup, data backup and recovery, version updates, server maintenance, and user support is charged according to the size of the facility. For details on pricing, please visit the Zebrabase webpage (https://zebrabase.org/faq). To obtain the demo access or request a new database instance, please use the web form at https://zebrabase.org/contact.

Thanks to the hosted character of the Zebrabase project, we can provide unparalleled possibilities, including automatic backup and recovery options or instant version upgrades automatically available for all instances, regardless of whether they are running on the free or paid plan. The sustainability of this project is guaranteed because the tool is in use in the fish facility of the Institute of Molecular Genetics, where most of the new features are designed and thoroughly tested. Feedback from users is regularly collected and used to prioritize new features, and users are encouraged to report new suggestions for improvement to the Zebrabase team. In the near future, we plan to implement batch actions, enterprise resource planning and a genome editing module to streamline the workflow of researchers and facility managers, and to enable automated fee collection for the use of facility services. For more information about the new functionalities, please visit our webpage (https://zebrabase.org/news).

Acknowledgments

This work was funded by the Czech Science Foundation (16-21024S) and by the Ministry of Education, Youth and Sports (NPU I-LO1419).

Disclosure Statement

The authors declare that there are no competing financial interests.

References

1. Monson CA, Sadler KC. Inbreeding depression and outbreeding depression are evident in wild-type zebrafish lines. Zebrafish 2010;7:189–197.
2. Donnelly CJ, McFarland M, Ames A, Sundberg B, Springer D, Blauth P, *et al.* JAX Colony Management System (JCMS): an extensible colony and phenotype data management system. Mamm Genome 2010;21:205–215.
3. Cousin X, Daouk T, Pean S, Lyphout L, Schwartz ME, Begout ML. Electronic individual identification of zebrafish using radio frequency identification (RFID) microtags. J Exp Biol 2012;215:2729–2734.
4. Castranova D, Lawton A, Lawrence C, Baumann DP, Best J, Coscolla J, *et al.* The effect of stocking densities on

reproductive performance in laboratory zebrafish (*Danio rerio*). Zebrafish 2011;8:141–146.
5. Ribas L, Valdivieso A, Diaz N, Piferrer F. Appropriate rearing density in domesticated zebrafish to avoid masculinization: links with the stress response. J Exp Biol 2017; 220:1056–1064.
6. Spence R, Gerlach G, Lawrence C, Smith C. The behaviour and ecology of the zebrafish, *Danio rerio*. Biol Rev Camb Philos Soc 2008;83:13–34.
7. Hensley MR, Hassenplug E, McPhail R, Leung YF. ZeBase: an open-source relational database for zebrafish laboratories. Zebrafish 2012;9:44–49.
8. Anderson JL, Macurak ML, Halpern ME, Farber SA. A versatile aquatics facility inventory system with real-time barcode scan entry. Zebrafish 2010;7:281–287.
9. Yakulov TA, Walz G. Zebrafish database: customizable, free, and open-source solution for facility management. Zebrafish 2015;12:462–469.

Address correspondence to:
Petr Bartunek, PhD
Department of Cell Differentiation
Institute of Molecular Genetics AS CR v.v.i.
Videnska 1083, 142 20
Prague 4
Czech Republic

E-mail: bartunek@img.cas.cz

ZEBRAFISH
Volume 00, Number 00, 2017

DOI: 10.1089/zeb.2017.1548

Review Article

10th European Zebrafish Meeting 2017, Budapest: Husbandry Workshop Summary

Jana Oltová,[1,*] Carrie Barton,[2,*] Ana Catarina Certal,[3,*] Francesco Argenton,[4,*] and Zoltán M. Varga[5]

Abstract

A husbandry workshop on July 3, 2017, at the 10th European Zebrafish Meeting in Budapest, Hungary (July 3–July 7, 2017), focused on the standardization, optimization, and streamlining of fish facility procedures. Standardization can be achieved for example by developing novel software and hardware tools, such as a fish facility database for husbandry and environmental facility management (Zebrabase, Oltova), or a hand-held, air-pressurized fish feeder for consistent food distribution (Blowfish, Argenton). Streamlining is achieved when work hours are reduced, as with the standardized fish feeder, or by limiting the number and types of fish diets and observing the effect on animal welfare and performance (Barton). Testing the characteristics of new fish diets and observing whether they produce better experimental outcomes (Certal) optimizes diets and improves fish productivity. Collectively, the workshop presentations emphasized how consistency and harmonization of husbandry procedures within and across aquatic facilities yield reproducible scientific outcomes.

Keywords: euthanasia, facility database, hand-held feeder, fish diet, food, feeding

Introduction

A 1-H HUSBANDRY WORKSHOP with ~150 attendees was held on July 3, 2017 during the 10th European Zebrafish Meeting in Budapest, Hungary (July 3–July 7, 2017).

Institutional or departmental animal facilities are tasked with providing fish to a variety of research laboratories, often with very diverse research goals. Concurrently, animal caretakers must provide efficient, standardized, high-quality animal care. Owing to differing expectations, the boundaries between standardized animal care and optimization for specific research outcomes (i.e., reproductive performance) are often fluid. In this workshop, tools were presented that address both the standardization of animal care, for example, a database and a feeder, and optimization for specific research needs, for example, streamlining with a single food and the reproductive performance of animals fed with a particular diet. Please note the summary of presentations is in the order of the workshop program, whereas the authors contributed equally to the workshop and this report.

Presentations

Zebrabase: an intuitive zebrafish tracking database solution

Jana Oltova (jana.oltova@img.cas.cz) reported on the Zebrabase database development project, which develops an animal tracking database solution at the Institute of Molecular Genetics in Prague (CZ). An interdisciplinary team of zebrafish researchers, programmers, and web designers was initially tasked with the development of an application for their own zebrafish facility use, but this solution has now been made available to fish facilities worldwide.

Zebrabase is a scalable, cross-platform, web-based, animal tracking database developed specifically for aquatic research facilities. It has been built around three key concepts—comprehensive animal tracking, interactive breeding history, and advanced management features, including requesting and experiment planning. Importantly, Zebrabase is suitable both for small or budget-conscious facilities (there is a free plan for up to 150 tanks or 3 racks) and for large facilities

[1]Department of Cell Differentiation, Institute of Molecular Genetics of the Czech Academy of Sciences, Prague, Czech Republic.
[2]Department of Environmental and Molecular Toxicology, Sinnhuber Aquatic Research Laboratory (SARL), Oregon State University, Corvallis, Oregon.
[3]Champalimaud Research, Champalimaud Centre for the Unknown, Lisbon, Portugal.
[4]Department of Biology, Università Degli Studi di Padova, Padova, Italy.
[5]Zebrafish International Resource Center, University of Oregon, Eugene, Oregon.
*These authors contributed equally to this workshop.

aiming to improve workflow, facility management, or extending animal reporting capabilities (e.g., fish census or usage reports). An additional aim is to provide an intuitive, robust, and secure tracking solution for diverse research projects. Therefore—each user (facility, laboratory, etc.) can create an individualized Zebrabase environment that includes facility layout and customized configurations. These customized databases can be hosted on a virtual server using Secure Sockets Layer-encrypted communication. Data are backed up daily and archived for up to 6 months. Every 30 min, recent activities are copied onto a separate secondary cluster to ensure maximum availability of the service in case the primary cluster becomes unavailable.

Zebrabase supports both desktop and mobile use on Mac, Linux, Windows, Android, and iOS and has a built-in QR code generator and QR code reader functionality that provide instant access to all the fish stock information and related actions on a mobile device. A demo database is available for testing (https://demo.zebrabase.org/) and additional information is updated on the Zebrabase webpage (https://zebrabase.org/).

Successful elimination of live feeds in a high-production zebrafish facility

Carrie L. Barton (Carrie.Barton@oregonstate.edu) from the Sinnhuber Aquatic Research Laboratory (SARL) at Oregon State University, Corvallis, Oregon (US) presented data from a diet study, in which a combination of traditional commercial dry and live feed (*Artemia nauplii*) was compared with a new commercial formula in the absence of any live supplementation. Different protocols were administered to three cohorts of fish and the long-term effects of the diets were assessed. Animals were split into two groups and fed either (1) a commonly used blend of Zeigler feeds: AP100 at the larval stages, transitioning to Aquatox at 90 days post-fertilization (dpf), Golden Pearls (Brine Shrimp Direct), and Cyclop-eeze (Argent) additionally supplemented with live *Artemia,* or (2) Gemma Micro (Skretting), a commercial diet that based on the manufacturer's recommendations did not require the use of live feed supplementation. Feeds were size matched to the life stage of the fish (75–300 μ). The number of embryos produced by adults and the survival of the larvae and juveniles between 5 and 90 dpf were the performance endpoints. Results demonstrated that adult zebrafish thrived and produced large numbers of embryos in the absence of live feeds. Fish on the Gemma Micro diet began spawning earlier and produced more embryos over their lifetime than animals on the Zeigler-based feed supplemented with *Artemia.* This study demonstrates the practicality of eliminating live feeds in high-production zebrafish facilities with the advantages of reduced labor costs and minimized diet-dependent research variability.

Different impact of dry feeds on zebrafish growth and reproductive performance

During the third presentation, Ana C. Certal reported on the impact of dry feeds on zebrafish growth and reproductive performance. The study was conducted at the Champalimaud Center for the unknown in Lisbon (PT) based on a previously published study where three commercial feeds were compared and one of them stood out as the best performing feed[1] (presented at the EZM 2015 in Oslo). Ana Catarina Certal reported on Zebrafeed (Sparos), a new dry feed, which presented a better alternative to the current feed used in her facility (Gemma Micro, Skretting).

Breeding fish were raised either only on the new Zebrafeed or on the current feed until 60 dpf and were then switched to the new Zebrafeed. The latter group showed a statistically significant increase in embryo viability as compared with the first group, showing that the new Zebrafeed diet supported reproduction of zebrafish better. The study validated both feeds for optimal zebrafish rearing and for breeding programs for which redundancy in feed suppliers is an important aspect of facility management. Thus, Zebrafeed is an optimal feed for ''goal-directed'' feeding protocols, for example, when a large number of progeny or fast growth rates are expected by facility users.

A pneumatic dispenser for fast delivery of fish food

In the last presentation, Francesco Argenton from the Department of Biology, Università degli Studi di Padova (IT), reported on a novel pneumatic dispenser for fast delivery of fish food. Zebrafish are usually fed several times per day by rotating students and technicians that need to be well trained for accurate food dosing and delivery. Overfeeding leads to the accumulation of excess food at the bottom of the tank and degrading food impacts water filters negatively, leading to fish health problems. In addition, food can accumulate on aquarium lids, near the feeding hole, leading to mold. Feeding too little, in contrast, impairs fish growth and reproductive fitness. Hence, the amount of food provided must be adjusted according to the number of fish, their age, weight, and function. Despite the importance of delivering the correct dose per tank, the amount of food delivered even by well-trained operators has a significant intra-, and inter-individual variance.

To overcome the variability intrinsic to the routine feeding of a varying number and ages of fish in a facility, a pneumatic device for fast and precise delivery of food was developed. A reservoir containing 80 g dry food of 100 μm diameter and larger was mounted on a portable pneumatic gun at low pressure (1.5 atm). A trigger is pressed to blow food through a short polypropylene tube into fish tanks. Because the amount of food released at each pulse is consistent (independent from the length of the pulse), it can be regulated by tightening or releasing a ring valve. The device has been successfully used in two fish rooms with 1500 fish tanks at the University of Padua since 2015, reducing the feeding time from 90 min (manual feeding) to 30 min with the pneumatic dispenser. Thus, the pneumatic feeder saved food and time, produced no waste around the feeding hole, and more time became available for other husbandry-related tasks, for example, for cleaning tanks or filters. Finally, by controlling the amount of delivered food, and improving facility hygiene, the use of this device supports animal health and the Replacement, Reduction, and Refinement (3Rs) Principles of animal welfare. The device is self-cleaning, lacks moving parts, and is low maintenance. A video is provided here: (www.bio.unipd.it/development/BLOWFISHVOICE.mov).

The feeder, manuals, and instructions can be obtained from the University of Padua with an Material Transfer Agreement (email: Francesco.argenton@unipd.it).

Zebrafish Euthanasia

Robert Geisler from the European Zebrafish Resource Center (EZRC, www.ezrc.kit.edu/), at the Karlsruhe Institute of Technology (KIT) in Germany, provided a brief report and update about the outcomes of an international Workshop entitled *Euthanasia for Zebrafish—A Matter of Welfare and Science*, which had been hosted by EZRC on March 9, 2017, at the KIT (sponsored by EuFishBioMed; www.eufishbiomed.kit.edu/). In brief, because the directive 2010/63/EU does not address adequately the euthanasia of small tropical aquarium fish that are used in biomedical science, various methods for euthanasia of zebrafish had been discussed and proposed at this workshop with the goal to identify methods that consider the physiology of zebrafish and its use as a key biomedical research organism. Importantly, the euthanasia methods discussed were to follow the 3Rs Principles in animal experimentation and focus on animal welfare during anesthesia and euthanasia. A report of this workshop has been published in this journal.[2]

Disclosure Statement

No competing financial interests exist.

References

1. Farias M, Certal AC. Different feeds and feeding regimens have an impact on zebrafish larval rearing and breeding performance. Int J Marine Biol Res 2016;1:1–8.
2. Köhler A, Collymore C, Finger-Baier K, Geisler R, Kaufmann L, Pounder KC, *et al*. Report of workshop on euthanasia for zebrafish—a matter of welfare and science. Zebrafish 2017; 14:547–551.

Address correspondence to:
Zoltán M. Varga, PhD
Zebrafish International Resource Center
University of Oregon
Eugene, OR 97403

E-mail: zoltan@zebrafish.org

www.nature.com/scientificreports

OPEN

Modulated DISP3/PTCHD2 expression influences neural stem cell fate decisions

Received: 03 June 2016
Accepted: 21 December 2016
Published: 30 January 2017

Jana Konířová, Jana Oltová, Alicia Corlett, Justyna Kopycińska, Michal Kolář, Petr Bartůněk & Martina Zíková

Neural stem cells (NSCs) are defined by their dual ability to self-renew through mitotic cell division or differentiate into the varied neural cell types of the CNS. DISP3/PTCHD2 is a sterol-sensing domain-containing protein, highly expressed in neural tissues, whose expression is regulated by thyroid hormone. In the present study, we used a mouse NSC line to investigate what effect DISP3 may have on the self-renewal and/or differentiation potential of the cells. We demonstrated that NSC differentiation triggered significant reduction in DISP3 expression in the resulting astrocytes, neurons and oligodendrocytes. Moreover, when DISP3 expression was disrupted, the NSC "stemness" was suppressed, leading to a larger population of cells undergoing spontaneous neuronal differentiation. Conversely, overexpression of DISP3 resulted in increased NSC proliferation. When NSCs were cultured under differentiation conditions, we observed that the lack of DISP3 augmented the number of NSCs differentiating into each of the neural cell lineages and that neuronal morphology was altered. In contrast, DISP3 overexpression resulted in impaired cell differentiation. Taken together, our findings imply that DISP3 may help dictate the NSC cell fate to either undergo self-renewal or switch to the terminal differentiation cell program.

Neural stem cells (NSCs) are defined by their ability to self-renew through mitotic cell division and to differentiate into the various neural cell types: neurons, astrocytes and oligodendrocytes[1,2]. In the developing brain, NSCs first undergo symmetric self-renewal to expand the stem cell pool, which is followed by asymmetric neurogenic and gliogenic cell division to generate neurons and glia, respectively[3]. In the adult brain, NSCs reside in niches with specific molecular and cellular characteristics and whose specification is regulated by a large number of factors in each niche. Transduction of extracellular niche signals triggers a signaling cascade that activates intracellular regulatory mechanisms, including transcription factors, epigenetics and metabolism that control cell proliferation and differentiation (reviewed in ref. 4).

NSCs isolated from fetal[5–7] and adult[8–11] mammalian central nervous systems have previously been propagated *in vitro* in the presence of epidermal growth factor (EGF) and fibroblast growth factor 2 (FGF-2) to generate multicellular aggregates called neurospheres[6,11,12]. An alternative method of producing NSCs *in vitro* is via embryonic stem (ES) cells[13–15]. To date, neural differentiation of ES cells has been achieved using several published protocols that include treating ES cell aggregates with retinoic acid[16] or co-culturing ES cells on monolayers of bone marrow-derived stromal PA-6 cells[17]. Interestingly, recent studies have revealed that neither multicellular aggregation nor co-culture is necessary for ES cell neural commitment. Instead, eliminating signals that trigger alternative cell fates and the presence of EGF and FGF-2 are sufficient for ES cells to develop into neural precursors[15].

The NS-5 cell line represents NSCs derived from mouse ES cells. Differentiation of ES cells into neural precursors was induced in monolayer; lineage selection for cells expressing pan-neural gene *Sox1* was used to eliminate NSCs from undifferentiated ES cells and from non-neural differentiated cells. Subsequent cultivation of cells in the presence of EGF and FGF-2 resulted in a homogenous population of adherent bipolar cells that can be continuously symmetrically expanded in adherent monoculture without any spontaneous differentiation. Moreover, NS-5 cells represent tripotent NSCs, so even after prolonged expansion, they are still capable of generating neurons, astrocytes and oligodendrocytes under particular conditions *in vitro*[18,19].

The Dispatched 3 gene (*Disp3*), also known as *Ptchd2* or *KIAA1337*, encodes a 13-transmembrane domain-containing protein, highly expressed in neural tissue and regulated both *in vivo* and *in vitro* by thyroid

Institute of Molecular Genetics AS CR v.v.i., Vídeňská 1083, 142 20 Prague 4, Czech Republic. Correspondence and requests for materials should be addressed to P.B. (email: bartunek@img.cas.cz) or M.Z. (email: mzikova@img.cas.cz)

hormone[20]. Previously, ectopic expression of DISP3 in multipotent cerebellar progenitor cells was shown to promote cell proliferation and modulate expression of the genes involved in tumorigenesis. Further investigation revealed that *DISP3* mRNA levels are significantly elevated in the human brain cancer medulloblastoma[21].

Sequence alignments with structurally related proteins (HMGCR, SCAP, NPC1, NPC1L1, 7DHCR, PTCH1, PTCH2, DISP1 and DISP2) have shown that DISP3 contains a putative sterol-sensing domain (SSD). Functional analysis of these SSD-containing proteins revealed a link between the SSD and cholesterol homeostasis or cholesterol-linked signaling[22].

Lipid metabolism is fundamental for the brain development, but deciphering its role under normal and pathological conditions is difficult due to the brain lipid content complexity. Under normal conditions, neurogenesis requires brain fatty acid synthesis[23] and moreover, the proliferation capacity of NSCs depends on fatty acid oxidation[24]. In the pathological conditions, the accumulation of lipids is often a hallmark of affected neurogenesis. It was found that triple-transgenic Alzheimer's disease mice accumulate neutral lipids within the subventricular zone niche, which is sufficient to inhibit NSC proliferation[25].

In the current study we have investigated whether the levels of DISP3 expression could affect the self-renewal and/or differentiation potential of NSCs. Given that DISP3 expression is elevated in medulloblastoma and that distinct molecular subtypes of medulloblastoma can be characterized by specific neural stem cell molecular signatures[26], we wished to elucidate what role DISP3 may play in the neural stem cell development.

Materials and Methods

Cell culture and differentiation. NS-5 cells were a generous gift from Dietman Spengler (Max-Planck Institute of Psychiatry, Munich, Germany) with the permission of Austin Smith (Wellcome Trust Centre for Stem Cell Research, University of Cambridge, Cambridge, United Kingdom). Cells were cultured in a growth medium prepared by combining DMEM/F12 medium (Sigma) containing N2 supplement (Gibco) and Neurobasal medium (Gibco) containing B27 supplement (Gibco) and 2 mM L-glutamine (Gibco). The final medium was supplemented with BSA (25 μg/ml, Gibco), insulin (12.5 μg/ml, Sigma), apo-transferrin (50 μg/ml, Sigma), FGF-2 (10 ng/ml, R&D Systems) and EGF (10 ng/ml, R&D Systems). Cells were passaged every other day using 0.025% trypsin/EDTA and reseeded onto gelatine-coated dishes at a density of $1.5 \times 10^4/cm^2$. For NSC differentiation experiments, cells were seeded onto poly-ornithine/laminin-coated dishes at a density of $0.5 \times 10^4/cm^2$ and grown in standard growth medium. After 24 h in culture, the growth medium was changed to allow differentiation. To induce astrocyte differentiation, cells were incubated for four days in the standard growth medium supplemented with 1% FCS without EGF and FGF-2. For neuronal and oligodendrocyte differentiation, cells were cultured in DMEM/F12 medium (Sigma) supplemented with N2 (Gibco), FGF-2 (10 ng/ml, R&D Systems), PDGF-AA (10 ng/ml, R&D Systems) and forskolin (10 μM, Sigma). After four days, the medium was changed to DMEM/F12 medium (Sigma) supplemented with N2 (Gibco), FGF-2 (7.5 ng/ml, R&D Systems), ascorbic acid (200 μM, Sigma) and T3 (30 ng/ml, Sigma). Starting from day 5, the amount of FGF-2 in the medium was gradually reduced by removing half of the medium and replacing it with fresh medium lacking FGF-2.

RNA preparation and real-time qRT-PCR. Total RNA was extracted from the cultured cells using a PureLink RNA Mini Kit (Ambion) according to the manufacturer's protocol. For real-time RT-PCR, 200 ng of total RNA was reverse transcribed using random hexamer primers (Invitrogen) and M-MLV Reverse Transcriptase (Promega). cDNAs were amplified by the LightCycler® 480 system (Roche) using the SYBR Green I Master mix (Roche). All reactions were run in triplicates; all mRNAs levels were normalized to *Ubb* mRNA.

Primers. The following primers were used: Ubb 5′-ATGTGAAGGCCAAGATCCAG-3′ and 5′-TAATAGCCACCCCTCAGACG-3′, Disp3 5′-CAGCAGCTTTGACCTCTTCA-3′ and 5′-GCAACATCTGCAGGAAGGA-3′, T7EI-Disp3 sgRNA#1 5′-GCGAATCGAGCTCATCTTTCTGG-3′ and 5′-GGAGGATGGAATAAACCCCTTT-3′, T7EI-Disp3 sgRNA#2 5′-TGTGTGATGTGTCGTCCGTA-3′ and 5′-TCACATGCGACTACACTGCT-3′, βIII-tubulin 5′-TGGACAGTGTTCGGTCTGG-3′ and 5′-CCCTCCGTATAGTGCCCTTTG-3′, GFAP 5′-TGAGGCAGAAGCTCCAAGA-3′ and 5′-CCAGGGTGGCTTCATCTGC-3′, Plp 5′-GTTCCAGAGGCCAACATCAAGC-3′ and 5′-AGCCATACAACAGTCAGGGCATAG-3′, nestin 5′-AGGCTGAGAACTCTCGCTTGC-3′ and 5′-GGTGCTGGTCCTCTGGTATCC-3′, Igfbp7 5′-TGGTGACCGGGAAAATCTGG-3′ and 5′-TGCGTGGCACTCATACTCTC-3′, Lipt1 5′-TCCACGTGGGTTGATTGAGT-3′ and 5′-GCTGCTGGGACCTTGTGCTG-3′, Dgka 5′-GCTCTGTGTCTCTAGACGAG-3′ and 5′-TGGTGAATCTCTTGGGTCTCC-3′, Brsk1 5′-CCCGAGAAAAGGCTCAGTC-3′ and 5′-GGCTACGCATGGCTACTCTG-3′, Edg8 5′-GGACCGCTGTTTCTCTTGC-3′ and 5′-GATGGGATTCAGCAGCGAGT-3′.

Immunofluorescence and imaging. To detect proteins via immunofluorescence, cells were grown on glass coverslips, fixed in 4% paraformaldehyde, permeabilized with 0.1% Triton X-100 and blocked in a mixture of 10% NGS (Jackson ImmunoResearch) and 5% BSA (Sigma) before incubation with a primary antibody. Antibodies used included polyclonal anti-DISP3 antibody[21] (1:500), mouse anti-βIII-tubulin (1:1000, R&D Systems), mouse anti-GFAP (1:400, Sigma), mouse anti-oligodendrocyte marker O4 (1:500, R&D Systems). DISP3 staining was visualized by the biotin-streptavidin method using streptavidin conjugated to Alexa Fluor 555 (Invitrogen), βIII-tubulin and GFAP staining by goat anti-mouse IgG Alexa Fluor 488 secondary antibody (Invitrogen) and O4 staining by goat anti-mouse IgM Alexa Fluor 555 secondary antibody (Invitrogen). To visualize nuclei, cells were stained with DAPI (Sigma). Images for automated image analysis were taken with an Operetta HTS imaging system (PerkinElmer) at 20x magnification using Harmony software. A minimum of 50 fields per slide were analyzed using the Columbus image analysis software (PerkinElmer). The number of βIII-tubulin-stained neurites was

evaluated using the neurite finding tool (CSIRO Neurite Analysis method)[27] in the Columbus software and plotted as the number of neurites in the field divided by the total number of cells in the same field. In differentiated neuronal culture, highly βIII-tubulin-positive cells with extending neurites and dense cytoplasm were considered as neurons. Neurons and primary neurites were tagged and counted manually using the ImageJ software (Cell Counter plugin). Multiple fields (20x magnification, approximately about 300 cells) per each of the cell culture types in each of the seven independent experiments were counted. Representative pictures were acquired using a Leica DMI4000B microscope.

Virus production, transduction and transfection of NS-5 cells. The CRISPR/Cas9 method was utilized to knock-out the *Disp3* gene in NS-5 cells. The E-CRISP tool (http://www.e-crisp.org/E-CRISP/) was used to find suitable targets for mutagenesis within the *Disp3* gene. Two sites were chosen and oligonucleotides were ordered. These were then annealed and cloned into the lentiCRISPRv1 vector (Addgene # 49535) as previously described by Shalem *et al.*[28].

Lentiviruses were prepared by co-transfecting HEK293FT cells (Thermo Fisher Scientific, R70007) with the pLentiCRISPRv1 expression vector, psPAX2 and pVSV-G plasmids using the Lipofectamine reagent (Invitrogen). Twenty-four hours post transfection viral supernatant was harvested and the virions precipitated using PEG/it (SBI). Precipitated virions were resuspended in PBS and then incubated for 24 h with NS-5 cells. Cell medium was then changed and puromycin was added 24 h later.

To generate DISP3-overexpressing NS-5 cells, the full-length human *DISP3* (GenBank AB037758.1) was cloned into the retroviral vector pBABE-Hygro. Retroviruses were prepared by transfecting the expression vector into Phoenix-ECO cells (ATCC CRL-3214) using the Lipofectamine reagent. Viral supernatant was harvested at 36 h post transfection. NS-5 cells were incubated with virus supernatant and polybrene (4 μg/ml) for 8 h before changing the medium. Hygromycin was added 48 h later.

To generate short hairpin RNAs (shRNAs) against the *Disp3* gene (exon 2, target sequences: 5′-AUCGAGCUCAUCUUUCUGG-3′, 5′-GUUCUCUCAUGACUUACUU-3′), we utilized the pSilencer Expression Vector Insert Design Tool (Ambion). The oligonucleotides for shRNA expression were manufactured by Ambion, annealed and ligated into the pSilencer 2.1-U6 puro vector (Ambion). A negative control plasmid, pSilencer 2.1-U6 puro-NC, was supplied by Ambion. NS-5 cells were transfected using the Lipofectamine reagent (Invitrogen) and puromycin was added 24 h later.

T7 endonuclease assays. Genomic DNA was isolated using a QIAamp DNA Mini Kit (Qiagen). The genomic regions surrounding the target sites #1 (Exon 2) and target sites #2 (Exon 7) were PCR amplified using Q5 High-Fidelity DNA Polymerase (New England BioLabs) and primers T7EI-Disp3 sgRNA#1 and T7EI-Disp3 sgRNA#2. A total of 200 ng of the purified PCR product was denatured and slowly reannealed to facilitate heteroduplex formation: 95 °C for 10 min, 95-85 °C temperature ramping −2 °C/s, 85-25 °C temperature ramping −0.1 °C/s and 25 °C for 5 min. The reannealed amplicon was digested with T7 endonuclease I (New England BioLabs) at 37 °C for 20 min and analyzed in 2% agarose gel.

Immunoblotting. Protein samples were separated by SDS-PAGE using 4–15% precast gradient polyacrylamide gels (Biorad). Proteins were transferred onto nitrocellulose membranes which were subsequently blocked in a solution containing 5% non-fat milk dissolved in TBS and 0.05% Tween-20 (TBST). Filters were incubated in primary antibody (anti-DISP3 antibody, 1:500; anti-actin, 1:500, Sigma) diluted in 1% milk/TBST overnight and then washed and incubated with secondary antibody (ECL kit, GE Life Sciences).

Proliferation assays. Cell proliferation was measured using thymidine incorporation assays. Cells were plated at a density of 4×10^3 cells/well in 96-well plates. After 12 hours, cells were pulsed with [methyl-^{3}H] thymidine (UJV Rez) and cultured for an additional 8 hours. Cells were harvested onto a Filtermat using a FilterMate Harvester. Incorporated radioactivity was quantified using a MicroBeta2 Microplate scintillation counter (PerkinElmer). A cumulative growth curve was established by reseeding cells at a density of 1.5×10^4/cm^2 every other day and counting cell numbers using a CASY Cell Counter and Analyzer System (Roche).

Cell cycle analysis. For cell cycle analysis, cells were trypsinized (0.025% trypsin/EDTA), collected and fixed in a solution of 70% ethanol. After incubation at −20 °C overnight the cells were placed in a staining solution containing 0.1% Triton X-100 in PBS, propidium iodide (20 μg/ml, Sigma) and RNase A (200 μg/ml) for 15 min. Samples were analyzed using a BD LSRII flow cytometer and Watson pragmatic univariate analysis[29] tool in software FlowJo (FlowJo LLC).

Microarray analysis. RNA quality and concentration was measured using a NanoDrop 2000 spectrophotometer (Thermo Fisher Scientific) and RNA integrity was analyzed by Agilent Bioanalyzer 2100 (Agilent). Illumina MouseRef-WG-6 v2 Expression BeadChips (Illumina) were used for microarray analysis according to the manufacturer's protocol. In brief, 250 ng of RNA was amplified using the Illumina TotalPrep RNA Amplification Kit (Ambion). The labeled RNA (1500 ng) was then hybridized onto the chip according to the manufacturer's instructions. The analysis was performed in three to four biological replicates per group. The raw data was preprocessed using GenomeStudio software (version 1.9.0.24624; Illumina) and analyzed within the limma package[30] of Bioconductor[31] as described elsewhere[32]. In short, we used the normal-exponential model to remove the background noise, quantile normalization to standardize the data and log-2 transform to stabilize variance of the data. A moderated t-test of limma was used to detect transcripts differentially expressed between the Disp3 sgRNA-treated samples and controls. As the analysis was considered exploratory, we used weak criteria to select candidate genes that were differentially transcribed (Storey's $q < 0.9$[33]), which corresponds to $p < 0.001$,

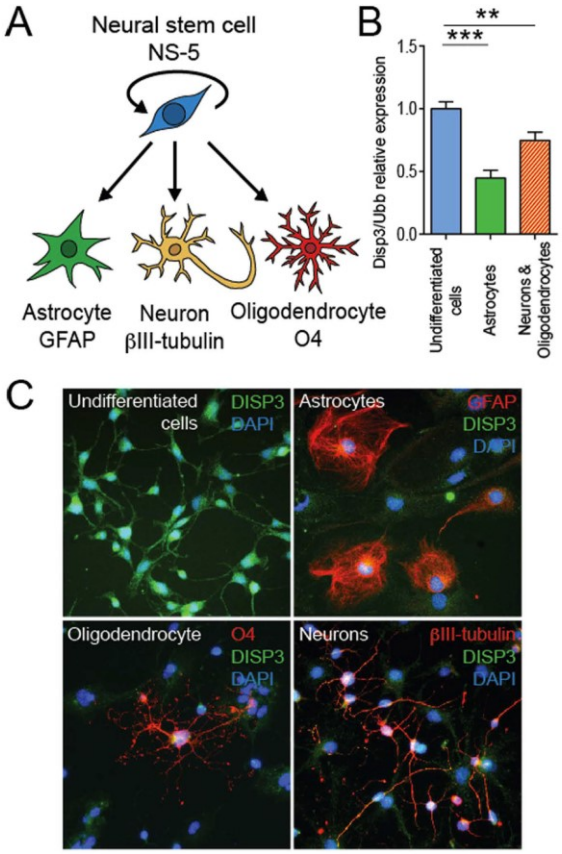

Figure 1. DISP3 expression alters during neural differentiation in NS-5 cells. (**A**) Multipotent neural stem cells NS-5 give rise to astrocytes, neurons and oligodendrocytes. Cell type-specific markers GFAP (astrocytes), βIII-tubulin (neurons) and O4 (oligodendrocytes) were analyzed. (**B**) Quantitative RT-PCR analysis of *Disp3* mRNA in undifferentiated and differentiated cells. *Ubb* was used as a reference gene. Bars represent the mean of three independent samples with error bars indicating standard deviation and the level of statistical significance (**$P < 0.01$, ***$P < 0.001$). Mean values: undifferentiated cells = 1.00, astrocytes = 0.45, neurons and oligodendrocytes = 0.75. (**C**) Immunofluorescence images of undifferentiated and differentiated cells stained with a polyclonal DISP3 antibody (green) and cell type-specific markers (red). DAPI (blue) was used to stain the nuclei.

and $|\log2FC| > 0.4$. The MIAME (Minimum Information About a Microarray Experiment) compliant transcription data was deposited in the ArrayExpress database (E-MTAB-4485).

Statistical analysis. The results obtained in the qRT-PCR analysis, proliferation measurement and automated microscopy image analysis were processed using GraphPad Prism software version 6. In the plots generated, each data point represents a biological replicate and the mean value is shown. Error bars specify standard deviation of the data. To determine the statistical significance of the results, an unpaired t-test with Welch's correction was used. Statistical significance is denoted by asterisks, *$P < 0.05$, **$P < 0.01$, ***$P < 0.001$, and ****$P < 0.0001$.

Results

DISP3 expression is reduced in differentiated neural stem cells. NS-5 mouse neural stem cells are capable of differentiating *in vitro* into the three neural cell types: astrocytes, neurons and oligodendrocytes. To identify each of these differentiated cell types, cell-specific markers can be used. These include GFAP (glial fibrillary acidic protein) for astrocytes, βIII-tubulin (part of the microtubular complex) for neurons, and O4 (oligodendrocyte surface antigen) and PLP (oligodendrocyte-specific transmembrane proteolipid) for oligodendrocytes (Fig. 1A).

To promote NS-5 cell differentiation we employed two strategies using two different types of differentiation media. Cells cultured in the first medium changed their morphology, finally generating astrocytes; the second medium promoted differentiation into a mixed culture of neurons and oligodendrocytes. To assess whether cell differentiation has an effect on *Disp3* expression, qRT-PCR was used to quantify and compare the levels of *Disp3* in each of the cell populations. This analysis revealed that *Disp3* levels are highest in undifferentiated cells and

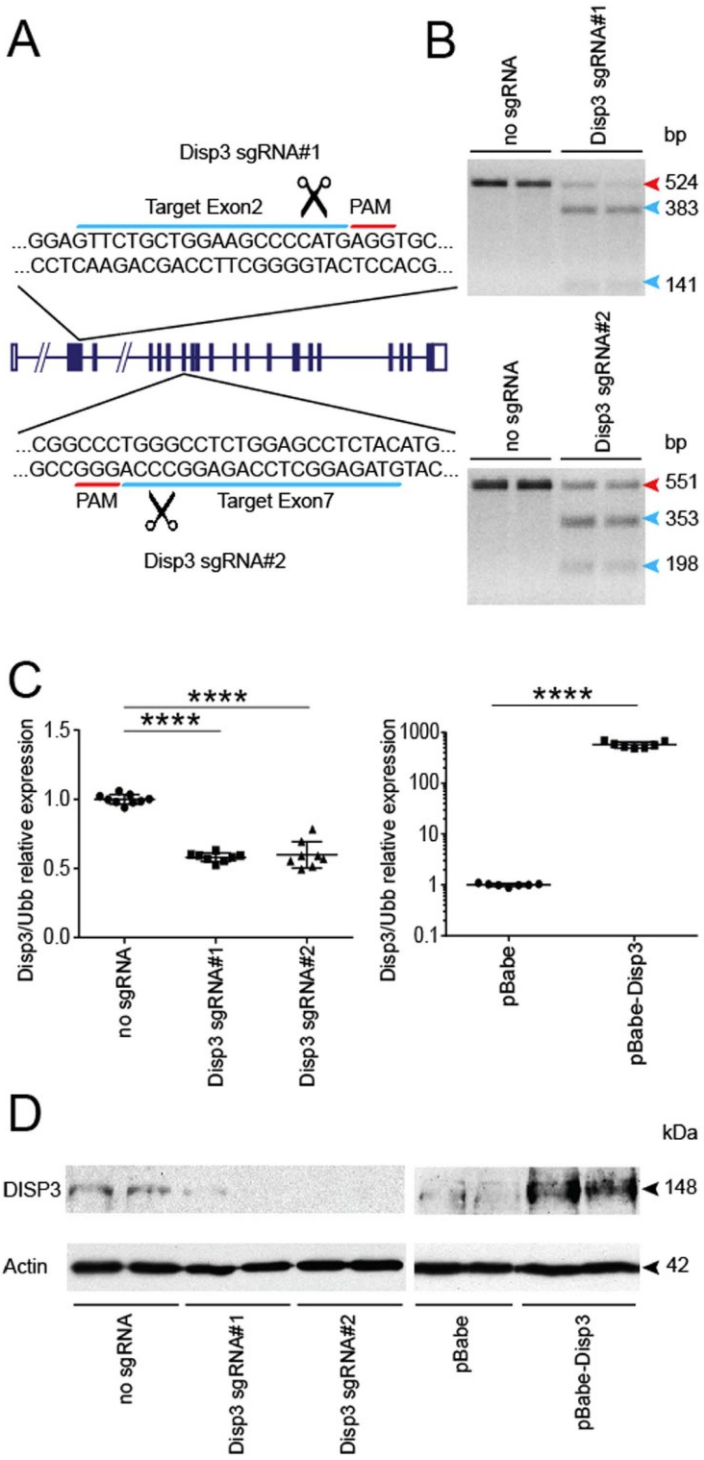

Figure 2. Modulation of DISP3 levels in NS-5 cells. (**A**) A scheme of the *Disp3* gene showing two sgRNA target sites for *Disp3* targeting via RNA-guided CRISPR/Cas9 endonuclease. The 20 nt target sequence (blue) is represented along with the neighboring PAM motif (red). (**B**) T7 endonuclease I assays confirm indels induced by Disp3 sgRNA#1 and Disp3 sgRNA#2 in two independent cell batches. The red arrow indicates the wild-type DNA fragment, blue arrows indicate mutant DNA fragments. (**C**) Quantitative RT-PCR analysis of *Disp3* mRNA. Cells infected with a lentivirus encoding Cas9 and Disp3 sgRNA#1 or Disp3 sgRNA#2 and control without sgRNA (left scatter plot); cells infected with a retrovirus encoding human *DISP3* (pBabe-Disp3) and control empty vector (pBabe) (right scatter plot). *Ubb* was used as a reference gene. Data represent the mean of biological replicates with error bars indicating standard deviation and the level of statistical significance (****$P < 0.0001$). Mean values: no sgRNA = 1.00, Disp3 sgRNA#1 = 0.58, Disp3 sgRNA#2 = 0.60, pBabe = 1.00, pBabe-Disp3 = 576. (**D**) Level of DISP3 protein confirmed by western blot. Actin served as a loading control.

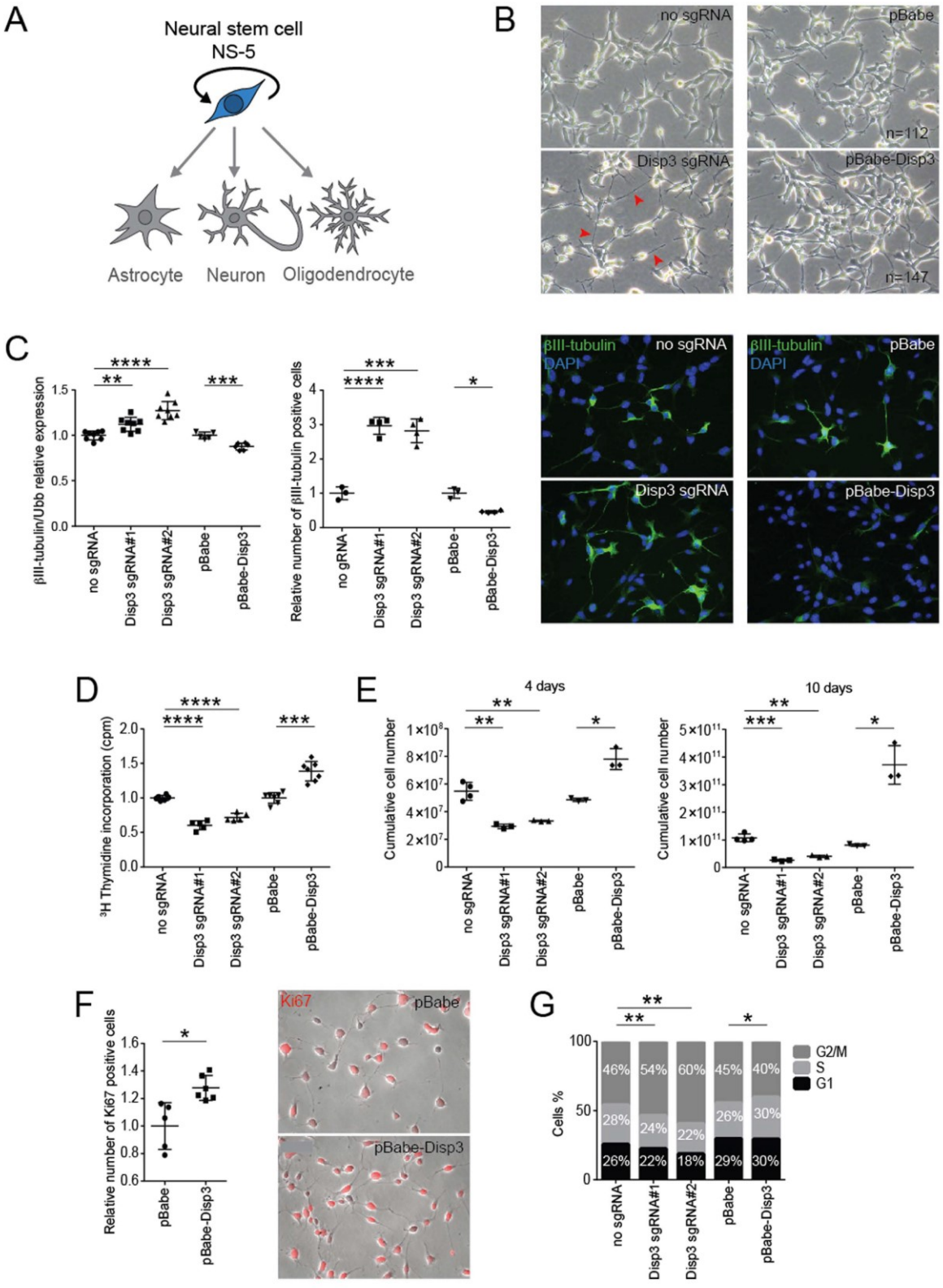

Figure 3. Modulation of DISP3 expression results in changes to undifferentiated NS-5 cells. (**A**) Under particular conditions, NS-5 cells are capable of self-renewal. (**B**) Modulation DISP3 expression leads to morphological changes in undifferentiated NS-5 cells. Representative phase-contrast images of Disp3 sgRNA, pBabe-Disp3 and relevant control cells are shown. Note the prolonged processes observed in Disp3 sgRNA cells (red arrows). (**C**) βIII-tubulin expression in Disp3 sgRNA, pBabe-Disp3 and control cells was quantified by qRT-PCR analysis (left scatter plot, *Ubb* was used as a reference gene) and by the Operetta High-Content

Imagining System followed by Columbus software analysis (right scatter plot). According to the intensity of staining, cells were divided into three groups: cells with basal, medium and high intensity of βIII-tubulin staining. This analysis shows the fraction of βIII-tubulin-positive cells with the staining intensity exceeding the basal level and normalized to the number of total cells (nuclei). Representative immunofluorescent images of cells stained with βIII-tubulin (green) and DAPI (blue) are also shown. All data represent the mean of biological replicates with error bars indicating standard deviation and the level of statistical significance (*$P < 0.05$, **$P < 0.01$, ***$P < 0.001$, ****$P < 0.0001$). Mean values - left scatter plot: no sgRNA = 1.00, Disp3 sgRNA#1 = 1.12, Disp3 sgRNA#2 = 1.27, pBabe = 1.00, pBabe-Disp3 = 0.88; - right scatter plot: no sgRNA = 1.00, Disp3 sgRNA#1 = 2.97, Disp3 sgRNA#2 = 2.82, pBabe = 1.00, pBabe-Disp3 = 0.46. (**D**) Proliferation of Disp3 sgRNA, pBabe-Disp3 and control cells was measured by ^{3}H-thymidine incorporation assays. All data represent the mean of biological replicates with error bars indicating standard deviation and the level of statistical significance (***$P < 0.001$, ****$P < 0.0001$). Mean values: no sgRNA = 1.00, Disp3 sgRNA#1 = 0.60, Disp3 sgRNA#2 = 0.72, pBabe = 1.00, pBabe-Disp3 = 1.39. (**E**) Disp3 sgRNA, pBabe-Disp3 and control cells were counted every other day. The growth rate was plotted as cumulative cell numbers. All data represent the mean of biological replicates with error bars indicating standard deviation and the level of statistical significance (*$P < 0.05$, **$P < 0.01$, ***$P < 0.001$). Mean values - left scatter plot (4 days): no sgRNA = 5.48×10^{7}, Disp3 sgRNA#1 = 2.94×10^{7}, Disp3 sgRNA#2 = 3.33×10^{7}, pBabe = 4.86×10^{7}, pBabe-Disp3 = 7.81×10^{7}; - right scatter plot (10 days): no sgRNA = 1.07×10^{11}, Disp3 sgRNA#1 = 0.27×10^{11}, Disp3 sgRNA#2 = 0.41×10^{11}, pBabe = 0.81×10^{11}, pBabe-Disp3 = 3.72×10^{11}. (**F**) Operetta High-Content Imaging System quantification of Ki-67 staining (left) and representative immunofluorescence images of pBabe-Disp3 and control cells stained with Ki-67 (red, right). All data represent the mean of biological replicates with error bars indicating standard deviation and the level of statistical significance (*$P < 0.05$). Mean values: pBabe = 1.00, pBabe-Disp3 = 1.28. (**G**) The effect of modified DISP3 expression on cell cycle progression was determined by flow cytometry analysis. The percentage of cells in the G1, S and G2/M phases of the cell cycle was counted and plotted. All data represent the mean of biological replicates, the level of statistical significance shows changes in the percentage of cells in the G2/M phase (*$P < 0.05$, **$P < 0.01$).

significantly decrease upon differentiation (Fig. 1B). The differentiation status of cells was verified by qRT-PCR using previously mentioned cell-type specific markers (Fig. S1). These results were further confirmed by immunofluorescence studies, which demonstrated reduced DISP3 protein expression when NS-5 cells differentiate (Fig. 1C). The status of cells in the various conditions was confirmed by immunofluorescence staining with specific markers. Staining of undifferentiated cells revealed either very low (βIII-tubulin) or undetectable (GFAP, O4) levels of neural cell-specific markers (not shown). To conclude, differentiation of NS-5 cells into astrocytes, neurons or oligodendrocytes results in reduced levels of both DISP3 mRNA and protein.

Modulation of DISP3 expression in NS-5 cells. To elucidate the effect of DISP3 expression on neural stem cell fate, the levels of *Disp3* expression were diminished using the CRISPR/Cas9 technology. Two custom designed single guide RNAs targeting exon 2 (Disp3 sgRNA#1) and exon 7 (Disp3 sgRNA#2) were used to impair expression of the *Disp3* gene (Fig. 2A). NS-5 cells were infected with a lentivirus containing Cas9 nuclease and either Disp3 sgRNA#1 or Disp3 sgRNA#2. After antibiotic selection, the presence of mutated alleles was confirmed using a batch T7 endonuclease I assay (Fig. 2B).

Additionally, NS-5 cells overexpressing DISP3 were generated by retroviral transduction with a DISP3-overexpression vector (pBabe-Disp3). The levels of *Disp3* mRNA in both novel NS-5 cell cultures (Disp3 sgRNAs and pBabe-Disp3) were determined by qRT-PCR (Fig. 2C) and later confirmed by Western blotting (Fig. 2D). Thus, using the CRISPR-Cas9 and retroviral transduction systems, we were able to efficiently modulate DISP3 expression in NS-5 cells.

Modulated DISP3 expression in NS-5 cells modifies the phenotype of undifferentiated NSCs. Previously, we have demonstrated that the process of NSC differentiation resulted in altered DISP3 expression. We next evaluated the possible effect of modulated DISP3 expression on undifferentiated cells maintained under self-renewal conditions (Fig. 3A).

Compared to control cells, both Disp3 sgRNAs and pBabe-Disp3 cell lines exhibited morphological changes upon cultivation in standard growth medium. The most evident change observed in Disp3 sgRNAs cells was formation of elongated cell processes, which indicated the onset of neuronal differentiation (Fig. 3B, left panels). Interestingly, cells overexpressing DISP3 (pBabe-Disp3) seemed to proliferate faster than the control cells. This phenomenon is illustrated in Fig. 3B, right panels, when after seeding a constant number of cells per dish and subsequent cultivation under the same conditions, there were more cells present in the pBabe-Disp3 culture compared to the pBabe control culture.

Moreover, the results of qRT-PCR and protein analysis demonstrated that in both Disp3 sgRNAs and pBabe-Disp3 cells, βIII-tubulin expression levels were altered (Fig. 3C). The same effect was observed using shRNA-induced knock-down in NS-5 cells (Fig. S2). Quantification of mRNA changes (Fig. 3C, left scatter plot) clearly illustrates that a decrease in DISP3 expression results in an increase in βIII-tubulin expression, whilst an increase in DISP3 levels causes the reverse effect. These results were confirmed by microscopy followed by automated image analysis of cells stained with a βIII-tubulin antibody. The analysis shows that compared to control cells, the number of βIII-tubulin-positive cells is higher in Disp3 sgRNA NS-5 cells and reduced in pBabe-Disp3 cells (Fig. 3C, right scatter plot). Representative images of this staining are shown in Fig. 3C, right panels. Moreover, in Disp3 sgRNA NS-5 cells, the fraction of highly and medium βIII-tubulin-stained cells is increased,

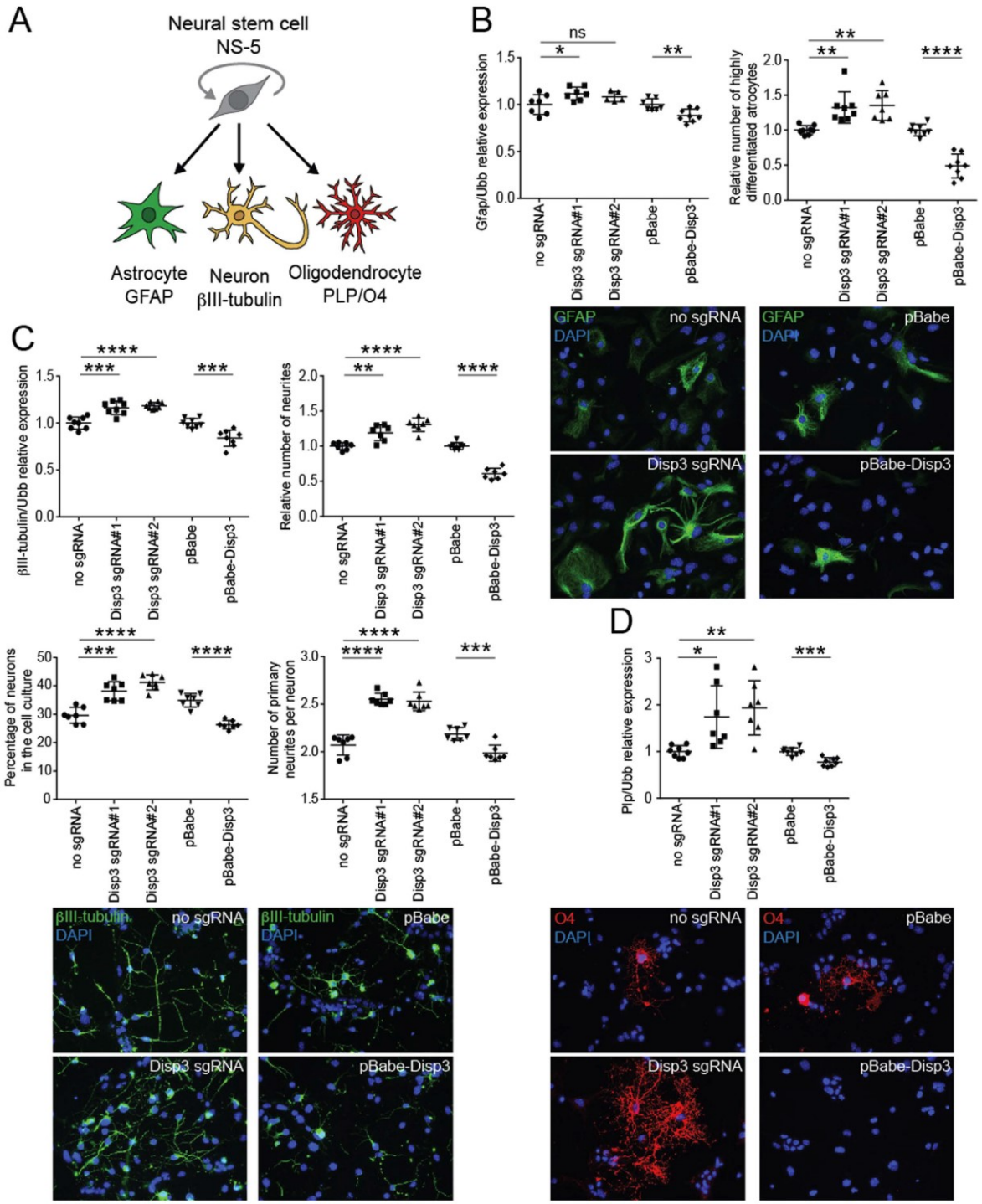

Figure 4. Changes in DISP3 expression levels affect NS-5 differentiation patterns. (**A**) Multipotent neural stem cells NS-5 give rise to astrocytes, neurons and oligodendrocytes. Cell type-specific markers GFAP (astrocytes), βIII-tubulin (neurons) and O4 (oligodendrocytes) were analyzed. (**B**) qRT-PCR analysis of *Gfap* mRNA expression (left scatter plot, *Ubb* was used as a reference gene) and GFAP staining of cells after astrocyte differentiation analyzed by the Operetta High-Content Imagining System followed by Columbus software analysis (right scatter plot). This analysis shows the fraction of highly differentiated astrocytes, which were recognized and quantified based on their shape, size, and intensity of staining and normalized to the number of total cells (nuclei). Representative immunofluorescent images of cells stained with GFAP (green) are shown. All data represent the mean of biological replicates with error bars indicating standard deviation and the level of statistical significance (*$P < 0.05$, **$P < 0.01$, ****$P < 0.0001$). Mean values - left scatter plot: no sgRNA = 1.00, Disp3 sgRNA#1 = 1.12, Disp3 sgRNA#2 = 1.08, pBabe = 1.00, pBabe-Disp3 = 0.88; - right scatter plot: no sgRNA = 1.00, Disp3 sgRNA#1 = 1.32, Disp3 sgRNA#2 = 1.35, pBabe = 1.00, pBabe-Disp3 = 0.49. (**C**) qRT-

PCR analysis of βIII-tubulin mRNA expression (upper left scatter plot, *Ubb* was used as a reference gene) and the numbers of βIII-tubulin-stained neurites (upper right scatter plot) after neuronal differentiation counted by the Operetta High-Content Imagining System followed by Columbus software analysis using the neurite finding tool. The analysis shows the relative number of neurites normalized to the number of total cells (nuclei). The lower left scatter plot displays the percentage of neurons in each cell culture analyzed manually with ImageJ. The lower right scatter plot shows the number of primary neurites recalculated per neuron. All data represent the mean of biological replicates with error bars indicating standard deviation and the level of statistical significance (**$P < 0.01$, ***$P < 0.001$, ****$P < 0.0001$). Representative immunofluorescent images of cells stained with β III-tubulin (green) are shown at the bottom. Mean values - upper left scatter plot: no sgRNA = 1.00, Disp3 sgRNA#1 = 1.16, Disp3 sgRNA#2 = 1.19, pBabe = 1.00, pBabe-Disp3 = 0.84; - upper right scatter plot: no sgRNA = 1.00, Disp3 sgRNA#1 = 1.19, Disp3 sgRNA#2 = 1.31, pBabe = 1.00, pBabe-Disp3 = 0.61; - lower left scatter plot: no sgRNA = 29.56, Disp3 sgRNA#1 = 38.13, Disp3 sgRNA#2 = 41.19, pBabe = 34.91, pBabe-Disp3 = 26.33; - lower right scatter plot: no sgRNA = 2.07, Disp3 sgRNA#1 = 2.55, Disp3 sgRNA#2 = 2.53, pBabe = 2.18, pBabe-Disp3 = 1.99. (**D**) qRT-PCR analysis of *Plp* mRNA expression after oligodendrocyte differentiation. *Ubb* was used as a reference gene. Representative immunofluorescent images of cells stained with O4 (red) are shown. All data represent the mean of biological replicates with error bars indicating standard deviation and the level of statistical significance (*$P < 0.05$, **$P < 0.01$, ***$P < 0.001$). Mean values: no sgRNA = 1.00, Disp3 sgRNA#1 = 1.74, Disp3 sgRNA#2 = 1.93, pBabe = 1.00, pBabe-Disp3 = 0.78.

whereas the percentage of cells with basal expression decreased (Fig. S3), which indicates that overall more cells have increased βIII-tubulin expression.

To elucidate the effect of DISP3 expression on maintaining the undifferentiated state of NS-5 cells, nestin (type-IV intermediate filament protein) mRNA levels were characterized by qRT-PCR. Analysis of both cell lines revealed changes in the nestin expression, which confirmed our previous data suggesting that reduction of DISP3 expression promotes spontaneous differentiation of NS-5 cells, whilst its overexpression helps to maintain the cell stemness (Fig. S4).

To quantify cell proliferation in Disp3 sgRNAs and pBabe-Disp3 cells, a thymidine incorporation assay was performed. The proliferation rate of NS-5 cells overexpressing DISP3 was increased compared to control cells, whilst the proliferation rate of Disp3 sgRNAs was reduced (Fig. 3D, Fig. S5). The growth rate of Disp3 sgRNAs and pBabe-Disp3 cells was quantified every other day and plotted as cumulative cell numbers. Figure 3E shows two selected days from the growth curve (Fig. S6) and corroborates that DISP3 overexpression provides a growth advantage. These results were confirmed using Ki-67 staining (marker of cell proliferation). Compared to control cells, pBabe-Disp3 cells displayed a significantly higher number of Ki-67-positive stained cells (Fig. 3F). Finally, to determine the effect of DISP3 expression on the cell cycle, flow cytometry analysis was performed. This analysis revealed that compared to control cells, both disruption and overexpression of the *Disp3* gene leads to an altered distribution of cells in distinct phases of the cell cycle (Fig. 3G).

Changes in DISP3 expression affect NS-5 cell fate decisions. Given that NS-5 cells can be driven to differentiate into neural cell types *in vitro*, we wondered whether modifying DISP3 expression would affect the NSC differentiation fates. Cells either under- or over-expressing DISP3 were analyzed to determine whether the expression levels of neural-specific markers were altered in NS-5 cells incubated under specific conditions to promote differentiation into either astrocytes, neurons or oligodendrocytes (Fig. 4A).

GFAP is a type-III intermediate filament protein that has previously been used to identify astrocytes. During astrocyte differentiation, the level of *Gfap* mRNA was significantly increased from undetectable on day 0 to relatively high in fully differentiated control NS-5 cells (Fig. S1). GFAP expression in Disp3 sgRNAs and pBabe-Disp3 astrocytes followed a similar pattern to control cells; however, at the end of differentiation the increased *Gfap* mRNA levels in Disp3 sgRNAs and the reduced *Gfap* mRNA levels in pBabe-Disp3 cells indicate an impact of DISP3 on the astrocyte differentiation (Fig. 4B left scatter plot, Fig. S7). Whilst *Gfap* mRNA expression did not differ greatly among the various cell types, there was a definite impact at the protein level. Cells stained with antibodies against GFAP were recognized and quantified based on their shape, size, and intensity of staining and the results revealed that compared to control cells, Disp3 sgRNAs cells in culture had an increased number of highly differentiated astrocytes. The reverse effect was observed in pBabe-Disp3 cells (Fig. 4B right scatter plot, representative images).

To examine neuronal differentiation in NS-5 cells, βIII-tubulin mRNA levels were quantified. Increased βIII-tubulin mRNA levels were observed in Disp3 sgRNA cells whilst pBabe-Disp3 cells showed a reduction (Fig. 4C upper left scatter plot, Fig. S7). This result demonstrates that modulation of DISP3 expression affects βIII-tubulin mRNA levels under neuronal differentiation conditions in the same direction as under the growth/proliferation conditions (Fig. S8). Analysis of the morphology of control NS-5-derived neurons revealed long prototypical neuronal projections (neurites), which expressed high levels of βIII-tubulin protein. The number of neurites normalized to the total cell number has been selected as an initial readout for neuronal differentiation.

The numbers of neurites derived from each NS-5 cell culture were automatically quantified and revealed that, compared to the control culture, there were more neurites per cell in Disp3 sgRNAs and less neurites in pBabe-Disp3 cell culture (Fig. 4C upper right scatter plot). Evaluation of the number of neurons in differentiated neuronal culture is difficult using the automated image analysis because of their dense cytoplasm and thin processes. Nevertheless, we were able to analyze the number of neurons manually using the ImageJ software. In differentiated culture, only βIII-tubulin-positive cells with extending neurites and dense cytoplasm were considered as neurons. The analysis shows that compared to control cells, the percentage of fully differentiated neurons is higher in Disp3 sgRNA NS-5 cell culture and reduced in pBabe-Disp3 cells (Fig. 4C lower left scatter plot).

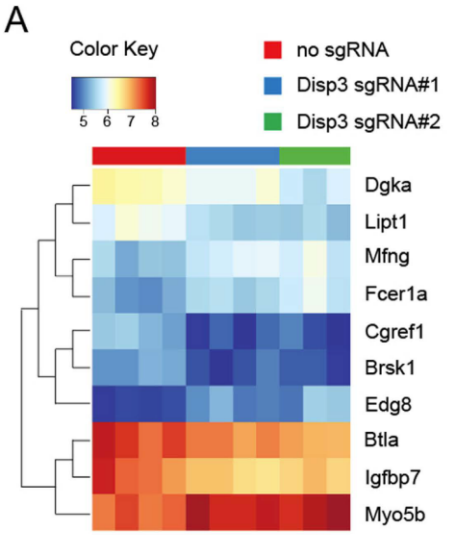

B

Symbol	Fold change	P-Value	RefSeq
Cgref1	0.64	2.40E-05	XM_181420.1
Igfbp7	0.65	0.00018	NM_008048.2
Lipt1	0.7	1.50E-05	NM_001037918.1
Dgka	0.71	4.70E-05	NM_016811.2
Btla	0.71	0.00012	NM_177584.3
Brsk1	0.73	3.40E-05	NM_001003920.2
Mfng	1.38	9.40E-05	NM_008595.2
Myo5b	1.39	9.90E-05	NM_201600.2
Fcer1a	1.43	5.60E-05	NM_010184.1
Edg8	1.46	0.00031	NM_053190.1

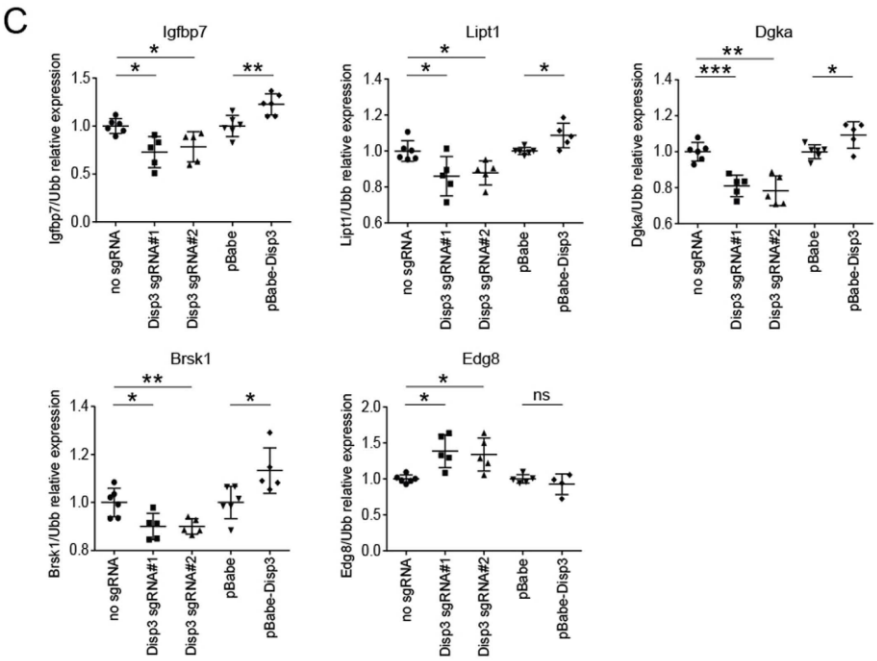

Figure 5. ***Disp3*** **gene expression modulation alters gene expression in NS-5 cells.** A heatmap (**A**) and a list of genes (**B**) with altered expression in Disp3 sgRNA cells relative to control cells was obtained by microarray expression profiling. (**C**) Relative expression of identified genes in Disp3 sgRNA, pBabe-Disp3 and control cells was confirmed by an independent qRT-PCR experiment. *Ubb* was used as a reference gene. Data represent the mean of biological replicates with error bars indicating standard deviation and the level of statistical significance (*P < 0.05, **P < 0.01, ***P < 0.001). Mean values - Igfbp7: no sgRNA = 1.00, Disp3 sgRNA#1 = 0.73, Disp3 sgRNA#2 = 0.78, pBabe = 1.00, pBabe-Disp3 = 1.23; - Lipt1: no sgRNA = 1.00, Disp3 sgRNA#1 = 0.86, Disp3 sgRNA#2 = 0.87, pBabe = 1.00, pBabe-Disp3 = 1.09; - Dgka: no sgRNA = 1.00, Disp3 sgRNA#1 = 0.81, Disp3 sgRNA#2 = 0.78, pBabe = 1.00, pBabe-Disp3 = 1.09; - Brsk1: no sgRNA = 1.00, Disp3 sgRNA#1 = 0.90, Disp3 sgRNA#2 = 0.90, pBabe = 1.00, pBabe-Disp3 = 1.13; - Edg8: no sgRNA = 1.00, Disp3 sgRNA#1 = 1.39, Disp3 sgRNA#2 = 1.34, pBabe = 1.00, pBabe-Disp3 = 0.93.

Moreover, ImageJ analysis of the absolute number of primary neurites recalculated per neuron in each NS-5 cell culture showed that, compared to the control culture, there were more primary neurites in Disp3 sgRNAs and less primary neurites in pBabe-Disp3 neurons (Fig. 4C lower right scatter plot, bottom representative images).

Finally, the effect of DISP3 expression on oligodendrocyte differentiation was determined by quantitating the level of *Plp* mRNA and O4 protein expression in NS-5 cell cultures after differentiation. PLP is an oligodendrocyte-specific transmembrane proteolipid protein that is required for neuronal myelination. O4 is

an antigen located on the surface of oligodendrocytes. *Plp* mRNA levels increased in Disp3 sgRNAs cells while decreased in pBabe-Disp3 cells. Similar findings were obtained when cells were stained with the O4 antibody (Fig. 4D, Fig. S7). Unfortunately, due to the small fraction of cells positive for oligodendrocyte markers (especially in pBabe-Disp3 cells), we were unable to quantify this staining and therefore, show only a representative picture.

In summary, modulation of DISP3 expression affects NS-5 differentiation. Compared to control cell cultures, Disp3 sgRNAs cells generated more highly differentiated astrocytes and showed increased expression of *Plp* mRNA, which is specific for oligodendrocytes. Similarly, the expression of neuron-specific βIII-tubulin mRNA was increased, and as such, these cells exhibited increased numbers of neurites. Furthermore, compared to control cells, the number of fully differentiated neurons was higher in Disp3 sgRNA NS-5 cell culture and these neurons had increased numbers of primary neurites. In pBabe-Disp3 cells, the differentiation potential was much lower regardless of the differentiation strategy used.

Modified levels of DISP3 lead to altered gene expression in NS-5 cells. To identify genes in NS-5 cells affected by altered DISP3 expression, we performed microarray analysis. Total RNAs isolated from Disp3 sgRNA#1, Disp3 sgRNA#2 and control cells were hybridized to the Illumina Mouse Expression BeadChips. On the basis of the obtained expression profiles we established a heatmap (Fig. 5A) and a compiled list of common genes (Fig. 5B) with significantly altered expression in both Disp3 sgRNA cultures. The expression levels of the identified genes were confirmed by qRT-PCR in independent Disp3 sgRNA, pBabe-Disp3 and control cell cultures. Our results show that modified expression levels of DISP3 lead to altered mRNA levels of insulin-like growth factor binding protein 7 (*Igfbp7*), lipoyltransferase 1 (*Lipt1*), diacylglycerol kinase alpha (*Dgka*), brain serine/threonine kinase 1 (*Brsk1*) and endothelial differentiation sphingolipid G-protein-coupled receptor 8 (*Edg8*) (Fig. 5C). Interestingly, all of these identified genes were described to function either in neurodevelopment and/or have been implicated in various tumors.

Discussion

In this study we examined the role of DISP3 in NSC proliferation and differentiation. We have demonstrated in NS-5 cells that the levels of DISP3 expression significantly decrease upon differentiation. We performed both loss-of-function and gain-of-function experiments to determine the effect of DISP3 on the NSC phenotype and differentiation potential. When NSCs were maintained under growth/proliferation conditions, both Disp3 sgRNAs and pBabe-Disp3 cells underwent significant morphological changes. The most obvious alteration was observed in Disp3 sgRNAs cells. Even though the mRNA expression of βIII-tubulin did not much differ from control cells, the number of βIII-tubulin-positive cells detected by immunofluorescence staining and automated counting was increased nearly three times. The analysis also revealed that not only the fraction of βIII-tubulin-positive cells was higher in Disp3 sgRNA NS-5 cell culture, but also that the number of highly stained cells was significantly increased. The observed high expression levels of NSC marker nestin in Disp3 sgRNA NS-5 cells under the growth/proliferation conditions, which were only slightly lower than in control cells, demonstrate the undifferentiated character of these cells. Nevertheless, the increased proportion of βIII-tubulin-positive cells indicates the onset of neuronal differentiation. Interestingly, cells overexpressing DISP3 demonstrated a significantly faster proliferation rate than control cells.

In the postnatal cerebellum, the expression of DISP3 is controlled by ATOH1, a transcription factor that plays a major role in cell proliferation, cell migration and initiation of the cell differentiation program[34]. Interestingly, ATOH1 is also implicated in promoting medulloblastoma formation[35]. Analysis of Oncomine datasets revealed that *DISP3* expression is significantly elevated in human medulloblastoma[21]. Medulloblastoma is the most common malignant pediatric brain tumor and can be classified into at least four distinct molecular subgroups that vary according to clinical signs and molecular markers. The most aggressive forms of the disease are the non-SHH/WNT subtypes[36]. Each of these subtypes is characterized by expression of markers that are found in embryonic or adult stem cells, as well as in neural "cancer stem cells" (CSC). It has been hypothesized that sustained tumor growth is restricted to CSCs, which display many similarities to NSCs in their capacity to self-renew and differentiate[37]. Neural CSCs are able to grow in serum-free media containing EGF and FGF, the two growth factors that promote its "dedifferentiated" status[8,38,39].

Immunohistochemical evidence suggests that particular medulloblastoma molecular subgroups arise from distinct cellular origins. WNT-subtype tumors infiltrate the dorsal brainstem, whereas SHH medulloblastomas originate from external germinal layer progenitor (EGL) cells[40]. The origins of non-SHH/WNT subtypes 3 and 4 remain to be defined; nevertheless, it has been demonstrated that the master regulator transcription factors of subgroup 4 are active in neurons that originate from early progenitors of the upper rhombic lip[41]. In our previous paper, we used the multipotent cerebellar progenitor cell line C17.2, which was generated from isolated cerebellar neural cells from the EGL layer. The study demonstrated that ectopic overexpression of DISP3 promotes cell proliferation, alters tumorigenic gene expression and modifies the differentiation profile of DISP3-expressing C17.2 cells[21].

To elucidate whether modulation of DISP3 expression has any effect on the NSC differentiation potential, we determined the expression levels of neural-specific markers in differentiated Disp3 sgRNA cells, pBabe-Disp3 and control cells using both manual and automated microscopy methods. Compared to control cell cultures, differentiated Disp3 sgRNAs cells yielded a greater proportion of neurons and highly differentiated astrocytes. Analysis of Disp3 sgRNA cell culture also showed a higher number of fully differentiated neurons with more primary neurites compared to control cells. In contrast, pBabe-Disp3 cells demonstrated impaired differentiation.

DISP3 is an SSD-containing protein with a phylogenetic relationship to other members of this family. Previously identified genetic mutations within SSD-containing protein family members have revealed NSC self-renewal and differentiation defects. Mutations in the *NPC1* gene cause the Niemann-Pick type C1 lysosomal lipid storage disorder that is characterized by multisystem defects including demyelination and progressive neurodegeneration[42].

Npc1 mutations lead to reduced NSC self-renewal, impaired neurosphere generation and altered astrocyte morphology[43]. Current research indicates that an imbalance between NSC proliferation and differentiation is the major cause of many neurodevelopmental disorders. To date, research of developmental disabilities was mostly based on gene mutation studies in case/control cohorts. However, induced pluripotent stem cells (iPSCs) generated from affected patients are now being used to measure the extent of the neural proliferation/differentiation deficit, which may, in many cases, correspond with the degree of impairment. This appears to be critical for formulating appropriate treatment strategies, as these neurodevelopmental disorders are considered as multi-cause, complex diseases of NSC proliferation and differentiation rather than as a cluster of particularly impaired molecular pathways[44]. Upon neuronal differentiation, human iPSCs containing the most frequent *NPC1* mutation exhibit premature cell death and dysfunction of important pathways, including calcium and WNT signaling[45]. Another neurological disease involving altered NSC function is the Smith-Lemli-Opitz syndrome (SLOS). SLOS is a cholesterol synthesis disorder caused by a mutation within the *DHCR7* gene. Impaired DHCR7 activity results in lower cholesterol biosynthesis and higher 7-dehydrocholesterol levels[46]. The altered sterol composition within cells then leads to central nervous system malformations, as well as cognitive and behavioral abnormalities[47,48]. SLOS-derived iPSCs exhibit accelerated neuronal differentiation, formation of long neuronal projections and increased expression of neuronal markers[49]. Importantly, *DISP3* was identified among the top differentially expressed transcripts in neurons derived from *TSC2*-deleted pluripotent stem cells. Mutations in either *TSC1* or *TSC2* have been determined to cause tuberous sclerosis, a severe multisystem disorder presented by neuropsychiatric symptoms including autism, intellectual disability, and epilepsy[50]. *TSC2* deletion alters neuronal proliferation and differentiation and leads to altered neuronal synaptogenesis and transmission paralleled by molecular changes in pathways associated with autism[51].

To support the observed phenotypes, we conducted gene expression profiling of NS-5 cells with disrupted DISP3 expression. The analysis revealed a number of genes with altered mRNA levels. These included *Igfbp7*, *Lipt1, Dgka, Brsk1* and *Edg8*, which have known neurodevelopmental functions and/or have been implicated in various tumors. Both neurodevelopment and oncogenesis are multi-step processes in which altered signal transduction pathway activation can have pleiotropic effects depending on the specific gene expression profile in the particular cell type and during the specific time-window, and recent findings show that many genes are implicated in both processes[52,53].

IGFBP7 belongs to the superfamily of insulin-like growth factor (IGF)-binding proteins (IGFBPs), which have been described to function in tumorigenesis in a tissue type- and tumor pathology-dependent manner[54–59]. In glioblastoma, IGFBP7 is upregulated and its expression level within the tumor correlates with its histological grade and patient prognosis[60]. In a noncarcinogenic brain, it was shown that IGFBP7 downregulation resulted in increased hippocampal neuron survival[61]. Interestingly, brain tissue and blood serum isolated from Alzheimer's disease patients demonstrated IGFBP7 upregulation[62]. Another gene whose expression was downregulated in Disp3-sgRNA cells was *Dgka*. DGKA is a member of the diacylglycerol kinase family and is expressed specifically within oligodendrocytes of the CNS. It has also been proposed to function in myelin formation and metabolism[63] and was identified as a marker for a depressive disorder relapse[64]. Many studies have also suggested a role for DGKA in tumorigenesis[65–67]. Interestingly, attenuation of DGKA activity in glioblastoma cells induced apoptosis[68,69]. BRSK1 is an AMP-activated serine/threonine kinase, which is specifically expressed in the brain and is known to play an essential role in neuronal polarization. It has been reported that the loss of both BRSK1 and its related protein BRSK2 is required to affect neuronal differentiation. Such double-knockout mice show a smaller forebrain and an abnormally thin cortex with disordered segregation of particular neuronal subtypes. Double-mutant neurons displayed changes in morphology and axons that were difficult to distinguish from dendrites[70]. BRSK1 also plays an important role in the regulation of cell cycle progression through controlling centrosome duplication via phosphorylation of γ-tubulin[71]. The only gene whose expression was upregulated in Disp3-sgRNA cells was *Edg8*. This gene encodes a sphingosine 1-phosphate G-protein-coupled receptor that is expressed predominantly in oligodendrocytes and astrocytes[72]. In the developing brain, EDG8 is expressed in radial glial cells and is involved in transforming these cells into astrocytes[73]. In the course of oligodendrocytes differentiation, EDG8 is expressed in both immature and mature stages of myelin-forming cell and promotes survival of mature oligodendrocytes[74]. Overall, the functions of the identified DISP3-sensitive genes correlate well with our experimental results that demonstrate that DISP3 expression levels impact NSC proliferation and differentiation.

In this study, we utilized the mouse neural stem cell line NS-5, which is capable of differentiating into neurons, astrocytes and oligodendrocytes. Currently, this is one of the few *in vitro* model systems available to investigate the effect of DISP3 downregulation on NSC self-renewal and differentiation. We used the CRISPR-Cas9 technology to reduce the endogenously high levels DISP3 in NS-5 cells in order to assess the ability of these transgenic cells to self-renew and differentiate. NSC proliferation and differentiation are tightly controlled processes that require subtle spatial and temporal adjustments; otherwise, NSCs that differentiate either prematurely or late will ultimately affect the overall number of neural cells generated. Taken together, our findings demonstrate that DISP3 may be one of the players that regulate the transition of NSC from self-renewal to differentiation.

References

1. Gage, F. H. Mammalian neural stem cells. *Science* **287,** 1433–1438, doi: 10.1126/science.287.5457.1433 (2000).
2. Temple, S. The development of neural stem cells. *Nature* **414,** 112–117, doi: 10.1038/35102174 (2001).
3. Gotz, M. & Huttner, W. B. The cell biology of neurogenesis. *Nat Rev Mol Cell Biol* **6,** 777–788, doi: 10.1038/nrm1739 (2005).
4. Bond, A. M., Ming, G. L. & Song, H. Adult Mammalian Neural Stem Cells and Neurogenesis: Five Decades Later. *Cell Stem Cell* **17,** 385–395, doi: 10.1016/j.stem.2015.09.003 (2015).
5. Davis, A. A. & Temple, S. A self-renewing multipotential stem cell in embryonic rat cerebral cortex. *Nature* **372,** 263–266, doi: 10.1038/372263a0 (1994).
6. Reynolds, B. A., Tetzlaff, W. & Weiss, S. A multipotent EGF-responsive striatal embryonic progenitor cell produces neurons and astrocytes. *J Neurosci* **12,** 4565–4574 (1992).

7. Vescovi, A. L. *et al.* Isolation and cloning of multipotential stem cells from the embryonic human CNS and establishment of transplantable human neural stem cell lines by epigenetic stimulation. *Exp Neurol* **156,** 71–83, doi: 10.1006/exnr.1998.6998 (1999).
8. Reynolds, B. A. & Weiss, S. Generation of neurons and astrocytes from isolated cells of the adult mammalian central nervous system. *Science* **255,** 1707–1710, doi: 10.1126/science.1553558 (1992).
9. Lois, C. & Alvarez-Buylla, A. Proliferating subventricular zone cells in the adult mammalian forebrain can differentiate into neurons and glia. *Proc Natl Acad Sci USA* **90,** 2074–2077, doi: 10.1073/pnas.90.5.2074 (1993).
10. Gritti, A. *et al.* Multipotential stem cells from the adult mouse brain proliferate and self-renew in response to basic fibroblast growth factor. *J Neurosci* **16,** 1091–1100 (1996).
11. Palmer, T. D., Markakis, E. A., Willhoite, A. R., Safar, F. & Gage, F. H. Fibroblast growth factor-2 activates a latent neurogenic program in neural stem cells from diverse regions of the adult CNS. *J Neurosci* **19,** 8487–8497 (1999).
12. Reynolds, B. A. & Weiss, S. Clonal and population analyses demonstrate that an EGF-responsive mammalian embryonic CNS precursor is a stem cell. *Dev Biol* **175,** 1–13, doi: 10.1006/dbio.1996.0090 (1996).
13. Keller, G. M. *In vitro* differentiation of embryonic stem cells. *Curr Opin Cell Biol* **7,** 862–869, doi: 10.1016/0955-0674(95)80071-9 (1995).
14. Tropepe, V. *et al.* Direct neural fate specification from embryonic stem cells: a primitive mammalian neural stem cell stage acquired through a default mechanism. *Neuron* **30,** 65–78, doi: 10.1016/S0896-6273(01)00263-X (2001).
15. Ying, Q. L., Stavridis, M., Griffiths, D., Li, M. & Smith, A. Conversion of embryonic stem cells into neuroectodermal precursors in adherent monoculture. *Nat Biotechnol* **21,** 183–186, doi: 10.1038/nbt780 (2003).
16. Bain, G., Kitchens, D., Yao, M., Huettner, J. E. & Gottlieb, D. I. Embryonic stem cells express neuronal properties *in vitro*. *Dev Biol* **168,** 342–357, doi: 10.1006/dbio.1995.1085 (1995).
17. Kawasaki, H. *et al.* Induction of midbrain dopaminergic neurons from ES cells by stromal cell-derived inducing activity. *Neuron* **28,** 31–40, doi: 10.1016/S0896-6273(00)00083-0 (2000).
18. Conti, L. *et al.* Niche-independent symmetrical self-renewal of a mammalian tissue stem cell. *PLoS Biol* **3,** e283, doi: 10.1371/journal.pbio.0030283 (2005).
19. Glaser, T., Pollard, S. M., Smith, A. & Brustle, O. Tripotential differentiation of adherently expandable neural stem (NS) cells. *PLoS One* **2,** e298, doi: 10.1371/journal.pone.0000298 (2007).
20. Zikova, M., Corlett, A., Bendova, Z., Pajer, P. & Bartunek, P. DISP3, a sterol-sensing domain-containing protein that links thyroid hormone action and cholesterol metabolism. *Mol Endocrinol* **23,** 520–528, doi: 10.1210/me.2008-0271 (2009).
21. Zikova, M. *et al.* DISP3 promotes proliferation and delays differentiation of neural progenitor cells. *FEBS Lett* **588,** 4071–4077, doi: 10.1016/j.febslet.2014.09.036 (2014).
22. Kuwabara, P. E. & Labouesse, M. The sterol-sensing domain: multiple families, a unique role? *Trends Genet* **18,** 193–201, doi: 10.1016/S0168-9525(02)02640-9 (2002).
23. Knobloch, M. *et al.* Metabolic control of adult neural stem cell activity by Fasn-dependent lipogenesis. *Nature* **493,** 226–230, doi: 10.1038/nature11689 (2013).
24. Stoll, E. A. *et al.* Neural Stem Cells in the Adult Subventricular Zone Oxidize Fatty Acids to Produce Energy and Support Neurogenic Activity. *Stem Cells* **33,** 2306–2319, doi: 10.1002/stem.2042 (2015).
25. Hamilton, L. K. *et al.* Aberrant Lipid Metabolism in the Forebrain Niche Suppresses Adult Neural Stem Cell Proliferation in an Animal Model of Alzheimer's Disease. *Cell Stem Cell* **17,** 397–411, doi: 10.1016/j.stem.2015.08.001 (2015).
26. Manoranjan, B. *et al.* Medulloblastoma stem cells: where development and cancer cross pathways. *Pediatr Res* **71,** 516–522, doi: 10.1038/pr.2011.62 (2012).
27. Wang, D. *et al.* HCA-vision: Automated neurite outgrowth analysis. *J Biomol Screen* **15,** 1165–1170, doi: 10.1177/1087057110382894 (2010).
28. Shalem, O. *et al.* Genome-scale CRISPR-Cas9 knockout screening in human cells. *Science* **343,** 84–87, doi: 10.1126/science.1247005 (2014).
29. Watson, J. V., Chambers, S. H. & Smith, P. J. A pragmatic approach to the analysis of DNA histograms with a definable G1 peak. *Cytometry* **8,** 1–8, doi: 10.1002/cyto.990080101 (1987).
30. Smyth, G. K. Linear models and empirical bayes methods for assessing differential expression in microarray experiments. *Stat Appl Genet Mol Biol* **3**, Article3, doi: 10.2202/1544-6115.1027 (2004).
31. Gentleman, R. C. *et al.* Bioconductor: open software development for computational biology and bioinformatics. *Genome Biol* **5,** R80, doi: 10.1186/gb-2004-5-10-r80 (2004).
32. Valach, J. *et al.* Smooth muscle actin-expressing stromal fibroblasts in head and neck squamous cell carcinoma: increased expression of galectin-1 and induction of poor prognosis factors. *Int J Cancer* **131,** 2499–2508, doi: 10.1002/ijc.27550 (2012).
33. Storey, J. D. & Tibshirani, R. Statistical significance for genomewide studies. *Proc Natl Acad Sci USA* **100,** 9440–9445, doi: 10.1073/pnas.1530509100 (2003).
34. Klisch, T. J. *et al. In vivo* Atoh1 targetome reveals how a proneural transcription factor regulates cerebellar development. *Proc Natl Acad Sci USA* **108,** 3288–3293, doi: 10.1073/pnas.1100230108 (2011).
35. Ayrault, O. *et al.* Atoh1 inhibits neuronal differentiation and collaborates with Gli1 to generate medulloblastoma-initiating cells. *Cancer Res* **70,** 5618–5627, doi: 10.1158/0008-5472.CAN-09-3740 (2010).
36. Northcott, P. A. *et al.* Medulloblastoma comprises four distinct molecular variants. *J Clin Oncol* **29,** 1408–1414, doi: 10.1200/JCO.2009.27.4324 (2011).
37. Lathia, J. D., Heddleston, J. M., Venere, M. & Rich, J. N. Deadly teamwork: neural cancer stem cells and the tumor microenvironment. *Cell Stem Cell* **8,** 482–485, doi: 10.1016/j.stem.2011.04.013 (2011).
38. Galli, R. *et al.* Isolation and characterization of tumorigenic, stem-like neural precursors from human glioblastoma. *Cancer Res* **64,** 7011–7021, doi: 10.1158/0008-5472.CAN-04-1364 (2004).
39. Hemmati, H. D. *et al.* Cancerous stem cells can arise from pediatric brain tumors. *Proc Natl Acad Sci USA* **100,** 15178–15183, doi: 10.1073/pnas.2036535100 (2003).
40. Gibson, P. *et al.* Subtypes of medulloblastoma have distinct developmental origins. *Nature* **468,** 1095–1099, doi: 10.1038/nature09587 (2010).
41. Lin, C. Y. *et al.* Active medulloblastoma enhancers reveal subgroup-specific cellular origins. *Nature* **530,** 57–62, doi: 10.1038/nature16546 (2016).
42. Ikonen, E. & Holtta-Vuori, M. Cellular pathology of Niemann-Pick type C disease. *Semin Cell Dev Biol* **15,** 445–454, doi: 10.1016/j.semcdb.2004.03.001 (2004).
43. Yang, S. R. *et al.* NPC1 gene deficiency leads to lack of neural stem cell self-renewal and abnormal differentiation through activation of p38 mitogen-activated protein kinase signaling. *Stem Cells* **24,** 292–298, doi: 10.1634/stemcells.2005-0221 (2006).
44. Ernst, C. Proliferation and Differentiation Deficits are a Major Convergence Point for Neurodevelopmental Disorders. *Trends Neurosci*, doi: 10.1016/j.tins.2016.03.001 (2016).
45. Efthymiou, A. G. *et al.* Rescue of an *in vitro* neuron phenotype identified in Niemann-Pick disease, type C1 induced pluripotent stem cell-derived neurons by modulating the WNT pathway and calcium signaling. *Stem Cells Transl Med* **4,** 230–238, doi: 10.5966/sctm.2014-0127 (2015).
46. Wassif, C. A. *et al.* Mutations in the human sterol delta7-reductase gene at 11q12-13 cause Smith-Lemli-Opitz syndrome. *Am J Hum Genet* **63,** 55–62, doi: 10.1086/301936 (1998).

47. Lee, R. W., Conley, S. K., Gropman, A., Porter, F. D. & Baker, E. H. Brain magnetic resonance imaging findings in Smith-Lemli-Opitz syndrome. *Am J Med Genet A* **161A,** 2407–2419, doi: 10.1002/ajmg.a.36096 (2013).
48. Tierney, E. *et al.* Behavior phenotype in the RSH/Smith-Lemli-Opitz syndrome. *Am J Med Genet* **98,** 191–200, doi: 10.1002/1096-8628(20010115)98:2%3C191::AID-AJMG1030%3E3.0.CO;2-M (2001).
49. Francis, K. R. *et al.* Modeling Smith-Lemli-Opitz syndrome with induced pluripotent stem cells reveals a causal role for Wnt/beta-catenin defects in neuronal cholesterol synthesis phenotypes. *Nat Med* **22,** 388–396, doi: 10.1038/nm.4067 (2016).
50. European Chromosome 16 Tuberous Sclerosis, C. Identification and characterization of the tuberous sclerosis gene on chromosome 16. *Cell* **75,** 1305–1315, doi: 10.1016/0092-8674(93)90618-Z (1993).
51. Costa, V. *et al.* mTORC1 Inhibition Corrects Neurodevelopmental and Synaptic Alterations in a Human Stem Cell Model of Tuberous Sclerosis. *Cell Rep* **15,** 86–95, doi: 10.1016/j.celrep.2016.02.090 (2016).
52. Frazier, T. W. *et al.* Molecular and phenotypic abnormalities in individuals with germline heterozygous PTEN mutations and autism. *Mol Psychiatry* **20,** 1132–1138, doi: 10.1038/mp.2014.125 (2015).
53. Sugathan, A. *et al.* CHD8 regulates neurodevelopmental pathways associated with autism spectrum disorder in neural progenitors. *Proc Natl Acad Sci USA* **111,** E4468–4477, doi: 10.1073/pnas.1405266111 (2014).
54. Sprenger, C. C., Damon, S. E., Hwa, V., Rosenfeld, R. G. & Plymate, S. R. Insulin-like growth factor binding protein-related protein 1 (IGFBP-rP1) is a potential tumor suppressor protein for prostate cancer. *Cancer Research* **59,** 2370–2375 (1999).
55. Ruan, W. J. *et al.* IGFBP7 plays a potential tumor suppressor role in colorectal carcinogenesis. *Cancer Biology & Therapy* **6,** 354–359, doi: 10.4161/cbt.6.3.3702 (2007).
56. Rupp, C. *et al.* IGFBP7, a novel tumor stroma marker, with growth-promoting effects in colon cancer through a paracrine tumor-stroma interaction. *Oncogene* **34,** 815–825, doi: 10.1038/onc.2014.18 (2015).
57. Smith, E., Ruszkiewicz, A. R., Jamieson, G. G. & Drew, P. A. IGFBP7 is associated with poor prognosis in oesophageal adenocarcinoma and is regulated by promoter DNA methylation. *British Journal of Cancer* **110,** 775–782, doi: 10.1038/bjc.2013.783 (2014).
58. Sato, Y. *et al.* Relationship between expression of IGFBP7 and clinicopathological variables in gastric cancer. *Journal of Clinical Pathology* **68,** 795–801, doi: 10.1136/jclinpath-2015-202987 (2015).
59. Benassi, M. S. *et al.* Tissue and serum IGFBP7 protein as biomarker in high-grade soft tissue sarcoma. *American Journal of Cancer Research* **5,** 3446–3454 (2015).
60. Jiang, W., Xiang, C. L., Cazacu, S., Brodie, C. & Mikkelsen, T. Insulin-like Growth Factor Binding Protein 7 Mediates Glioma Cell Growth and Migration. *Neoplasia* **10,** 1335–1342, doi: 10.1593/Neo.08694 (2008).
61. Agis-Balboa, R. C. *et al.* A hippocampal insulin-growth factor 2 pathway regulates the extinction of fear memories. *Embo Journal* **30,** 4071–4083, doi: 10.1038/emboj.2011.293 (2011).
62. Agbemenyah, H. Y., Agis-Balboa, R. C., Burkhardt, S., Delalle, I. & Fischer, A. Insulin growth factor binding protein 7 is a novel target to treat dementia. *Neurobiology of Disease* **62,** 135–143, doi: 10.1016/j.nbd.2013.09.011 (2014).
63. Goto, K. *et al.* Gene Cloning, Sequence, Expression and Insitu Localization of 80-Kda Diacylglycerol Kinase Specific to Oligodendrocyte of Rat-Brain. *Molecular Brain Research* **16,** 75–87, doi: 10.1016/0169-328x(92)90196-I (1992).
64. Redei, E. E. *et al.* Blood transcriptomic biomarkers in adult primary care patients with major depressive disorder undergoing cognitive behavioral therapy. *Transl Psychiatry* **4,** e442, doi: 10.1038/tp.2014.66 (2014).
65. Yanagisawa, K. *et al.* Diacylglycerol kinase alpha suppresses tumor necrosis factor-alpha- -induced apoptosis of human melanoma cells through NF-kappa B activation. *Biochimica Et Biophysica Acta-Molecular and Cell Biology of Lipids* **1771,** 462–474, doi: 10.1016/j.bbalip.2006.12.008 (2007).
66. Carter, H., Samayoa, J., Hruban, R. H. & Karchin, R. Prioritization of driver mutations in pancreatic cancer using cancer-specific high-throughput annotation of somatic mutations (CHASM). *Cancer Biology & Therapy* **10,** 582–587, doi: 10.4161/cbt.10.6.12537 (2010).
67. Takeishi, K. *et al.* Diacylglycerol kinase alpha enhances hepatocellular carcinoma progression by activation of Ras-Raf-MEK-ERK pathway. *Journal of Hepatology* **57,** 77–83, doi: 10.1016/j.jhep.2012.02.026 (2012).
68. Kefas, B. *et al.* A miR-297/hypoxia/DGK- axis regulating glioblastoma survival. *Neuro-Oncology* **15,** 1652–1663, doi: 10.1093/neuonc/not118 (2013).
69. Dominguez, C. L. *et al.* Diacylglycerol Kinase a Is a Critical Signaling Node and Novel Therapeutic Target in Glioblastoma and Other Cancers. *Cancer Discovery* **3,** 782–797, doi: 10.1158/2159-8290.CD-12-0215 (2013).
70. Kishi, M., Pan, Y. A., Crump, J. G. & Sanes, J. R. Mammalian SAD kinases are required for neuronal polarization. *Science* **307,** 929–932, doi: 10.1126/science.1107403 (2005).
71. Alvarado-Kristensson, M., Rodriguez, M. J., Silio, V., Valpuesta, J. M. & Carrera, A. C. SADB phosphorylation of gamma-tubulin regulates centrosome duplication. *Nature Cell Biology* **11,** 1081–U1086, doi: 10.1038/Ncb1921 (2009).
72. Im, D. S. *et al.* Characterization of a novel sphingosine 1-phosphate receptor, Edg-8. *Journal of Biological Chemistry* **275,** 14281–14286, doi: 10.1074/jbc.275.19.14281 (2000).
73. Ulfig, N. & Briese, M. Evidence for the presence of the sphingosine-1-phosphate receptor Edg-8 in human radial glial fibers. *Acta Histochemica* **106,** 373–378, doi: 10.1016/j.acthis.2004.08.002 (2004).
74. Jaillard, C. *et al.* Edg8/S1P5: An oligodendroglial receptor with dual function on process retraction and cell survival. *Journal of Neuroscience* **25,** 1459–1469, doi: 10.1523/Jneurosci.4645-04.2005 (2005).

Acknowledgements

We thank S. Takacova for proofreading the manuscript and Ondrej Horvath for cell cycle analysis. This work was supported by Czech Science Foundation project P301-12-1478, MEYS project LO1419, CUGA project 1272214 and IMG institutional support RVO 6878050.

Author Contributions

P.B. and M.Z. proposed the experiments and supervised the work. Ja.K. performed the experiments and analyzed the data. J.O., A.C. and Ju.K. performed the experiments. M.K. analyzed the microarray data. M.Z., J.K., J.O., A.C. and P.B. prepared the manuscript. All authors discussed the results and reviewed the manuscript.

Additional Information

Supplementary information accompanies this paper at http://www.nature.com/srep

Competing financial interests: The authors declare no competing financial interests.

How to cite this article: Konířová, J. *et al.* Modulated DISP3/PTCHD2 expression influences neural stem cell fate decisions. *Sci. Rep.* **7**, 41597; doi: 10.1038/srep41597 (2017).

Supplementary information

Modulated DISP3/PTCHD2 expression influences neural stem cell fate decisions

Jana Konířová, Jana Oltová, Alicia Corlett, Justyna Kopycińska, Michal Kolář, Petr Bartůněk* and Martina Zíková*

Institute of Molecular Genetics AS CR v.v.i., Vídeňská 1083, 142 20 Prague 4, Czech Republic

*Corresponding author:

Petr Bartůněk
Institute of Molecular Genetics AS CR v.v.i.
Vídeňská 1083, 142 20 Prague 4, Czech Republic
Tel. +420-241063117
Email: bartunek@img.cas.cz

Martina Zíková
Institute of Molecular Genetics AS CR v.v.i.
Vídeňská 1083, 142 20 Prague 4, Czech Republic
Tel. +420-241063113
Email: mzikova@img.cas.cz

Supplementary information

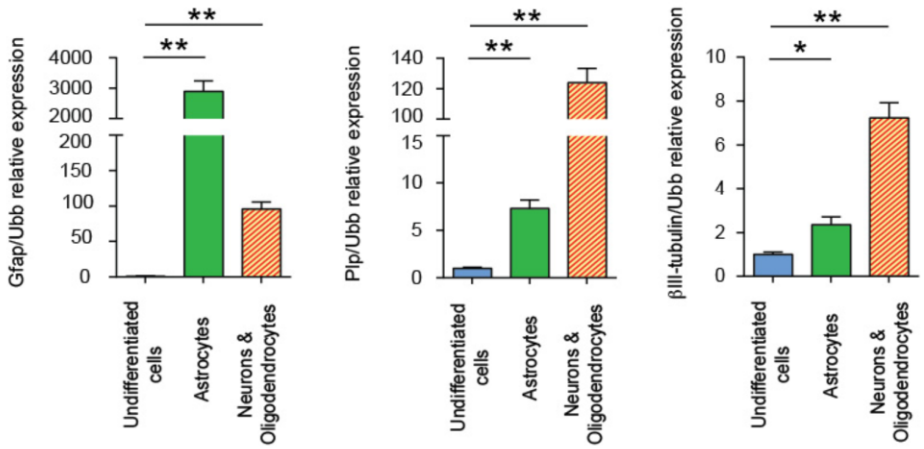

Supplementary Figure 1: Quantitative RT-PCR analysis of *Gfap, Plp* and βIII-tubulin mRNA expression in undifferentiated and differentiated NS-5 cells. *Ubb* was used as a reference gene. Bars represent the mean of three independent samples with error bars indicating standard deviation and the level of statistical significance (*P< 0.05, **P< 0.01). Mean values - Gfap relative expression: undifferentiated cells=1.00, astrocytes=2900, neurons and oligodendrocytes=96; - Plp relative expression: undifferentiated cells=1.00, astrocytes=7.30, neurons and oligodendrocytes=124; - βIII-tubulin relative expression: undifferentiated cells=1.00, astrocytes=2.36, neurons and oligodendrocytes=7.23.

Supplementary information

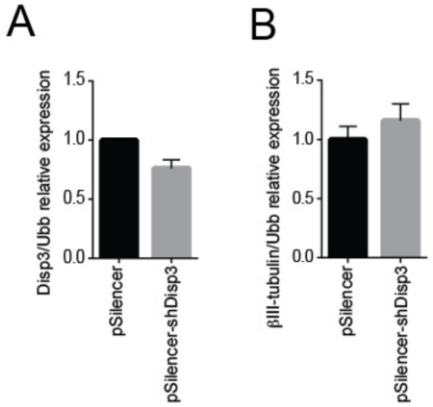

Supplementary Figure 2: Downregulation of DISP3 by shRNA leads to altered expression levels of βIII-tubulin.

(A) qRT-PCR analysis of *Disp3* expression in control (pSilencer) and shDisp3-treated NS-5 cells. *Ubb* was used as a reference gene. Bars represent the mean of three biological replicates with error bars indicating standard deviation. Mean values: pSilencer=1.00, pSilencer-shDisp3=0.76.

(B) qRT-PCR analysis of βIII-tubulin mRNA expression in control (pSilencer) and shDisp3-treated NS-5 cells. *Ubb* was used as a reference gene. Bars represent the mean of three biological replicates with error bars indicating standard deviation. Mean values: pSilencer=1.00, pSilencer-shDisp3=1.16.

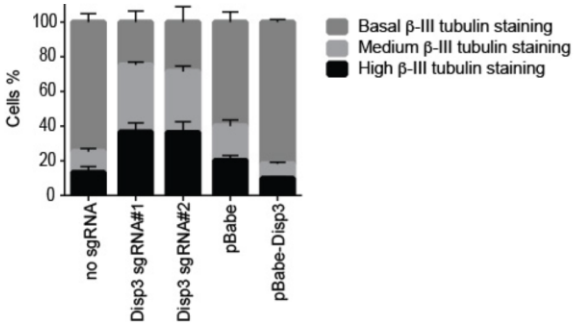

Supplementary Figure 3: Distribution of undifferentiated NS-5 cells based on β-III tubulin staining.

βIII-tubulin staining of undifferentiated NS-5 cells quantified by the Operetta High-Content Imagining System followed by Columbus software analysis. According to the intensity of βIII-tubulin staining, cells were divided into three groups: basal, medium and high intensity of staining. Data represent the percentage of cells in each particular group and the mean of biological replicates with error bars indicating standard deviation. Mean values - high βIII-tubulin staining: no sgRNA=13.47, Disp3 sgRNA#1=36.76, Disp3 sgRNA#2=36.40, pBabe=20.29, pBabe-Disp3=9.91; - medium βIII-tubulin staining: no sgRNA=11.92, Disp3 sgRNA#1=38.56, Disp3 sgRNA#2=35.18, pBabe=19.93, pBabe-Disp3=8.50; - basal βIII-tubulin staining: no sgRNA=74.61, Disp3 sgRNA#1=24.68, Disp3 sgRNA#2=28.42, pBabe=59.78, pBabe-Disp3=81.59.

Supplementary information

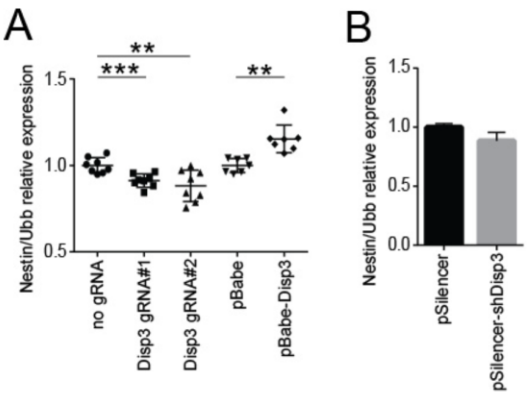

Supplementary Figure 4: Altered expression of nestin in Disp3 sgRNA (pSilencer-shDisp3) and pBabe-Disp3 cells.

(A) qRT-PCR analysis of nestin mRNA expression in Disp3 sgRNA, pBabe-Disp3 and control cells. *Ubb* was used as a reference gene. Data represent the mean of biological replicates with error bars indicating standard deviation and the level of statistical significance (**P< 0.01, ***P< 0.001). Mean values: no sgRNA=1.00, Disp3 sgRNA#1=0.91, Disp3 sgRNA#2=0.88, pBabe=1.00, pBabe-Disp3=1.15.

(B) qRT-PCR analysis of nestin mRNA expression in control (pSilencer) and shDisp3-treated NS-5 cells. *Ubb* was used as a reference gene. Data represent the mean of three biological replicates with error bars indicating standard deviation. Mean values: pSilencer=1, pSilencer-shDisp3=0.88.

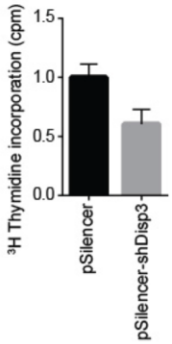

Supplementary Figure 5: Downregulation of DISP3 expression levels by shRNA leads to reduced NS-5 cell proliferation.

Proliferation of control (pSilencer) and shDisp3-treated NS-5 cells was measured by a ^{3}H-thymidine incorporation assay. Bars represent the mean of three biological replicates with error bars indicating standard deviation. Mean values: pSilencer=1.00, pSilencer-shDisp3=0.60.

Supplementary information

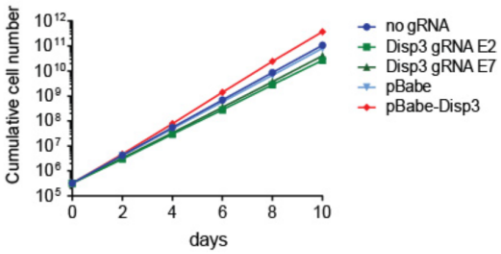

Supplementary Figure 6: Cell proliferation is altered in Disp3 sgRNA and pBabe-Disp3 NS-5 cells. Disp3 sgRNA, pBabe-Disp3 and control cells were counted every other day. The growth rate was plotted as cumulative cell numbers.

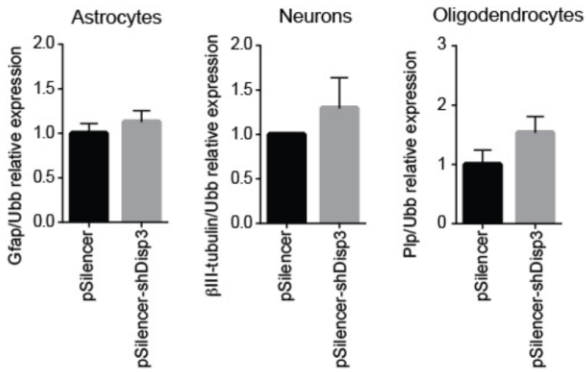

Supplementary Figure 7: Downregulation of DISP3 expression by shRNA promotes differentiation of NS-5 cells.

qRT-PCR analysis of *Gfap*, βIII-tubulin and *Plp* mRNA expression in control (pSilencer) and shDisp3 cells at days 4 (astrocytes) and 9 (neurons and oligodendrocytes) of differentiation. *Ubb* was used as a reference gene. Bars represent the mean of three biological replicates with error bars indicating standard deviation. Mean values - Gfap relative expression: pSilencer=1.00, pSilencer-shDisp3=1.13; - βIII-tubulin relative expression: pSilencer=1.00, pSilencer-shDisp3=1.30; - Plp relative expression: pSilencer=1.00, pSilencer-shDisp3=1.54.

Supplementary information

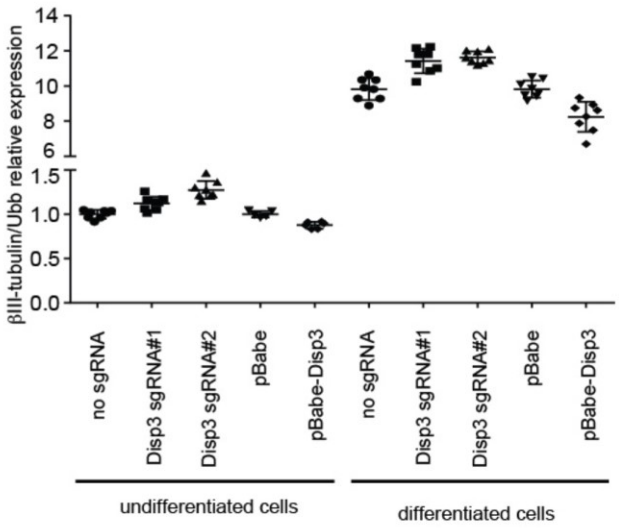

Supplementary Figure 8: Changes in DISP3 expression levels affect βIII-tubulin expression under both growth/proliferation and differentiation conditions. βIII-tubulin expression was quantified by qRT-PCR analysis (*Ubb* was used as a reference gene). Data represent the mean of biological replicates with error bars indicating standard deviation. Mean values - undifferentiated cells: no sgRNA=1.00, Disp3 sgRNA#1=1.12, Disp3 sgRNA#2=1.27, pBabe=1.00, pBabe-Disp3=0.88; - differentiated cells: no sgRNA=9.82, Disp3 sgRNA#1=11.42, Disp3 sgRNA#2=11.63, pBabe=9.82, pBabe-Disp3=8.24.